ISYA 2024 – THE INTERSTELLAR MEDIUM (ISM): LECTURE 2.
Atoms, Molecules & Dust

Frédéric GALLIANO

CEA Paris-Saclay, France

September 29, 2024

Outline of the Lecture

1. **ATOMS & IONS**
   - A reminder of atomic physics
   - The neutral gas
   - The ionized gas

Outline of the Lecture

1. **ATOMS & IONS**
   - A reminder of atomic physics
   - The neutral gas
   - The ionized gas
2. **MOLECULES IN SPACE**
   - The quantum molecular modes
   - Molecular bonding
   - Astrophysical molecular lines and features

Outline of the Lecture

1. **ATOMS & IONS**
   - A reminder of atomic physics
   - The neutral gas
   - The ionized gas
2. **MOLECULES IN SPACE**
   - The quantum molecular modes
   - Molecular bonding
   - Astrophysical molecular lines and features
3. **INTERSTELLAR DUST GRAINS**
   - Optical properties
   - Grain heating & cooling
   - State-of-the-art dust models

Outline of the Lecture

1. **ATOMS & IONS**
   - A reminder of atomic physics
   - The neutral gas
   - The ionized gas
2. **MOLECULES IN SPACE**
   - The quantum molecular modes
   - Molecular bonding
   - Astrophysical molecular lines and features
3. **INTERSTELLAR DUST GRAINS**
   - Optical properties
   - Grain heating & cooling
   - State-of-the-art dust models
4. **CONCLUSION**
   - Take-away points
   - References

Outline of the Lecture

1. **ATOMS & IONS**
   - A reminder of atomic physics
   - The neutral gas
   - The ionized gas
2. **MOLECULES IN SPACE**
   - The quantum molecular modes
   - Molecular bonding
   - Astrophysical molecular lines and features
3. **INTERSTELLAR DUST GRAINS**
   - Optical properties
   - Grain heating & cooling
   - State-of-the-art dust models
4. **CONCLUSION**
   - Take-away points
   - References

The Schrödinger equation applied to the H atom (see Bransden & Joachain 1983)

The Schrödinger equation applied to the H atom (see Bransden & Joachain 1983)

Assumptions: $m_e/m_p \simeq 5 \times 10^{-4} \Rightarrow$ fixed nucleus & spherically symmetric potential.

The Schrödinger equation applied to the H atom (see Bransden & Joachain 1983)

Assumptions: $m_e/m_p \simeq 5 \times 10^{-4} \Rightarrow$ fixed nucleus & spherically symmetric potential.

$$\overbrace{\left(\underbrace{-\frac{\hbar^2}{2m_e}\vec{\nabla}^2}_{\text{kinetic energy}} \qquad\qquad \right)}$$

The Schrödinger equation applied to the H atom (see Bransden & Joachain 1983)

Assumptions: $m_e/m_p \simeq 5 \times 10^{-4} \Rightarrow$ fixed nucleus & spherically symmetric potential.

$$\overbrace{\left(\underbrace{-\frac{\hbar^2}{2m_e}\vec{\nabla}^2}_{\text{kinetic energy}} \underbrace{-\frac{e^2}{4\pi\epsilon_0 r}}_{\text{Coulomb potential}}\right)}$$

The Schrödinger equation applied to the H atom (see Bransden & Joachain 1983)

Assumptions: $m_e/m_p \simeq 5\times10^{-4}$ $\Rightarrow$ fixed nucleus & spherically symmetric potential.

$$\overbrace{\left(\underbrace{-\frac{\hbar^2}{2m_e}\vec{\nabla}^2}_{\text{kinetic energy}}\underbrace{-\frac{e^2}{4\pi\epsilon_0 r}}_{\text{Coulomb potential}}\right)}^{\text{Hamiltonian operator}}\psi(r,\theta,\phi)$$

The Schrödinger equation applied to the H atom (see Bransden & Joachain 1983)

Assumptions: $m_e/m_p \simeq 5\times10^{-4} \Rightarrow$ fixed nucleus & spherically symmetric potential.

$$\overbrace{\left(\underbrace{-\frac{\hbar^2}{2m_e}\vec{\nabla}^2}_{\text{kinetic energy}}\ \underbrace{-\frac{e^2}{4\pi\epsilon_0 r}}_{\text{Coulomb potential}}\right)}^{\text{Hamiltonian operator}}\psi(r,\theta,\phi) = E\,\underbrace{\psi(r,\theta,\phi)}_{\text{wave function}}.$$

The Schrödinger equation applied to the H atom (see Bransden & Joachain 1983)

Assumptions: $m_e/m_p \simeq 5 \times 10^{-4} \Rightarrow$ fixed nucleus & spherically symmetric potential.

$$\overbrace{\left(\underbrace{-\frac{\hbar^2}{2m_e}\vec{\nabla}^2}_{\text{kinetic energy}} \underbrace{-\frac{e^2}{4\pi\epsilon_0 r}}_{\text{Coulomb potential}} \right)}^{\text{Hamiltonian operator}} \psi(r,\theta,\phi) = E\,\underbrace{\psi(r,\theta,\phi)}_{\text{wave function}}.$$

Solution: 1. Eigenvalues of E *i.e. energy levels*: $E_n = -\frac{m_e e^4}{8h^2\epsilon_0^2}\frac{1}{n^2}$

The Schrödinger equation applied to the H atom (see Bransden & Joachain 1983)

Assumptions: $m_e/m_p \simeq 5 \times 10^{-4} \Rightarrow$ fixed nucleus & spherically symmetric potential.

$$\overbrace{\left(\underbrace{-\frac{\hbar^2}{2m_e}\vec{\nabla}^2}_{\text{kinetic energy}} \underbrace{-\frac{e^2}{4\pi\epsilon_0 r}}_{\text{Coulomb potential}} \right)}^{\text{Hamiltonian operator}} \psi(r,\theta,\phi) = E \underbrace{\psi(r,\theta,\phi)}_{\text{wave function}}.$$

Solution: 1. Eigenvalues of E *i.e. energy levels*: $E_n = -\frac{m_e e^4}{8h^2\epsilon_0^2}\frac{1}{n^2} \Rightarrow \boxed{E_n = -\frac{13.6\text{ eV}}{n^2}}$.

The Schrödinger equation applied to the H atom (see Bransden & Joachain 1983)

Assumptions: $m_e/m_p \simeq 5 \times 10^{-4} \Rightarrow$ fixed nucleus & spherically symmetric potential.

$$\overbrace{\left(\underbrace{-\frac{\hbar^2}{2m_e}\vec{\vec{\nabla}}^2}_{\text{kinetic energy}} \underbrace{-\frac{e^2}{4\pi\epsilon_0 r}}_{\text{Coulomb potential}} \right)}^{\text{Hamiltonian operator}} \psi(r,\theta,\phi) = E\,\underbrace{\psi(r,\theta,\phi)}_{\text{wave function}}.$$

Solution:

1. Eigenvalues of E *i.e. energy levels*: $E_n = -\frac{m_e e^4}{8h^2\epsilon_0^2}\frac{1}{n^2} \Rightarrow \boxed{E_n = -\frac{13.6\text{ eV}}{n^2}}$.
2. A set of wave functions corresponding to each one of the possible energy levels $\rightarrow$ combination of *spherical harmonic* functions.

The Schrödinger equation applied to the H atom (see Bransden & Joachain 1983)

Assumptions: $m_e/m_p \simeq 5 \times 10^{-4} \Rightarrow$ fixed nucleus & spherically symmetric potential.

$$\overbrace{\left(\underbrace{-\frac{\hbar^2}{2m_e}\vec{\nabla}^2}_{\text{kinetic energy}} \underbrace{-\frac{e^2}{4\pi\epsilon_0 r}}_{\text{Coulomb potential}}\right)}^{\text{Hamiltonian operator}} \psi(r,\theta,\phi) = E\,\underbrace{\psi(r,\theta,\phi)}_{\text{wave function}}.$$

Solution:

1. Eigenvalues of E *i.e. energy levels*: $E_n = -\frac{m_e e^4}{8h^2\epsilon_0^2}\frac{1}{n^2} \Rightarrow \boxed{E_n = -\frac{13.6\text{ eV}}{n^2}}$.
2. A set of wave functions corresponding to each one of the possible energy levels $\rightarrow$ combination of *spherical harmonic* functions.

Quantum numbers characterizing each individual solution

The Schrödinger equation applied to the H atom (see Bransden & Joachain 1983)

Assumptions: $m_e/m_p \simeq 5\times10^{-4} \Rightarrow$ fixed nucleus & spherically symmetric potential.

$$\overbrace{\left(\underbrace{-\frac{\hbar^2}{2m_e}\vec{\nabla}^2}_{\text{kinetic energy}}\;\underbrace{-\frac{e^2}{4\pi\epsilon_0 r}}_{\text{Coulomb potential}}\right)}^{\text{Hamiltonian operator}}\psi(r,\theta,\phi) = E\,\underbrace{\psi(r,\theta,\phi)}_{\text{wave function}}.$$

Solution:

1. Eigenvalues of E *i.e. energy levels*: $E_n = -\frac{m_e e^4}{8h^2\epsilon_0^2}\frac{1}{n^2} \Rightarrow \boxed{E_n = -\frac{13.6\text{ eV}}{n^2}}.$
2. A set of wave functions corresponding to each one of the possible energy levels $\rightarrow$ combination of *spherical harmonic* functions.

Quantum numbers characterizing each individual solution

Name	Symbol	Values	Signification
Principal	n	$1,2,\ldots,\infty$	Energy ($E\propto 1/n^2$) or size of the shell

The Schrödinger equation applied to the H atom (see Bransden & Joachain 1983)

Assumptions: $m_e/m_p \simeq 5\times10^{-4} \Rightarrow$ fixed nucleus & spherically symmetric potential.

$$\overbrace{\left(\underbrace{-\frac{\hbar^2}{2m_e}\vec{\nabla}^2}_{\text{kinetic energy}}\;\underbrace{-\frac{e^2}{4\pi\epsilon_0 r}}_{\text{Coulomb potential}}\right)}^{\text{Hamiltonian operator}}\psi(r,\theta,\phi) = E\,\underbrace{\psi(r,\theta,\phi)}_{\text{wave function}}.$$

Solution:

1. Eigenvalues of E *i.e. energy levels*: $E_n = -\frac{m_e e^4}{8h^2\epsilon_0^2}\frac{1}{n^2} \Rightarrow \boxed{E_n = -\frac{13.6\text{ eV}}{n^2}}$.
2. A set of wave functions corresponding to each one of the possible energy levels $\rightarrow$ combination of *spherical harmonic* functions.

Quantum numbers characterizing each individual solution

Name	Symbol	Values	Signification
Principal	n	$1,2,\ldots,\infty$	Energy ($E\propto 1/n^2$) or size of the shell
Azimuthal	l	$0,1,\ldots,n-1$	Angular momentum ($L\propto\sqrt{l(l+1)}$)

The Schrödinger equation applied to the H atom (see Bransden & Joachain 1983)

Assumptions: $m_e/m_p \simeq 5\times10^{-4} \Rightarrow$ fixed nucleus & spherically symmetric potential.

$$\overbrace{\left(\underbrace{-\frac{\hbar^2}{2m_e}\vec{\nabla}^2}_{\text{kinetic energy}}\underbrace{-\frac{e^2}{4\pi\epsilon_0 r}}_{\text{Coulomb potential}}\right)}^{\text{Hamiltonian operator}}\psi(r,\theta,\phi) = E\,\underbrace{\psi(r,\theta,\phi)}_{\text{wave function}}.$$

Solution:

1. Eigenvalues of E *i.e. energy levels*: $E_n = -\frac{m_e e^4}{8h^2\epsilon_0^2}\frac{1}{n^2} \Rightarrow \boxed{E_n = -\frac{13.6\text{ eV}}{n^2}}$.
2. A set of wave functions corresponding to each one of the possible energy levels $\rightarrow$ combination of *spherical harmonic* functions.

Quantum numbers characterizing each individual solution

Name	Symbol	Values	Signification
Principal	n	$1, 2, \ldots, \infty$	Energy ($E \propto 1/n^2$) or size of the shell
Azimuthal	l	$0, 1, \ldots, n-1$	Angular momentum ($L \propto \sqrt{l(l+1)}$)
Magnetic	m_l	$l, l-1, \ldots, -l$	Orientation (spherical harmonic combination)

The Schrödinger equation applied to the H atom (see Bransden & Joachain 1983)

Assumptions: $m_e/m_p \simeq 5 \times 10^{-4} \Rightarrow$ fixed nucleus & spherically symmetric potential.

$$\overbrace{\left(\underbrace{-\frac{\hbar^2}{2m_e}\vec{\nabla}^2}_{\text{kinetic energy}} \underbrace{-\frac{e^2}{4\pi\epsilon_0 r}}_{\text{Coulomb potential}}\right)}^{\text{Hamiltonian operator}} \psi(r,\theta,\phi) = E\,\underbrace{\psi(r,\theta,\phi)}_{\text{wave function}}.$$

Solution:

1. Eigenvalues of E *i.e. energy levels*: $E_n = -\frac{m_e e^4}{8h^2\epsilon_0^2}\frac{1}{n^2} \Rightarrow \boxed{E_n = -\frac{13.6\text{ eV}}{n^2}}$.
2. A set of wave functions corresponding to each one of the possible energy levels $\rightarrow$ combination of *spherical harmonic* functions.

Quantum numbers characterizing each individual solution

Name	Symbol	Values	Signification
Principal	n	$1, 2, \ldots, \infty$	Energy ($E \propto 1/n^2$) or size of the shell
Azimuthal	l	$0, 1, \ldots, n-1$	Angular momentum ($L \propto \sqrt{l(l+1)}$)
Magnetic	m_l	$l, l-1, \ldots, -l$	Orientation (spherical harmonic combination)
Spin	m_s	$+1/2, -1/2$	Magnetic moment (spin direction)

At a given energy (n) $\rightarrow$ different values of the angular momentum (l).

At a given energy (n) $\rightarrow$ different values of the angular momentum (l).

l=0
(s)

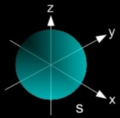

m_l=0

Credit: surfaces corresponding to 90 % probability presence of the electron (UC Davis Chemwiki).

At a given energy (n) $\rightarrow$ different values of the angular momentum (l).

l=0
(s)

l=1
(p)

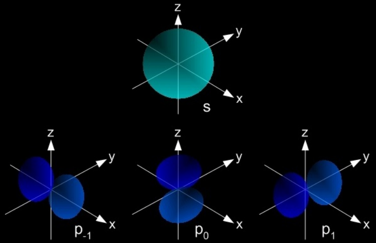

m_l=-1 m_l=0 m_l=1

Credit: surfaces corresponding to 90 % probability presence of the electron (UC Davis Chemwiki).

Atoms | Electronic Orbitals of the Hydrogen Atom

At a given energy (n) $\rightarrow$ different values of the angular momentum (l).

l=0 (s)

l=1 (p)

l=2 (d)

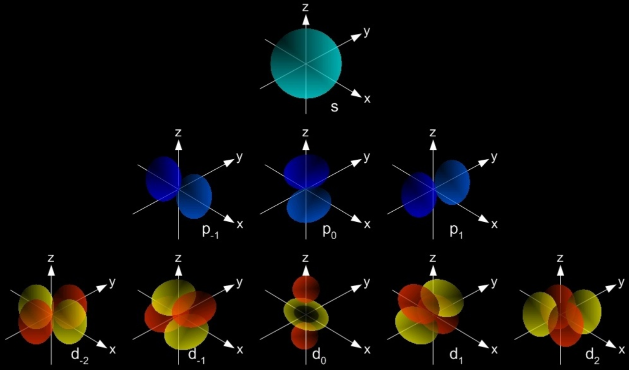

m_l=-2 m_l=-1 m_l=0 m_l=1 m_l=2

Credit: surfaces corresponding to 90 % probability presence of the electron (UC Davis Chemwiki).

At a given energy (n) $\rightarrow$ different values of the angular momentum (l).

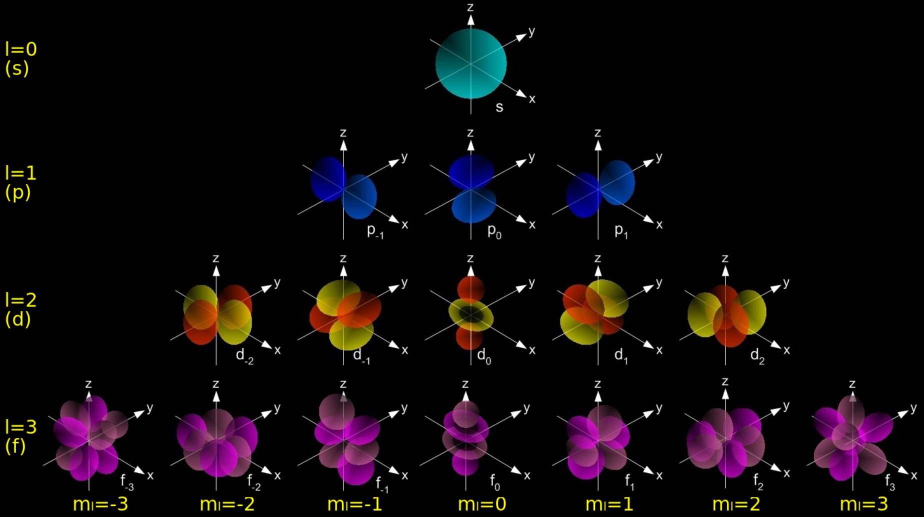

Credit: surfaces corresponding to 90 % probability presence of the electron (UC Davis Chemwiki).

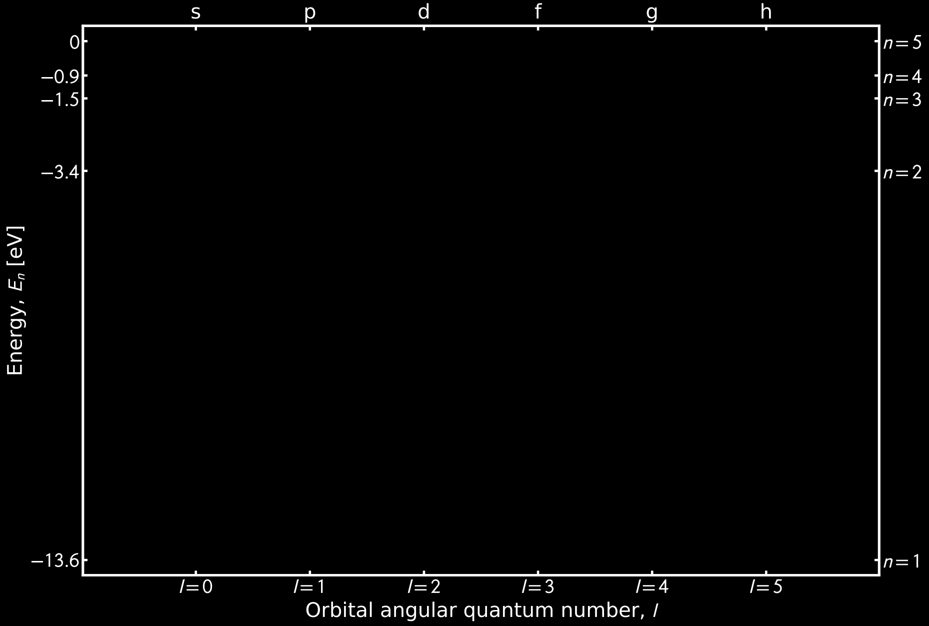
s
p
d
f
g
h
0
−0.9
−1.5
−3.4
−13.6
Energy, E_n [eV]
$n=5$
$n=4$
$n=3$
$n=2$
$n=1$
$l=0$
$l=1$
$l=2$
$l=3$
$l=4$
$l=5$
Orbital angular quantum number, l

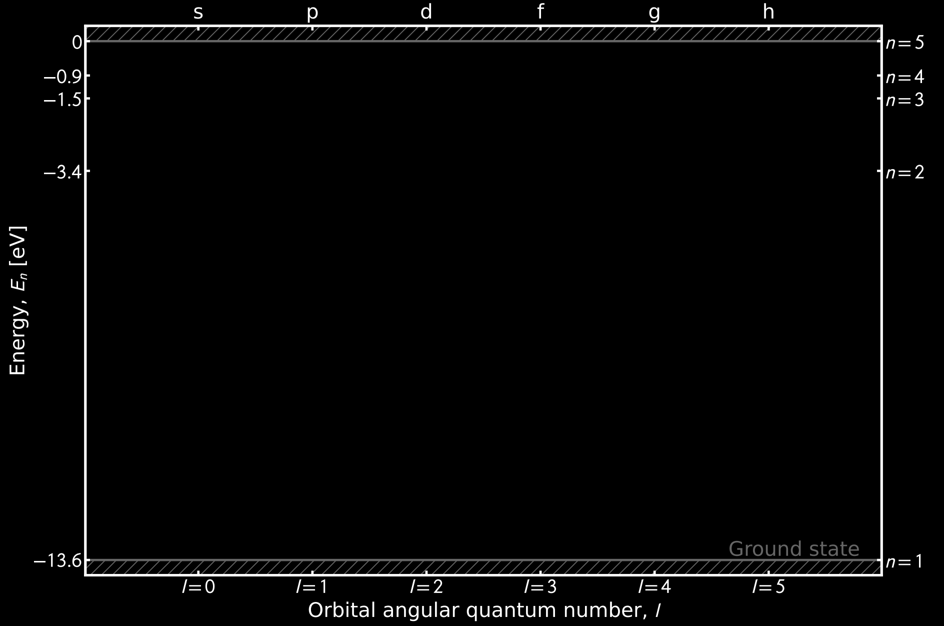
s
p
d
f
g
h
0
−0.9
−1.5
−3.4
−13.6
n = 5
n = 4
n = 3
n = 2
n = 1
Energy, E_n [eV]
Ground state
l = 0
l = 1
l = 2
l = 3
l = 4
l = 5
Orbital angular quantum number, l

The Gross Structure of the H Atom: Resonant Lines

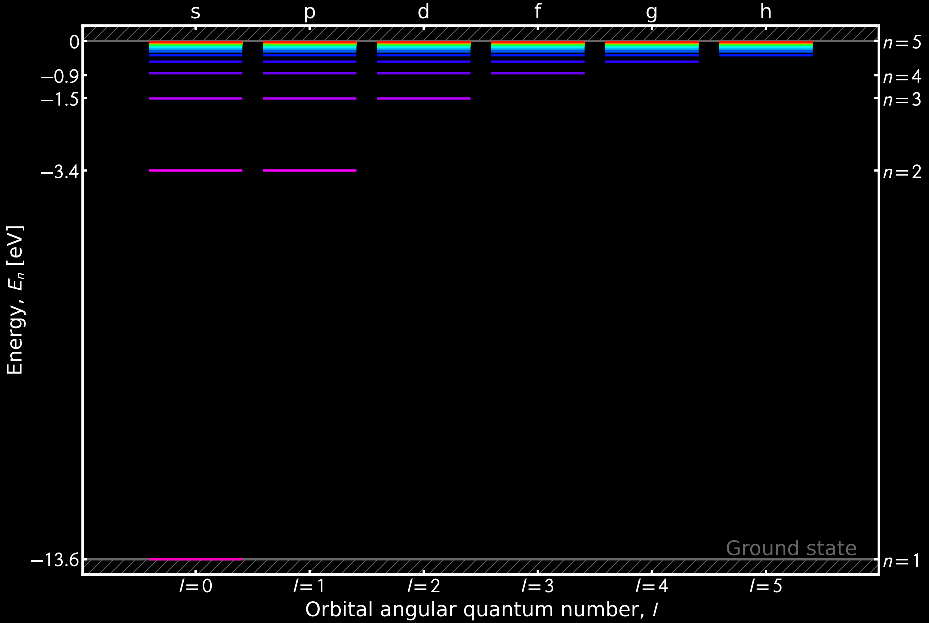

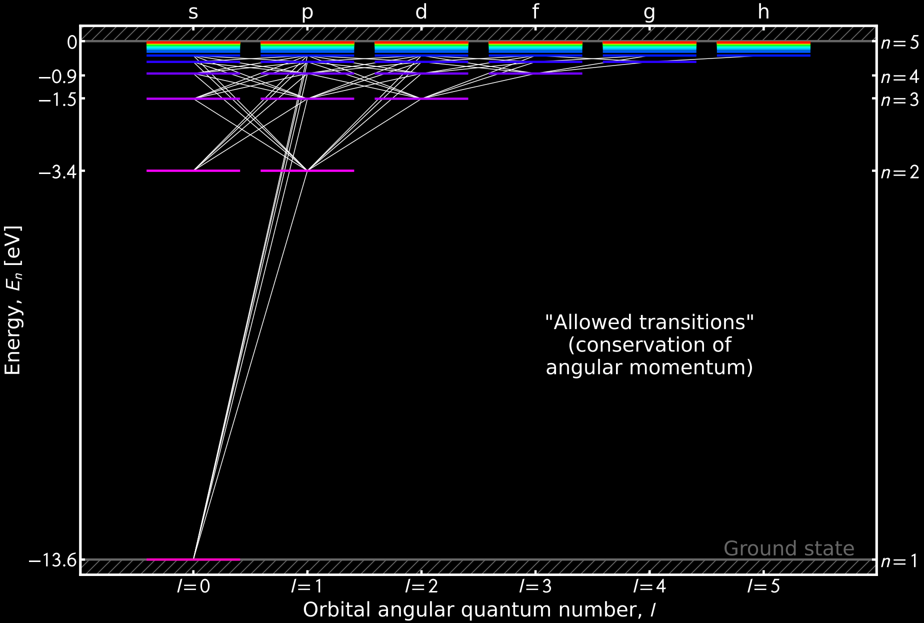
s
p
d
f
g
h
0
−0.9
−1.5
−3.4
−13.6
n = 5
n = 4
n = 3
n = 2
n = 1
Energy, E_n [eV]
"Allowed transitions"
(conservation of
angular momentum)
Ground state
l = 0
l = 1
l = 2
l = 3
l = 4
l = 5
Orbital angular quantum number, l

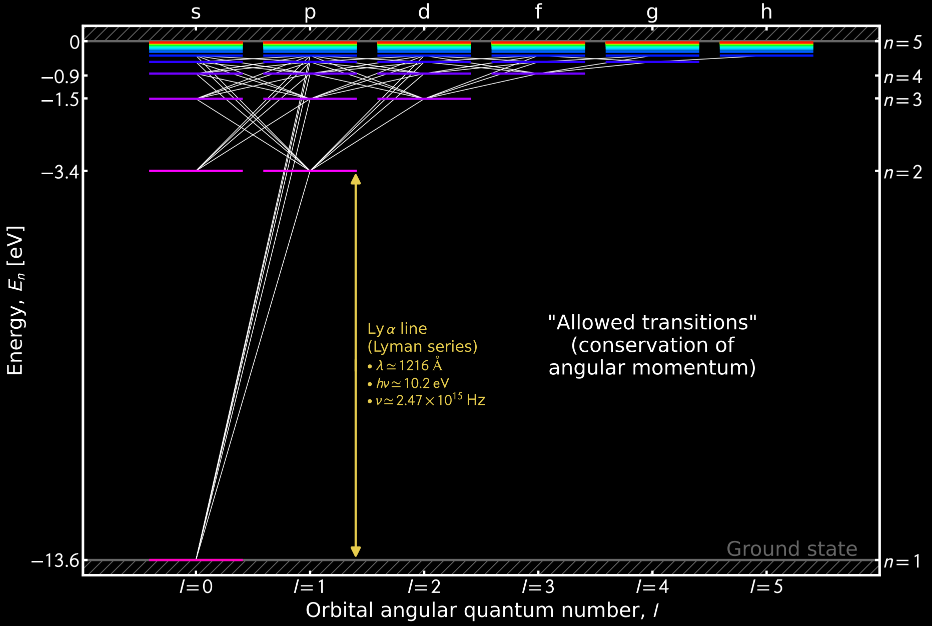
s
p
d
f
g
h
0
−0.9
−1.5
−3.4
−13.6
n = 5
n = 4
n = 3
n = 2
n = 1
Energy, E_n [eV]
Ly α line
(Lyman series)
• $\lambda \simeq 1216$ Å
• $h\nu \simeq 10.2$ eV
• $\nu \simeq 2.47 \times 10^{15}$ Hz
"Allowed transitions"
(conservation of
angular momentum)
Ground state
$l = 0$
$l = 1$
$l = 2$
$l = 3$
$l = 4$
$l = 5$
Orbital angular quantum number, l

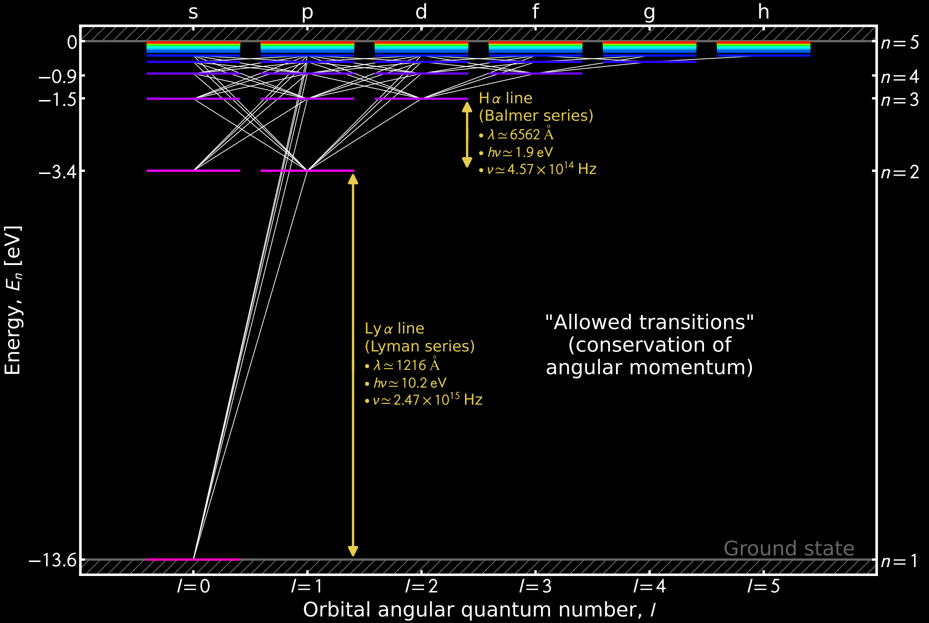
s
p
d
f
g
h
0
−0.9
−1.5
−3.4
−13.6
n = 5
n = 4
n = 3
n = 2
n = 1
Energy, E_n [eV]
H α line
(Balmer series)
• $\lambda \simeq 6562$ Å
• $h\nu \simeq 1.9$ eV
• $\nu \simeq 4.57 \times 10^{14}$ Hz
Ly α line
(Lyman series)
• $\lambda \simeq 1216$ Å
• $h\nu \simeq 10.2$ eV
• $\nu \simeq 2.47 \times 10^{15}$ Hz
"Allowed transitions"
(conservation of
angular momentum)
Ground state
$l = 0$
$l = 1$
$l = 2$
$l = 3$
$l = 4$
$l = 5$
Orbital angular quantum number, l

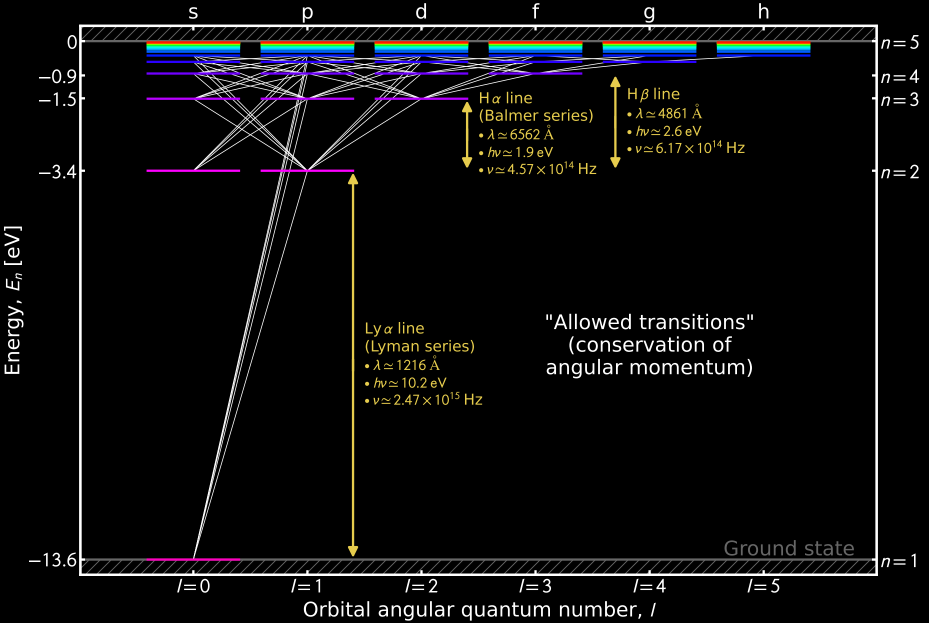
s
p
d
f
g
h
0
−0.9
−1.5
−3.4
−13.6
n = 5
n = 4
n = 3
n = 2
n = 1
Energy, E_n [eV]
H α line
(Balmer series)
• $\lambda \simeq 6562$ Å
• $h\nu \simeq 1.9$ eV
• $\nu \simeq 4.57 \times 10^{14}$ Hz
H β line
• $\lambda \simeq 4861$ Å
• $h\nu \simeq 2.6$ eV
• $\nu \simeq 6.17 \times 10^{14}$ Hz
Ly α line
(Lyman series)
• $\lambda \simeq 1216$ Å
• $h\nu \simeq 10.2$ eV
• $\nu \simeq 2.47 \times 10^{15}$ Hz
"Allowed transitions"
(conservation of
angular momentum)
Ground state
l = 0
l = 1
l = 2
l = 3
l = 4
l = 5
Orbital angular quantum number, l

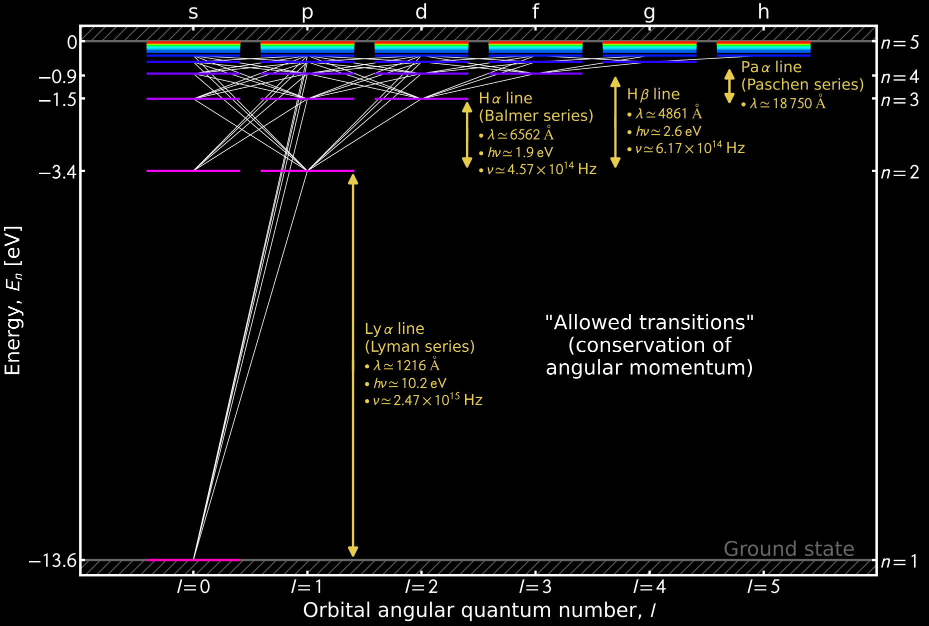

s
p
d
f
g
h
0
−0.9
−1.5
−3.4
−13.6
n = 5
n = 4
n = 3
n = 2
n = 1
Energy, E_n [eV]
H α line
(Balmer series)
• λ ≃ 6562 Å
• hν ≃ 1.9 eV
• ν ≃ 4.57 × 10^14 Hz
H β line
• λ ≃ 4861 Å
• hν ≃ 2.6 eV
• ν ≃ 6.17 × 10^14 Hz
Pa α line
(Paschen series)
• λ ≃ 18 750 Å
Ly α line
(Lyman series)
• λ ≃ 1216 Å
• hν ≃ 10.2 eV
• ν ≃ 2.47 × 10^15 Hz
"Allowed transitions"
(conservation of
angular momentum)
Ground state
l = 0
l = 1
l = 2
l = 3
l = 4
l = 5
Orbital angular quantum number, l

Gross structure

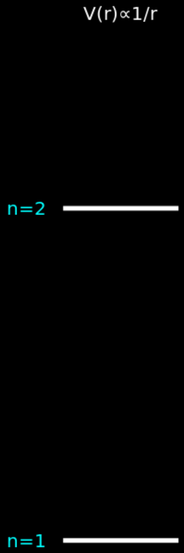

Gross structure

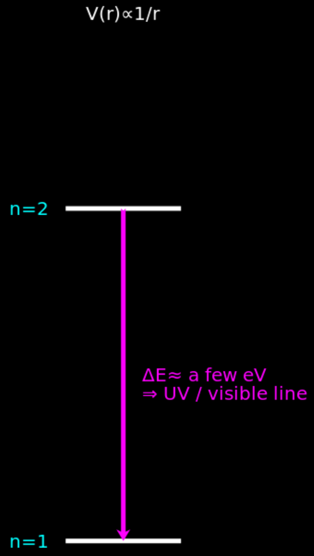

Gross structure

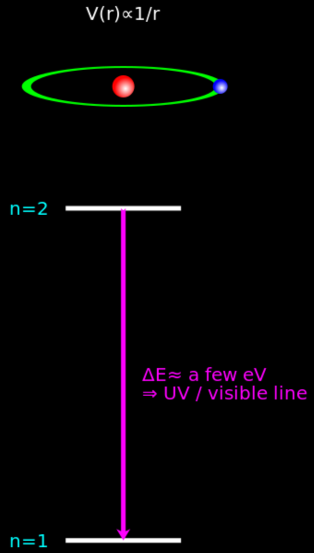

Gross structure

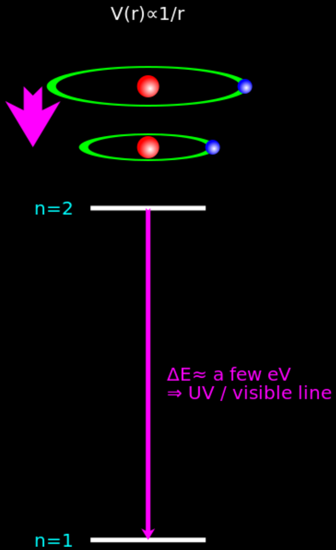

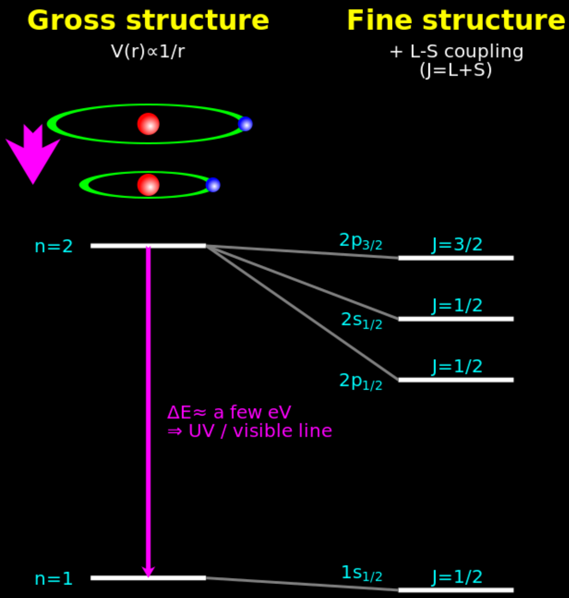
Gross structure
V(r)∝1/r
Fine structure
+ L-S coupling
(J=L+S)
n=2
2p3/2
J=3/2
J=1/2
2s1/2
J=1/2
2p1/2
ΔE≈ a few eV
⇒ UV / visible line
n=1
1s1/2
J=1/2

Atoms | Level Splitting: the Fine & Hyperfine Structures

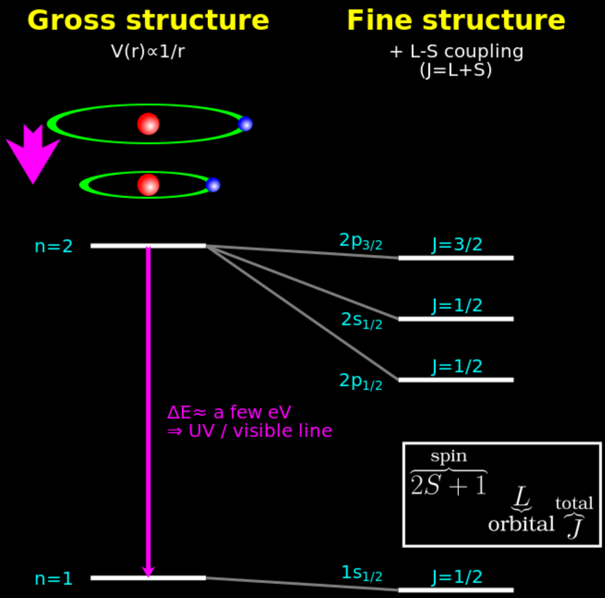

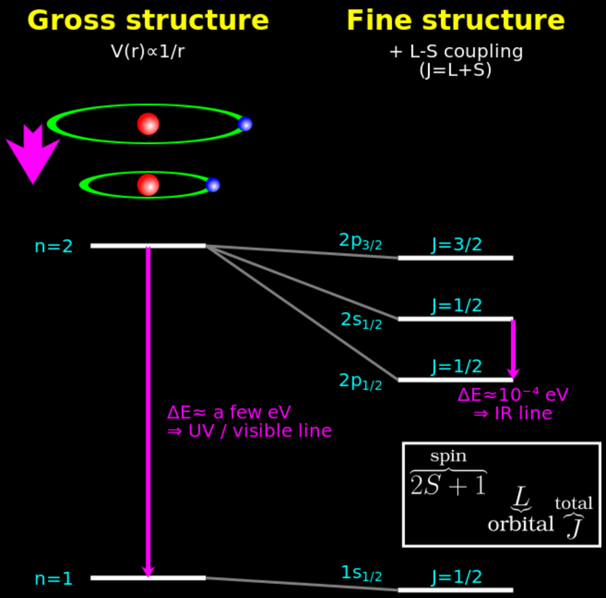
Gross structure
V(r)∝1/r
Fine structure
+ L-S coupling
(J=L+S)
n=2
2p3/2
J=3/2
J=1/2
2s1/2
J=1/2
2p1/2
ΔE≈10⁻⁴ eV
⇒ IR line
ΔE≈ a few eV
⇒ UV / visible line
spin
2S + 1
L
orbital
total
J
n=1
1s1/2
J=1/2

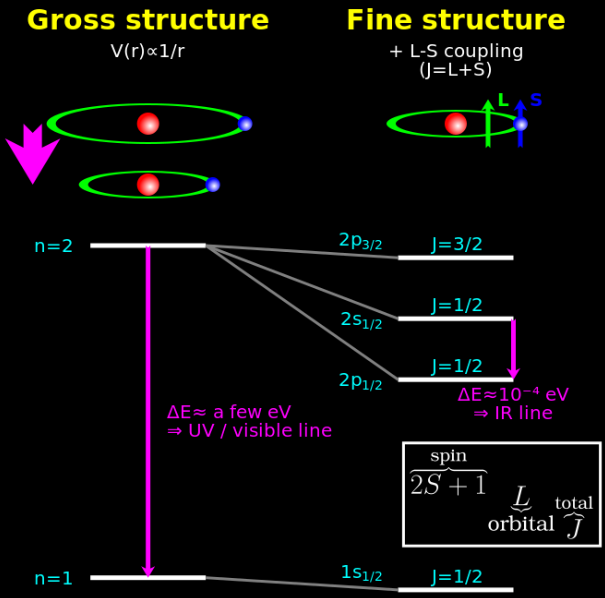
Gross structure
V(r)∝1/r
Fine structure
+ L-S coupling
(J=L+S)
L
S
n=2
n=1
2p3/2
2s1/2
2p1/2
1s1/2
J=3/2
J=1/2
J=1/2
J=1/2
ΔE≈ a few eV
⇒ UV / visible line
ΔE≈10⁻⁴ eV
⇒ IR line
spin
2S + 1
L
orbital
total
J

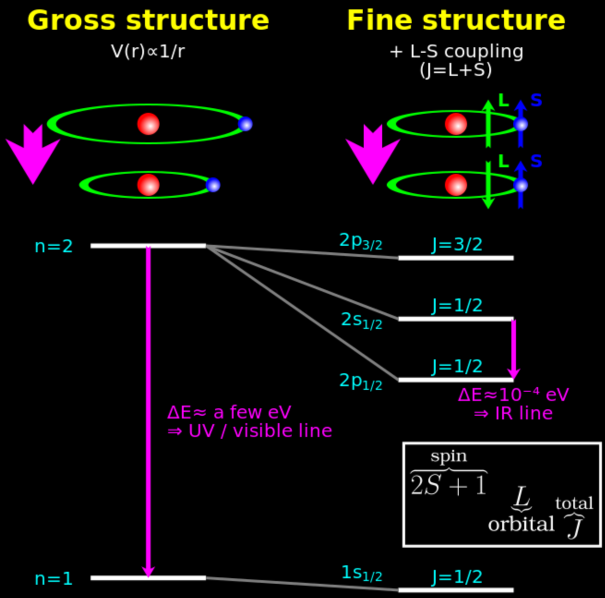
Gross structure
V(r)∝1/r
Fine structure
+ L-S coupling
(J=L+S)
L
S
L
S
n=2
$2p_{3/2}$
J=3/2
J=1/2
$2s_{1/2}$
J=1/2
$2p_{1/2}$
ΔE≈10^{-4} eV
⇒ IR line
ΔE≈ a few eV
⇒ UV / visible line
$\overbrace{2S+1}^{\text{spin}} \underbrace{L}_{\text{orbital}} \overbrace{J}^{\text{total}}$
n=1
$1s_{1/2}$
J=1/2

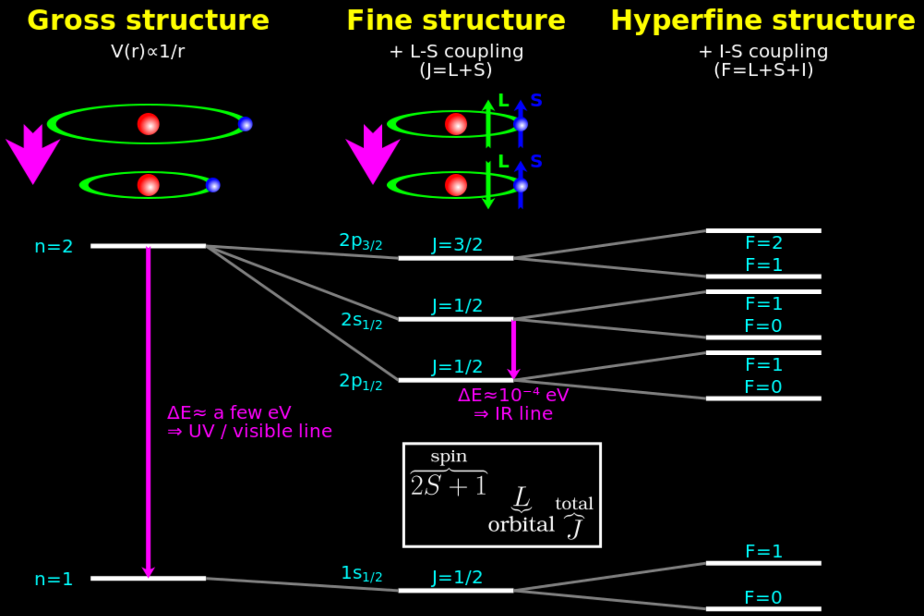
Gross structure
V(r)∝1/r
Fine structure
+ L-S coupling
(J=L+S)
Hyperfine structure
+ I-S coupling
(F=L+S+I)
L
S
L
S
n=2
2p3/2
J=3/2
F=2
F=1
2s1/2
J=1/2
F=1
F=0
2p1/2
J=1/2
F=1
F=0
ΔE≈10⁻⁴ eV
⇒ IR line
ΔE≈ a few eV
⇒ UV / visible line
spin 2S+1
L orbital
total J
n=1
1s1/2
J=1/2
F=1
F=0

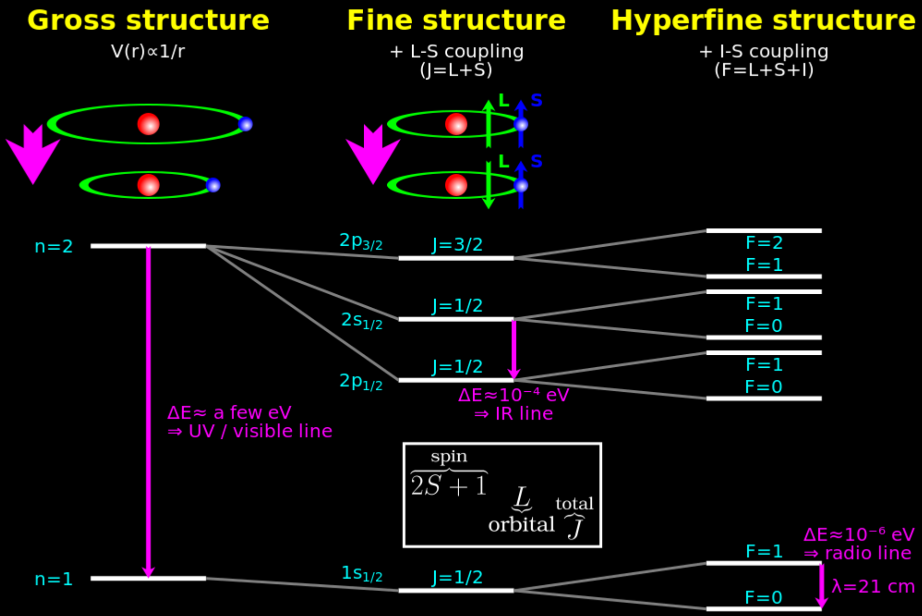
Gross structure
V(r)∝1/r
Fine structure
+ L-S coupling
(J=L+S)
Hyperfine structure
+ I-S coupling
(F=L+S+I)
L
S
L
S
n=2
n=1
2p3/2
J=3/2
2s1/2
J=1/2
2p1/2
J=1/2
1s1/2
J=1/2
F=2
F=1
F=1
F=0
F=1
F=0
F=1
F=0
ΔE≈ a few eV
⇒ UV / visible line
ΔE≈10⁻⁴ eV
⇒ IR line
ΔE≈10⁻⁶ eV
⇒ radio line
λ=21 cm
spin
2S+1
L
orbital
total
J

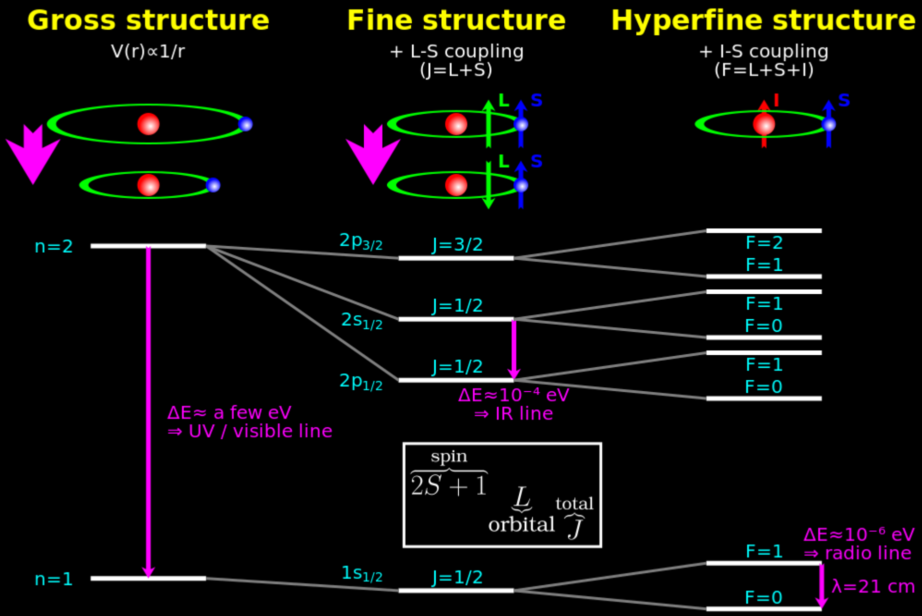
Gross structure
V(r)∝1/r
Fine structure
+ L-S coupling
(J=L+S)
Hyperfine structure
+ I-S coupling
(F=L+S+I)
L
S
I
n=2
n=1
2p3/2
J=3/2
2s1/2
J=1/2
2p1/2
J=1/2
1s1/2
J=1/2
F=2
F=1
F=1
F=0
F=1
F=0
F=1
F=0
ΔE≈ a few eV
⇒ UV / visible line
ΔE≈10⁻⁴ eV
⇒ IR line
ΔE≈10⁻⁶ eV
⇒ radio line
λ=21 cm
spin
2S + 1
L
orbital
total
J

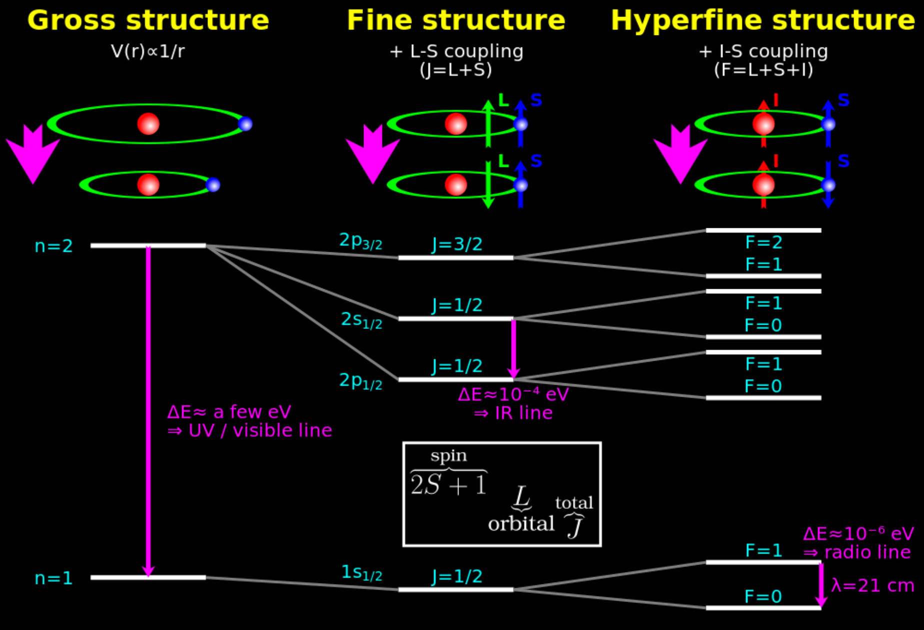
Gross structure
V(r)∝1/r
Fine structure
+ L-S coupling
(J=L+S)
Hyperfine structure
+ I-S coupling
(F=L+S+I)
L
S
I
n=2
n=1
2p3/2
J=3/2
2s1/2
J=1/2
2p1/2
J=1/2
1s1/2
J=1/2
F=2
F=1
F=1
F=0
F=1
F=0
F=1
F=0
ΔE≈ a few eV
⇒ UV / visible line
ΔE≈10⁻⁴ eV
⇒ IR line
ΔE≈10⁻⁶ eV
⇒ radio line
λ=21 cm
spin
2S + 1
L
orbital
total
J

Filling the orbitals

Filling the orbitals

- Other atoms → the different orbitals have the same characteristics as for H.

Filling the orbitals

- Other atoms → the different orbitals have the same characteristics as for H.
- The lowest energy levels are filled first.

Filling the orbitals

- Other atoms → the different orbitals have the same characteristics as for H.
- The lowest energy levels are filled first.
- *Pauli exclusion principle* → no more than 2 electrons per l, with antiparallel spins: ↑↓.

Filling the orbitals

- Other atoms → the different orbitals have the same characteristics as for H.
- The lowest energy levels are filled first.
- *Pauli exclusion principle* → no more than 2 electrons per l, with antiparallel spins: ↑↓.

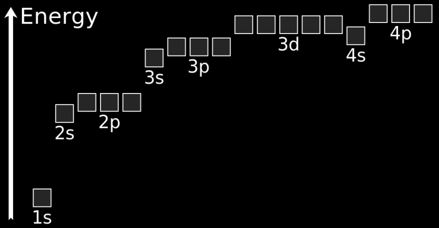

Filling the orbitals

- Other atoms → the different orbitals have the same characteristics as for H.
- The lowest energy levels are filled first.
- *Pauli exclusion principle* → no more than 2 electrons per l, with antiparallel spins: ↑↓.

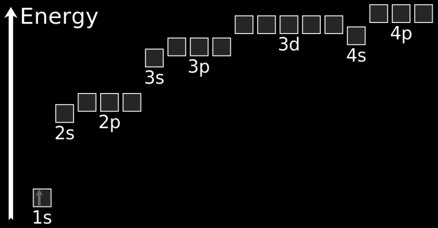

Filling the orbitals

- Other atoms → the different orbitals have the same characteristics as for H.
- The lowest energy levels are filled first.
- *Pauli exclusion principle* → no more than 2 electrons per l, with antiparallel spins: ↑↓.

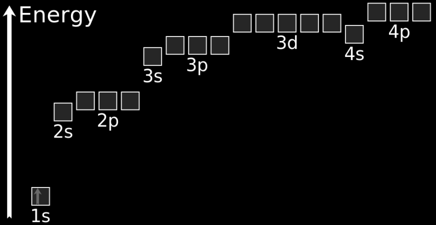

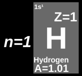

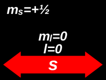

Filling the orbitals

- Other atoms $\rightarrow$ the different orbitals have the same characteristics as for H.
- The lowest energy levels are filled first.
- *Pauli exclusion principle* $\rightarrow$ no more than 2 electrons per l, with antiparallel spins: ↑↓.

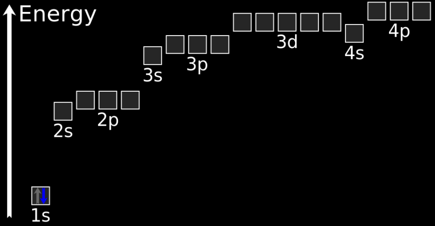

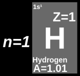

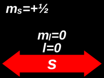

Filling the orbitals

- Other atoms → the different orbitals have the same characteristics as for H.
- The lowest energy levels are filled first.
- *Pauli exclusion principle* → no more than 2 electrons per l, with antiparallel spins: ↑↓.

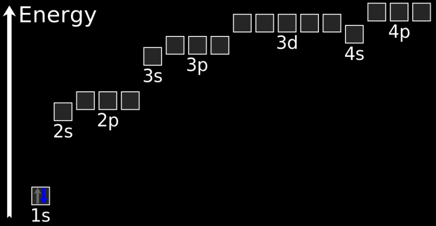

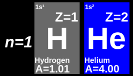

Noble gas

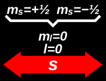

Filling the orbitals

- Other atoms → the different orbitals have the same characteristics as for H.
- The lowest energy levels are filled first.
- *Pauli exclusion principle* → no more than 2 electrons per *l*, with antiparallel spins: ↑↓.

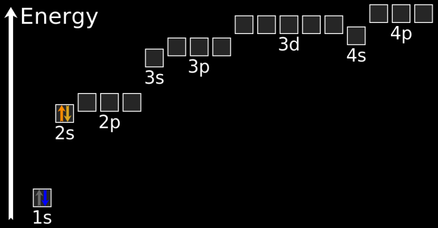

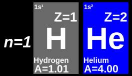

Noble gas

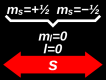

Filling the orbitals

- Other atoms → the different orbitals have the same characteristics as for H.
- The lowest energy levels are filled first.
- *Pauli exclusion principle* → no more than 2 electrons per l, with antiparallel spins: ↑↓.

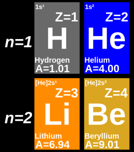

Noble gas
Alkali metal
Alkaline earth metal

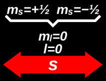

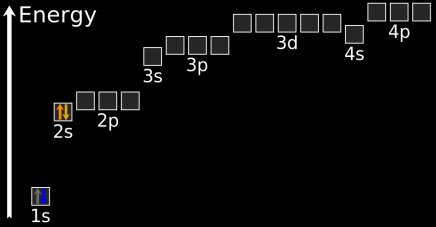

Filling the orbitals

- Other atoms → the different orbitals have the same characteristics as for H.
- The lowest energy levels are filled first.
- *Pauli exclusion principle* → no more than 2 electrons per l, with antiparallel spins: ↑↓.

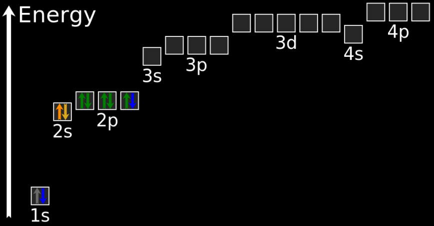

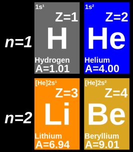

Noble gas
Alkali metal
Alkaline earth metal

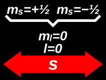

Filling the orbitals

- Other atoms → the different orbitals have the same characteristics as for H.
- The lowest energy levels are filled first.
- *Pauli exclusion principle* → no more than 2 electrons per l, with antiparallel spins: ↑↓.

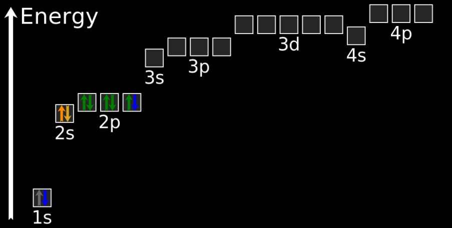

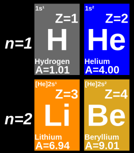

Noble gas
Alkali metal
Alkaline earth metal
Non metal

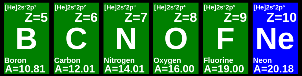

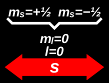

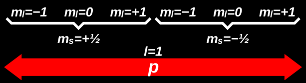

Filling the orbitals

- Other atoms → the different orbitals have the same characteristics as for H.
- The lowest energy levels are filled first.
- *Pauli exclusion principle* → no more than 2 electrons per l, with antiparallel spins: ↑↓.

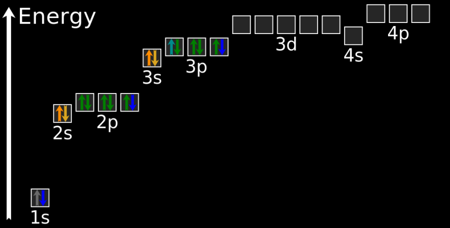

Noble gas
Alkali metal
Alkaline earth metal
Non metal

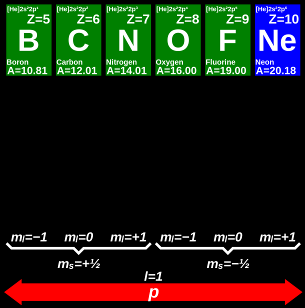

Filling the orbitals

- Other atoms → the different orbitals have the same characteristics as for H.
- The lowest energy levels are filled first.
- *Pauli exclusion principle* → no more than 2 electrons per l, with antiparallel spins: ↑↓.

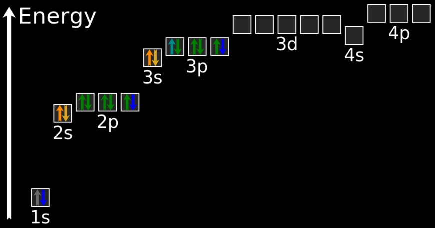

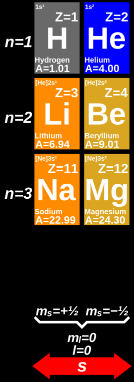

Noble gas

Alkali metal

Alkaline earth metal

Non metal

Poor metal

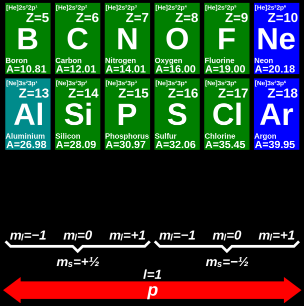

Filling the orbitals

- Other atoms → the different orbitals have the same characteristics as for H.
- The lowest energy levels are filled first.
- *Pauli exclusion principle* → no more than 2 electrons per l, with antiparallel spins: ↑↓.

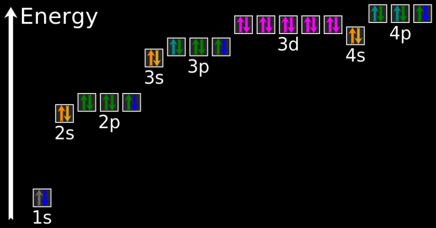

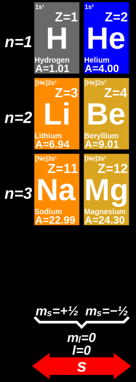

Noble gas
Alkali metal
Alkaline earth metal
Non metal
Poor metal

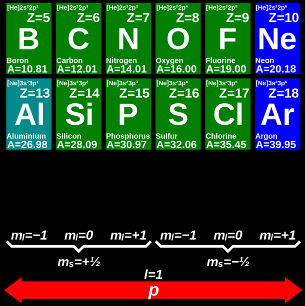

Filling the orbitals

- Other atoms → the different orbitals have the same characteristics as for H.
- The lowest energy levels are filled first.
- *Pauli exclusion principle* → no more than 2 electrons per *l*, with antiparallel spins: ↑↓.

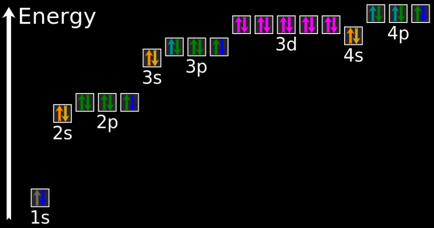

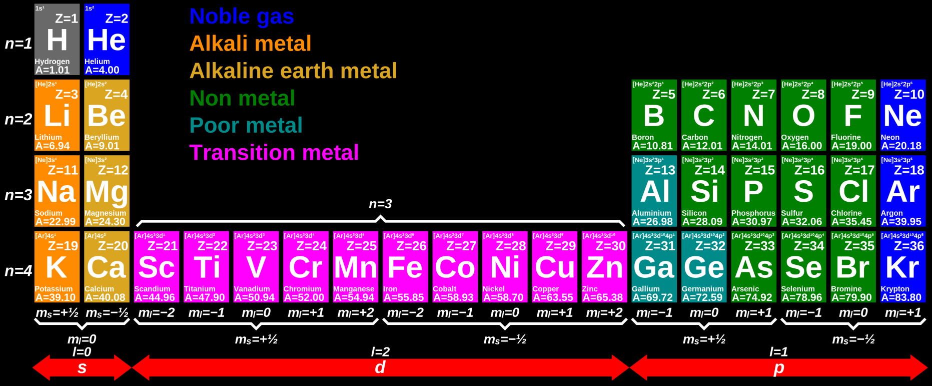

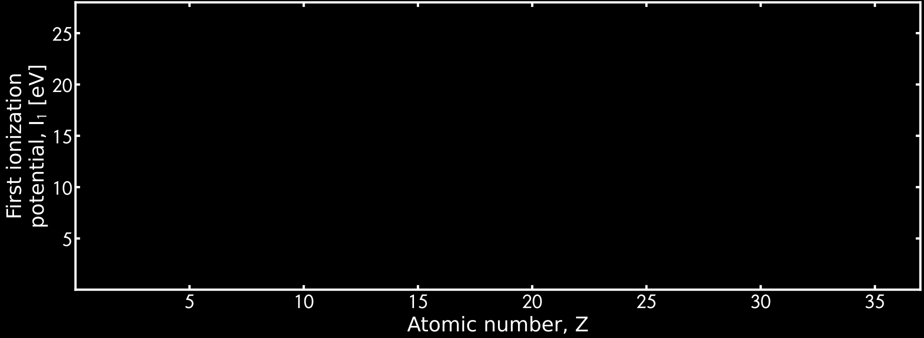
25
20
15
10
5
First ionization potential, I_1 [eV]
5
10
15
20
25
30
35
Atomic number, Z

Atoms | First Ionization Potentials & Electron Affinity

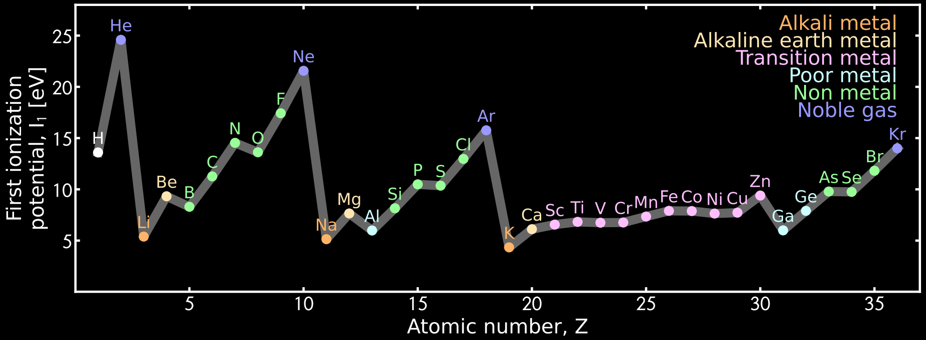

Atoms | First Ionization Potentials & Electron Affinity

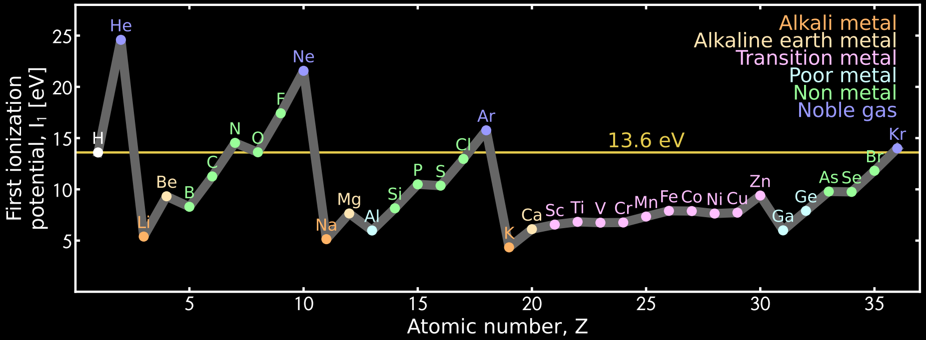

Atoms | First Ionization Potentials & Electron Affinity

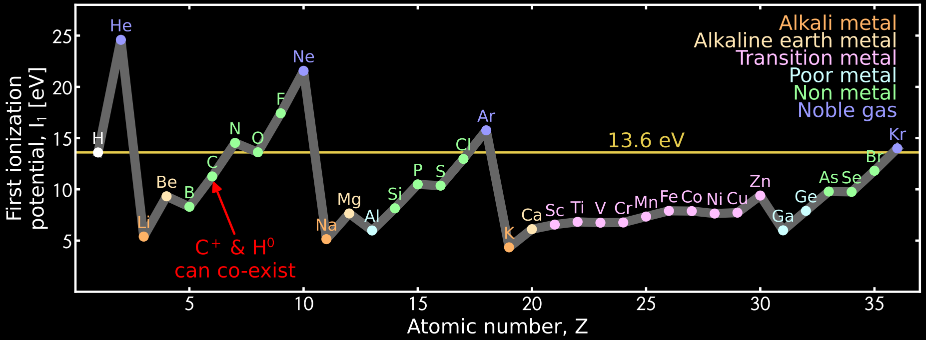

Atoms | First Ionization Potentials & Electron Affinity

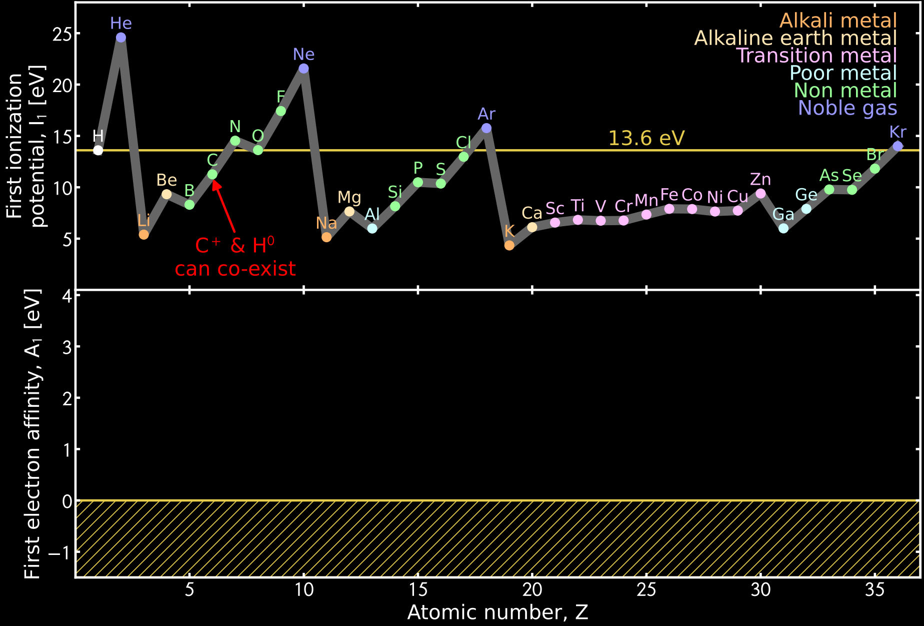

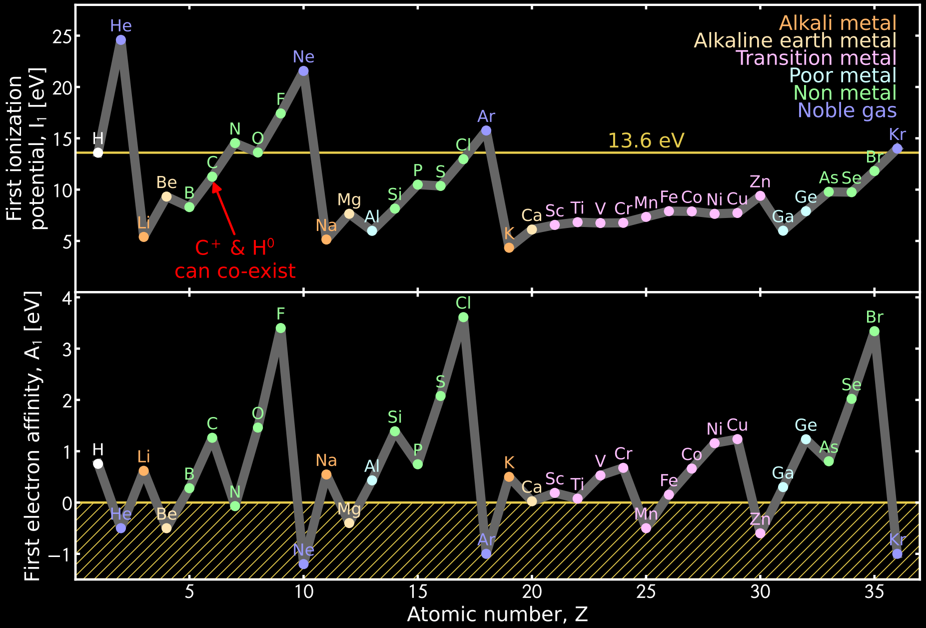
Alkali metal
Alkaline earth metal
Transition metal
Poor metal
Non metal
Noble gas
First ionization potential, I_1 [eV]
13.6 eV
C^+ & H^0 can co-exist
H
He
Li
Be
B
C
N
O
F
Ne
Na
Mg
Al
Si
P
S
Cl
Ar
K
Ca
Sc
Ti
V
Cr
Mn
Fe
Co
Ni
Cu
Zn
Ga
Ge
As
Se
Br
Kr
First electron affinity, A_1 [eV]
Atomic number, Z

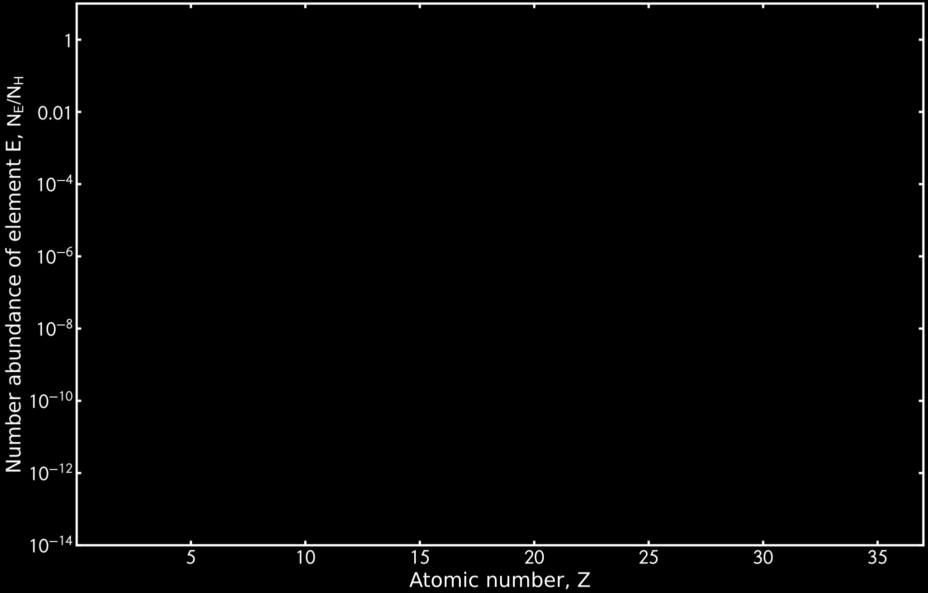

(Data from Asplund et al. 2009)

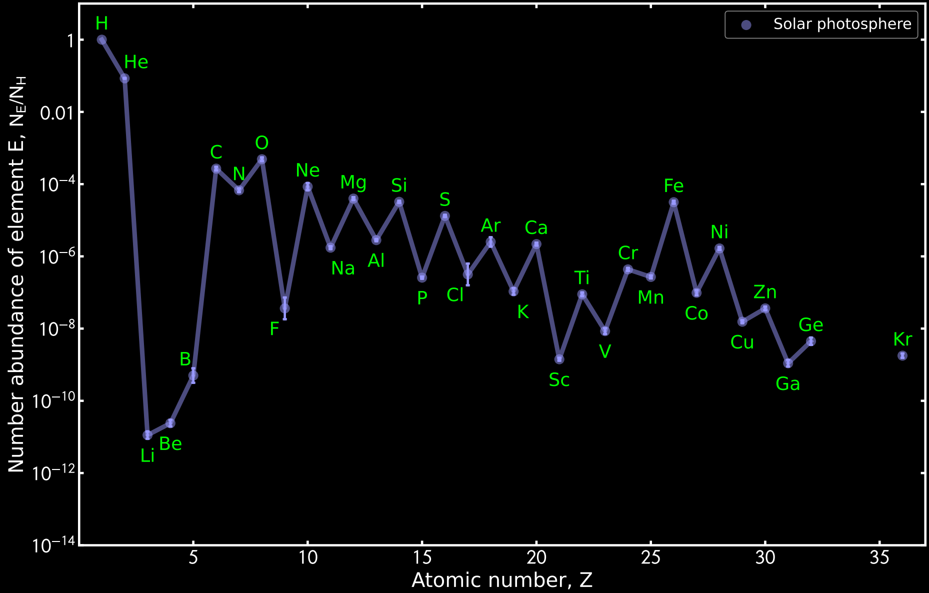

(Data from Asplund et al. 2009)

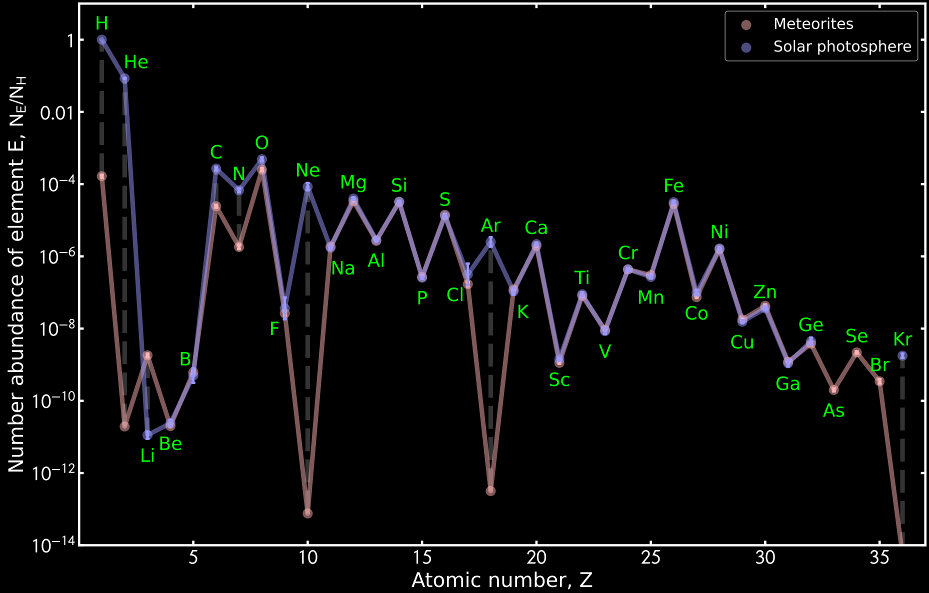

(Data from Asplund et al. 2009)

Atoms | Solar Elemental Abundances

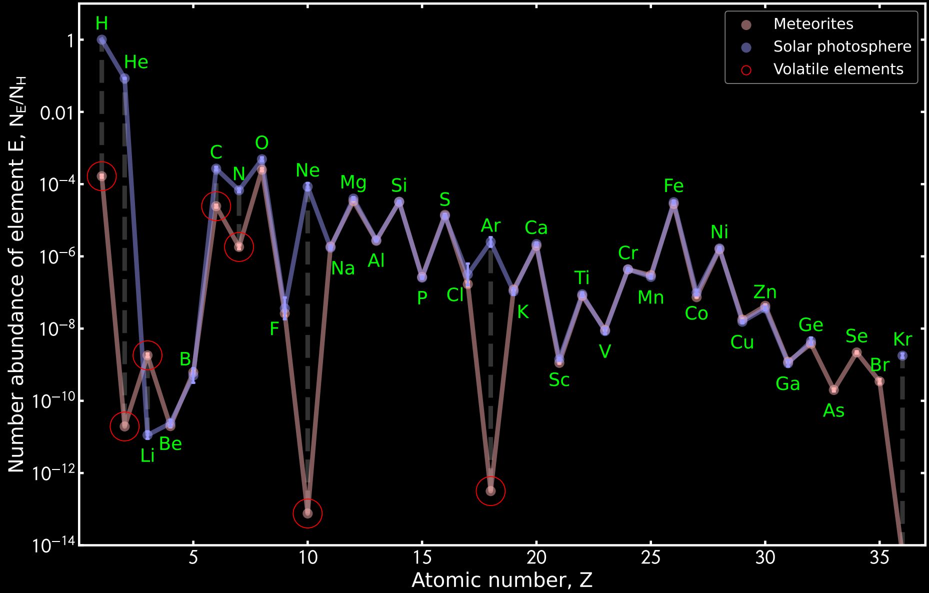

(Data from Asplund et al. 2009)

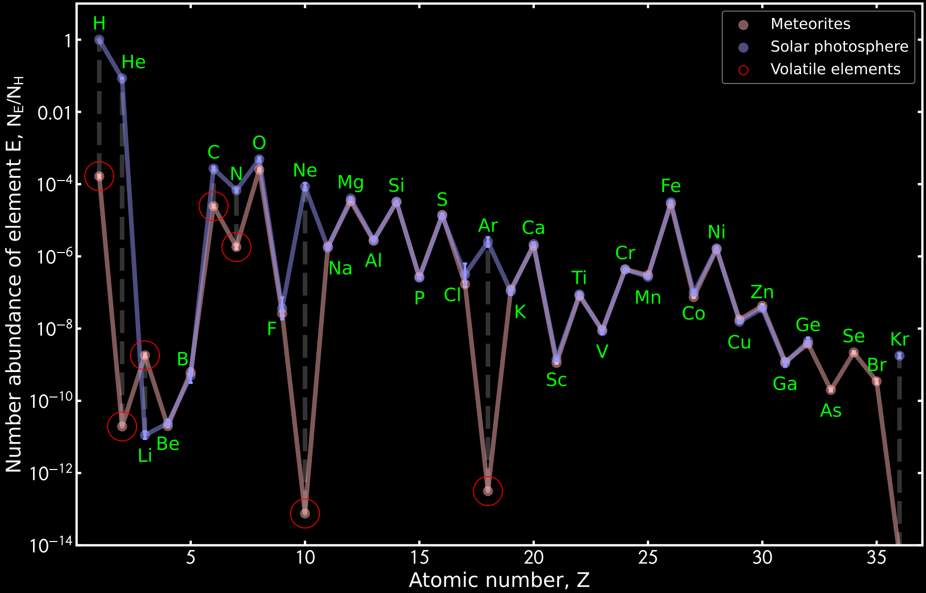

☉ ⇒ good approximation for the Galactic ISM. (Data from Asplund et al. 2009)

Selection rules		
Spontaneous emission rates (Einstein coefficients)		

Credit: adapted from Dopita & Sutherland (2003, Chap. 2) and Tielens (2005, Chap. 2).

Resonance lines *Electric dipole*		
Selection rules		
$\Delta J = 0, \pm 1$ $(0 \not\leftrightarrow 0)$ $\Delta l = \pm 1$ (parity change) Δn arbitrary $\Delta L = 0, \pm 1$ $(0 \not\leftrightarrow 0)$ $\Delta S = 0$		
Spontaneous emission rates (Einstein coefficients)		

Credit: adapted from Dopita & Sutherland (2003, Chap. 2) and Tielens (2005, Chap. 2).

Resonance lines *Electric dipole*		
Selection rules		
$\Delta J = 0, \pm 1$ $(0 \not\leftrightarrow 0)$ $\Delta l = \pm 1$ (parity change) Δn arbitrary $\Delta L = 0, \pm 1$ $(0 \not\leftrightarrow 0)$ $\Delta S = 0$		
Spontaneous emission rates (Einstein coefficients)		
$A_{\rm res} \simeq 10^5 - 10^9\ {\rm s}^{-1}$		

Credit: adapted from Dopita & Sutherland (2003, Chap. 2) and Tielens (2005, Chap. 2).

Resonance lines *Electric dipole*	Intercombination lines *Electric quadrupole*	
Selection rules		
$\Delta J = 0, \pm 1$ $(0 \not\leftrightarrow 0)$	$\Delta J = 0, \pm 1, \pm 2$ $(0 \not\leftrightarrow 0,$ $1/2 \not\leftrightarrow 1/2,\ 0 \not\leftrightarrow 1)$	
$\Delta l = \pm 1$ (parity change)	$\Delta l = 0, \pm 2$ (no parity change)	
Δn arbitrary	Δn arbitrary	
$\Delta L = 0, \pm 1$ $(0 \not\leftrightarrow 0)$	$\Delta L = 0, \pm 1, \pm 2$ $(0 \not\leftrightarrow 0,\ 0 \not\leftrightarrow 1)$	
$\Delta S = 0$	$\Delta S = 0$	
Spontaneous emission rates (Einstein coefficients)		
$A_{\rm res} \simeq 10^5 - 10^9\ {\rm s}^{-1}$		

Credit: adapted from Dopita & Sutherland (2003, Chap. 2) and Tielens (2005, Chap. 2).

Atoms | Selection Rules & Forbidden Lines

Resonance lines *Electric dipole*	**Intercombination lines** *Electric quadrupole*	
	Selection rules	
$\Delta J = 0, \pm 1$ $(0 \not\leftrightarrow 0)$	$\Delta J = 0, \pm 1, \pm 2$ $(0 \not\leftrightarrow 0,$ $1/2 \not\leftrightarrow 1/2,\ 0 \not\leftrightarrow 1)$	
$\Delta l = \pm 1$ (parity change)	$\Delta l = 0, \pm 2$ (no parity change)	
Δn arbitrary	Δn arbitrary	
$\Delta L = 0, \pm 1$ $(0 \not\leftrightarrow 0)$	$\Delta L = 0, \pm 1, \pm 2$ $(0 \not\leftrightarrow 0,\ 0 \not\leftrightarrow 1)$	
$\Delta S = 0$	$\Delta S = 0$	
	Spontaneous emission rates (Einstein coefficients)	
$A_{\rm res} \simeq 10^5 - 10^9\ {\rm s}^{-1}$	$A_{\rm int} \simeq \alpha^2 A_{\rm res} \simeq 10^1 - 10^5\ {\rm s}^{-1}$	

Credit: adapted from Dopita & Sutherland (2003, Chap. 2) and Tielens (2005, Chap. 2).

Resonance lines *Electric dipole*	Intercombination lines *Electric quadrupole*	
Selection rules		
$\Delta J = 0, \pm 1$ $(0 \not\leftrightarrow 0)$	$\Delta J = 0, \pm 1, \pm 2$ $(0 \not\leftrightarrow 0,$ $1/2 \not\leftrightarrow 1/2,\ 0 \not\leftrightarrow 1)$	
$\Delta l = \pm 1$ (parity change)	$\Delta l = 0, \pm 2$ (no parity change)	
Δn arbitrary	Δn arbitrary	
$\Delta L = 0, \pm 1$ $(0 \not\leftrightarrow 0)$	$\Delta L = 0, \pm 1, \pm 2$ $(0 \not\leftrightarrow 0,\ 0 \not\leftrightarrow 1)$	
$\Delta S = 0$	$\Delta S = 0$	
Spontaneous emission rates (Einstein coefficients)		
$A_{\rm res} \simeq 10^5 - 10^9\ {\rm s}^{-1}$	$A_{\rm int} \simeq \alpha^2 A_{\rm res} \simeq 10^1 - 10^5\ {\rm s}^{-1}$	

Credit: adapted from Dopita & Sutherland (2003, Chap. 2) and Tielens (2005, Chap. 2).

Fine-structure constant: $\alpha \equiv \dfrac{e^2}{4\pi\epsilon_0\hbar c} \simeq \dfrac{1}{137}$ (dimensionless).

Atoms | Selection Rules & Forbidden Lines

Resonance lines *Electric dipole*	**Intercombination lines** *Electric quadrupole*	**Forbidden lines** *Magnetic dipole*
Selection rules		
$\Delta J = 0, \pm 1$ ($0 \not\leftrightarrow 0$)	$\Delta J = 0, \pm 1, \pm 2$ ($0 \not\leftrightarrow 0$, $1/2 \not\leftrightarrow 1/2$, $0 \not\leftrightarrow 1$)	$\Delta J = 0, \pm 1$ ($0 \not\leftrightarrow 0$)
$\Delta l = \pm 1$ (parity change)	$\Delta l = 0, \pm 2$ (no parity change)	$\Delta l = 0$
Δn arbitrary	Δn arbitrary	$\Delta n = 0$
$\Delta L = 0, \pm 1$ ($0 \not\leftrightarrow 0$)	$\Delta L = 0, \pm 1, \pm 2$ ($0 \not\leftrightarrow 0$, $0 \not\leftrightarrow 1$)	$\Delta L = 0$
$\Delta S = 0$	$\Delta S = 0$	$\Delta S = 0$
Spontaneous emission rates (Einstein coefficients)		
$A_{\rm res} \simeq 10^5 - 10^9\ {\rm s}^{-1}$	$A_{\rm int} \simeq \alpha^2 A_{\rm res} \simeq 10^1 - 10^5\ {\rm s}^{-1}$	

Credit: adapted from Dopita & Sutherland (2003, Chap. 2) and Tielens (2005, Chap. 2).

Fine-structure constant: $\alpha \equiv \frac{e^2}{4\pi\epsilon_0\hbar c} \simeq \frac{1}{137}$ (dimensionless).

Resonance lines *Electric dipole*	**Intercombination lines** *Electric quadrupole*	**Forbidden lines** *Magnetic dipole*
Selection rules		
$\Delta J = 0, \pm 1$ ($0 \not\leftrightarrow 0$)	$\Delta J = 0, \pm 1, \pm 2$ ($0 \not\leftrightarrow 0$, $1/2 \not\leftrightarrow 1/2$, $0 \not\leftrightarrow 1$)	$\Delta J = 0, \pm 1$ ($0 \not\leftrightarrow 0$)
$\Delta l = \pm 1$ (parity change)	$\Delta l = 0, \pm 2$ (no parity change)	$\Delta l = 0$
Δn arbitrary	Δn arbitrary	$\Delta n = 0$
$\Delta L = 0, \pm 1$ ($0 \not\leftrightarrow 0$)	$\Delta L = 0, \pm 1, \pm 2$ ($0 \not\leftrightarrow 0$, $0 \not\leftrightarrow 1$)	$\Delta L = 0$
$\Delta S = 0$	$\Delta S = 0$	$\Delta S = 0$
Spontaneous emission rates (Einstein coefficients)		
$A_{\rm res} \simeq 10^5 - 10^9\ {\rm s}^{-1}$	$A_{\rm int} \simeq \alpha^2 A_{\rm res} \simeq 10^1 - 10^5\ {\rm s}^{-1}$	$A_{\rm for} \simeq \alpha^4 A_{\rm res} \simeq 10^{-4} - 1\ {\rm s}^{-1}$

Credit: adapted from Dopita & Sutherland (2003, Chap. 2) and Tielens (2005, Chap. 2).

Fine-structure constant: $\alpha \equiv \dfrac{e^2}{4\pi\epsilon_0\hbar c} \simeq \dfrac{1}{137}$ (dimensionless).

Resonance lines *Electric dipole*	**Intercombination lines** *Electric quadrupole*	**Forbidden lines** *Magnetic dipole*
Selection rules		
$\Delta J = 0, \pm 1$ ($0 \not\leftrightarrow 0$)	$\Delta J = 0, \pm 1, \pm 2$ ($0 \not\leftrightarrow 0$, $1/2 \not\leftrightarrow 1/2$, $0 \not\leftrightarrow 1$)	$\Delta J = 0, \pm 1$ ($0 \not\leftrightarrow 0$)
$\Delta l = \pm 1$ (parity change)	$\Delta l = 0, \pm 2$ (no parity change)	$\Delta l = 0$
Δn arbitrary	Δn arbitrary	$\Delta n = 0$
$\Delta L = 0, \pm 1$ ($0 \not\leftrightarrow 0$)	$\Delta L = 0, \pm 1, \pm 2$ ($0 \not\leftrightarrow 0$, $0 \not\leftrightarrow 1$)	$\Delta L = 0$
$\Delta S = 0$	$\Delta S = 0$	$\Delta S = 0$
Spontaneous emission rates (Einstein coefficients)		
$A_{res} \simeq 10^5 - 10^9\ s^{-1}$	$A_{int} \simeq \alpha^2 A_{res} \simeq 10^1 - 10^5\ s^{-1}$	$A_{for} \simeq \alpha^4 A_{res} \simeq 10^{-4} - 1\ s^{-1}$

Credit: adapted from Dopita & Sutherland (2003, Chap. 2) and Tielens (2005, Chap. 2).

Fine-structure constant: $\alpha \equiv \frac{e^2}{4\pi\epsilon_0 \hbar c} \simeq \frac{1}{137}$ (dimensionless).

Spectroscopic notation

Resonance lines *Electric dipole*	Intercombination lines *Electric quadrupole*	Forbidden lines *Magnetic dipole*
Selection rules		
$\Delta J = 0, \pm 1$ ($0 \not\leftrightarrow 0$)	$\Delta J = 0, \pm 1, \pm 2$ ($0 \not\leftrightarrow 0$, $1/2 \not\leftrightarrow 1/2$, $0 \not\leftrightarrow 1$)	$\Delta J = 0, \pm 1$ ($0 \not\leftrightarrow 0$)
$\Delta l = \pm 1$ (parity change)	$\Delta l = 0, \pm 2$ (no parity change)	$\Delta l = 0$
Δn arbitrary	Δn arbitrary	$\Delta n = 0$
$\Delta L = 0, \pm 1$ ($0 \not\leftrightarrow 0$)	$\Delta L = 0, \pm 1, \pm 2$ ($0 \not\leftrightarrow 0$, $0 \not\leftrightarrow 1$)	$\Delta L = 0$
$\Delta S = 0$	$\Delta S = 0$	$\Delta S = 0$
Spontaneous emission rates (Einstein coefficients)		
$A_{\rm res} \simeq 10^5 - 10^9\ {\rm s}^{-1}$	$A_{\rm int} \simeq \alpha^2 A_{\rm res} \simeq 10^1 - 10^5\ {\rm s}^{-1}$	$A_{\rm for} \simeq \alpha^4 A_{\rm res} \simeq 10^{-4} - 1\ {\rm s}^{-1}$

Credit: adapted from Dopita & Sutherland (2003, Chap. 2) and Tielens (2005, Chap. 2).

Fine-structure constant: $\alpha \equiv \dfrac{e^2}{4\pi\epsilon_0\hbar c} \simeq \dfrac{1}{137}$ (dimensionless).

Spectroscopic notation

1. Charge of species noted in roman numeral: C I $\Leftrightarrow$ C^0, C II $\Leftrightarrow$ C^+, C III $\Leftrightarrow$ C^{2+}, *etc.*

Resonance lines *Electric dipole*	**Intercombination lines** *Electric quadrupole*	**Forbidden lines** *Magnetic dipole*
Selection rules		
$\Delta J = 0, \pm 1$ $(0 \not\leftrightarrow 0)$	$\Delta J = 0, \pm 1, \pm 2$ $(0 \not\leftrightarrow 0,$ $1/2 \not\leftrightarrow 1/2,\ 0 \not\leftrightarrow 1)$	$\Delta J = 0, \pm 1$ $(0 \not\leftrightarrow 0)$
$\Delta l = \pm 1$ (parity change)	$\Delta l = 0, \pm 2$ (no parity change)	$\Delta l = 0$
Δn arbitrary	Δn arbitrary	$\Delta n = 0$
$\Delta L = 0, \pm 1$ $(0 \not\leftrightarrow 0)$	$\Delta L = 0, \pm 1, \pm 2$ $(0 \not\leftrightarrow 0,\ 0 \not\leftrightarrow 1)$	$\Delta L = 0$
$\Delta S = 0$	$\Delta S = 0$	$\Delta S = 0$
Spontaneous emission rates (Einstein coefficients)		
$A_{\rm res} \simeq 10^5 - 10^9\ {\rm s}^{-1}$	$A_{\rm int} \simeq \alpha^2 A_{\rm res} \simeq 10^1 - 10^5\ {\rm s}^{-1}$	$A_{\rm for} \simeq \alpha^4 A_{\rm res} \simeq 10^{-4} - 1\ {\rm s}^{-1}$

Credit: adapted from Dopita & Sutherland (2003, Chap. 2) and Tielens (2005, Chap. 2).

Fine-structure constant: $\alpha \equiv \frac{e^2}{4\pi\epsilon_0\hbar c} \simeq \frac{1}{137}$ (dimensionless).

Spectroscopic notation

1. Charge of species noted in roman numeral: C I $\Leftrightarrow$ C^0, C II $\Leftrightarrow$ C^+, C III $\Leftrightarrow$ C^{2+}, *etc.*
2. Forbidden lines between square brackets: *e.g.* $[\text{C II}]_{158\mu\text{m}}$ (forbidden), but $\text{C II}_{1335\text{Å}}$ (allowed).

Collisional

Excitation

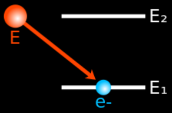

Excitation

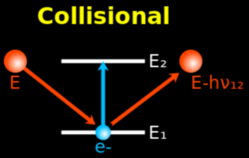

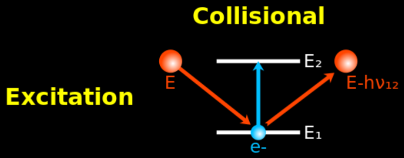

Transition energy

$h\nu_{21} \equiv E_2 - E_1.$

Collisional

Excitation

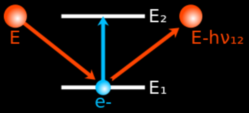

Transition energy

$h\nu_{21} \equiv E_2 - E_1.$

Statistical equilibrium

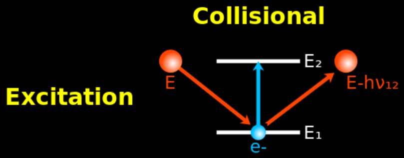

Transition energy

$h\nu_{21} \equiv E_2 - E_1$.

Statistical equilibrium

$$\underbrace{n_1\, n_{\rm coll}\, \overbrace{\gamma_{12}(T|{\rm coll})}^{[{\rm cm^3/s}]}}_{\text{collisional excitation}} \qquad [{\rm cm^{-3}s^{-1}}]$$

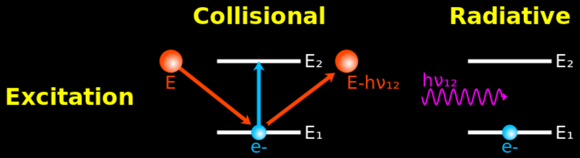

Transition energy

$h\nu_{21} \equiv E_2 - E_1.$

Statistical equilibrium

$$\underbrace{n_1\, n_{\rm coll}\, \overbrace{\gamma_{12}(T|{\rm coll})}^{[{\rm cm^3/s}]}}_{\text{collisional excitation}} \qquad [{\rm cm^{-3}s^{-1}}]$$

Collisional **Radiative**

Excitation

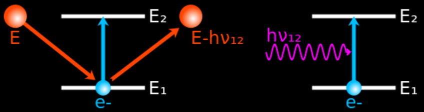

Transition energy

$h\nu_{21} \equiv E_2 - E_1 .$

Statistical equilibrium

$$\underbrace{n_1\, n_{\rm coll}\, \overbrace{\gamma_{12}(T|\mathrm{coll})}^{[\mathrm{cm^3/s}]}}_{\text{collisional excitation}} \qquad [\mathrm{cm^{-3}s^{-1}}]$$

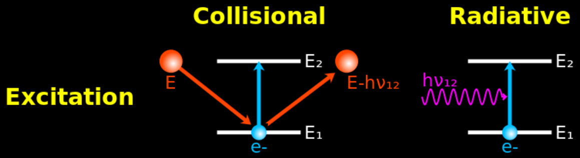

Transition energy

$h\nu_{21} \equiv E_2 - E_1.$

Statistical equilibrium

$$\underbrace{n_1\, n_{\rm coll}\, \overbrace{\gamma_{12}(T|{\rm coll})}^{[{\rm cm}^3/{\rm s}]}}_{\text{collisional excitation}} + \underbrace{n_1\, J_{21}\, \overbrace{B_{12}}^{[{\rm m}^2{\rm sr/J}]}}_{\text{radiative excitation}} \qquad [{\rm cm}^{-3}{\rm s}^{-1}]$$

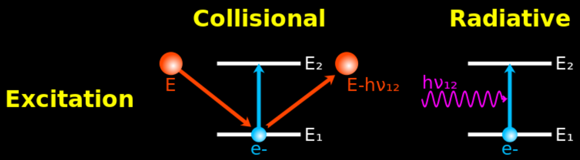

Transition energy

$h\nu_{21} \equiv E_2 - E_1.$

$$J_{21} \equiv \int_0^\infty \underbrace{J_\nu(\nu)}_{\text{mean intensity}} \times \underbrace{\phi_{21}(\nu)}_{\text{line profile}} \, d\nu \; [\mathrm{W/m^2/sr}].$$

Statistical equilibrium

$$\underbrace{n_1 n_{\text{coll}} \overbrace{\gamma_{12}(T|\text{coll})}^{[\mathrm{cm^3/s}]}}_{\text{collisional excitation}} + \underbrace{n_1 J_{21} \overbrace{B_{12}}^{[\mathrm{m^2 sr/J}]}}_{\text{radiative excitation}} \qquad [\mathrm{cm^{-3}s^{-1}}]$$

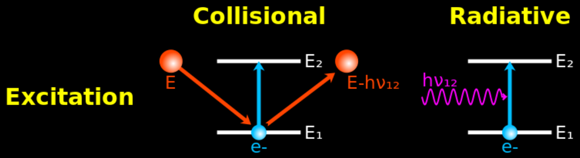

Transition energy

$h\nu_{21} \equiv E_2 - E_1.$

$$J_{21} \equiv \int_0^\infty \underbrace{J_\nu(\nu)}_{\text{mean intensity}} \times \underbrace{\phi_{21}(\nu)}_{\text{line profile}} \, d\nu \;\; [\text{W/m}^2/\text{sr}].$$

Einstein coefficients

$g_1 B_{12} = g_2 B_{21}.$

$$A_{21} = \frac{2h\nu_{21}^3}{c^2} B_{21}.$$

From *detailed balance* (Rybicky & Lightman, 1979). Level degeneracies: g_1 & g_2.

Statistical equilibrium

$$\underbrace{n_1 n_{\text{coll}} \overbrace{\gamma_{12}(T|\text{coll})}^{[\text{cm}^3/\text{s}]}}_{\text{collisional excitation}} + \underbrace{n_1 J_{21} \overbrace{B_{12}}^{[\text{m}^2\text{sr/J}]}}_{\text{radiative excitation}} \qquad [\text{cm}^{-3}\text{s}^{-1}]$$

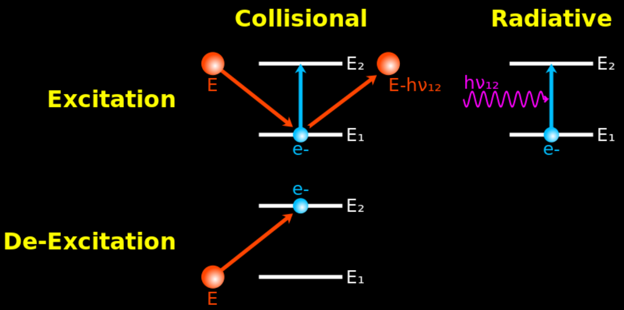

Transition energy

$h\nu_{21} \equiv E_2 - E_1.$

$$J_{21} \equiv \int_0^\infty \underbrace{J_\nu(\nu)}_{\text{mean intensity}} \times \underbrace{\phi_{21}(\nu)}_{\text{line profile}} \, d\nu \; [\mathrm{W/m^2/sr}].$$

Einstein coefficients

$g_1 B_{12} = g_2 B_{21}.$

$$A_{21} = \frac{2h\nu_{21}^3}{c^2} B_{21}.$$

From *detailed balance* (Rybicky & Lightman, 1979). Level degeneracies: g_1 & g_2.

Statistical equilibrium

$$\underbrace{n_1 n_{\text{coll}} \overbrace{\gamma_{12}(T|\text{coll})}^{[\mathrm{cm^3/s}]}}_{\text{collisional excitation}} + \underbrace{n_1 J_{21} \overbrace{B_{12}}^{[\mathrm{m^2 sr/J}]}}_{\text{radiative excitation}} \qquad [\mathrm{cm^{-3}s^{-1}}]$$

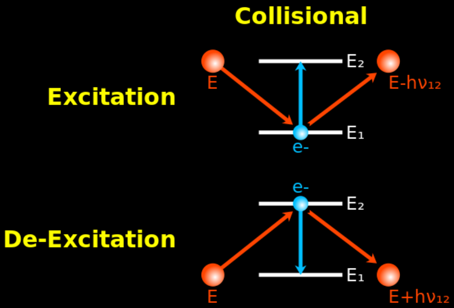

Transition energy

$h\nu_{21} \equiv E_2 - E_1$.

$$J_{21} \equiv \int_0^\infty \underbrace{J_\nu(\nu)}_{\text{mean intensity}} \times \underbrace{\phi_{21}(\nu)}_{\text{line profile}} \, d\nu \; [\text{W/m}^2/\text{sr}].$$

Einstein coefficients

$g_1 B_{12} = g_2 B_{21}$.

$$A_{21} = \frac{2h\nu_{21}^3}{c^2} B_{21}.$$

From *detailed balance* (Rybicky & Lightman, 1979). Level degeneracies: g_1 & g_2.

Statistical equilibrium

$$\underbrace{n_1 n_{\text{coll}} \overbrace{\gamma_{12}(T|\text{coll})}^{[\text{cm}^3/\text{s}]}}_{\text{collisional excitation}} + \underbrace{n_1 J_{21} \overbrace{B_{12}}^{[\text{m}^2\text{sr/J}]}}_{\text{radiative excitation}} \quad [\text{cm}^{-3}\text{s}^{-1}]$$

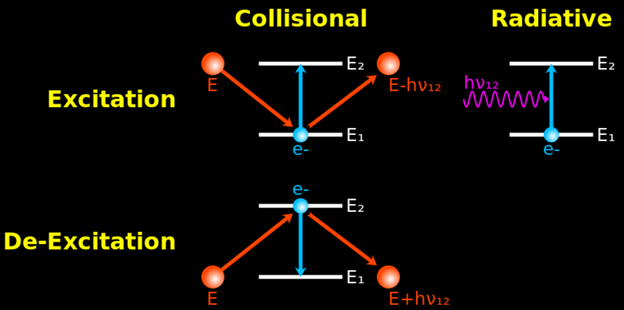

Transition energy

$$h\nu_{21} \equiv E_2 - E_1.$$

$$J_{21} \equiv \int_0^\infty \underbrace{J_\nu(\nu)}_{\text{mean intensity}} \times \underbrace{\phi_{21}(\nu)}_{\text{line profile}} \, d\nu \; [\text{W/m}^2/\text{sr}].$$

Einstein coefficients

$$g_1 B_{12} = g_2 B_{21}.$$

$$A_{21} = \frac{2h\nu_{21}^3}{c^2} B_{21}.$$

From *detailed balance* (Rybicky & Lightman, 1979). Level degeneracies: g_1 & g_2.

Statistical equilibrium

$$\underbrace{n_1 n_{\text{coll}} \overbrace{\gamma_{12}(T|\text{coll})}^{[\text{cm}^3/\text{s}]}}_{\text{collisional excitation}} + \underbrace{n_1 J_{21} \overbrace{B_{12}}^{[\text{m}^2\text{sr/J}]}}_{\text{radiative excitation}} = \underbrace{n_2 n_{\text{coll}} \overbrace{\gamma_{21}(T|\text{coll})}^{[\text{cm}^3/\text{s}]}}_{\text{collisional de-excitation}} \quad [\text{cm}^{-3}\text{s}^{-1}]$$

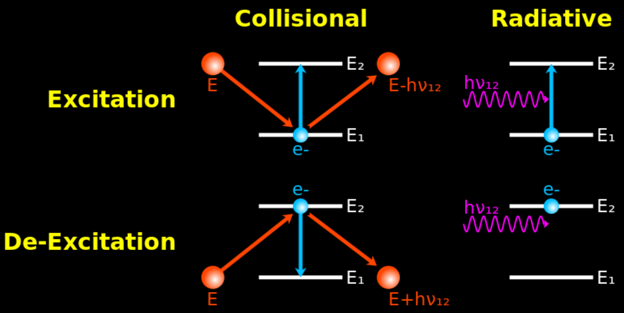

Transition energy

$$h\nu_{21} \equiv E_2 - E_1.$$

$$J_{21} \equiv \int_0^\infty \underbrace{J_\nu(\nu)}_{\text{mean intensity}} \times \underbrace{\phi_{21}(\nu)}_{\text{line profile}} \, d\nu \; [\text{W/m}^2/\text{sr}].$$

Einstein coefficients

$$g_1 B_{12} = g_2 B_{21}.$$

$$A_{21} = \frac{2h\nu_{21}^3}{c^2} B_{21}.$$

From *detailed balance* (Rybicky & Lightman, 1979). Level degeneracies: g_1 & g_2.

Statistical equilibrium

$$\underbrace{n_1 n_{\text{coll}} \overbrace{\gamma_{12}(T|\text{coll})}^{[\text{cm}^3/\text{s}]}}_{\text{collisional excitation}} + \underbrace{n_1 J_{21} \overbrace{B_{12}}^{[\text{m}^2\text{sr/J}]}}_{\text{radiative excitation}} = \underbrace{n_2 n_{\text{coll}} \overbrace{\gamma_{21}(T|\text{coll})}^{[\text{cm}^3/\text{s}]}}_{\text{collisional de-excitation}} \quad [\text{cm}^{-3}\text{s}^{-1}]$$

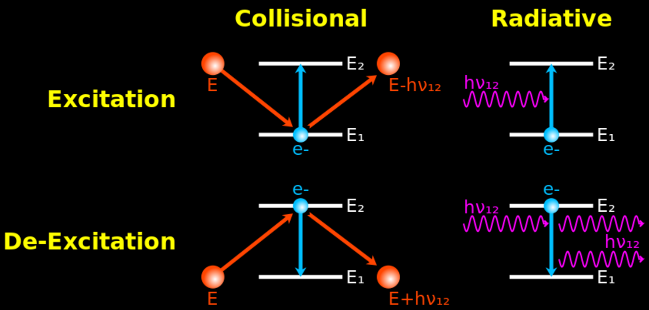

Transition energy

$h\nu_{21} \equiv E_2 - E_1$.

$$J_{21} \equiv \int_0^\infty \underbrace{J_\nu(\nu)}_{\text{mean intensity}} \times \underbrace{\phi_{21}(\nu)}_{\text{line profile}} \, d\nu \; [\text{W/m}^2/\text{sr}].$$

Einstein coefficients

$g_1 B_{12} = g_2 B_{21}$.

$A_{21} = \dfrac{2h\nu_{21}^3}{c^2} B_{21}$.

From *detailed balance* (Rybicky & Lightman, 1979). Level degeneracies: g_1 & g_2.

Statistical equilibrium

$$\underbrace{n_1 n_{\text{coll}} \overbrace{\gamma_{12}(T|\text{coll})}^{[\text{cm}^3/\text{s}]}}_{\text{collisional excitation}} + \underbrace{n_1 J_{21} \overbrace{B_{12}}^{[\text{m}^2\text{sr/J}]}}_{\text{radiative excitation}} = \underbrace{n_2 n_{\text{coll}} \overbrace{\gamma_{21}(T|\text{coll})}^{[\text{cm}^3/\text{s}]}}_{\text{collisional de-excitation}} \quad [\text{cm}^{-3}\text{s}^{-1}]$$

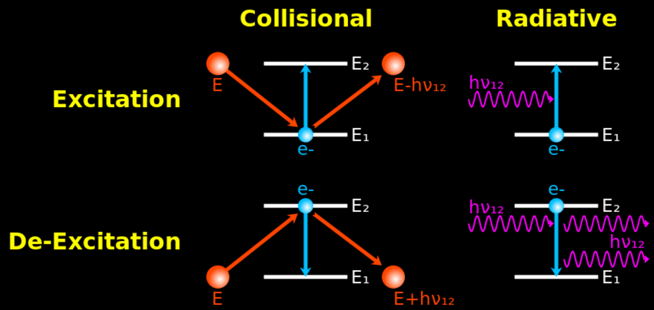

Transition energy

$h\nu_{21} \equiv E_2 - E_1.$

$$J_{21} \equiv \int_0^\infty \underbrace{J_\nu(\nu)}_{\text{mean intensity}} \times \underbrace{\phi_{21}(\nu)}_{\text{line profile}} \, d\nu \ [\mathrm{W/m^2/sr}].$$

Einstein coefficients

$g_1 B_{12} = g_2 B_{21}.$

$A_{21} = \frac{2h\nu_{21}^3}{c^2} B_{21}.$

From *detailed balance* (Rybicky & Lightman, 1979). Level degeneracies: g_1 & g_2.

Statistical equilibrium

$$\underbrace{n_1 n_{\rm coll} \overbrace{\gamma_{12}(T|\mathrm{coll})}^{[\mathrm{cm^3/s}]}}_{\text{collisional excitation}} + \underbrace{n_1 J_{21} \overbrace{B_{12}}^{[\mathrm{m^2 sr/J}]}}_{\text{radiative excitation}} = \underbrace{n_2 n_{\rm coll} \overbrace{\gamma_{21}(T|\mathrm{coll})}^{[\mathrm{cm^3/s}]}}_{\text{collisional de-excitation}} + \underbrace{n_2 J_{21} \overbrace{B_{21}}^{[\mathrm{m^2 sr/J}]}}_{\text{radiative de-excitation}} \quad [\mathrm{cm^{-3} s^{-1}}]$$

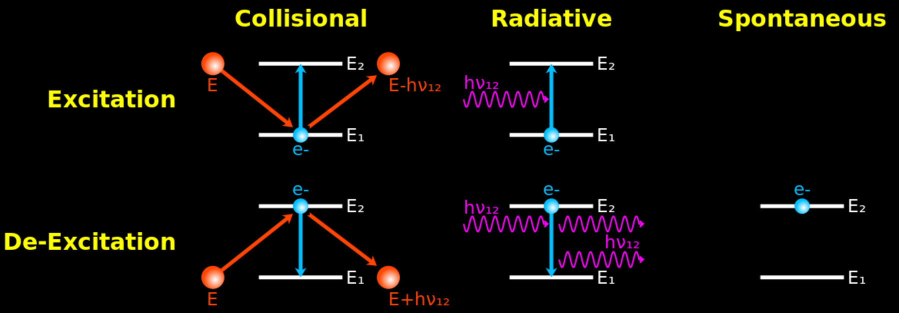

Transition energy

$$h\nu_{21} \equiv E_2 - E_1.$$

$$J_{21} \equiv \int_0^\infty \underbrace{J_\nu(\nu)}_{\text{mean intensity}} \times \underbrace{\phi_{21}(\nu)}_{\text{line profile}} \, d\nu \;\; [\text{W/m}^2/\text{sr}].$$

Einstein coefficients

$$g_1 B_{12} = g_2 B_{21}.$$

$$A_{21} = \frac{2h\nu_{21}^3}{c^2} B_{21}.$$

From *detailed balance* (Rybicky & Lightman, 1979). Level degeneracies: g_1 & g_2.

Statistical equilibrium

$$\underbrace{n_1 n_{\text{coll}} \overbrace{\gamma_{12}(T|\text{coll})}^{[\text{cm}^3/\text{s}]}}_{\text{collisional excitation}} + \underbrace{n_1 J_{21} \overbrace{B_{12}}^{[\text{m}^2\text{sr/J}]}}_{\text{radiative excitation}} = \underbrace{n_2 n_{\text{coll}} \overbrace{\gamma_{21}(T|\text{coll})}^{[\text{cm}^3/\text{s}]}}_{\text{collisional de-excitation}} + \underbrace{n_2 J_{21} \overbrace{B_{21}}^{[\text{m}^2\text{sr/J}]}}_{\text{radiative de-excitation}} \quad [\text{cm}^{-3}\text{s}^{-1}]$$

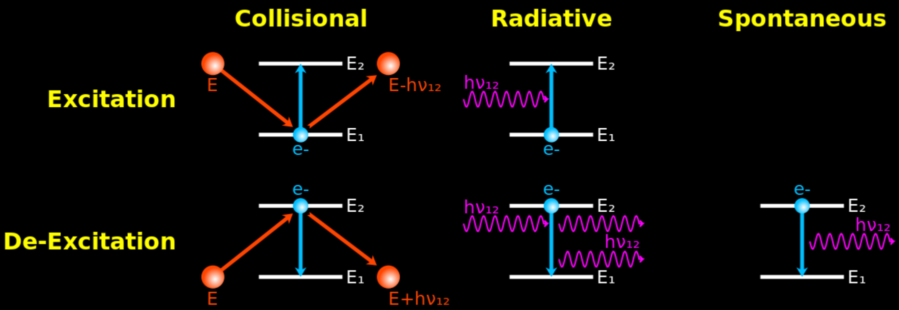

Transition energy

$h\nu_{21} \equiv E_2 - E_1$.

$$J_{21} \equiv \int_0^\infty \underbrace{J_\nu(\nu)}_{\text{mean intensity}} \times \underbrace{\phi_{21}(\nu)}_{\text{line profile}} \, d\nu \ [\text{W/m}^2/\text{sr}].$$

Einstein coefficients

$g_1 B_{12} = g_2 B_{21}$.

$A_{21} = \frac{2h\nu_{21}^3}{c^2} B_{21}$.

From *detailed balance* (Rybicky & Lightman, 1979). Level degeneracies: g_1 & g_2.

Statistical equilibrium

$$\underbrace{n_1 n_{\text{coll}} \overbrace{\gamma_{12}(T|\text{coll})}^{[\text{cm}^3/\text{s}]}}_{\text{collisional excitation}} + \underbrace{n_1 J_{21} \overbrace{B_{12}}^{[\text{m}^2\text{sr/J}]}}_{\text{radiative excitation}} = \underbrace{n_2 n_{\text{coll}} \overbrace{\gamma_{21}(T|\text{coll})}^{[\text{cm}^3/\text{s}]}}_{\text{collisional de-excitation}} + \underbrace{n_2 J_{21} \overbrace{B_{21}}^{[\text{m}^2\text{sr/J}]}}_{\text{radiative de-excitation}} \quad [\text{cm}^{-3}\text{s}^{-1}]$$

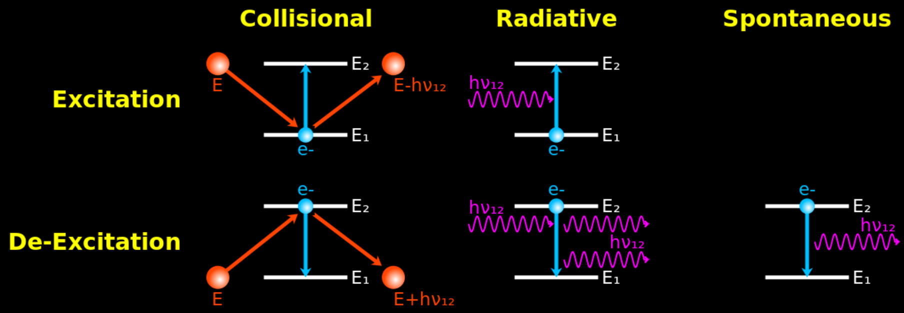

Transition energy

$h\nu_{21} \equiv E_2 - E_1.$

$$J_{21} \equiv \int_0^\infty \underbrace{J_\nu(\nu)}_{\text{mean intensity}} \times \underbrace{\phi_{21}(\nu)}_{\text{line profile}} \, d\nu \ [\text{W/m}^2/\text{sr}].$$

Einstein coefficients

$g_1 B_{12} = g_2 B_{21}.$

$$A_{21} = \frac{2h\nu_{21}^3}{c^2} B_{21}.$$

From *detailed balance* (Rybicky & Lightman, 1979). Level degeneracies: g_1 & g_2.

Statistical equilibrium

$$\underbrace{n_1 n_{coll} \overbrace{\gamma_{12}(T|\text{coll})}^{[\text{cm}^3/\text{s}]}}_{\text{collisional excitation}} + \underbrace{n_1 J_{21} \overbrace{B_{12}}^{[\text{m}^2\text{sr/J}]}}_{\text{radiative excitation}} = \underbrace{n_2 n_{coll} \overbrace{\gamma_{21}(T|\text{coll})}^{[\text{cm}^3/\text{s}]}}_{\text{collisional de-excitation}} + \underbrace{n_2 J_{21} \overbrace{B_{21}}^{[\text{m}^2\text{sr/J}]}}_{\text{radiative de-excitation}} + \underbrace{n_2 \overbrace{A_{21}}^{[\text{s}^{-1}]}}_{\text{spontaneous emission}} \quad [\text{cm}^{-3}\text{s}^{-1}]$$

Line intensity, for a two-level atom, in the optically-thin limit, with no external radiation

Line intensity, for a two-level atom, in the optically-thin limit, with no external radiation

$$\underbrace{\frac{\mathrm{d}P_{21}}{\mathrm{d}V}\ [\mathrm{W/cm^3}]}_{\text{power emitted per unit volume}}$$

Line intensity, for a two-level atom, in the optically-thin limit, with no external radiation

$$\underbrace{\frac{\mathrm{d}P_{21}}{\mathrm{d}V}\ [\mathrm{W/cm^3}]}_{\text{power emitted per unit volume}} = \underbrace{n_2\ [\mathrm{cm^{-3}}]}_{\text{number of excited atoms per unit volume}}$$

Line intensity, for a two-level atom, in the optically-thin limit, with no external radiation

$$\underbrace{\frac{\mathrm{d}P_{21}}{\mathrm{d}V}\ [\mathrm{W/cm^3}]}_{\text{power emitted per unit volume}} = \underbrace{n_2\ [\mathrm{cm^{-3}}]}_{\text{number of excited atoms per unit volume}} \times \underbrace{A_{21}\ [\mathrm{s^{-1}}]}_{\text{emission rate per atom}}$$

Line intensity, for a two-level atom, in the optically-thin limit, with no external radiation

$$\underbrace{\frac{\mathrm{d}P_{21}}{\mathrm{d}V}\;[\mathrm{W/cm^3}]}_{\text{power emitted per unit volume}} = \underbrace{n_2\;[\mathrm{cm^{-3}}]}_{\text{number of excited atoms per unit volume}} \times \underbrace{A_{21}\;[\mathrm{s^{-1}}]}_{\text{emission rate per atom}} \times \underbrace{h\nu_{21}\;[\mathrm{J}]}_{\text{single photon energy}}.$$

Line intensity, for a two-level atom, in the optically-thin limit, with no external radiation

$$\underbrace{\frac{\mathrm{d}P_{21}}{\mathrm{d}V}\ [\mathrm{W/cm^3}]}_{\text{power emitted per unit volume}} = \underbrace{n_2\ [\mathrm{cm^{-3}}]}_{\text{number of excited atoms per unit volume}} \times \underbrace{A_{21}\ [\mathrm{s^{-1}}]}_{\text{emission rate per atom}} \times \underbrace{h\nu_{21}\ [\mathrm{J}]}_{\text{single photon energy}}.$$

Detailed balance (equilibrium between a process and its reverse): $\frac{\gamma_{12}}{\gamma_{21}} = \frac{g_2}{g_1}\exp\left(-\frac{h\nu_{21}}{kT}\right)$.

Line intensity, for a two-level atom, in the optically-thin limit, with no external radiation

$$\underbrace{\frac{dP_{21}}{dV}\ [\mathrm{W/cm^3}]}_{\text{power emitted per unit volume}} = \underbrace{n_2\ [\mathrm{cm^{-3}}]}_{\text{number of excited atoms per unit volume}} \times \underbrace{A_{21}\ [\mathrm{s^{-1}}]}_{\text{emission rate per atom}} \times \underbrace{h\nu_{21}\ [\mathrm{J}]}_{\text{single photon energy}} .$$

Detailed balance (equilibrium between a process and its reverse): $\dfrac{\gamma_{12}}{\gamma_{21}} = \dfrac{g_2}{g_1}\exp\left(-\dfrac{h\nu_{21}}{kT}\right)$.

Statistical equilibrium: $n_1 n_{\mathrm{coll}}\gamma_{12} = n_2 n_{\mathrm{coll}}\gamma_{21} + n_2 A_{21}$

Line intensity, for a two-level atom, in the optically-thin limit, with no external radiation

$$\underbrace{\frac{dP_{21}}{dV}\ [\mathrm{W/cm^3}]}_{\text{power emitted per unit volume}} = \underbrace{n_2\ [\mathrm{cm^{-3}}]}_{\text{number of excited atoms per unit volume}} \times \underbrace{A_{21}\ [\mathrm{s^{-1}}]}_{\text{emission rate per atom}} \times \underbrace{h\nu_{21}\ [\mathrm{J}]}_{\text{single photon energy}}.$$

Detailed balance (equilibrium between a process and its reverse): $\frac{\gamma_{12}}{\gamma_{21}} = \frac{g_2}{g_1}\exp\left(-\frac{h\nu_{21}}{kT}\right)$.

Statistical equilibrium: $n_1 n_{\rm coll}\gamma_{12} = n_2 n_{\rm coll}\gamma_{21} + n_2 A_{21} \Rightarrow \frac{n_2}{n_1} = \frac{\gamma_{12}}{\gamma_{21}}\frac{1}{1+\frac{A_{21}}{n_{\rm coll}\gamma_{21}}}$

Line intensity, for a two-level atom, in the optically-thin limit, with no external radiation

$$\underbrace{\frac{\mathrm{d}P_{21}}{\mathrm{d}V}\ [\mathrm{W/cm^3}]}_{\text{power emitted per unit volume}} = \underbrace{n_2\ [\mathrm{cm^{-3}}]}_{\text{number of excited atoms per unit volume}} \times \underbrace{A_{21}\ [\mathrm{s^{-1}}]}_{\text{emission rate per atom}} \times \underbrace{h\nu_{21}\ [\mathrm{J}]}_{\text{single photon energy}}.$$

Detailed balance (equilibrium between a process and its reverse): $\frac{\gamma_{12}}{\gamma_{21}} = \frac{g_2}{g_1}\exp\left(-\frac{h\nu_{21}}{kT}\right)$.

Statistical equilibrium: $n_1 n_{\rm coll}\gamma_{12} = n_2 n_{\rm coll}\gamma_{21} + n_2 A_{21} \Rightarrow \frac{n_2}{n_1} = \frac{\gamma_{12}}{\gamma_{21}}\frac{1}{1+\frac{A_{21}}{n_{\rm coll}\gamma_{21}}} = \frac{g_2}{g_1}\frac{\exp\left(-\frac{h\nu_{21}}{kT}\right)}{1+\frac{A_{21}}{n_{\rm coll}\gamma_{21}}}$.

Line intensity, for a two-level atom, in the optically-thin limit, with no external radiation

$$\underbrace{\frac{dP_{21}}{dV}\ [\mathrm{W/cm^3}]}_{\text{power emitted per unit volume}} = \underbrace{n_2\ [\mathrm{cm^{-3}}]}_{\text{number of excited atoms per unit volume}} \times \underbrace{A_{21}\ [\mathrm{s^{-1}}]}_{\text{emission rate per atom}} \times \underbrace{h\nu_{21}\ [\mathrm{J}]}_{\text{single photon energy}}.$$

Detailed balance (equilibrium between a process and its reverse): $\frac{\gamma_{12}}{\gamma_{21}} = \frac{g_2}{g_1} \exp\left(-\frac{h\nu_{21}}{kT}\right)$.

Statistical equilibrium: $n_1 n_{\mathrm{coll}} \gamma_{12} = n_2 n_{\mathrm{coll}} \gamma_{21} + n_2 A_{21} \Rightarrow \frac{n_2}{n_1} = \frac{\gamma_{12}}{\gamma_{21}} \frac{1}{1 + \frac{A_{21}}{n_{\mathrm{coll}}\gamma_{21}}} = \frac{g_2}{g_1} \frac{\exp\left(-\frac{h\nu_{21}}{kT}\right)}{1 + \frac{A_{21}}{n_{\mathrm{coll}}\gamma_{21}}}$.

Low-density cooling function

Line intensity, for a two-level atom, in the optically-thin limit, with no external radiation

$$\underbrace{\frac{\mathrm{d}P_{21}}{\mathrm{d}V}\;[\mathrm{W/cm^3}]}_{\text{power emitted per unit volume}} = \underbrace{n_2\;[\mathrm{cm^{-3}}]}_{\text{number of excited atoms per unit volume}} \times \underbrace{A_{21}\;[\mathrm{s^{-1}}]}_{\text{emission rate per atom}} \times \underbrace{h\nu_{21}\;[\mathrm{J}]}_{\text{single photon energy}}.$$

Detailed balance (equilibrium between a process and its reverse): $\frac{\gamma_{12}}{\gamma_{21}} = \frac{g_2}{g_1}\exp\left(-\frac{h\nu_{21}}{kT}\right)$.

Statistical equilibrium: $n_1 n_{\mathrm{coll}}\gamma_{12} = n_2 n_{\mathrm{coll}}\gamma_{21} + n_2 A_{21} \Rightarrow \frac{n_2}{n_1} = \frac{\gamma_{12}}{\gamma_{21}}\frac{1}{1+\frac{A_{21}}{n_{\mathrm{coll}}\gamma_{21}}} = \frac{g_2}{g_1}\frac{\exp\left(-\frac{h\nu_{21}}{kT}\right)}{1+\frac{A_{21}}{n_{\mathrm{coll}}\gamma_{21}}}$.

Low-density cooling function

If $A_{21} \gg n_{\mathrm{coll}}\gamma_{21}$ & posing $n_1 = X_1 n_{\mathrm{coll}}$

Line intensity, for a two-level atom, in the optically-thin limit, with no external radiation

$$\underbrace{\frac{dP_{21}}{dV}\;[\mathrm{W/cm^3}]}_{\text{power emitted per unit volume}} = \underbrace{n_2\;[\mathrm{cm^{-3}}]}_{\text{number of excited atoms per unit volume}} \times \underbrace{A_{21}\;[\mathrm{s^{-1}}]}_{\text{emission rate per atom}} \times \underbrace{h\nu_{21}\;[\mathrm{J}]}_{\text{single photon energy}}.$$

Detailed balance (equilibrium between a process and its reverse): $\frac{\gamma_{12}}{\gamma_{21}} = \frac{g_2}{g_1}\exp\left(-\frac{h\nu_{21}}{kT}\right)$.

Statistical equilibrium: $n_1 n_{\mathrm{coll}}\gamma_{12} = n_2 n_{\mathrm{coll}}\gamma_{21} + n_2 A_{21} \Rightarrow \frac{n_2}{n_1} = \frac{\gamma_{12}}{\gamma_{21}}\frac{1}{1+\frac{A_{21}}{n_{\mathrm{coll}}\gamma_{21}}} = \frac{g_2}{g_1}\frac{\exp\left(-\frac{h\nu_{21}}{kT}\right)}{1+\frac{A_{21}}{n_{\mathrm{coll}}\gamma_{21}}}$.

Low-density cooling function

If $A_{21} \gg n_{\mathrm{coll}}\gamma_{21}$ & posing $n_1 = X_1 n_{\mathrm{coll}} \rightarrow \frac{dP_{21}}{dV} \simeq n_{\mathrm{coll}}^2 h\nu_{21} X_1 \frac{\gamma_{21}}{A_{21}}\frac{g_2}{g_1}\exp\left(-\frac{h\nu_{21}}{kT}\right)$

Line intensity, for a two-level atom, in the optically-thin limit, with no external radiation

$$\underbrace{\frac{dP_{21}}{dV}\,[\mathrm{W/cm^3}]}_{\text{power emitted per unit volume}} = \underbrace{n_2\,[\mathrm{cm^{-3}}]}_{\text{number of excited atoms per unit volume}} \times \underbrace{A_{21}\,[\mathrm{s^{-1}}]}_{\text{emission rate per atom}} \times \underbrace{h\nu_{21}\,[\mathrm{J}]}_{\text{single photon energy}}.$$

Detailed balance (equilibrium between a process and its reverse): $\frac{\gamma_{12}}{\gamma_{21}} = \frac{g_2}{g_1}\exp\left(-\frac{h\nu_{21}}{kT}\right)$.

Statistical equilibrium: $n_1 n_{\rm coll}\gamma_{12} = n_2 n_{\rm coll}\gamma_{21} + n_2 A_{21} \Rightarrow \frac{n_2}{n_1} = \frac{\gamma_{12}}{\gamma_{21}}\frac{1}{1+\frac{A_{21}}{n_{\rm coll}\gamma_{21}}} = \frac{g_2}{g_1}\frac{\exp\left(-\frac{h\nu_{21}}{kT}\right)}{1+\frac{A_{21}}{n_{\rm coll}\gamma_{21}}}$.

Low-density cooling function

If $A_{21} \gg n_{\rm coll}\gamma_{21}$ & posing $n_1 = X_1 n_{\rm coll} \rightarrow \frac{dP_{21}}{dV} \simeq n_{\rm coll}^2 h\nu_{21} X_1 \frac{\gamma_{21}}{A_{21}}\frac{g_2}{g_1}\exp\left(-\frac{h\nu_{21}}{kT}\right) \equiv n_{\rm coll}^2 \underbrace{\Lambda_{21}(T)}_{\text{cooling function}}$.

Line intensity, for a two-level atom, in the optically-thin limit, with no external radiation

$$\underbrace{\frac{dP_{21}}{dV}\;[\mathrm{W/cm^3}]}_{\text{power emitted per unit volume}} = \underbrace{n_2\;[\mathrm{cm^{-3}}]}_{\text{number of excited atoms per unit volume}} \times \underbrace{A_{21}\;[\mathrm{s^{-1}}]}_{\text{emission rate per atom}} \times \underbrace{h\nu_{21}\;[\mathrm{J}]}_{\text{single photon energy}}.$$

Detailed balance (equilibrium between a process and its reverse): $\frac{\gamma_{12}}{\gamma_{21}} = \frac{g_2}{g_1}\exp\left(-\frac{h\nu_{21}}{kT}\right)$.

Statistical equilibrium: $n_1 n_{\rm coll}\gamma_{12} = n_2 n_{\rm coll}\gamma_{21} + n_2 A_{21} \Rightarrow \frac{n_2}{n_1} = \frac{\gamma_{12}}{\gamma_{21}}\frac{1}{1+\frac{A_{21}}{n_{\rm coll}\gamma_{21}}} = \frac{g_2}{g_1}\frac{\exp\left(-\frac{h\nu_{21}}{kT}\right)}{1+\frac{A_{21}}{n_{\rm coll}\gamma_{21}}}$.

Low-density cooling function

If $A_{21} \gg n_{\rm coll}\gamma_{21}$ & posing $n_1 = X_1 n_{\rm coll} \rightarrow \frac{dP_{21}}{dV} \simeq n_{\rm coll}^2 h\nu_{21} X_1 \frac{\gamma_{21}}{A_{21}}\frac{g_2}{g_1}\exp\left(-\frac{h\nu_{21}}{kT}\right) \equiv n_{\rm coll}^2 \underbrace{\Lambda_{21}(T)}_{\text{cooling function}}$.

Line surface brightness: $I_{21} = \frac{1}{4\pi}\int_{\text{sightline } s}\frac{dP_{21}}{dV}\,ds$

Line intensity, for a two-level atom, in the optically-thin limit, with no external radiation

$$\underbrace{\frac{\mathrm{d}P_{21}}{\mathrm{d}V}\,[\mathrm{W/cm^3}]}_{\text{power emitted per unit volume}} = \underbrace{n_2\,[\mathrm{cm^{-3}}]}_{\text{number of excited atoms per unit volume}} \times \underbrace{A_{21}\,[\mathrm{s^{-1}}]}_{\text{emission rate per atom}} \times \underbrace{h\nu_{21}\,[\mathrm{J}]}_{\text{single photon energy}} .$$

Detailed balance (equilibrium between a process and its reverse): $\frac{\gamma_{12}}{\gamma_{21}} = \frac{g_2}{g_1}\exp\left(-\frac{h\nu_{21}}{kT}\right)$.

Statistical equilibrium: $n_1 n_{\mathrm{coll}}\gamma_{12} = n_2 n_{\mathrm{coll}}\gamma_{21} + n_2 A_{21} \Rightarrow \frac{n_2}{n_1} = \frac{\gamma_{12}}{\gamma_{21}}\frac{1}{1+\frac{A_{21}}{n_{\mathrm{coll}}\gamma_{21}}} = \frac{g_2}{g_1}\frac{\exp\left(-\frac{h\nu_{21}}{kT}\right)}{1+\frac{A_{21}}{n_{\mathrm{coll}}\gamma_{21}}}$.

Low-density cooling function

If $A_{21} \gg n_{\mathrm{coll}}\gamma_{21}$ & posing $n_1 = X_1 n_{\mathrm{coll}} \rightarrow \frac{\mathrm{d}P_{21}}{\mathrm{d}V} \simeq n_{\mathrm{coll}}^2 h\nu_{21} X_1 \frac{\gamma_{21}}{A_{21}}\frac{g_2}{g_1}\exp\left(-\frac{h\nu_{21}}{kT}\right) \equiv n_{\mathrm{coll}}^2 \underbrace{\Lambda_{21}(T)}_{\text{cooling function}}$.

Line surface brightness: $I_{21} = \frac{1}{4\pi}\int_{\text{sightline s}} \frac{\mathrm{d}P_{21}}{\mathrm{d}V}\,\mathrm{d}s = \frac{1}{4\pi}\langle n_{\mathrm{coll}}^2\rangle \underbrace{\Delta s}_{\text{cloud depth}} \times \underbrace{\Lambda(T)}_{[\mathrm{W.cm^3}]}$ $[\mathrm{W/m^2/sr}]$.

Two line emissivity regimes

Two line emissivity regimes

Optically-thin & no external radiation $\Rightarrow$ no J_{21}.

Two line emissivity regimes

Optically-thin & no external radiation ⇒ no J_{21}.

$$\frac{n_2}{n_1} = \frac{g_2}{g_1} \frac{\exp\left(-\frac{h\nu_{21}}{kT}\right)}{1 + \frac{n_{\rm crit}}{n_{\rm coll}}}.$$

Two line emissivity regimes

Optically-thin & no external radiation ⇒ no J_{21}.

$$\frac{n_2}{n_1} = \frac{g_2}{g_1} \frac{\exp\left(-\frac{h\nu_{21}}{kT}\right)}{1 + \frac{n_{\rm crit}}{n_{\rm coll}}}.$$

Critical density: $\boxed{n_{\rm crit}(T|{\rm coll}) \equiv \frac{A_{21}}{\gamma_{21}(T)}}.$

Two line emissivity regimes

Optically-thin & no external radiation ⇒ no J_{21}.

$$\frac{n_2}{n_1} = \frac{g_2}{g_1} \frac{\exp\left(-\frac{h\nu_{21}}{kT}\right)}{1+\frac{n_{\rm crit}}{n_{\rm coll}}}.$$

Critical density: $\boxed{n_{\rm crit}(T|{\rm coll}) \equiv \frac{A_{21}}{\gamma_{21}(T)}}$.

Line emissivity, with $\rho_{\rm line} \simeq n_1\,[{\rm X_{line}/H}]\,m_{\rm H}$:

Two line emissivity regimes

Optically-thin & no external radiation ⇒ no J_{21}.

$$\frac{n_2}{n_1} = \frac{g_2}{g_1} \frac{\exp\left(-\frac{h\nu_{21}}{kT}\right)}{1+\frac{n_{\rm crit}}{n_{\rm coll}}}.$$

Critical density: $\boxed{n_{\rm crit}(T|\text{coll}) \equiv \frac{A_{21}}{\gamma_{21}(T)}}$.

Line emissivity, with $\rho_{\rm line} \simeq n_1\,[\text{X}_{\rm line}/\text{H}]\,m_{\rm H}$:

$$\epsilon_{21} = h\nu_{21}\frac{n_2}{\rho_{\rm line}}A_{21}$$

Two line emissivity regimes

Optically-thin & no external radiation $\Rightarrow$ no J_{21}.

$$\frac{n_2}{n_1} = \frac{g_2}{g_1} \frac{\exp\left(-\frac{h\nu_{21}}{kT}\right)}{1 + \frac{n_{\rm crit}}{n_{\rm coll}}}.$$

Critical density: $\boxed{n_{\rm crit}(T|{\rm coll}) \equiv \frac{A_{21}}{\gamma_{21}(T)}}$.

Line emissivity, with $\rho_{\rm line} \simeq n_1\,[{\rm X}_{\rm line}/{\rm H}]\,m_{\rm H}$:

$$\begin{aligned}\epsilon_{21} &= h\nu_{21}\frac{n_2}{\rho_{\rm line}}A_{21} \\ &= \frac{h\nu_{21}}{m_{\rm H}}\left[\frac{{\rm X}_{\rm line}}{\rm H}\right]\frac{g_2}{g_1}A_{21}\frac{\exp\left(-\frac{h\nu_{21}}{kT}\right)}{1+\frac{n_{\rm crit}}{n_{\rm coll}}}.\end{aligned}$$

Two line emissivity regimes

Optically-thin & no external radiation ⇒ no J_{21}.

$$\frac{n_2}{n_1} = \frac{g_2}{g_1}\frac{\exp\left(-\frac{h\nu_{21}}{kT}\right)}{1+\frac{n_{\rm crit}}{n_{\rm coll}}}.$$

Critical density: $\boxed{n_{\rm crit}(T|{\rm coll}) \equiv \frac{A_{21}}{\gamma_{21}(T)}}.$

Line emissivity, with $\rho_{\rm line} \simeq n_1\,[{\rm X_{line}}/{\rm H}]\,m_{\rm H}$:

$$\begin{aligned}\epsilon_{21} &= h\nu_{21}\frac{n_2}{\rho_{\rm line}}A_{21}\\ &= \frac{h\nu_{21}}{m_{\rm H}}\left[\frac{\rm X_{line}}{\rm H}\right]\frac{g_2}{g_1}A_{21}\frac{\exp\left(-\frac{h\nu_{21}}{kT}\right)}{1+\frac{n_{\rm crit}}{n_{\rm coll}}}.\end{aligned}$$

Two regimes:

Two line emissivity regimes

Optically-thin & no external radiation ⇒ no J_{21}.

$$\frac{n_2}{n_1} = \frac{g_2}{g_1} \frac{\exp\left(-\frac{h\nu_{21}}{kT}\right)}{1 + \frac{n_{\rm crit}}{n_{\rm coll}}}.$$

Critical density: $\boxed{n_{\rm crit}(T|{\rm coll}) \equiv \frac{A_{21}}{\gamma_{21}(T)}}$.

Line emissivity, with $\rho_{\rm line} \simeq n_1\,[{\rm X}_{\rm line}/{\rm H}]\,m_{\rm H}$:

$$\begin{aligned} \epsilon_{21} &= h\nu_{21}\frac{n_2}{\rho_{\rm line}}A_{21} \\ &= \frac{h\nu_{21}}{m_{\rm H}}\left[\frac{{\rm X}_{\rm line}}{\rm H}\right]\frac{g_2}{g_1}A_{21}\frac{\exp\left(-\frac{h\nu_{21}}{kT}\right)}{1+\frac{n_{\rm crit}}{n_{\rm coll}}}. \end{aligned}$$

Two regimes:

$n_{\rm coll} \gg n_{\rm crit}$: collisional de-excitation dominates ⇒ ≃ LTE.

Two line emissivity regimes

Optically-thin & no external radiation $\Rightarrow$ no J_{21}.

$$\frac{n_2}{n_1} = \frac{g_2}{g_1} \frac{\exp\left(-\frac{h\nu_{21}}{kT}\right)}{1+\frac{n_{crit}}{n_{coll}}}.$$

Critical density: $\boxed{n_{crit}(T|\text{coll}) \equiv \frac{A_{21}}{\gamma_{21}(T)}}$.

Line emissivity, with $\rho_{line} \simeq n_1\,[X_{line}/H]\,m_H$:

$$\begin{aligned} \epsilon_{21} &= h\nu_{21}\frac{n_2}{\rho_{line}}A_{21} \\ &= \frac{h\nu_{21}}{m_H}\left[\frac{X_{line}}{H}\right]\frac{g_2}{g_1}A_{21}\frac{\exp\left(-\frac{h\nu_{21}}{kT}\right)}{1+\frac{n_{crit}}{n_{coll}}}. \end{aligned}$$

Two regimes:

$n_{coll} \gg n_{crit}$: collisional de-excitation dominates $\Rightarrow \simeq$ LTE.

$n_{coll} \ll n_{crit}$: spontaneous emission dominates $\Rightarrow$ less emissive.

Two line emissivity regimes

Optically-thin & no external radiation ⇒ no J_{21}.

$$\frac{n_2}{n_1} = \frac{g_2}{g_1} \frac{\exp\left(-\frac{h\nu_{21}}{kT}\right)}{1 + \frac{n_{\rm crit}}{n_{\rm coll}}}.$$

Critical density: $\boxed{n_{\rm crit}(T|{\rm coll}) \equiv \frac{A_{21}}{\gamma_{21}(T)}}$.

Line emissivity, with $\rho_{\rm line} \simeq n_1\,[{\rm X_{line}/H}]\,m_{\rm H}$:

$$\begin{aligned}\epsilon_{21} &= h\nu_{21}\frac{n_2}{\rho_{\rm line}}A_{21} \\ &= \frac{h\nu_{21}}{m_{\rm H}}\left[\frac{\rm X_{line}}{\rm H}\right]\frac{g_2}{g_1}A_{21}\frac{\exp\left(-\frac{h\nu_{21}}{kT}\right)}{1 + \frac{n_{\rm crit}}{n_{\rm coll}}}.\end{aligned}$$

Two regimes:

$n_{\rm coll} \gg n_{\rm crit}$: collisional de-excitation dominates ⇒ ≃ LTE.

$n_{\rm coll} \ll n_{\rm crit}$: spontaneous emission dominates ⇒ less emissive.

Example: the $[{\rm C\,II}]_{158\mu m}$ line in an H I cloud

Two line emissivity regimes

Optically-thin & no external radiation ⇒ no J_{21}.

$$\frac{n_2}{n_1} = \frac{g_2}{g_1} \frac{\exp\left(-\frac{h\nu_{21}}{kT}\right)}{1+\frac{n_{\rm crit}}{n_{\rm coll}}}.$$

Critical density: $\boxed{n_{\rm crit}(T|{\rm coll}) \equiv \frac{A_{21}}{\gamma_{21}(T)}}$.

Line emissivity, with $\rho_{\rm line} \simeq n_1\,[{\rm X_{line}/H}]\,m_{\rm H}$:

$$\begin{aligned}\epsilon_{21} &= h\nu_{21}\frac{n_2}{\rho_{\rm line}}A_{21} \\ &= \frac{h\nu_{21}}{m_{\rm H}}\left[\frac{\rm X_{line}}{\rm H}\right]\frac{g_2}{g_1}A_{21}\frac{\exp\left(-\frac{h\nu_{21}}{kT}\right)}{1+\frac{n_{\rm crit}}{n_{\rm coll}}}.\end{aligned}$$

Two regimes:

$n_{\rm coll} \gg n_{\rm crit}$: collisional de-excitation dominates ⇒ $\simeq$ LTE.

$n_{\rm coll} \ll n_{\rm crit}$: spontaneous emission dominates ⇒ less emissive.

Example: the $[{\rm C\,II}]_{158\mu{\rm m}}$ line in an H I cloud

- $n_{\rm coll} = n_{\rm H}$, $m_{\rm line} = 12 m_{\rm H}$, $\lambda_{21} = 158\ \mu$m.

Atoms | Optically-Thin Limit & the Concept of Critical Density

Two line emissivity regimes

Optically-thin & no external radiation ⇒ no J_{21}.

$$\frac{n_2}{n_1} = \frac{g_2}{g_1} \frac{\exp\left(-\frac{h\nu_{21}}{kT}\right)}{1+\frac{n_{crit}}{n_{coll}}}.$$

Critical density: $\boxed{n_{crit}(T|\text{coll}) \equiv \frac{A_{21}}{\gamma_{21}(T)}}$.

Line emissivity, with $\rho_{line} \simeq n_1\,[X_{line}/H]\,m_H$:

$$\epsilon_{21} = h\nu_{21}\frac{n_2}{\rho_{line}}A_{21}$$
$$= \frac{h\nu_{21}}{m_H}\left[\frac{X_{line}}{H}\right]\frac{g_2}{g_1}A_{21}\frac{\exp\left(-\frac{h\nu_{21}}{kT}\right)}{1+\frac{n_{crit}}{n_{coll}}}.$$

Two regimes:

$n_{coll} \gg n_{crit}$: collisional de-excitation dominates ⇒ $\simeq$ LTE.

$n_{coll} \ll n_{crit}$: spontaneous emission dominates ⇒ less emissive.

Example: the $[\text{C II}]_{158\mu m}$ line in an H I cloud

- $n_{coll} = n_H$, $m_{line} = 12 m_H$, $\lambda_{21} = 158\ \mu$m.
- Atomic data → $A_{21} = 2.4\times10^{-6}\ \text{s}^{-1}$, $g_1 = 2$, $g_2 = 4$, $n_{crit}(\text{H I}) = 2993\ \text{cm}^{-3}$.

Two line emissivity regimes

Optically-thin & no external radiation ⇒ no J_{21}.

$$\frac{n_2}{n_1} = \frac{g_2}{g_1} \frac{\exp\left(-\frac{h\nu_{21}}{kT}\right)}{1+\frac{n_{\rm crit}}{n_{\rm coll}}}.$$

Critical density: $\boxed{n_{\rm crit}(T|{\rm coll}) \equiv \frac{A_{21}}{\gamma_{21}(T)}}$.

Line emissivity, with $\rho_{\rm line} \simeq n_1\,[{\rm X_{line}/H}]\,m_{\rm H}$:

$$\epsilon_{21} = h\nu_{21}\frac{n_2}{\rho_{\rm line}}A_{21}$$

$$= \frac{h\nu_{21}}{m_{\rm H}}\left[\frac{\rm X_{line}}{\rm H}\right]\frac{g_2}{g_1}A_{21}\frac{\exp\left(-\frac{h\nu_{21}}{kT}\right)}{1+\frac{n_{\rm crit}}{n_{\rm coll}}}.$$

Two regimes:

$n_{\rm coll} \gg n_{\rm crit}$: collisional de-excitation dominates ⇒ $\simeq$ LTE.

$n_{\rm coll} \ll n_{\rm crit}$: spontaneous emission dominates ⇒ less emissive.

Example: the $[\rm C\,II]_{158\mu m}$ line in an H I cloud

- $n_{\rm coll} = n_{\rm H}$, $m_{\rm line} = 12 m_{\rm H}$, $\lambda_{21} = 158\ \mu$m.
- Atomic data → $A_{21} = 2.4\times10^{-6}\ {\rm s}^{-1}$, $g_1 = 2$, $g_2 = 4$, $n_{\rm crit}({\rm H\,I}) = 2993\ {\rm cm}^{-3}$.

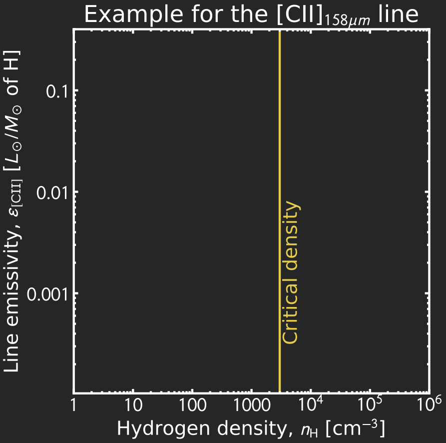

Two line emissivity regimes

Optically-thin & no external radiation ⇒ no J_{21}.

$$\frac{n_2}{n_1} = \frac{g_2}{g_1} \frac{\exp\left(-\frac{h\nu_{21}}{kT}\right)}{1 + \frac{n_{crit}}{n_{coll}}}.$$

Critical density: $\boxed{n_{crit}(T|\text{coll}) \equiv \frac{A_{21}}{\gamma_{21}(T)}}$.

Line emissivity, with $\rho_{line} \simeq n_1\,[X_{line}/H]\,m_H$:

$$\begin{aligned} \epsilon_{21} &= h\nu_{21}\frac{n_2}{\rho_{line}}A_{21} \\ &= \frac{h\nu_{21}}{m_H}\left[\frac{X_{line}}{H}\right]\frac{g_2}{g_1}A_{21}\frac{\exp\left(-\frac{h\nu_{21}}{kT}\right)}{1+\frac{n_{crit}}{n_{coll}}}. \end{aligned}$$

Two regimes:

$n_{coll} \gg n_{crit}$: collisional de-excitation dominates ⇒ $\simeq$ LTE.

$n_{coll} \ll n_{crit}$: spontaneous emission dominates ⇒ less emissive.

Example: the [C II]$_{158\mu m}$ line in an H I cloud

- $n_{coll} = n_H$, $m_{line} = 12 m_H$, $\lambda_{21} = 158\ \mu$m.
- Atomic data → $A_{21} = 2.4 \times 10^{-6}\ \text{s}^{-1}$, $g_1 = 2$, $g_2 = 4$, $n_{crit}(\text{H I}) = 2993\ \text{cm}^{-3}$.

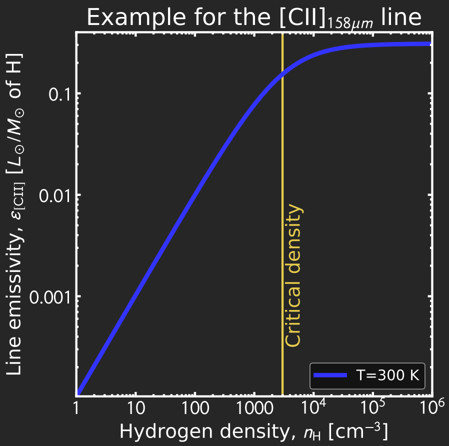

Two line emissivity regimes

Optically-thin & no external radiation ⇒ no J_{21}.

$$\frac{n_2}{n_1} = \frac{g_2}{g_1} \frac{\exp\left(-\frac{h\nu_{21}}{kT}\right)}{1+\frac{n_{\text{crit}}}{n_{\text{coll}}}}.$$

Critical density: $\boxed{n_{\text{crit}}(T|\text{coll}) \equiv \frac{A_{21}}{\gamma_{21}(T)}}$.

Line emissivity, with $\rho_{\text{line}} \simeq n_1\,[X_{\text{line}}/H]\,m_H$:

$$\begin{aligned}\epsilon_{21} &= h\nu_{21}\frac{n_2}{\rho_{\text{line}}}A_{21} \\ &= \frac{h\nu_{21}}{m_H}\left[\frac{X_{\text{line}}}{H}\right]\frac{g_2}{g_1}A_{21}\frac{\exp\left(-\frac{h\nu_{21}}{kT}\right)}{1+\frac{n_{\text{crit}}}{n_{\text{coll}}}}.\end{aligned}$$

Two regimes:

$n_{\text{coll}} \gg n_{\text{crit}}$: collisional de-excitation dominates ⇒ ≃ LTE.

$n_{\text{coll}} \ll n_{\text{crit}}$: spontaneous emission dominates ⇒ less emissive.

Example: the $[\text{C II}]_{158\mu m}$ line in an H I cloud

- $n_{\text{coll}} = n_H$, $m_{\text{line}} = 12 m_H$, $\lambda_{21} = 158\ \mu$m.
- Atomic data → $A_{21} = 2.4 \times 10^{-6}\ \text{s}^{-1}$, $g_1 = 2$, $g_2 = 4$, $n_{\text{crit}}(\text{H I}) = 2993\ \text{cm}^{-3}$.

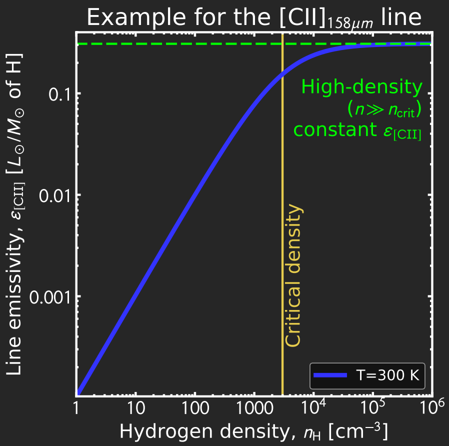

Atoms | Optically-Thin Limit & the Concept of Critical Density

Two line emissivity regimes

Optically-thin & no external radiation ⇒ no J_{21}.

$$\frac{n_2}{n_1} = \frac{g_2}{g_1} \frac{\exp\left(-\frac{h\nu_{21}}{kT}\right)}{1 + \frac{n_{\rm crit}}{n_{\rm coll}}}.$$

Critical density: $\boxed{n_{\rm crit}(T|{\rm coll}) \equiv \frac{A_{21}}{\gamma_{21}(T)}}$.

Line emissivity, with $\rho_{\rm line} \simeq n_1 \,[{\rm X_{line}/H}]\, m_{\rm H}$:

$$\epsilon_{21} = h\nu_{21} \frac{n_2}{\rho_{\rm line}} A_{21}$$

$$= \frac{h\nu_{21}}{m_{\rm H}} \left[\frac{\rm X_{line}}{\rm H}\right] \frac{g_2}{g_1} A_{21} \frac{\exp\left(-\frac{h\nu_{21}}{kT}\right)}{1 + \frac{n_{\rm crit}}{n_{\rm coll}}}.$$

Two regimes:

$n_{\rm coll} \gg n_{\rm crit}$: collisional de-excitation dominates ⇒ $\simeq$ LTE.

$n_{\rm coll} \ll n_{\rm crit}$: spontaneous emission dominates ⇒ less emissive.

Example: the [C II]$_{158\mu m}$ line in an H I cloud

- $n_{\rm coll} = n_{\rm H}$, $m_{\rm line} = 12 m_{\rm H}$, $\lambda_{21} = 158\ \mu$m.
- Atomic data → $A_{21} = 2.4 \times 10^{-6}$ s^{-1}, $g_1 = 2$, $g_2 = 4$, $n_{\rm crit}$(H I) $= 2993$ cm^{-3}.

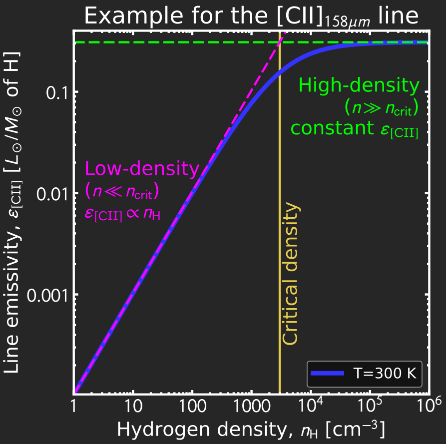

Two line emissivity regimes

Optically-thin & no external radiation ⇒ no J_{21}.

$$\frac{n_2}{n_1} = \frac{g_2}{g_1} \frac{\exp\left(-\frac{h\nu_{21}}{kT}\right)}{1+\frac{n_{\rm crit}}{n_{\rm coll}}}.$$

Critical density: $\boxed{n_{\rm crit}(T|{\rm coll}) \equiv \frac{A_{21}}{\gamma_{21}(T)}}$.

Line emissivity, with $\rho_{\rm line} \simeq n_1\,[{\rm X_{line}/H}]\,m_{\rm H}$:

$$\epsilon_{21} = h\nu_{21}\frac{n_2}{\rho_{\rm line}}A_{21}$$

$$= \frac{h\nu_{21}}{m_{\rm H}}\left[\frac{\rm X_{line}}{\rm H}\right]\frac{g_2}{g_1}A_{21}\frac{\exp\left(-\frac{h\nu_{21}}{kT}\right)}{1+\frac{n_{\rm crit}}{n_{\rm coll}}}.$$

Two regimes:

$n_{\rm coll} \gg n_{\rm crit}$: collisional de-excitation dominates ⇒ $\simeq$ LTE.

$n_{\rm coll} \ll n_{\rm crit}$: spontaneous emission dominates ⇒ less emissive.

Example: the $[{\rm C\,II}]_{158\mu m}$ line in an H I cloud

- $n_{\rm coll} = n_{\rm H}$, $m_{\rm line} = 12 m_{\rm H}$, $\lambda_{21} = 158\ \mu$m.
- Atomic data → $A_{21} = 2.4 \times 10^{-6}\ {\rm s^{-1}}$, $g_1 = 2$, $g_2 = 4$, $n_{\rm crit}({\rm H\,I}) = 2993\ {\rm cm^{-3}}$.

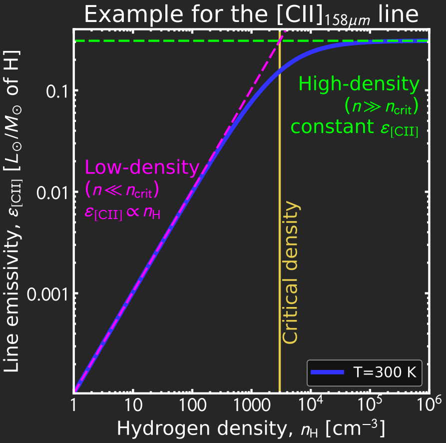

Optically-thin & $n_{\rm H} \gg n_{\rm crit}$ ⇒ $L_{21} \propto$ mass.

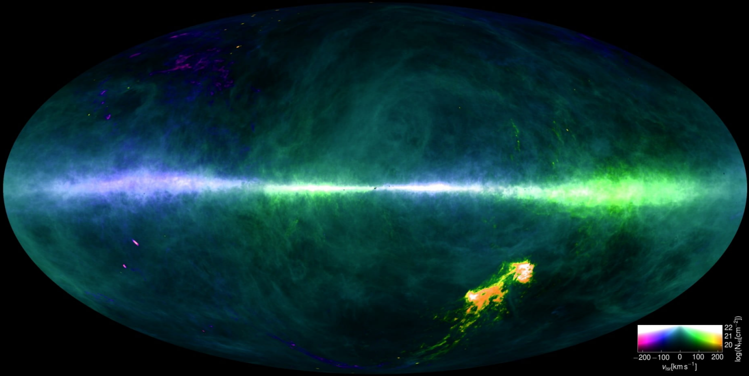

Credit: [H I]$_{21\,cm}$ map of the Milky Way HI4PI Collaboration et al. (2016).

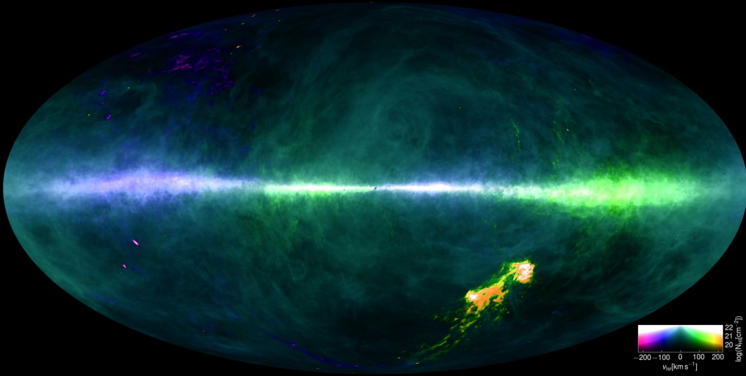

Credit: [H I]$_{21\,cm}$ map of the Milky Way HI4PI Collaboration et al. (2016).

Tracing neutral Hydrogen in galaxies (Kalberla & Kerp, 2009; Walter et al., 2008)

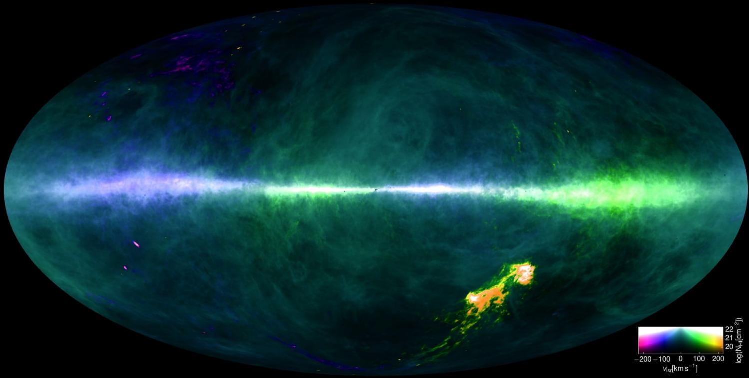

Credit: [H I]$_{21\,cm}$ map of the Milky Way HI4PI Collaboration et al. (2016).

Tracing neutral Hydrogen in galaxies (Kalberla & Kerp, 2009; Walter et al., 2008)

- Absorption by atmosphere & dust negligible. Self-absorbed towards dense regions.

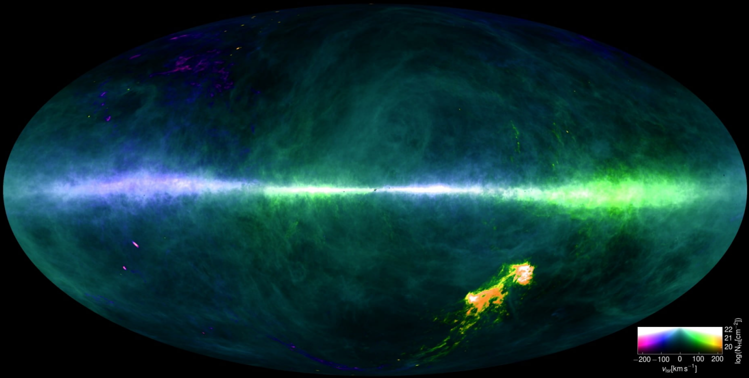

Credit: [H I]$_{21\,cm}$ map of the Milky Way HI4PI Collaboration et al. (2016).

Tracing neutral Hydrogen in galaxies (Kalberla & Kerp, 2009; Walter et al., 2008)

- Absorption by atmosphere & dust negligible. Self-absorbed towards dense regions.
- Used to trace the spiral structure of galaxies and their rotation curves.

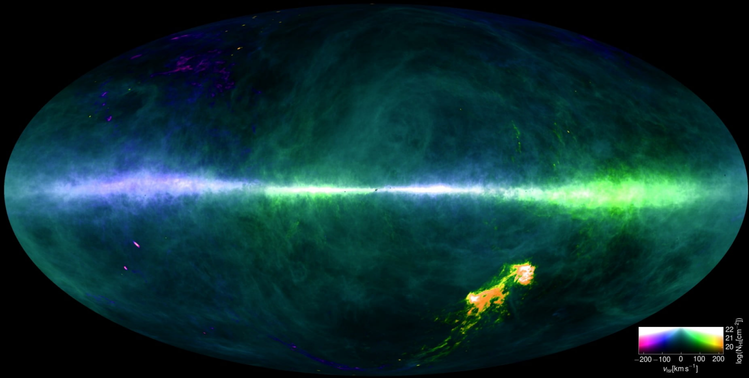

Credit: [H I]$_{21\,cm}$ map of the Milky Way HI4PI Collaboration et al. (2016).

Tracing neutral Hydrogen in galaxies (Kalberla & Kerp, 2009; Walter et al., 2008)

- Absorption by atmosphere & dust negligible. Self-absorbed towards dense regions.
- Used to trace the spiral structure of galaxies and their rotation curves.
- Zeeman effect (energy level splitting by $\vec{B}$) → magnetic field tracer.

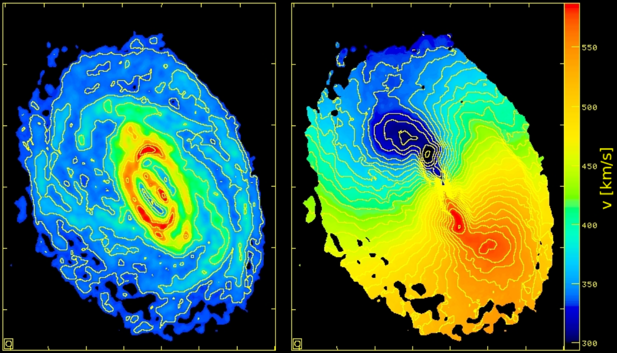

Credit: Circinus, $[H\,I]_{21\,cm}$ mass (left) & radial velocity (right) (Jones et al., 1999).

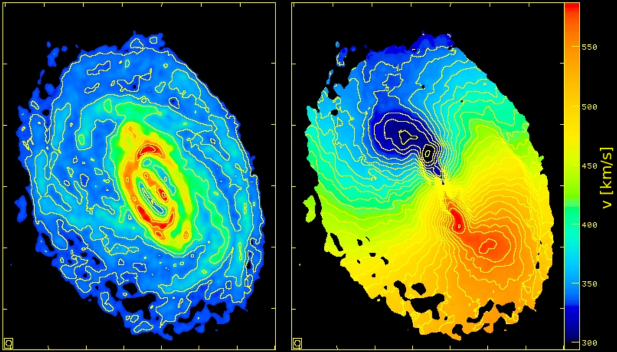

Credit: Circinus, [H I]$_{21\,cm}$ mass (left) & radial velocity (right) (Jones et al., 1999).

Atomic data for H I$_{21cm}$

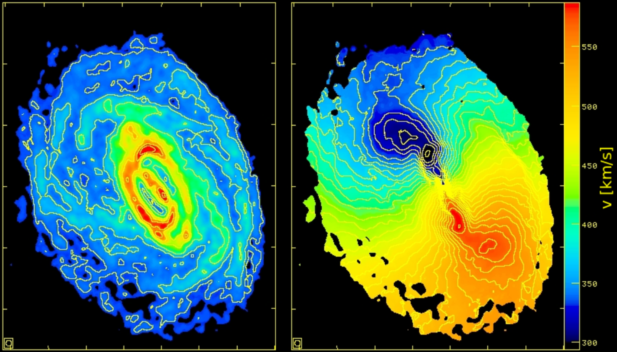

Credit: Circinus, [H I]$_{21\,\mathrm{cm}}$ mass (left) & radial velocity (right) (Jones et al., 1999).

Atomic data for H I$_{21cm}$

- $A_{21} = 2.9 \times 10^{-15}$ s^{-1} $\simeq$ 1 every 11 Myr.

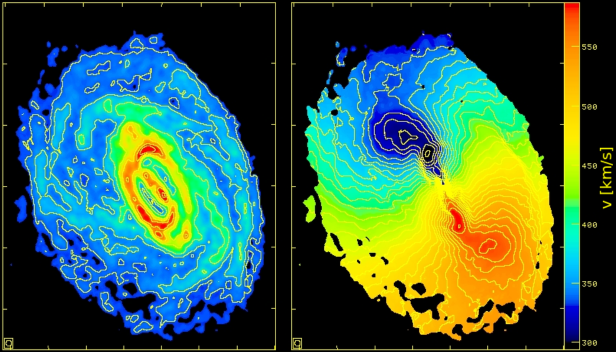

Credit: Circinus, $[\text{H I}]_{21\,\text{cm}}$ mass (left) & radial velocity (right) (Jones et al., 1999).

Atomic data for H I$_{21cm}$

- $A_{21} = 2.9 \times 10^{-15}\ \text{s}^{-1}$ $\simeq$ 1 every 11 Myr.
- $g_1 = 1$ & $g_2 = 3$.

The H I$_{21cm}$ Line in the Optically-Thin Limit

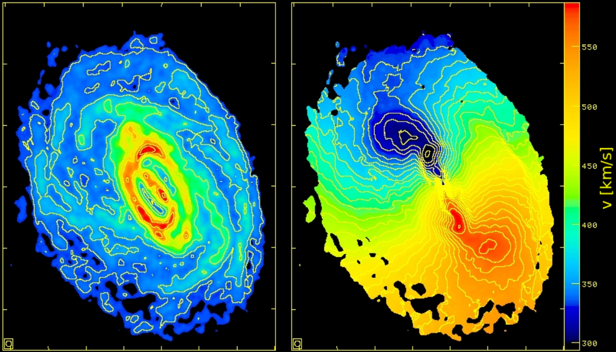

Credit: Circinus, [H I]$_{21\,cm}$ mass (left) & radial velocity (right) (Jones et al., 1999).

Atomic data for H I$_{21cm}$

- $A_{21} = 2.9 \times 10^{-15}$ s^{-1} $\simeq$ 1 every 11 Myr.
- $g_1 = 1$ & $g_2 = 3$.
- $E_{21} = 5.87$ μeV $\Rightarrow$ $\exp\left(-E_{21}/kT\right) \simeq 1$ for all relevant T.

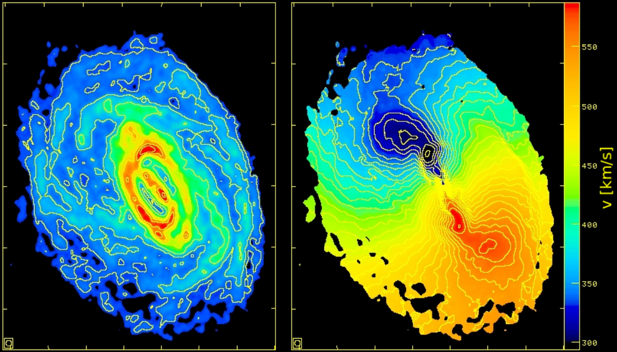

Credit: Circinus, [H I]$_{21\ cm}$ mass (left) & radial velocity (right) (Jones et al., 1999).

Atomic data for H I$_{21cm}$

- $A_{21} = 2.9 \times 10^{-15}$ s^{-1} $\simeq$ 1 every 11 Myr.
- $g_1 = 1$ & $g_2 = 3$.
- $E_{21} = 5.87$ μeV $\Rightarrow$ $\exp(-E_{21}/kT) \simeq 1$ for all relevant T.
- $n_{crit} \simeq 3 \times 10^{-5}$ cm^{-3} $\Rightarrow$ LTE regime.

Atoms | The H I$_{21cm}$ Line in the Optically-Thin Limit

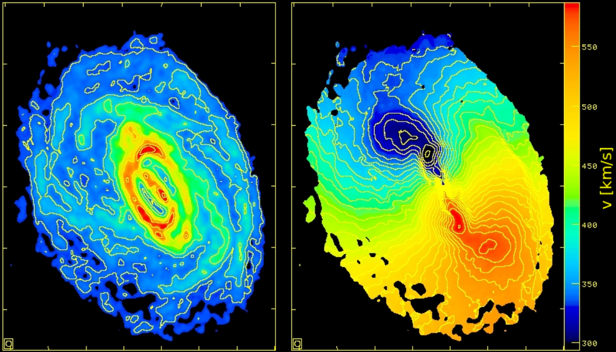

Credit: Circinus, [H I]$_{21\,cm}$ mass (left) & radial velocity (right) (Jones et al., 1999).

Atomic data for H I$_{21cm}$

- $A_{21} = 2.9 \times 10^{-15}$ s^{-1} $\simeq$ 1 every 11 Myr.
- $g_1 = 1$ & $g_2 = 3$.
- $E_{21} = 5.87$ μeV $\Rightarrow$ $\exp(-E_{21}/kT) \simeq 1$ for all relevant T.
- $n_{crit} \simeq 3 \times 10^{-5}$ cm^{-3} $\Rightarrow$ LTE regime.

H I$_{21cm}$ as a neutral gas mass tracer (assuming no absorption)

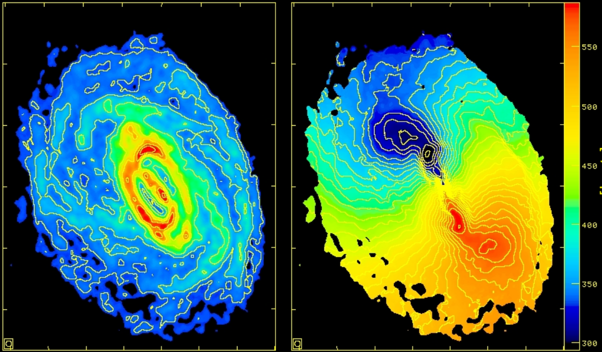

Credit: Circinus, [H I]$_{21\,cm}$ mass (left) & radial velocity (right) (Jones et al., 1999).

Atomic data for H I$_{21cm}$

- $A_{21} = 2.9 \times 10^{-15}$ s^{-1} $\simeq$ 1 every 11 Myr.
- $g_1 = 1$ & $g_2 = 3$.
- $E_{21} = 5.87$ μeV $\Rightarrow$ $\exp(-E_{21}/kT) \simeq 1$ for all relevant T.
- $n_{crit} \simeq 3 \times 10^{-5}$ cm^{-3} $\Rightarrow$ LTE regime.

H I$_{21cm}$ as a neutral gas mass tracer (assuming no absorption)

Level population: $\frac{n_2}{n_1} = \frac{g_2}{g_1} \exp\left(-\frac{h\nu_{21}}{kT}\right) = 3 \exp\left(-\frac{0.0682\text{ K}}{T}\right) \simeq 3$

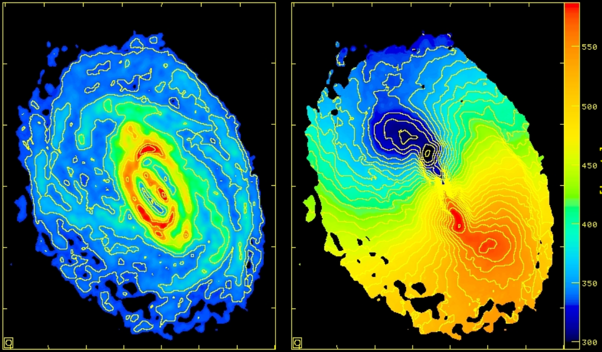

Credit: Circinus, [H I]$_{21\,cm}$ mass (left) & radial velocity (right) (Jones et al., 1999).

Atomic data for H I$_{21cm}$

- $A_{21} = 2.9 \times 10^{-15}\ s^{-1} \simeq 1$ every 11 Myr.
- $g_1 = 1$ & $g_2 = 3$.
- $E_{21} = 5.87\ \mu eV \Rightarrow \exp\left(-E_{21}/kT\right) \simeq 1$ for all relevant T.
- $n_{crit} \simeq 3 \times 10^{-5}\ cm^{-3} \Rightarrow$ LTE regime.

H I$_{21cm}$ as a neutral gas mass tracer (assuming no absorption)

Level population: $\frac{n_2}{n_1} = \frac{g_2}{g_1} \exp\left(-\frac{h\nu_{21}}{kT}\right) = 3 \exp\left(-\frac{0.0682\ K}{T}\right) \simeq 3 \Rightarrow n_2 \simeq \frac{3}{4} n(H\,I)$.

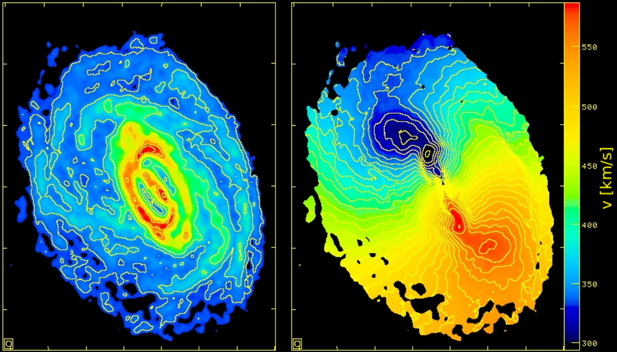

Credit: Circinus, $[\mathrm{H\,I}]_{21\,\rm cm}$ mass (left) & radial velocity (right) (Jones et al., 1999).

Atomic data for H I$_{21\rm cm}$

- $A_{21} = 2.9 \times 10^{-15}\ \mathrm{s}^{-1}$ $\simeq$ 1 every 11 Myr.
- $g_1 = 1$ & $g_2 = 3$.
- $E_{21} = 5.87\ \mu\mathrm{eV} \Rightarrow \exp(-E_{21}/kT) \simeq 1$ for all relevant T.
- $n_{\rm crit} \simeq 3 \times 10^{-5}\ \mathrm{cm}^{-3}$ $\Rightarrow$ LTE regime.

H I$_{21\rm cm}$ as a neutral gas mass tracer (assuming no absorption)

Level population: $\frac{n_2}{n_1} = \frac{g_2}{g_1}\exp\left(-\frac{h\nu_{21}}{kT}\right) = 3\exp\left(-\frac{0.0682\ \mathrm{K}}{T}\right) \simeq 3 \Rightarrow n_2 \simeq \frac{3}{4}n(\mathrm{H\,I})$.

Emitted power: $L_{\rm H\,I} = h\nu_{21} \underbrace{\frac{M_{\rm H\,I}}{m_{\rm H}}}_{\text{number of atoms}} A_{21}\frac{3}{4}\underbrace{\exp\left(-\frac{h\nu_{21}}{kT}\right)}_{\simeq 1}$

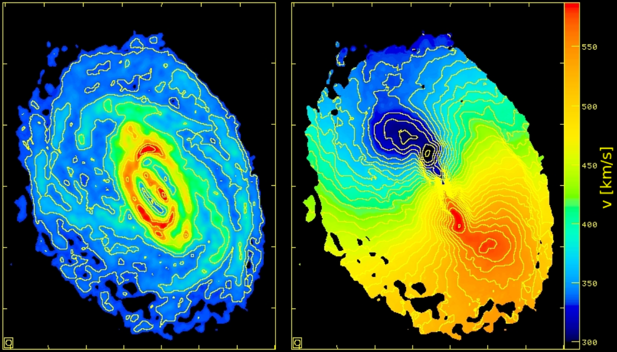

Credit: Circinus, $[\mathrm{H\,I}]_{21\,\mathrm{cm}}$ mass (left) & radial velocity (right) (Jones et al., 1999).

Atomic data for H I$_{21cm}$

- $A_{21} = 2.9 \times 10^{-15}$ s^{-1} $\simeq$ 1 every 11 Myr.
- $g_1 = 1$ & $g_2 = 3$.
- $E_{21} = 5.87$ μeV $\Rightarrow$ $\exp(-E_{21}/kT) \simeq 1$ for all relevant T.
- $n_{crit} \simeq 3 \times 10^{-5}$ cm^{-3} $\Rightarrow$ LTE regime.

H I$_{21cm}$ as a neutral gas mass tracer (assuming no absorption)

Level population: $$\frac{n_2}{n_1} = \frac{g_2}{g_1}\exp\left(-\frac{h\nu_{21}}{kT}\right) = 3\exp\left(-\frac{0.0682\text{ K}}{T}\right) \simeq 3 \Rightarrow n_2 \simeq \frac{3}{4}n(\mathrm{H\,I}).$$

Emitted power: $$L_{\mathrm{H\,I}} = h\nu_{21}\underbrace{\frac{M_{\mathrm{H\,I}}}{m_{\mathrm{H}}}}_{\text{number of atoms}} A_{21}\frac{3}{4}\underbrace{\exp\left(-\frac{h\nu_{21}}{kT}\right)}_{\simeq 1} \Rightarrow \epsilon_{\mathrm{H\,I}} \equiv \frac{L_{\mathrm{H\,I}}}{M_{\mathrm{H\,I}}} \simeq 6.2 \times 10^{-9}\ L_{\odot}/M_{\odot}.$$

Photo-ionization cross-sections

Photo-ionization cross-sections

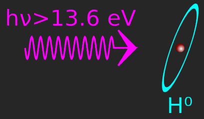

Photo-ionization cross-sections

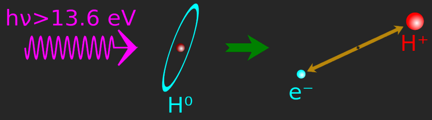

Photo-ionization cross-sections

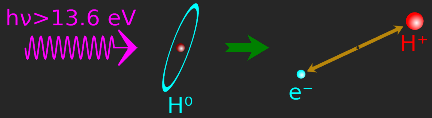

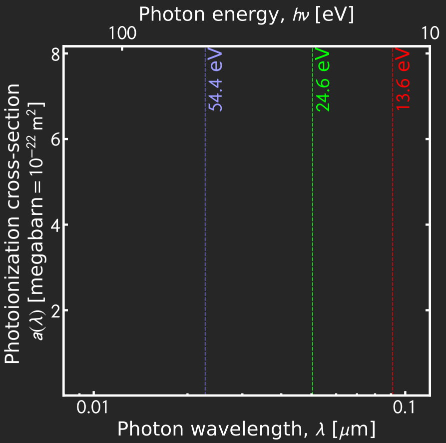

(Osterbrock & Ferland, 2006, Chap. 2)

Photo-ionization cross-sections

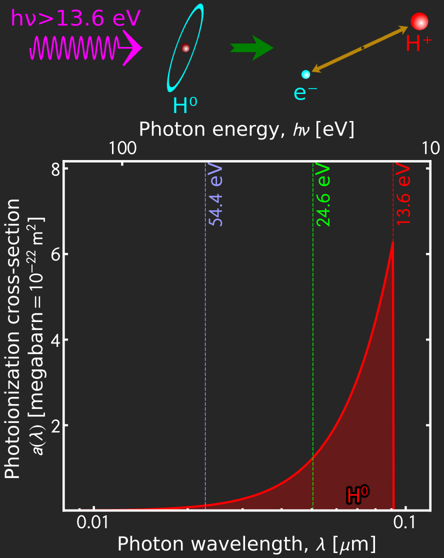

(Osterbrock & Ferland, 2006, Chap. 2)

Photo-ionization cross-sections

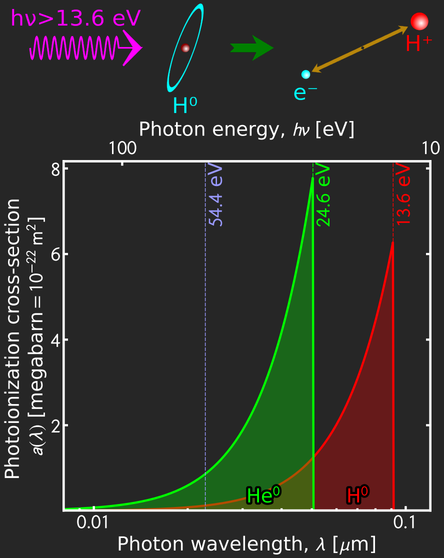

(Osterbrock & Ferland, 2006, Chap. 2)

Photo-ionization cross-sections

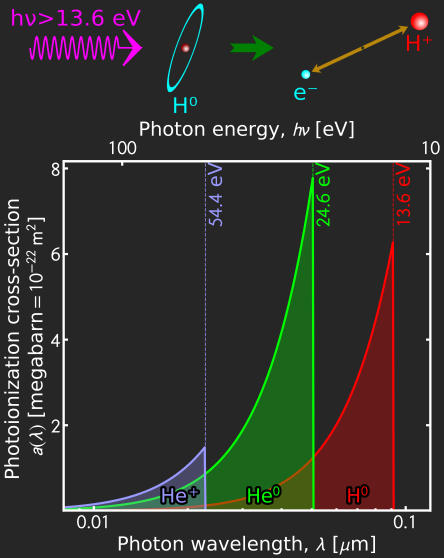

(Osterbrock & Ferland, 2006, Chap. 2)

Photo-ionization cross-sections

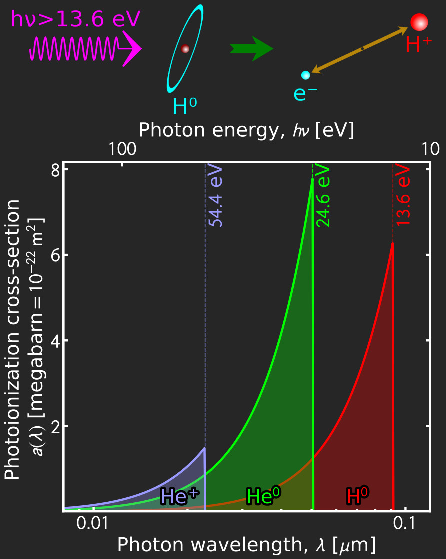

(Osterbrock & Ferland, 2006, Chap. 2)

The Lyman Break & photometric redshifts

Photo-ionization cross-sections

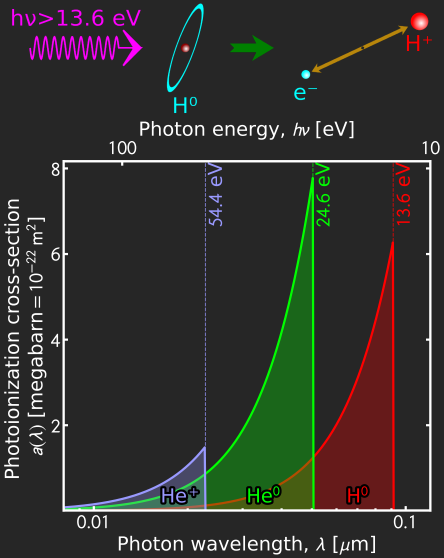

(Osterbrock & Ferland, 2006, Chap. 2)

The Lyman Break & photometric redshifts

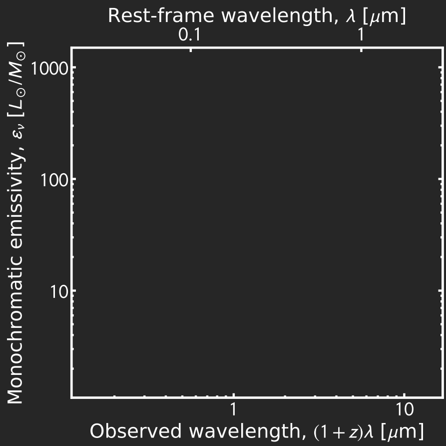

Photo-ionization cross-sections

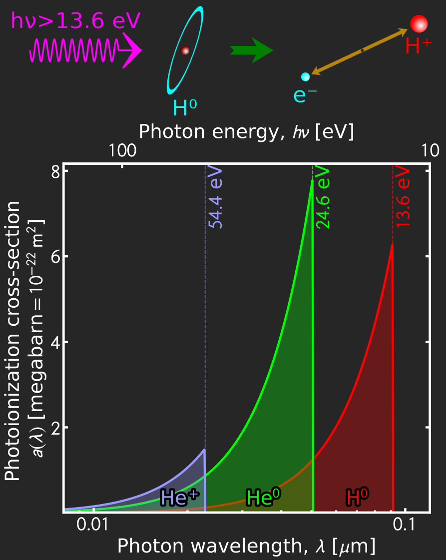

(Osterbrock & Ferland, 2006, Chap. 2)

The Lyman Break & photometric redshifts

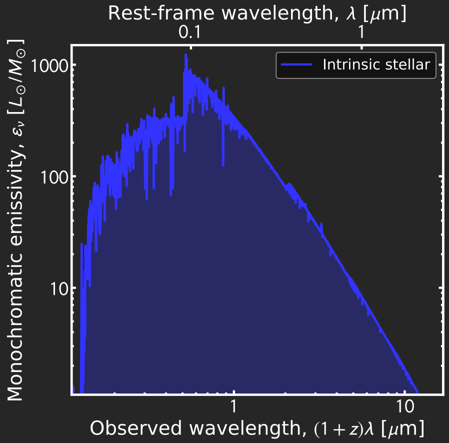

Photo-ionization cross-sections

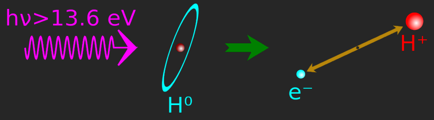

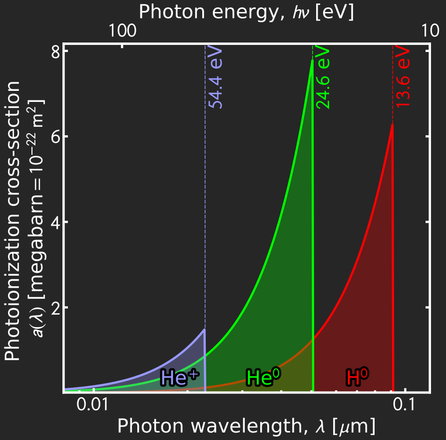

(Osterbrock & Ferland, 2006, Chap. 2)

The Lyman Break & photometric redshifts

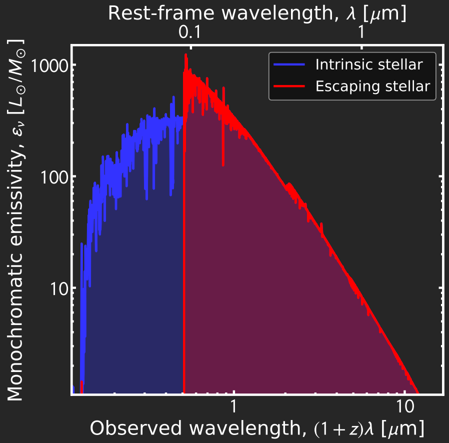

Photo-ionization cross-sections

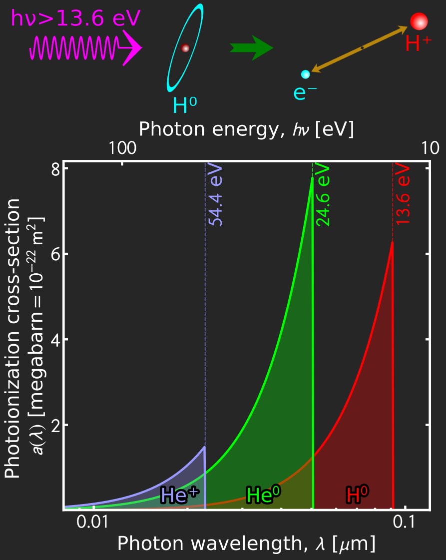

(Osterbrock & Ferland, 2006, Chap. 2)

The Lyman Break & photometric redshifts

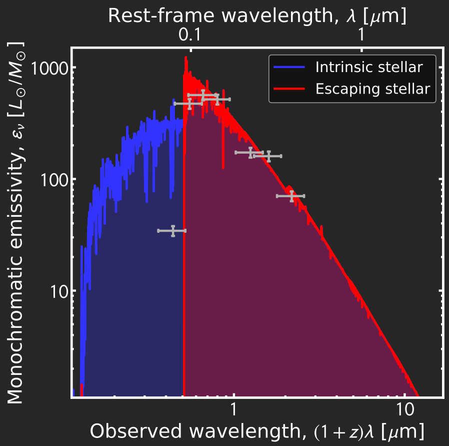

Photo-ionization cross-sections

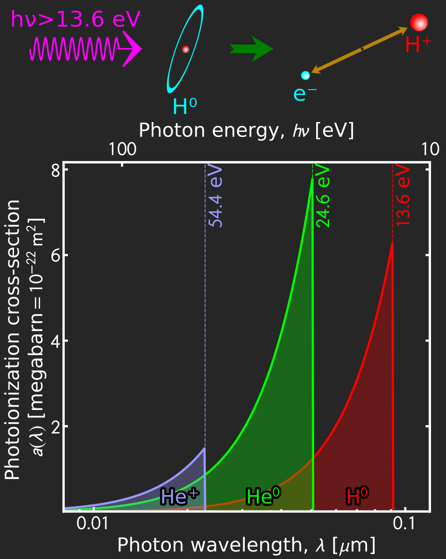

(Osterbrock & Ferland, 2006, Chap. 2)

The Lyman Break & photometric redshifts

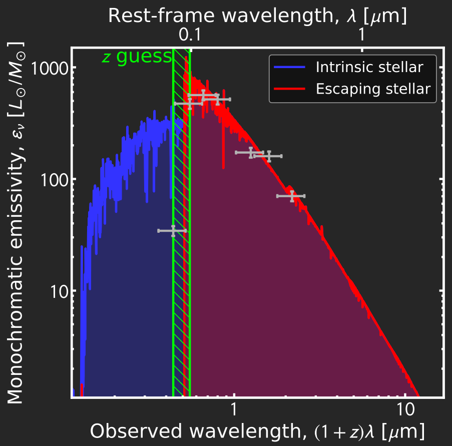

Photo-ionization cross-sections

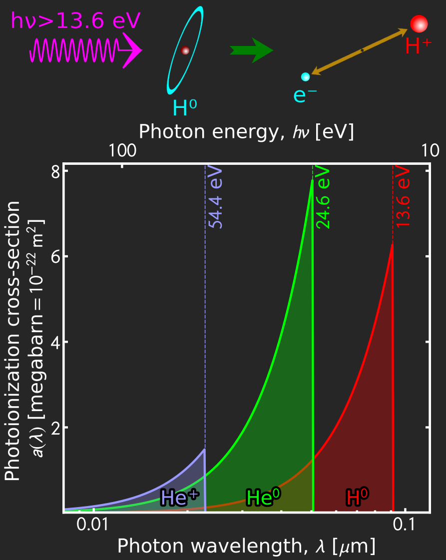

(Osterbrock & Ferland, 2006, Chap. 2)

The Lyman Break & photometric redshifts

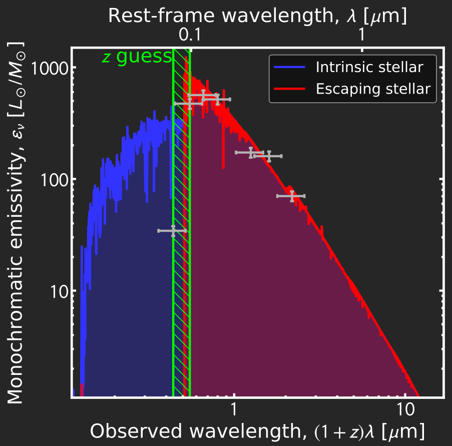

- H^+ is transparent to ionizing photons.

Photo-ionization cross-sections

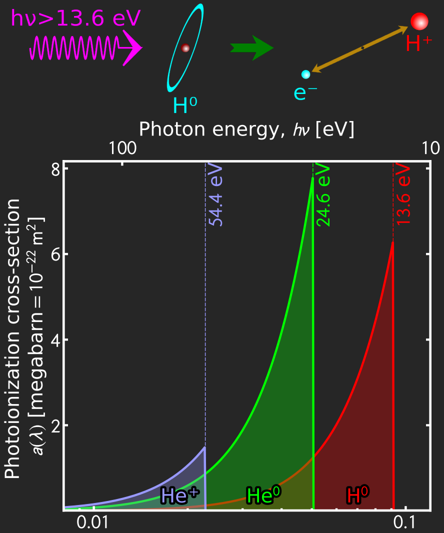

(Osterbrock & Ferland, 2006, Chap. 2)

The Lyman Break & photometric redshifts

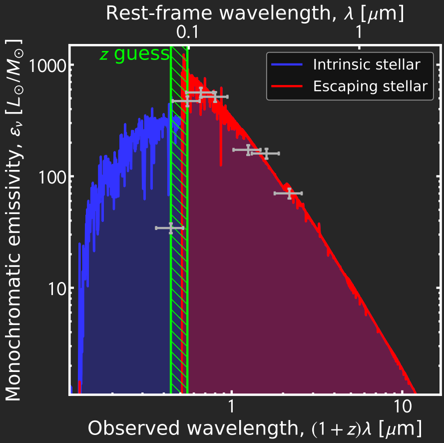

- H^+ is transparent to ionizing photons.
- H^0 is opaque to ionizing photons.

The recombination cascade

The recombination cascade

The recombination cascade

The recombination cascade

1. Electrons can recombine to any level, *nl*:

The recombination cascade

1. Electrons can recombine to any level, nl: $\underbrace{h\nu_1}_{\text{first emitted photon}}$

The recombination cascade

1. Electrons can recombine to any level, *nl*:

$$\underbrace{h\nu_1}_{\text{first emitted photon}} = \underbrace{E_k}_{\text{electron kinetic energy} \simeq 1\text{ eV}}$$

The recombination cascade

1. Electrons can recombine to any level, nl:

$$\underbrace{h\nu_1}_{\text{first emitted photon}} = \underbrace{E_k}_{\text{electron kinetic energy} \simeq 1\text{ eV}} + \underbrace{E_{nl}}_{nl\text{ state binding energy}}.$$

The recombination cascade

1. Electrons can recombine to any level, nl:

$$\underbrace{h\nu_1}_{\text{first emitted photon}} = \underbrace{E_k}_{\text{electron kinetic energy} \simeq 1\text{ eV}} + \underbrace{E_{nl}}_{nl\text{ state binding energy}}.$$

2. Several photons are then emitted down to $n = 1$:

The recombination cascade

1. Electrons can recombine to any level, *nl*:
$$\underbrace{h\nu_1}_{\text{first emitted photon}} = \underbrace{E_k}_{\text{electron kinetic energy} \simeq 1\text{ eV}} + \underbrace{E_{nl}}_{nl \text{ state binding energy}} .$$
2. Several photons are then emitted down to $n = 1$: $\sum_i h\nu_i = E_k + 13.6$ eV.

The recombination cascade

1. Electrons can recombine to any level, *nl*:
$$\underbrace{h\nu_1}_{\text{first emitted photon}} = \underbrace{E_k}_{\text{electron kinetic energy} \simeq 1\text{ eV}} + \underbrace{E_{nl}}_{nl\text{ state binding energy}}.$$
2. Several photons are then emitted down to $n=1$: $\sum_i h\nu_i = E_k + 13.6$ eV.

Volume recombination rate: $R = n_e n_p \alpha_A(T_e)$.

The recombination cascade

1. Electrons can recombine to any level, nl:
$$\underbrace{h\nu_1}_{\text{first emitted photon}} = \underbrace{E_k}_{\text{electron kinetic energy} \simeq 1\text{ eV}} + \underbrace{E_{nl}}_{nl\text{ state binding energy}}.$$
2. Several photons are then emitted down to $n=1$: $\sum_i h\nu_i = E_k + 13.6$ eV.

Volume recombination rate: $R = n_e n_p \alpha_A(T_e)$.

Two limiting cases

The recombination cascade

1. Electrons can recombine to any level, nl:
$$\underbrace{h\nu_1}_{\text{first emitted photon}} = \underbrace{E_k}_{\text{electron kinetic energy} \simeq 1\text{ eV}} + \underbrace{E_{nl}}_{nl\text{ state binding energy}}.$$
2. Several photons are then emitted down to $n = 1$: $\sum_i h\nu_i = E_k + 13.6$ eV.

Volume recombination rate: $R = n_e n_p \alpha_A(T_e)$.

Two limiting cases

Case A: recombination down to all levels: $\alpha_A(T_e) \rightarrow$ relevant for $\tau_{Ly} \ll 1$.

The recombination cascade

1. Electrons can recombine to any level, nl:
$$\underbrace{h\nu_1}_{\text{first emitted photon}} = \underbrace{E_k}_{\text{electron kinetic energy} \simeq 1\text{ eV}} + \underbrace{E_{nl}}_{nl\text{ state binding energy}}.$$
2. Several photons are then emitted down to $n = 1$: $\sum_i h\nu_i = E_k + 13.6$ eV.

Volume recombination rate: $R = n_e n_p \alpha_A(T_e)$.

Two limiting cases

Case A: recombination down to all levels: $\alpha_A(T_e) \rightarrow$ relevant for $\tau_{Ly} \ll 1$.

Case B: recombination down to $n > 1$: $\alpha_B(T_e) \equiv \alpha_A(T_e) - \alpha_{1s}(T_e) \rightarrow$ relevant for $\tau_{Ly} \gg 1$.

The recombination cascade

1. Electrons can recombine to any level, nl:
$$\underbrace{h\nu_1}_{\text{first emitted photon}} = \underbrace{E_k}_{\text{electron kinetic energy} \simeq 1\text{ eV}} + \underbrace{E_{nl}}_{nl\text{ state binding energy}}.$$
2. Several photons are then emitted down to $n=1$: $\sum_i h\nu_i = E_k + 13.6$ eV.

Volume recombination rate: $R = n_\mathrm{e} n_\mathrm{p} \alpha_\mathrm{A}(T_\mathrm{e})$.

Two limiting cases

Case A: recombination down to all levels: $\alpha_\mathrm{A}(T_\mathrm{e}) \rightarrow$ relevant for $\tau_\mathrm{Ly} \ll 1$.

Case B: recombination down to $n > 1$: $\alpha_\mathrm{B}(T_\mathrm{e}) \equiv \alpha_\mathrm{A}(T_\mathrm{e}) - \alpha_\mathrm{1s}(T_\mathrm{e}) \rightarrow$ relevant for $\tau_\mathrm{Ly} \gg 1$.

Recombination rates

The recombination cascade

1. Electrons can recombine to any level, nl:

$$\underbrace{h\nu_1}_{\text{first emitted photon}} = \underbrace{E_k}_{\text{electron kinetic energy} \simeq 1\text{ eV}} + \underbrace{E_{nl}}_{nl\text{ state binding energy}} .$$

2. Several photons are then emitted down to $n=1$: $\sum_i h\nu_i = E_k + 13.6$ eV.

Volume recombination rate: $R = n_\mathrm{e} n_\mathrm{p} \alpha_\mathrm{A}(T_\mathrm{e})$.

Two limiting cases

Case A: recombination down to all levels: $\alpha_\mathrm{A}(T_\mathrm{e}) \rightarrow$ relevant for $\tau_\mathrm{Ly} \ll 1$.

Case B: recombination down to $n > 1$: $\alpha_\mathrm{B}(T_\mathrm{e}) \equiv \alpha_\mathrm{A}(T_\mathrm{e}) - \alpha_\mathrm{1s}(T_\mathrm{e}) \rightarrow$ relevant for $\tau_\mathrm{Ly} \gg 1$.

Recombination rates

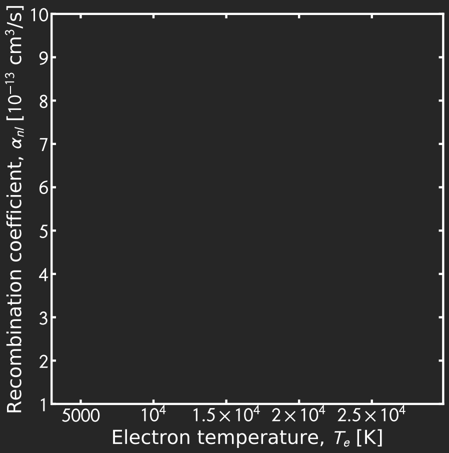

Data from Hummer & Storey (1987).

Atoms | Radiative Recombination of Hydrogen

The recombination cascade

1. Electrons can recombine to any level, nl:

$$\underbrace{h\nu_1}_{\text{first emitted photon}} = \underbrace{E_k}_{\text{electron kinetic energy } \simeq \text{ 1 eV}} + \underbrace{E_{nl}}_{nl \text{ state binding energy}} .$$

2. Several photons are then emitted down to $n = 1$: $\sum_i h\nu_i = E_k + 13.6$ eV.

Volume recombination rate: $R = n_e n_p \alpha_A(T_e)$.

Two limiting cases

Case A: recombination down to all levels: $\alpha_A(T_e) \rightarrow$ relevant for $\tau_{Ly} \ll 1$.

Case B: recombination down to $n > 1$: $\alpha_B(T_e) \equiv \alpha_A(T_e) - \alpha_{1s}(T_e) \rightarrow$ relevant for $\tau_{Ly} \gg 1$.

Recombination rates

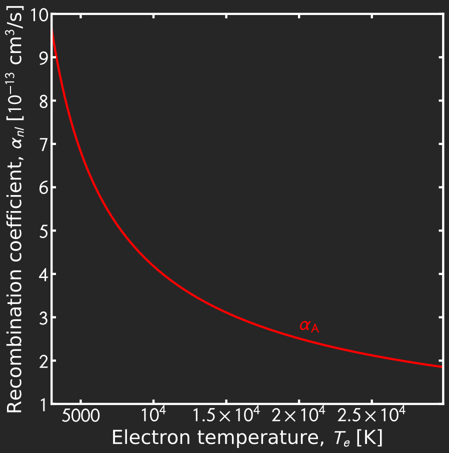

Data from Hummer & Storey (1987).

Atoms | Radiative Recombination of Hydrogen

The recombination cascade

1. Electrons can recombine to any level, nl:
$$\underbrace{h\nu_1}_{\text{first emitted photon}} = \underbrace{E_k}_{\text{electron kinetic energy} \simeq 1 \text{ eV}} + \underbrace{E_{nl}}_{nl \text{ state binding energy}} .$$
2. Several photons are then emitted down to $n = 1$: $\sum_i h\nu_i = E_k + 13.6$ eV.

Volume recombination rate: $R = n_e n_p \alpha_A(T_e)$.

Two limiting cases

Case A: recombination down to all levels: $\alpha_A(T_e) \rightarrow$ relevant for $\tau_{Ly} \ll 1$.

Case B: recombination down to $n > 1$: $\alpha_B(T_e) \equiv \alpha_A(T_e) - \alpha_{1s}(T_e) \rightarrow$ relevant for $\tau_{Ly} \gg 1$.

Recombination rates

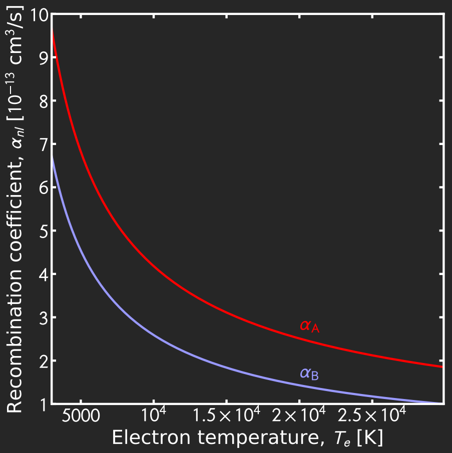

Data from Hummer & Storey (1987).

The Balmer line series

The Balmer line series

- Lyman series line are resonantly scattered $\Rightarrow$ they are re-absorbed by the gas in the case B.

The Balmer line series

- Lyman series line are resonantly scattered $\Rightarrow$ they are re-absorbed by the gas in the case B.
- The strongest escaping ionic resonant lines are from the Balmer series:

The Balmer line series

- Lyman series line are resonantly scattered $\Rightarrow$ they are re-absorbed by the gas in the case B.
- The strongest escaping ionic resonant lines are from the Balmer series:

  Hα line at $\lambda = 6564.6$ Å ($\in$ R band);

The Balmer line series

- Lyman series line are resonantly scattered $\Rightarrow$ they are re-absorbed by the gas in the case B.
- The strongest escaping ionic resonant lines are from the Balmer series:
  Hα line at $\lambda = 6564.6$ Å ($\in$ R band);
  Hβ line at $\lambda = 4862.7$ Å ($\in$ V band).

The Balmer line series

- Lyman series line are resonantly scattered $\Rightarrow$ they are re-absorbed by the gas in the case B.
- The strongest escaping ionic resonant lines are from the Balmer series:
  Hα line at $\lambda = 6564.6$ Å ($\in$ R band);
  Hβ line at $\lambda = 4862.7$ Å ($\in$ V band).
- In case B, $I(\mathrm{H}\alpha)/I(\mathrm{H}\beta) \simeq 3$ (mild T dependence)

The Balmer line series

- Lyman series line are resonantly scattered $\Rightarrow$ they are re-absorbed by the gas in the case B.
- The strongest escaping ionic resonant lines are from the Balmer series:
  Hα line at $\lambda = 6564.6$ Å ($\in$ R band);
  Hβ line at $\lambda = 4862.7$ Å ($\in$ V band).
- In case B, $I(\text{H}\alpha)/I(\text{H}\beta) \simeq 3$ (mild T dependence) $\Rightarrow$ extinction estimator.

The Balmer line series

- Lyman series line are resonantly scattered $\Rightarrow$ they are re-absorbed by the gas in the case B.
- The strongest escaping ionic resonant lines are from the Balmer series:
  Hα line at $\lambda = 6564.6$ Å ($\in$ R band);
  Hβ line at $\lambda = 4862.7$ Å ($\in$ V band).
- In case B, $I(\text{H}\alpha)/I(\text{H}\beta) \simeq 3$ (mild T dependence) $\Rightarrow$ extinction estimator.

Line intensity & Emission Measure (EM)

The Balmer line series

- Lyman series line are resonantly scattered $\Rightarrow$ they are re-absorbed by the gas in the case B.
- The strongest escaping ionic resonant lines are from the Balmer series:
  Hα line at $\lambda = 6564.6$ Å ($\in$ R band);
  Hβ line at $\lambda = 4862.7$ Å ($\in$ V band).
- In case B, $I(\mathrm{H}\alpha)/I(\mathrm{H}\beta) \simeq 3$ (mild T dependence) $\Rightarrow$ extinction estimator.

Line intensity & Emission Measure (EM)

- Optically-thin limit, below critical density:

$$I_{\mathrm{line}} = \int_0^L \frac{n_e^2}{4\pi}\Lambda(T)\,\mathrm{d}s$$

The Balmer line series

- Lyman series line are resonantly scattered $\Rightarrow$ they are re-absorbed by the gas in the case B.
- The strongest escaping ionic resonant lines are from the Balmer series:
  Hα line at $\lambda = 6564.6$ Å ($\in$ R band);
  Hβ line at $\lambda = 4862.7$ Å ($\in$ V band).
- In case B, $I(\text{H}\alpha)/I(\text{H}\beta) \simeq 3$ (mild T dependence) $\Rightarrow$ extinction estimator.

Line intensity & Emission Measure (EM)

- Optically-thin limit, below critical density:

$$I_{\text{line}} = \int_0^L \frac{n_e^2}{4\pi} \Lambda(T)\,\text{d}s \propto \underbrace{EM}_{\text{cm}^{-6}\text{pc}} \times \Lambda(T);$$

The Balmer line series

- Lyman series line are resonantly scattered $\Rightarrow$ they are re-absorbed by the gas in the case B.
- The strongest escaping ionic resonant lines are from the Balmer series:
  Hα line at $\lambda = 6564.6$ Å ($\in$ R band);
  Hβ line at $\lambda = 4862.7$ Å ($\in$ V band).
- In case B, $I(\mathrm{H}\alpha)/I(\mathrm{H}\beta) \simeq 3$ (mild T dependence) $\Rightarrow$ extinction estimator.

Line intensity & Emission Measure (EM)

- Optically-thin limit, below critical density:
  $$I_{\rm line} = \int_0^L \frac{n_e^2}{4\pi}\Lambda(T)\,\mathrm{d}s \propto \underbrace{EM}_{\rm cm^{-6}pc} \times\Lambda(T);$$
- With $EM \equiv \int_0^L n_e^2\,\mathrm{d}s$

The Balmer line series

- Lyman series line are resonantly scattered $\Rightarrow$ they are re-absorbed by the gas in the case B.
- The strongest escaping ionic resonant lines are from the Balmer series:
  Hα line at $\lambda = 6564.6$ Å ($\in$ R band);
  Hβ line at $\lambda = 4862.7$ Å ($\in$ V band).
- In case B, $I(\mathrm{H}\alpha)/I(\mathrm{H}\beta) \simeq 3$ (mild T dependence) $\Rightarrow$ extinction estimator.

Line intensity & Emission Measure (EM)

- Optically-thin limit, below critical density:
  $$I_{\mathrm{line}} = \int_0^L \frac{n_e^2}{4\pi}\Lambda(T)\,\mathrm{d}s \propto \underbrace{EM}_{\mathrm{cm}^{-6}\mathrm{pc}} \times \Lambda(T);$$
- With $EM \equiv \displaystyle\int_0^L n_e^2\,\mathrm{d}s \Rightarrow \boxed{EM \simeq \langle n_e^2 \rangle L}$.

The Balmer line series

- Lyman series line are resonantly scattered $\Rightarrow$ they are re-absorbed by the gas in the case B.
- The strongest escaping ionic resonant lines are from the Balmer series:
  Hα line at $\lambda = 6564.6$ Å ($\in$ R band);
  Hβ line at $\lambda = 4862.7$ Å ($\in$ V band).
- In case B, $I(\mathrm{H}\alpha)/I(\mathrm{H}\beta) \simeq 3$ (mild T dependence) $\Rightarrow$ extinction estimator.

Line intensity & Emission Measure (EM)

- Optically-thin limit, below critical density:
$$I_{\rm line} = \int_0^L \frac{n_e^2}{4\pi}\Lambda(T)\,{\rm d}s \propto \underbrace{EM}_{\rm cm^{-6}pc} \times \Lambda(T);$$
- With $EM \equiv \int_0^L n_e^2\,{\rm d}s \Rightarrow \boxed{EM \simeq \langle n_e^2 \rangle L}$.

The Large Magellanic Cloud (LMC)

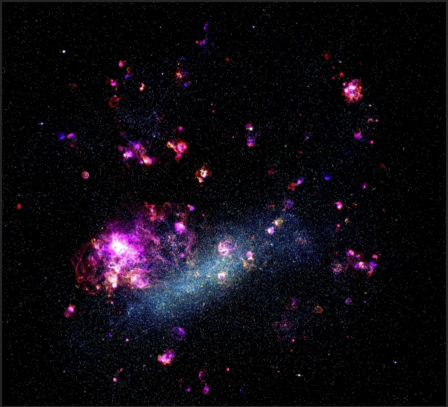

Credit: Hα + [S II]$_{6725Å}$ + [O III]$_{5007Å}$ (Smith et al., 2005).

The Balmer line series

- Lyman series line are resonantly scattered $\Rightarrow$ they are re-absorbed by the gas in the case B.
- The strongest escaping ionic resonant lines are from the Balmer series:
  Hα line at $\lambda = 6564.6$ Å ($\in$ R band);
  Hβ line at $\lambda = 4862.7$ Å ($\in$ V band).
- In case B, $I(\mathrm{H}\alpha)/I(\mathrm{H}\beta) \simeq 3$ (mild T dependence) $\Rightarrow$ extinction estimator.

Line intensity & Emission Measure (EM)

- Optically-thin limit, below critical density:

$$I_{\text{line}} = \int_0^L \frac{n_e^2}{4\pi}\Lambda(T)\,\mathrm{d}s \propto \underbrace{EM}_{\text{cm}^{-6}\text{pc}} \times \Lambda(T);$$

- With $EM \equiv \int_0^L n_e^2\,\mathrm{d}s \Rightarrow \boxed{EM \simeq \langle n_e^2 \rangle L}$.

The Large Magellanic Cloud (LMC)

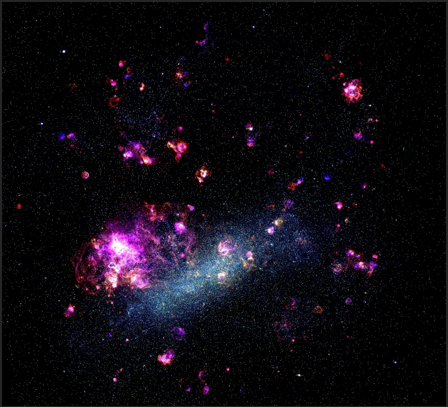

Credit: Hα + [S II]$_{6725\text{Å}}$ + [O III]$_{5007\text{Å}}$ (Smith et al., 2005).

$\Rightarrow$ Hα traces essentially dense ionized gas (H II regions).

Thermal plasma

Thermal plasma

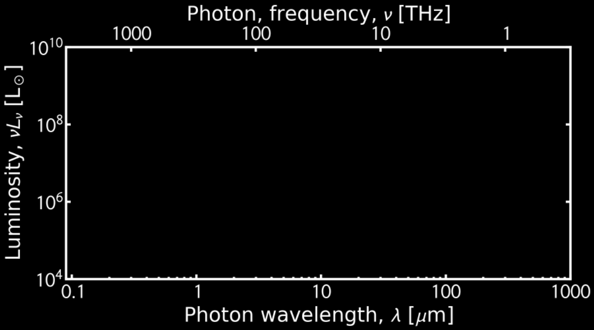

Thermal plasma

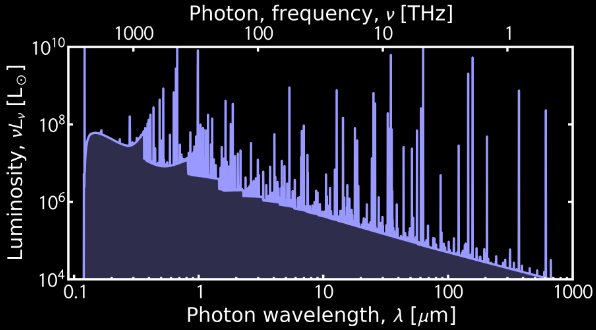

Thermal plasma

Bound-bound transitions: recombination lines.

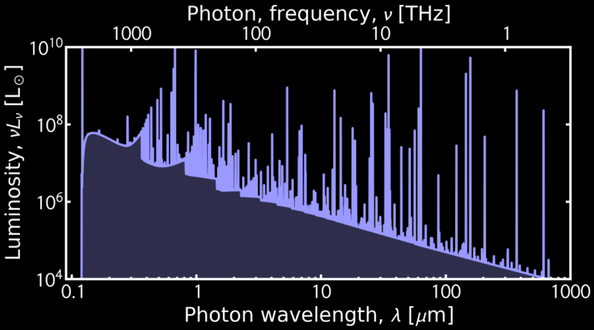

Thermal plasma

Bound-bound transitions: recombination lines.

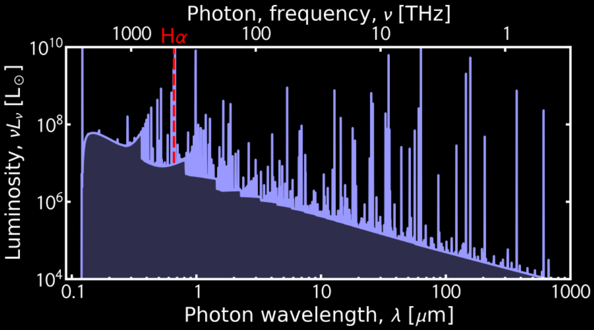

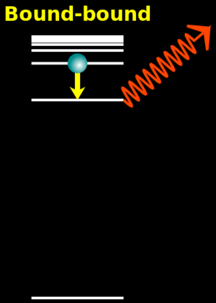

Thermal plasma

Bound-bound transitions: recombination lines.

Free-bound transitions: first transition of the recombination cascade.

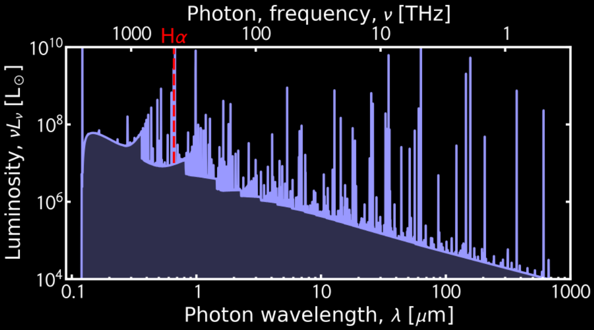

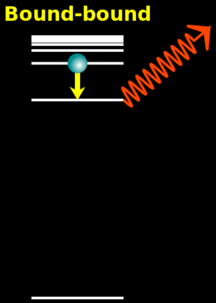

Thermal plasma

Bound-bound transitions: recombination lines.

Free-bound transitions: first transition of the recombination cascade.

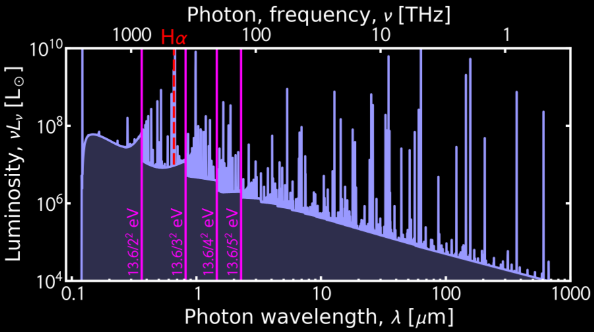

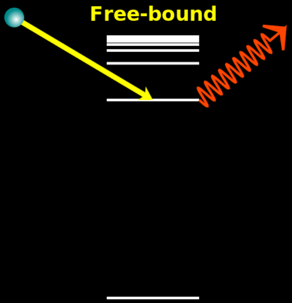

Thermal plasma

Bound-bound transitions: recombination lines.

Free-bound transitions: first transition of the recombination cascade.

Free-free transitions: deceleration of a free electron by the charge of a proton → inelastic collision.

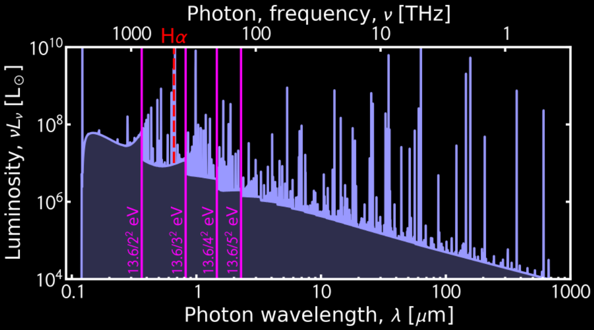

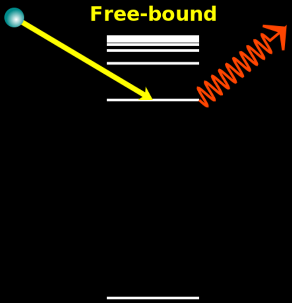

Thermal plasma

Bound-bound transitions: recombination lines.

Free-bound transitions: first transition of the recombination cascade.

Free-free transitions: deceleration of a free electron by the charge of a proton → in-elastic collision.

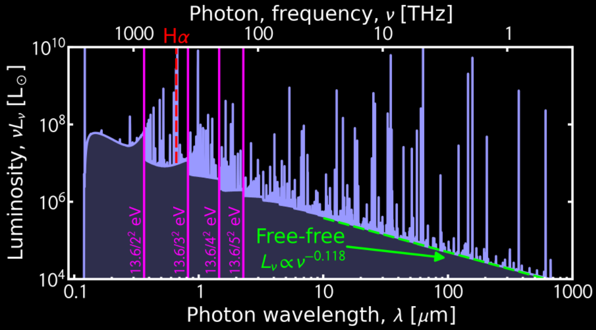

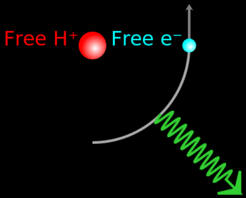

Thermal plasma

Bound-bound transitions: recombination lines.

Free-bound transitions: first transition of the recombination cascade.

Free-free transitions: deceleration of a free electron by the charge of a proton → inelastic collision.

Hydrogen free-free spectrum (Draine, 2011)

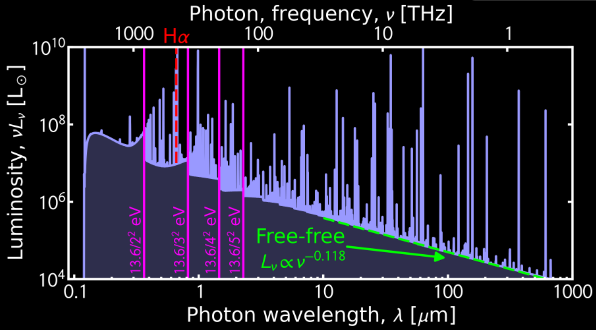

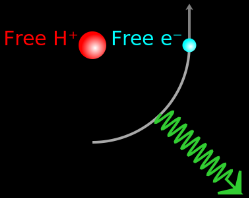

Thermal plasma

Bound-bound transitions: recombination lines.

Free-bound transitions: first transition of the recombination cascade.

Free-free transitions: deceleration of a free electron by the charge of a proton → inelastic collision.

Hydrogen free-free spectrum (Draine, 2011)

$$\underbrace{\frac{dP_\nu^{ff}}{dV}}_{[\text{W cm}^3/\text{Hz}]} \simeq 6.841\times10^{-47}\underbrace{g_{ff}(\nu)}_{\text{Gaunt factor}}\sqrt{\frac{T}{10^4\text{ K}}}\times\exp\left(-\frac{h\nu}{kT}\right)n_e^2$$

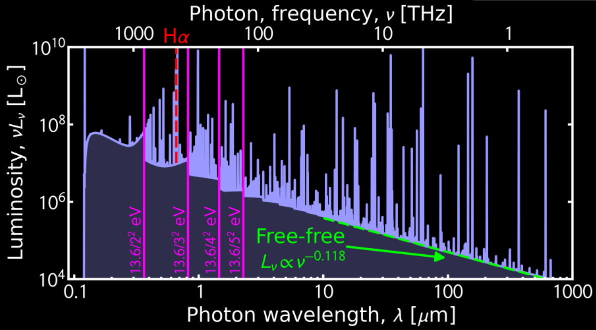

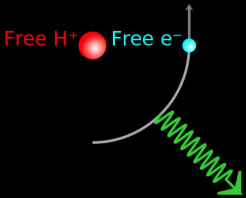

Thermal plasma

Bound-bound transitions: recombination lines.

Free-bound transitions: first transition of the recombination cascade.

Free-free transitions: deceleration of a free electron by the charge of a proton → inelastic collision.

Hydrogen free-free spectrum (Draine, 2011)

$$\underbrace{\frac{\mathrm{d}P_\nu^{ff}}{\mathrm{d}V}}_{[\mathrm{W\,cm^3/Hz}]} \simeq 6.841\times10^{-47}\underbrace{g_{ff}(\nu)}_{\text{Gaunt factor}}\sqrt{\frac{T}{10^4\text{ K}}} \times \exp\left(-\frac{h\nu}{kT}\right)n_e^2$$

$$\rightarrow g_{ff} \simeq 6.155\left(\frac{\nu}{1\text{ GHz}}\right)^{-0.118}\left(\frac{T}{10^4\text{ K}}\right)^{0.177}.$$

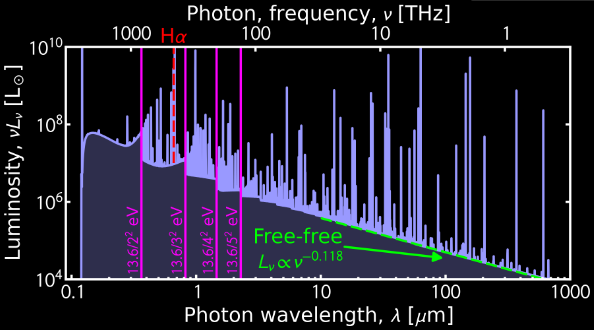

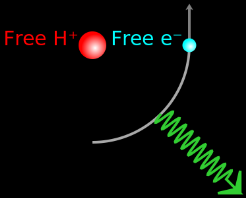

Outline of the Lecture

Molecules | Electronic, Rotational & Vibrational Modes

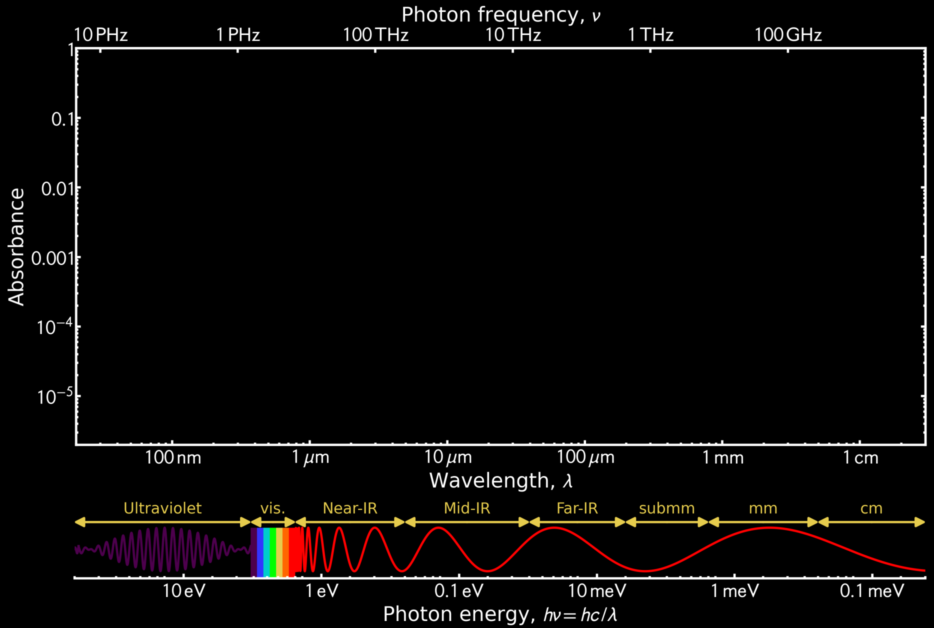

Molecules | Electronic, Rotational & Vibrational Modes

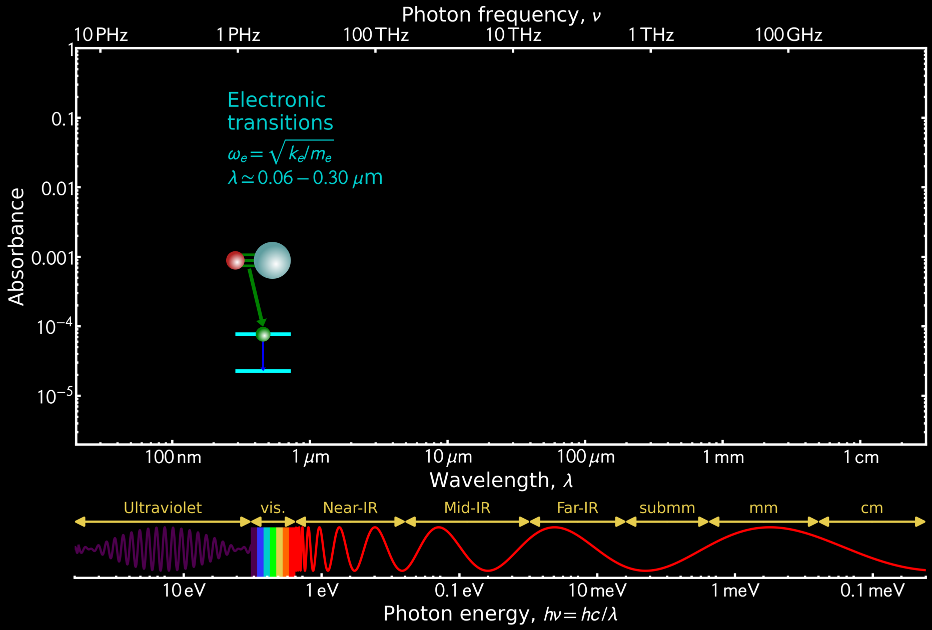

Molecules | Electronic, Rotational & Vibrational Modes

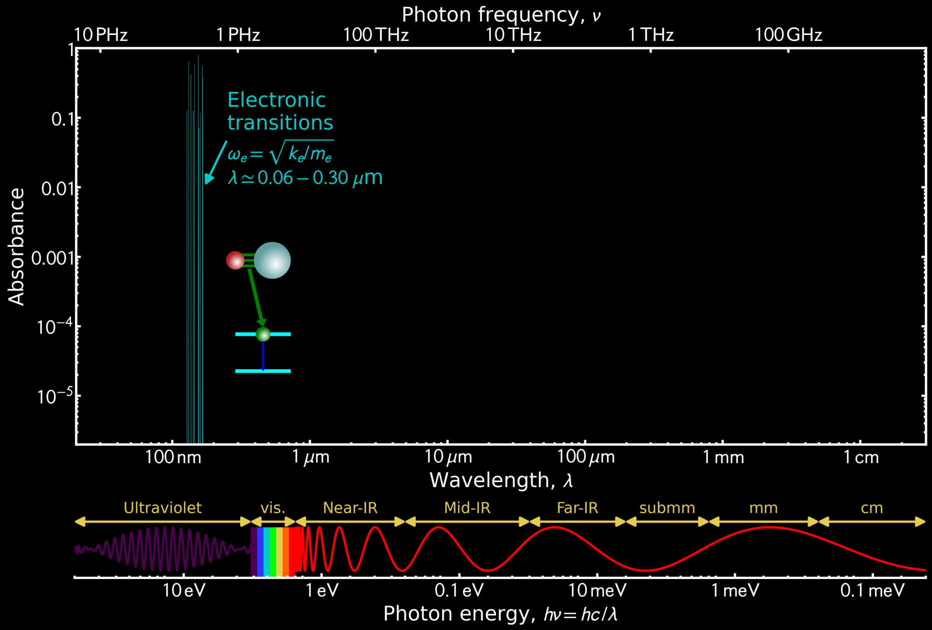

Molecules | Electronic, Rotational & Vibrational Modes

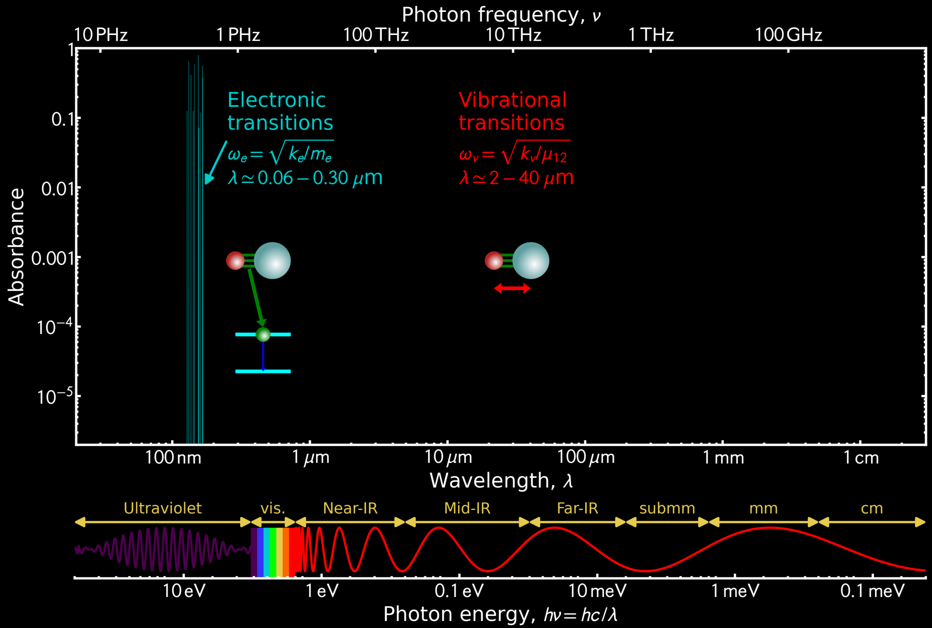

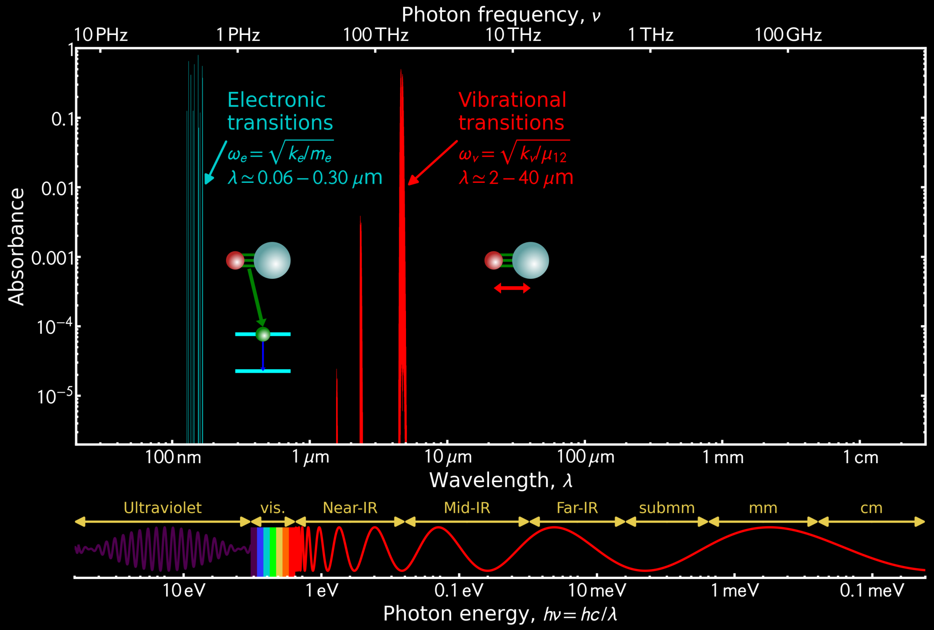

Photon frequency, ν
10 PHz
1 PHz
100 THz
10 THz
1 THz
100 GHz
Absorbance
1
0.1
0.01
0.001
10^{-4}
10^{-5}
Electronic transitions
$\omega_e = \sqrt{k_e/m_e}$
$\lambda \simeq 0.06 - 0.30\ \mu m$
Vibrational transitions
$\omega_v = \sqrt{k_v/\mu_{12}}$
$\lambda \simeq 2 - 40\ \mu m$
100 nm
1 μm
10 μm
100 μm
1 mm
1 cm
Wavelength, λ
Ultraviolet
vis.
Near-IR
Mid-IR
Far-IR
submm
mm
cm
10 eV
1 eV
0.1 eV
10 meV
1 meV
0.1 meV
Photon energy, $h\nu = hc/\lambda$

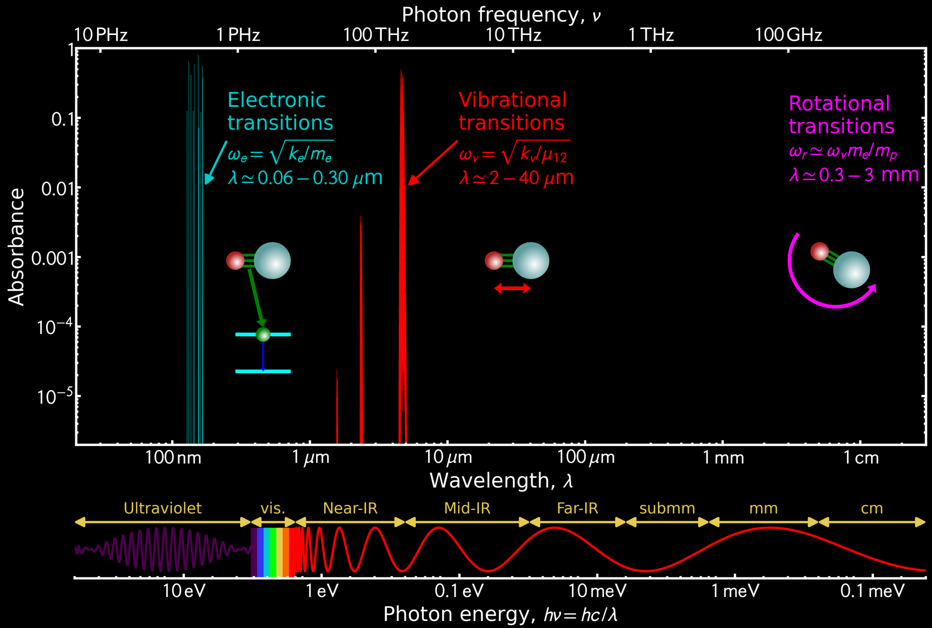
Photon frequency, ν
10 PHz
1 PHz
100 THz
10 THz
1 THz
100 GHz
Absorbance
1
0.1
0.01
0.001
10^{-4}
10^{-5}
Electronic transitions
$\omega_e = \sqrt{k_e/m_e}$
$\lambda \simeq 0.06 - 0.30\,\mu$m
Vibrational transitions
$\omega_v = \sqrt{k_v/\mu_{12}}$
$\lambda \simeq 2 - 40\,\mu$m
Rotational transitions
$\omega_r \simeq \omega_v m_e/m_p$
$\lambda \simeq 0.3 - 3$ mm
100 nm
1 μm
10 μm
100 μm
1 mm
1 cm
Wavelength, λ
Ultraviolet
vis.
Near-IR
Mid-IR
Far-IR
submm
mm
cm
10 eV
1 eV
0.1 eV
10 meV
1 meV
0.1 meV
Photon energy, $h\nu = hc/\lambda$

Molecules | Electronic, Rotational & Vibrational Modes

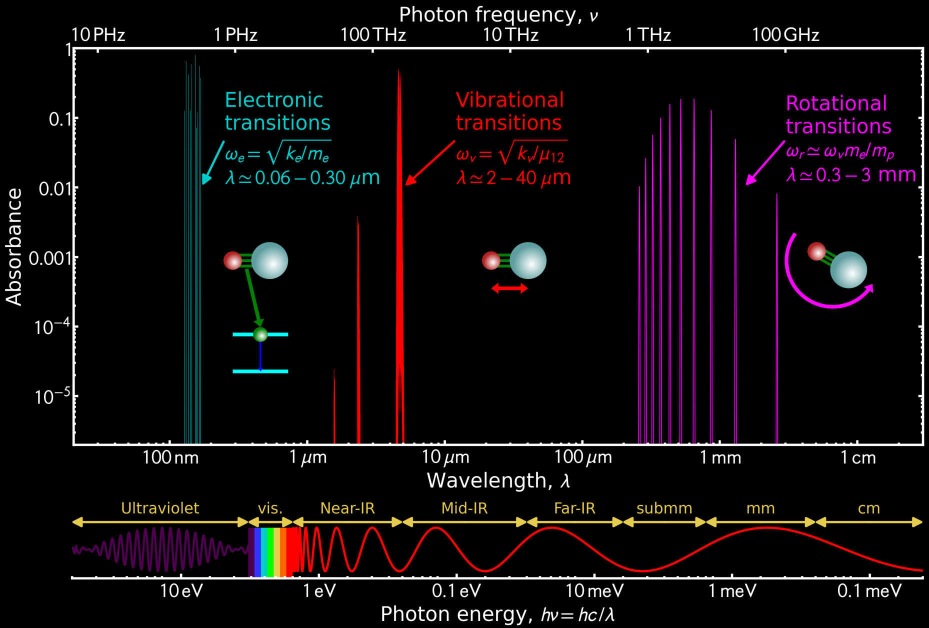

Level notation

Level notation

- Angular momentum of a bonding electron: $\lambda = 0 \Leftrightarrow \sigma$, $\lambda = 1 \Leftrightarrow \pi$, $\lambda = 2 \Leftrightarrow \delta$, ...

Level notation

- Angular momentum of a bonding electron: $\lambda = 0 \Leftrightarrow \sigma$, $\lambda = 1 \Leftrightarrow \pi$, $\lambda = 2 \Leftrightarrow \delta$, ...
- $\Lambda = \sum_i \lambda_i$, for all electrons, with: $\Lambda = 0 \Leftrightarrow \Sigma$, $\Lambda = 1 \Leftrightarrow \Pi$, $\Lambda = 2 \Leftrightarrow \Delta$, ...

Level notation

- Angular momentum of a bonding electron: $\lambda = 0 \Leftrightarrow \sigma$, $\lambda = 1 \Leftrightarrow \pi$, $\lambda = 2 \Leftrightarrow \delta$, ...
- $\Lambda = \sum_i \lambda_i$, for all electrons, with: $\Lambda = 0 \Leftrightarrow \Sigma$, $\Lambda = 1 \Leftrightarrow \Pi$, $\Lambda = 2 \Leftrightarrow \Delta$, ...
- Electronic levels are noted $n = 1 \Leftrightarrow X$, $n = 2 \Leftrightarrow A$, $n = 3 \Leftrightarrow B$, $\ldots \Rightarrow$ level notation: $\boxed{X^{2S+1}\Lambda}$.

Molecules | Energy Levels of H_2

Level notation

- Angular momentum of a bonding electron: $\lambda = 0 \Leftrightarrow \sigma$, $\lambda = 1 \Leftrightarrow \pi$, $\lambda = 2 \Leftrightarrow \delta$, ...
- $\Lambda = \sum_i \lambda_i$, for all electrons, with: $\Lambda = 0 \Leftrightarrow \Sigma$, $\Lambda = 1 \Leftrightarrow \Pi$, $\Lambda = 2 \Leftrightarrow \Delta$, ...
- Electronic levels are noted $n = 1 \Leftrightarrow X$, $n = 2 \Leftrightarrow A$, $n = 3 \Leftrightarrow B$, ... $\Rightarrow$ level notation: $\boxed{X^{2S+1}\Lambda}$.

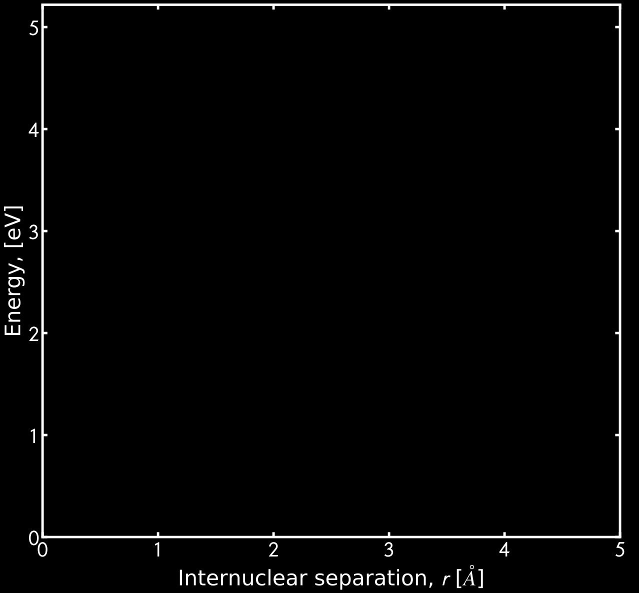

Level notation

- Angular momentum of a bonding electron: $\lambda = 0 \Leftrightarrow \sigma$, $\lambda = 1 \Leftrightarrow \pi$, $\lambda = 2 \Leftrightarrow \delta$, ...
- $\Lambda = \sum_i \lambda_i$, for all electrons, with: $\Lambda = 0 \Leftrightarrow \Sigma$, $\Lambda = 1 \Leftrightarrow \Pi$, $\Lambda = 2 \Leftrightarrow \Delta$, ...
- Electronic levels are noted $n = 1 \Leftrightarrow X$, $n = 2 \Leftrightarrow A$, $n = 3 \Leftrightarrow B$, ... $\Rightarrow$ level notation: $\boxed{X^{2S+1}\Lambda}$.

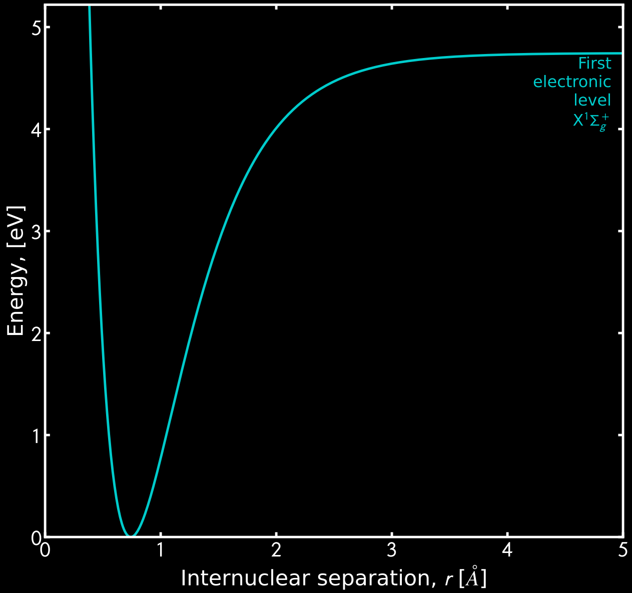

Level notation

- Angular momentum of a bonding electron: $\lambda = 0 \Leftrightarrow \sigma$, $\lambda = 1 \Leftrightarrow \pi$, $\lambda = 2 \Leftrightarrow \delta$, ...
- $\Lambda = \sum_i \lambda_i$, for all electrons, with: $\Lambda = 0 \Leftrightarrow \Sigma$, $\Lambda = 1 \Leftrightarrow \Pi$, $\Lambda = 2 \Leftrightarrow \Delta$, ...
- Electronic levels are noted $n = 1 \Leftrightarrow X$, $n = 2 \Leftrightarrow A$, $n = 3 \Leftrightarrow B$, $\ldots \Rightarrow$ level notation: $\boxed{X^{2S+1}\Lambda}$.

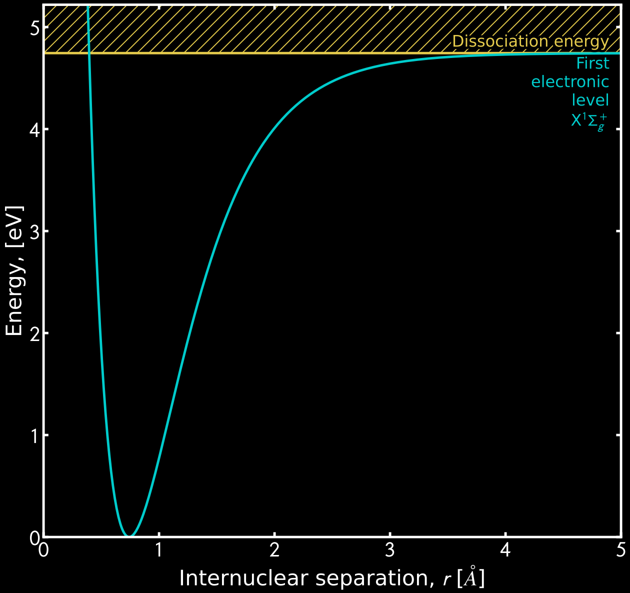

Level notation

- Angular momentum of a bonding electron: $\lambda = 0 \Leftrightarrow \sigma$, $\lambda = 1 \Leftrightarrow \pi$, $\lambda = 2 \Leftrightarrow \delta$, ...
- $\Lambda = \sum_i \lambda_i$, for all electrons, with: $\Lambda = 0 \Leftrightarrow \Sigma$, $\Lambda = 1 \Leftrightarrow \Pi$, $\Lambda = 2 \Leftrightarrow \Delta$, ...
- Electronic levels are noted $n = 1 \Leftrightarrow X$, $n = 2 \Leftrightarrow A$, $n = 3 \Leftrightarrow B$, $\ldots \Rightarrow$ level notation: $\boxed{X^{2S+1}\Lambda}$.

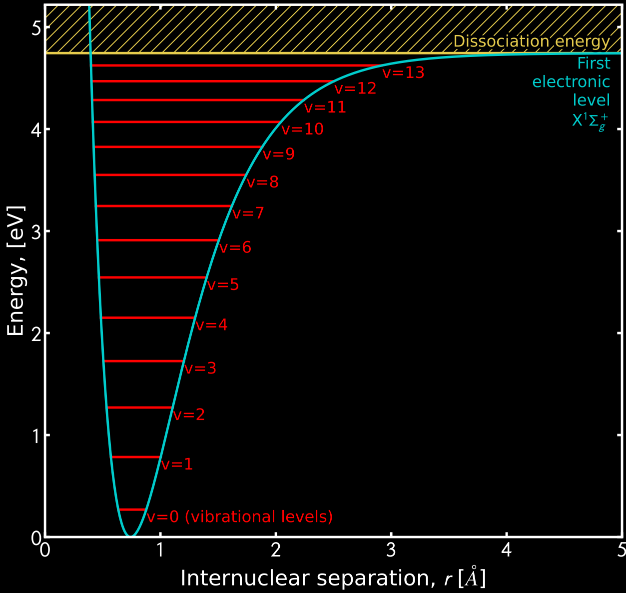

Level notation

- Angular momentum of a bonding electron: $\lambda = 0 \Leftrightarrow \sigma$, $\lambda = 1 \Leftrightarrow \pi$, $\lambda = 2 \Leftrightarrow \delta$, ...
- $\Lambda = \sum_i \lambda_i$, for all electrons, with: $\Lambda = 0 \Leftrightarrow \Sigma$, $\Lambda = 1 \Leftrightarrow \Pi$, $\Lambda = 2 \Leftrightarrow \Delta$, ...
- Electronic levels are noted $n = 1 \Leftrightarrow X$, $n = 2 \Leftrightarrow A$, $n = 3 \Leftrightarrow B$, ... $\Rightarrow$ level notation: $\boxed{X^{2S+1}\Lambda}$.

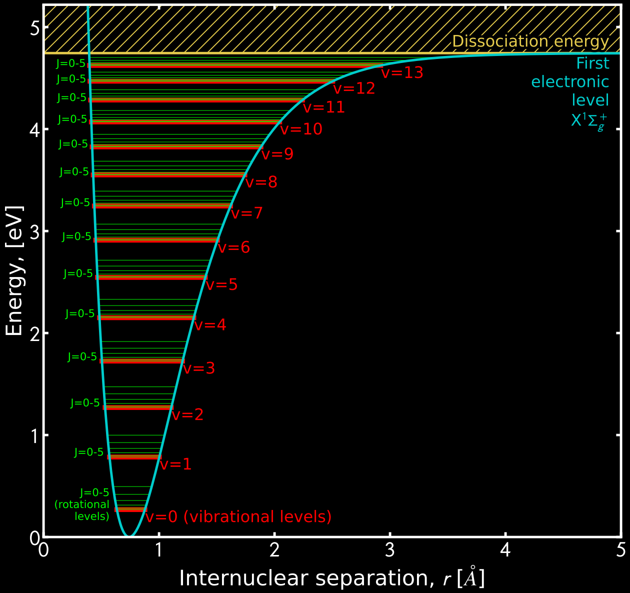

Level notation

- Angular momentum of a bonding electron: $\lambda = 0 \Leftrightarrow \sigma$, $\lambda = 1 \Leftrightarrow \pi$, $\lambda = 2 \Leftrightarrow \delta$, ...
- $\Lambda = \sum_i \lambda_i$, for all electrons, with: $\Lambda = 0 \Leftrightarrow \Sigma$, $\Lambda = 1 \Leftrightarrow \Pi$, $\Lambda = 2 \Leftrightarrow \Delta$, ...
- Electronic levels are noted $n = 1 \Leftrightarrow X$, $n = 2 \Leftrightarrow A$, $n = 3 \Leftrightarrow B$, $\ldots \Rightarrow$ level notation: $\boxed{X^{2S+1}\Lambda}$.
- Ro-vibrational lines: transitions between different vibrational & rotational levels of the same electronic state.

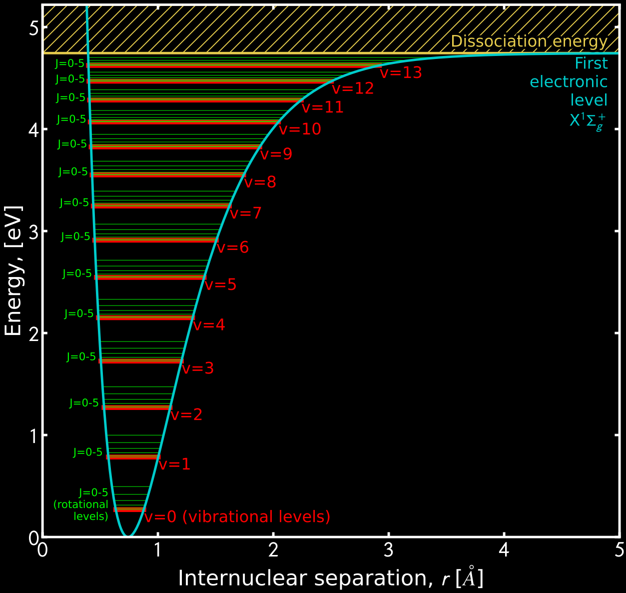

Level notation

- Angular momentum of a bonding electron: $\lambda = 0 \Leftrightarrow \sigma$, $\lambda = 1 \Leftrightarrow \pi$, $\lambda = 2 \Leftrightarrow \delta$, ...
- $\Lambda = \sum_i \lambda_i$, for all electrons, with: $\Lambda = 0 \Leftrightarrow \Sigma$, $\Lambda = 1 \Leftrightarrow \Pi$, $\Lambda = 2 \Leftrightarrow \Delta$, ...
- Electronic levels are noted $n = 1 \Leftrightarrow X$, $n = 2 \Leftrightarrow A$, $n = 3 \Leftrightarrow B$, ... $\Rightarrow$ level notation: $\boxed{X^{2S+1}\Lambda}$.
- Ro-vibrational lines: transitions between different vibrational & rotational levels of the same electronic state.

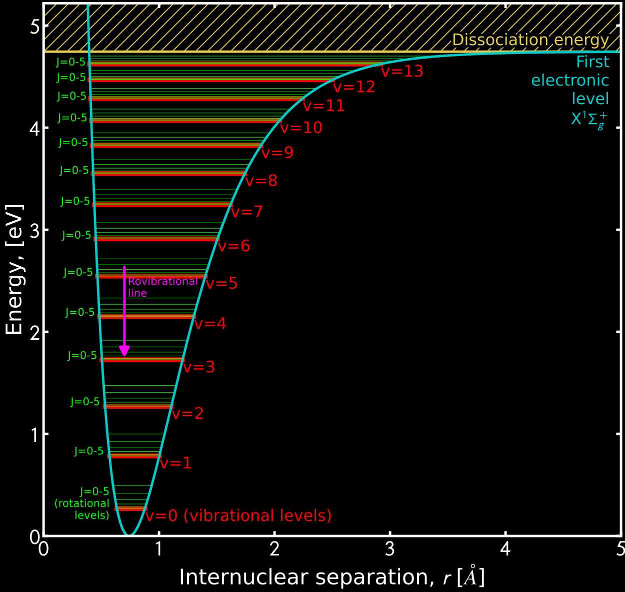

Level notation

- Angular momentum of a bonding electron: $\lambda = 0 \Leftrightarrow \sigma$, $\lambda = 1 \Leftrightarrow \pi$, $\lambda = 2 \Leftrightarrow \delta$, ...
- $\Lambda = \sum_i \lambda_i$, for all electrons, with: $\Lambda = 0 \Leftrightarrow \Sigma$, $\Lambda = 1 \Leftrightarrow \Pi$, $\Lambda = 2 \Leftrightarrow \Delta$, ...
- Electronic levels are noted $n = 1 \Leftrightarrow X$, $n = 2 \Leftrightarrow A$, $n = 3 \Leftrightarrow B$, ... $\Rightarrow$ level notation: $\boxed{X^{2S+1}\Lambda}$.
- Ro-vibrational lines: transitions between different vibrational & rotational levels of the same electronic state.

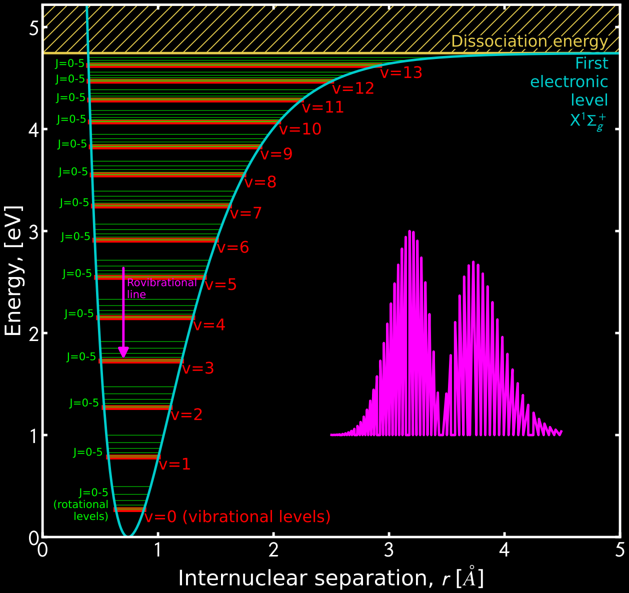

Level notation

- Angular momentum of a bonding electron: $\lambda = 0 \Leftrightarrow \sigma$, $\lambda = 1 \Leftrightarrow \pi$, $\lambda = 2 \Leftrightarrow \delta$, ...
- $\Lambda = \sum_i \lambda_i$, for all electrons, with: $\Lambda = 0 \Leftrightarrow \Sigma$, $\Lambda = 1 \Leftrightarrow \Pi$, $\Lambda = 2 \Leftrightarrow \Delta$, ...
- Electronic levels are noted $n = 1 \Leftrightarrow X$, $n = 2 \Leftrightarrow A$, $n = 3 \Leftrightarrow B$, ... ⇒ level notation: $\boxed{X^{2S+1}\Lambda}$.
- Ro-vibrational lines: transitions between different vibrational & rotational levels of the same electronic state.

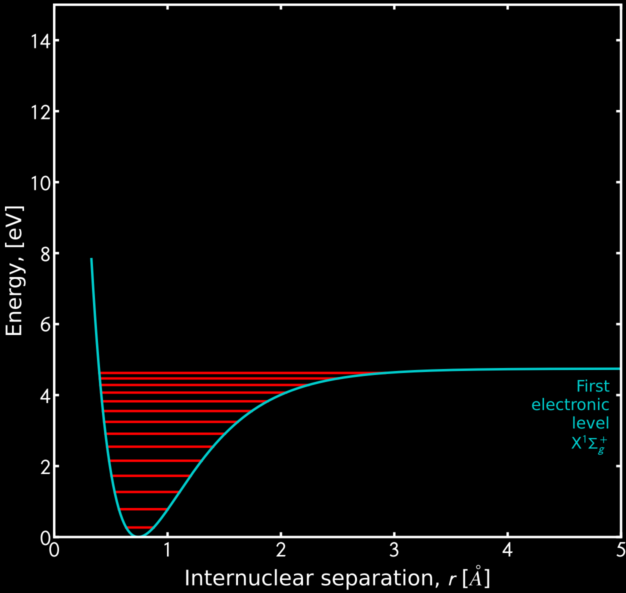

Level notation

- Angular momentum of a bonding electron: $\lambda = 0 \Leftrightarrow \sigma$, $\lambda = 1 \Leftrightarrow \pi$, $\lambda = 2 \Leftrightarrow \delta$, ...
- $\Lambda = \sum_i \lambda_i$, for all electrons, with: $\Lambda = 0 \Leftrightarrow \Sigma$, $\Lambda = 1 \Leftrightarrow \Pi$, $\Lambda = 2 \Leftrightarrow \Delta$, ...
- Electronic levels are noted $n = 1 \Leftrightarrow X$, $n = 2 \Leftrightarrow A$, $n = 3 \Leftrightarrow B$, ... ⇒ level notation: $\boxed{X^{2S+1}\Lambda}$.
- Ro-vibrational lines: transitions between different vibrational & rotational levels of the same electronic state.

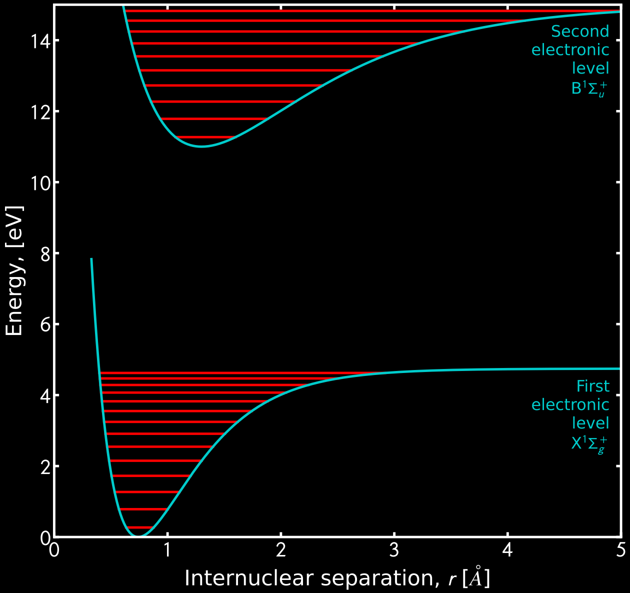

Level notation

- Angular momentum of a bonding electron: $\lambda = 0 \Leftrightarrow \sigma$, $\lambda = 1 \Leftrightarrow \pi$, $\lambda = 2 \Leftrightarrow \delta$, $\ldots$
- $\Lambda = \sum_i \lambda_i$, for all electrons, with: $\Lambda = 0 \Leftrightarrow \Sigma$, $\Lambda = 1 \Leftrightarrow \Pi$, $\Lambda = 2 \Leftrightarrow \Delta$, $\ldots$
- Electronic levels are noted $n = 1 \Leftrightarrow X$, $n = 2 \Leftrightarrow A$, $n = 3 \Leftrightarrow B$, $\ldots \Rightarrow$ level notation: $\boxed{X^{2S+1}\Lambda}$.
- Ro-vibrational lines: transitions between different vibrational & rotational levels of the same electronic state.

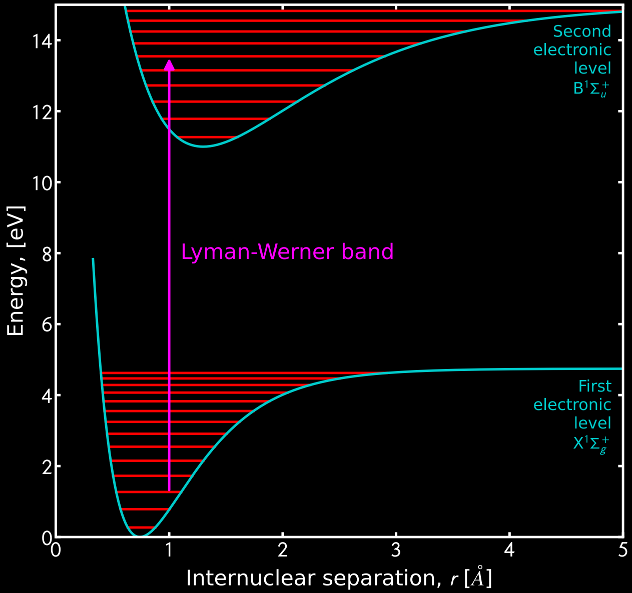

Strong Bonds (several eV)

Strong Bonds (several eV)

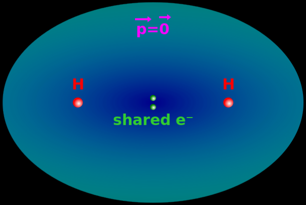

(a) Covalent bond: H_2
(between 2 non-metal atoms)

Strong Bonds (several eV)

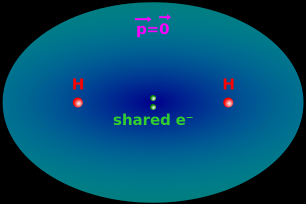

(a) Covalent bond: H_2
(between 2 non-metal atoms)

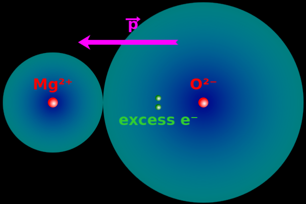

(b) Ionic bond: Mg-O in silicates
(between 1 metal & 1 non-metal atoms)

Strong Bonds (several eV)

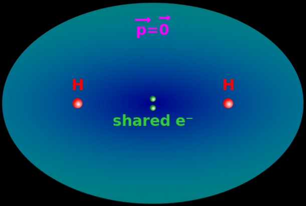

(a) Covalent bond: H_2
(between 2 non-metal atoms)

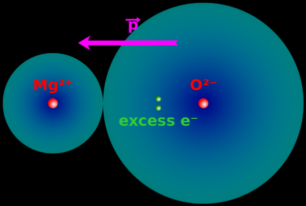

(b) Ionic bond: Mg-O in silicates
(between 1 metal & 1 non-metal atoms)

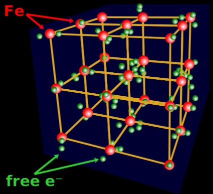

(c) Metallic bond: Fe
(between metal atoms)

Strong Bonds (several eV)

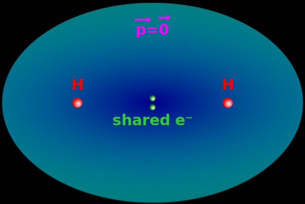

(a) Covalent bond: H_2
(between 2 non-metal atoms)

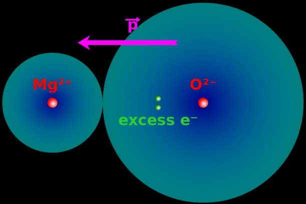

(b) Ionic bond: Mg-O in silicates
(between 1 metal & 1 non-metal atoms)

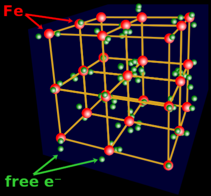

(c) Metallic bond: Fe
(between metal atoms)

Weak Bonds (a few 0.1 eV)

Strong Bonds (several eV)

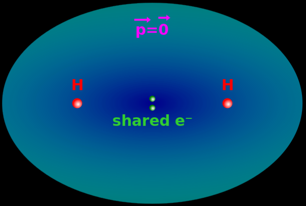

(a) Covalent bond: H_2
(between 2 non-metal atoms)

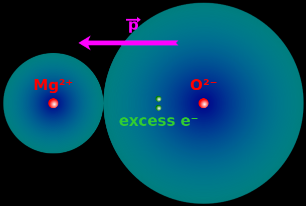

(b) Ionic bond: Mg-O in silicates
(between 1 metal & 1 non-metal atoms)

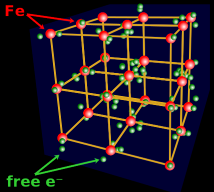

(c) Metallic bond: Fe
(between metal atoms)

Weak Bonds (a few 0.1 eV)

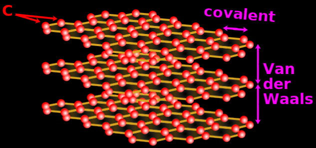

(d) Van der Waals force: graphite

Strong Bonds (several eV)

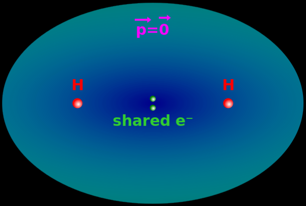

(a) Covalent bond: H_2
(between 2 non-metal atoms)

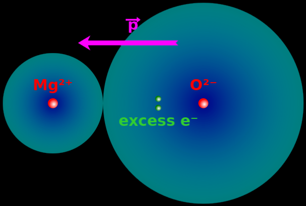

(b) Ionic bond: Mg-O in silicates
(between 1 metal & 1 non-metal atoms)

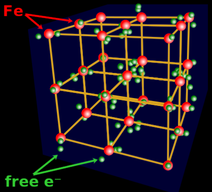

(c) Metallic bond: Fe
(between metal atoms)

Weak Bonds (a few 0.1 eV)

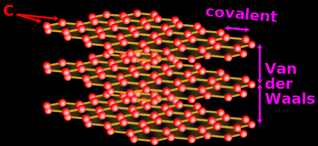

(d) Van der Waals force: graphite

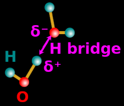

(e) Hydrogen bridge: H_2O ice

The principle of orbital hybridization

The principle of orbital hybridization

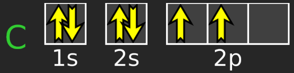

The principle of orbital hybridization

The principle of orbital hybridization

The principle of orbital hybridization

sp^3 hybrid

The principle of orbital hybridization

sp^3 hybrid

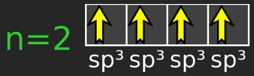

The principle of orbital hybridization

sp^3 hybrid

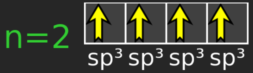

Example: methane (CH_4).

The principle of orbital hybridization

sp^3 hybrid

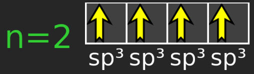

Example: methane (CH_4).

Mix: $1/4$ s + $3/4$ p.

The principle of orbital hybridization

sp^3 hybrid

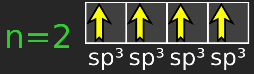

Example: methane (CH_4).

Mix: 1/4 s + 3/4 p.

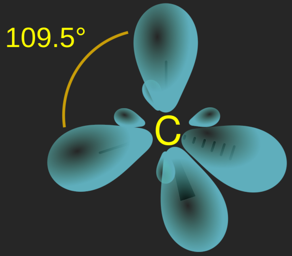

The principle of orbital hybridization

sp^3 hybrid

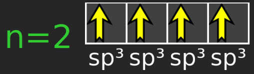

Example: methane (CH_4).

Mix: 1/4 s + 3/4 p.

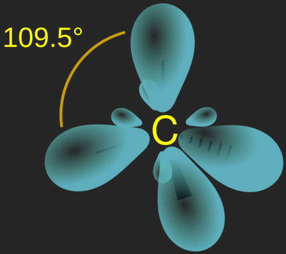

sp^2 hybrid

The principle of orbital hybridization

C [↑↓] 1s [↑↓] 2s [↑][↑][ ] 2p — **Electron promotion** (4.2 eV) → C* [↑↓] 1s [↑] 2s [↑][↑][↑] 2p

sp^3 hybrid

n=2 [↑][↑][↑][↑]
sp^3 sp^3 sp^3 sp^3

Example: methane (CH_4).

Mix: 1/4 s + 3/4 p.

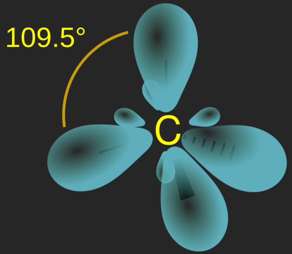

sp^2 hybrid

n=2 [↑][↑][↑][↑]
sp^2 sp^2 sp^2 p

The principle of orbital hybridization

C: 1s 2s 2p —— Electron promotion (4.2 eV) ——> C*: 1s 2s 2p

sp^3 hybrid

n=2: sp^3 sp^3 sp^3 sp^3

Example: methane (CH_4).

Mix: 1/4 s + 3/4 p.

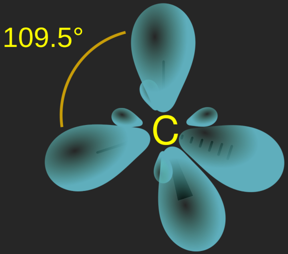

sp^2 hybrid

n=2: sp^2 sp^2 sp^2 p

Example: benzene (C_6H_6).

The principle of orbital hybridization

sp^3 hybrid

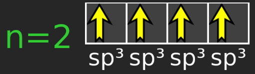

Example: methane (CH_4).

Mix: 1/4 s + 3/4 p.

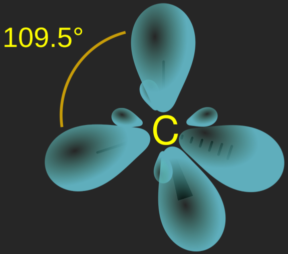

sp^2 hybrid

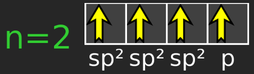

Example: benzene (C_6H_6).

Mix: 1/3 s + 2/3 p.

The principle of orbital hybridization

sp^3 hybrid

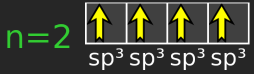

Example: methane (CH_4).

Mix: 1/4 s + 3/4 p.

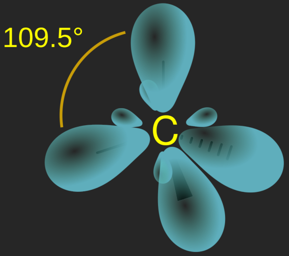

sp^2 hybrid

Example: benzene (C_6H_6).

Mix: 1/3 s + 2/3 p.

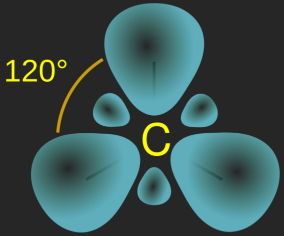

The principle of orbital hybridization

sp^3 hybrid

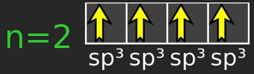

Example: methane (CH_4).

Mix: 1/4 s + 3/4 p.

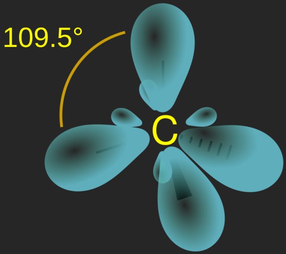

sp^2 hybrid

Example: benzene (C_6H_6).

Mix: 1/3 s + 2/3 p.

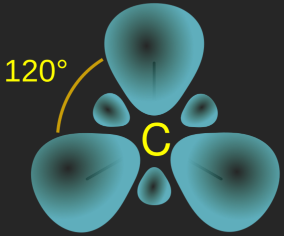

sp hybrid

The principle of orbital hybridization

C: 1s ↑↓ 2s ↑↓ 2p ↑ ↑ _ —— Electron promotion (4.2 eV) ——→ C*: 1s ↑↓ 2s ↑ 2p ↑ ↑ ↑

sp^3 hybrid

n=2: ↑ ↑ ↑ ↑ (sp^3 sp^3 sp^3 sp^3)

Example: methane (CH_4).

Mix: 1/4 s + 3/4 p.

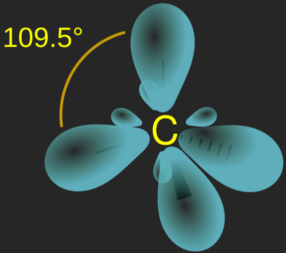

sp^2 hybrid

n=2: ↑ ↑ ↑ ↑ (sp^2 sp^2 sp^2 p)

Example: benzene (C_6H_6).

Mix: 1/3 s + 2/3 p.

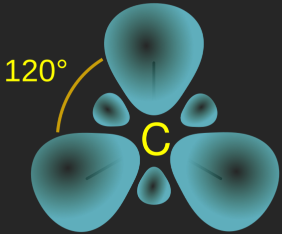

sp hybrid

n=2: ↑ ↑ ↑ ↑ (sp sp p p)

The principle of orbital hybridization

sp^3 hybrid

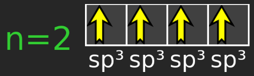

Example: methane (CH_4).

Mix: 1/4 s + 3/4 p.

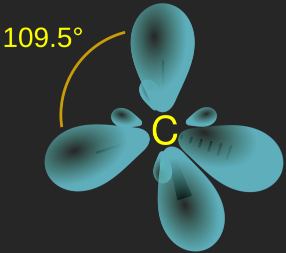

sp^2 hybrid

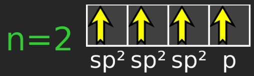

Example: benzene (C_6H_6).

Mix: 1/3 s + 2/3 p.

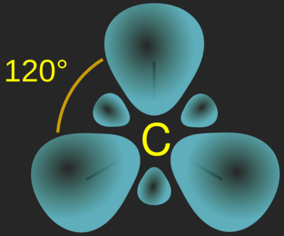

sp hybrid

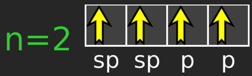

Example: acetylene (C_2H_2).

The principle of orbital hybridization

sp^3 hybrid

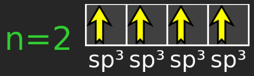

Example: methane (CH_4).

Mix: 1/4 s + 3/4 p.

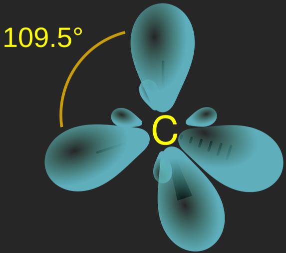

sp^2 hybrid

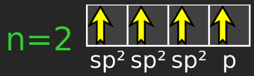

Example: benzene (C_6H_6).

Mix: 1/3 s + 2/3 p.

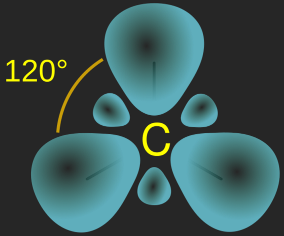

sp hybrid

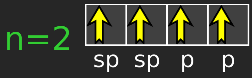

Example: acetylene (C_2H_2).

Mix: 1/2 s + 1/2 p.

The principle of orbital hybridization

sp^3 hybrid

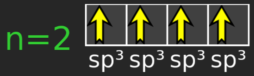

Example: methane (CH_4).

Mix: 1/4 s + 3/4 p.

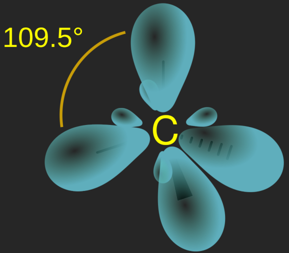

sp^2 hybrid

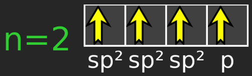

Example: benzene (C_6H_6).

Mix: 1/3 s + 2/3 p.

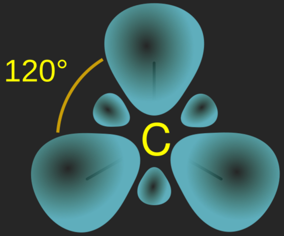

sp hybrid

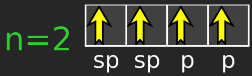

Example: acetylene (C_2H_2).

Mix: 1/2 s + 1/2 p.

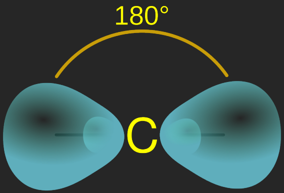

σ **bonds**

σ bonds

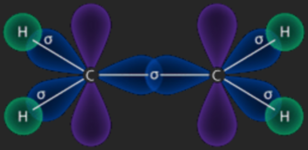

Credit: acetylene (Chemistry Library, CC BY-NC 4.0).

σ bonds

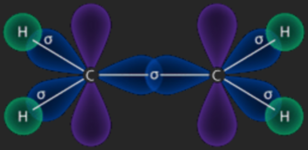

Credit: acetylene (Chemistry Library, CC BY-NC 4.0).

- Overlap of 2 s, p or sp^n orbitals.

σ bonds

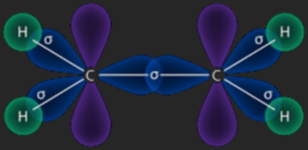

Credit: acetylene (Chemistry Library, CC BY-NC 4.0).

- Overlap of 2 s, p or sp^n orbitals.

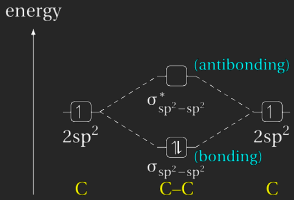

σ bonds

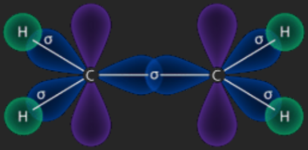

Credit: acetylene (Chemistry Library, CC BY-NC 4.0).

- Overlap of 2 s, p or sp^n orbitals.
- Rotational symmetry.

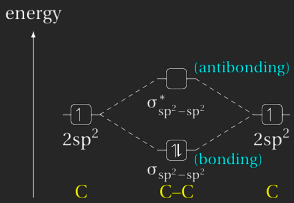

σ bonds

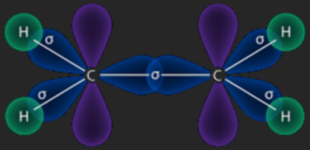

Credit: acetylene (Chemistry Library, CC BY-NC 4.0).

- Overlap of 2 s, p or sp^n orbitals.
- Rotational symmetry.
- Strongest covalent bond.

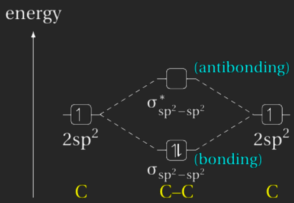

σ bonds

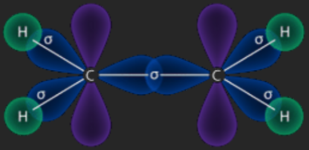

Credit: acetylene (Chemistry Library, CC BY-NC 4.0).

- Overlap of 2 s, p or sp^n orbitals.
- Rotational symmetry.
- Strongest covalent bond.

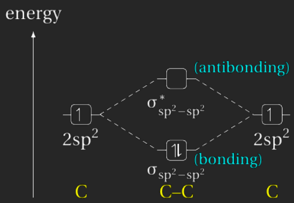

π bonds

σ bonds

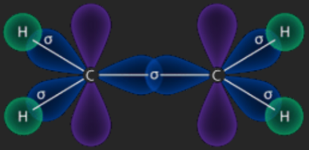

Credit: acetylene (Chemistry Library, CC BY-NC 4.0).

- Overlap of 2 s, p or sp^n orbitals.
- Rotational symmetry.
- Strongest covalent bond.

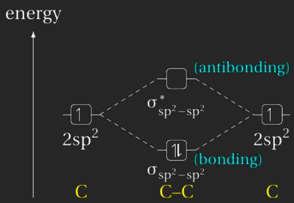

π bonds

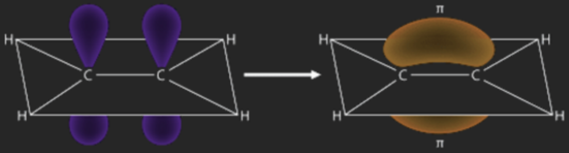

Credit: acetylene (Chemistry Library, CC BY-NC 4.0).

σ bonds

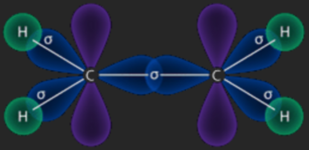

Credit: acetylene (Chemistry Library, CC BY-NC 4.0).

- Overlap of 2 s, p or sp^n orbitals.
- Rotational symmetry.
- Strongest covalent bond.

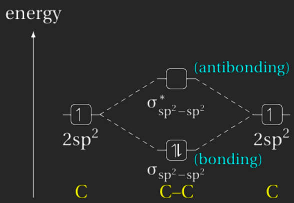

π bonds

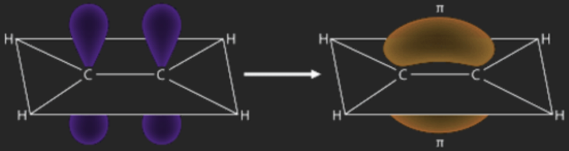

Credit: acetylene (Chemistry Library, CC BY-NC 4.0).

- Side-by-side overlap of the 2 lobes of 2 p orbitals.

σ bonds

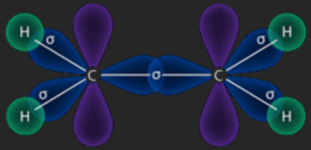

Credit: acetylene (Chemistry Library, CC BY-NC 4.0).

- Overlap of 2 s, p or sp^n orbitals.
- Rotational symmetry.
- Strongest covalent bond.

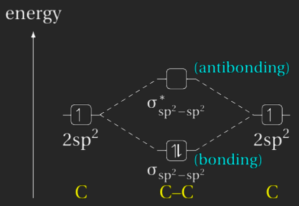

π bonds

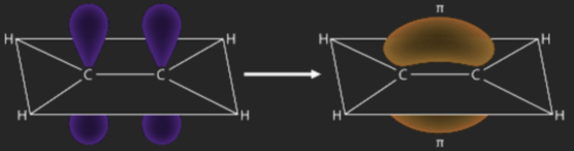

Credit: acetylene (Chemistry Library, CC BY-NC 4.0).

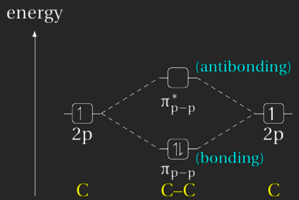

- Side-by-side overlap of the 2 lobes of 2 p orbitals.

σ bonds

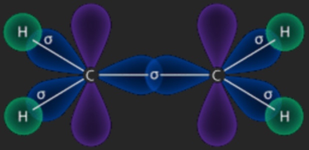

Credit: acetylene (Chemistry Library, CC BY-NC 4.0).

- Overlap of 2 s, p or sp^n orbitals.
- Rotational symmetry.
- Strongest covalent bond.

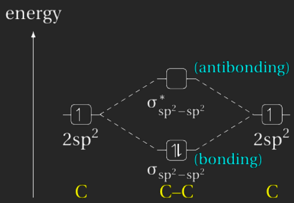

π bonds

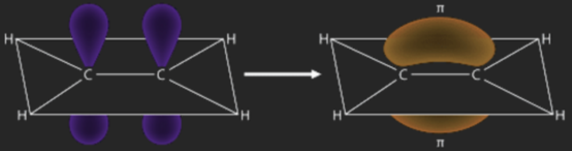

Credit: acetylene (Chemistry Library, CC BY-NC 4.0).

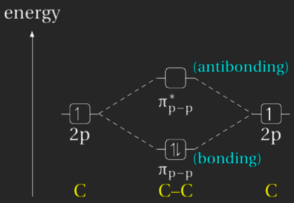

- Side-by-side overlap of the 2 lobes of 2 p orbitals.
- Weaker than σ bonds.

General properties

General properties

- Most abundant molecule in the Universe.

General properties

- Most abundant molecule in the Universe.
- Found in all regions with sufficient UV-shielding ($A(V) \gtrsim 0.1$).

General properties

- Most abundant molecule in the Universe.
- Found in all regions with sufficient UV-shielding ($A(V) \gtrsim 0.1$).
- Forms on dust grains (gas-phase formation inefficient).

General properties

- Most abundant molecule in the Universe.
- Found in all regions with sufficient UV-shielding ($A(V) \gtrsim 0.1$).
- Forms on dust grains (gas-phase formation inefficient).

Ortho / Para

General properties

- Most abundant molecule in the Universe.
- Found in all regions with sufficient UV-shielding ($A(V) \gtrsim 0.1$).
- Forms on dust grains (gas-phase formation inefficient).

Ortho / Para

- H_2 exists in two forms with parallel or anti-parallel nuclear spins: 2/3 Ortho + 1/3 Para.

General properties

- Most abundant molecule in the Universe.
- Found in all regions with sufficient UV-shielding ($A(V) \gtrsim 0.1$).
- Forms on dust grains (gas-phase formation inefficient).

Ortho / Para

- H_2 exists in two forms with parallel or anti-parallel nuclear spins: 2/3 Ortho + 1/3 Para.

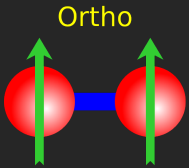

General properties

- Most abundant molecule in the Universe.
- Found in all regions with sufficient UV-shielding ($A(V) \gtrsim 0.1$).
- Forms on dust grains (gas-phase formation inefficient).

Ortho / Para

- H_2 exists in two forms with parallel or anti-parallel nuclear spins: 2/3 Ortho + 1/3 Para.

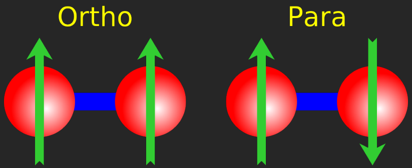

General properties

- Most abundant molecule in the Universe.
- Found in all regions with sufficient UV-shielding ($A(V) \gtrsim 0.1$).
- Forms on dust grains (gas-phase formation inefficient).

Ortho / Para

- H_2 exists in two forms with parallel or anti-parallel nuclear spins: 2/3 Ortho + 1/3 Para.
- No radiative transitions (Ortho $\leftrightarrow$ Para)

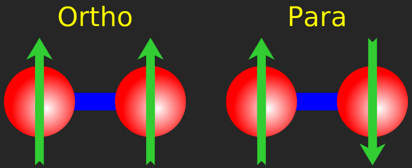

General properties

- Most abundant molecule in the Universe.
- Found in all regions with sufficient UV-shielding ($A(V) \gtrsim 0.1$).
- Forms on dust grains (gas-phase formation inefficient).

Ortho / Para

- H_2 exists in two forms with parallel or anti-parallel nuclear spins: 2/3 Ortho + 1/3 Para.
- No radiative transitions (Ortho $\leftrightarrow$ Para) $\Rightarrow$ conversion on the grains.

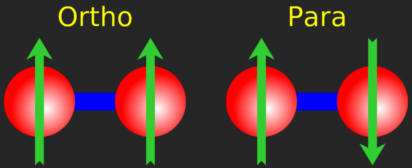

General properties

- Most abundant molecule in the Universe.
- Found in all regions with sufficient UV-shielding ($A(V) \gtrsim 0.1$).
- Forms on dust grains (gas-phase formation inefficient).

Ortho / Para

- H_2 exists in two forms with parallel or anti-parallel nuclear spins: $2/3$ Ortho $+$ $1/3$ Para.
- No radiative transitions (Ortho $\leftrightarrow$ Para) $\Rightarrow$ conversion on the grains.

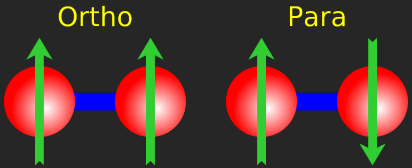

Consequence of the symmetry of H_2

General properties

- Most abundant molecule in the Universe.
- Found in all regions with sufficient UV-shielding ($A(V) \gtrsim 0.1$).
- Forms on dust grains (gas-phase formation inefficient).

Ortho / Para

- H_2 exists in two forms with parallel or anti-parallel nuclear spins: 2/3 Ortho + 1/3 Para.
- No radiative transitions (Ortho $\leftrightarrow$ Para) $\Rightarrow$ conversion on the grains.

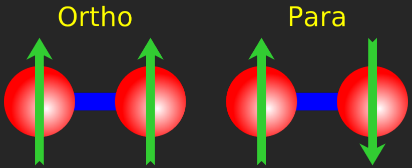

Consequence of the symmetry of H_2

- No dipolar moment $\Rightarrow$ no rotational lines

General properties

- Most abundant molecule in the Universe.
- Found in all regions with sufficient UV-shielding ($A(V) \gtrsim 0.1$).
- Forms on dust grains (gas-phase formation inefficient).

Ortho / Para

- H_2 exists in two forms with parallel or anti-parallel nuclear spins: 2/3 Ortho + 1/3 Para.
- No radiative transitions (Ortho $\leftrightarrow$ Para) $\Rightarrow$ conversion on the grains.

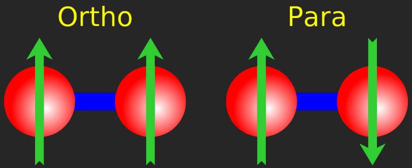

Consequence of the symmetry of H_2

- No dipolar moment $\Rightarrow$ no rotational lines

$\Rightarrow$ No line $\lesssim 300$ K $\rightarrow$ rovibrational MIR lines.

General properties

- Most abundant molecule in the Universe.
- Found in all regions with sufficient UV-shielding ($A(V) \gtrsim 0.1$).
- Forms on dust grains (gas-phase formation inefficient).

Ortho / Para

- H_2 exists in two forms with parallel or anti-parallel nuclear spins: 2/3 Ortho + 1/3 Para.
- No radiative transitions (Ortho $\leftrightarrow$ Para) $\Rightarrow$ conversion on the grains.

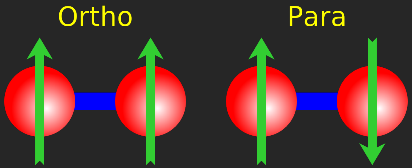

Consequence of the symmetry of H_2

- No dipolar moment $\Rightarrow$ no rotational lines

$\Rightarrow$ No line $\lesssim$ 300 K $\rightarrow$ rovibrational MIR lines.

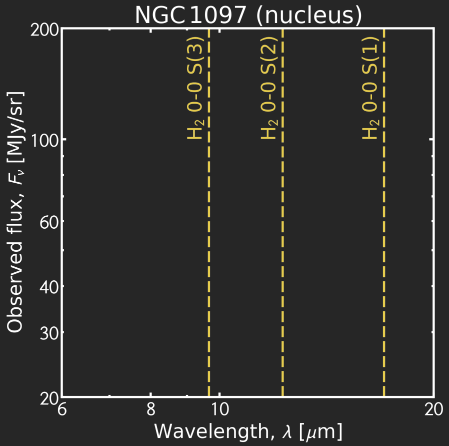

(Wu et al., 2018)

General properties

- Most abundant molecule in the Universe.
- Found in all regions with sufficient UV-shielding ($A(V) \gtrsim 0.1$).
- Forms on dust grains (gas-phase formation inefficient).

Ortho / Para

- H_2 exists in two forms with parallel or anti-parallel nuclear spins: 2/3 Ortho + 1/3 Para.
- No radiative transitions (Ortho ↔ Para) ⇒ conversion on the grains.

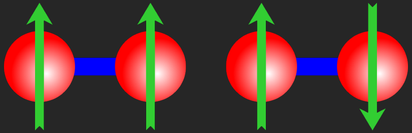

Consequence of the symmetry of H_2

- No dipolar moment ⇒ no rotational lines

⇒ No line $\lesssim$ 300 K → rovibrational MIR lines.

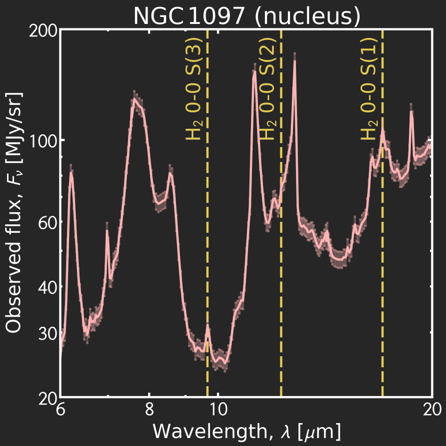

(Wu et al., 2018)

Ice properties

Ice properties

- Dense, UV-shielded regions ($A(V) \gtrsim 1$) $\rightarrow$ molecules freeze on grains.

Ice properties

- Dense, UV-shielded regions ($A(V) \gtrsim 1$) $\rightarrow$ molecules freeze on grains.
- Most abundant species: H_2O, CO & CO_2.

Ice properties

- Dense, UV-shielded regions ($A(V) \gtrsim 1$) $\rightarrow$ molecules freeze on grains.
- Most abundant species: H_2O, CO & CO_2.
- Characteristic spectral signatures: MIR absorption bands.

Ice properties

- Dense, UV-shielded regions ($A(V) \gtrsim 1$) $\rightarrow$ molecules freeze on grains.
- Most abundant species: H_2O, CO & CO_2.
- Characteristic spectral signatures: MIR absorption bands.

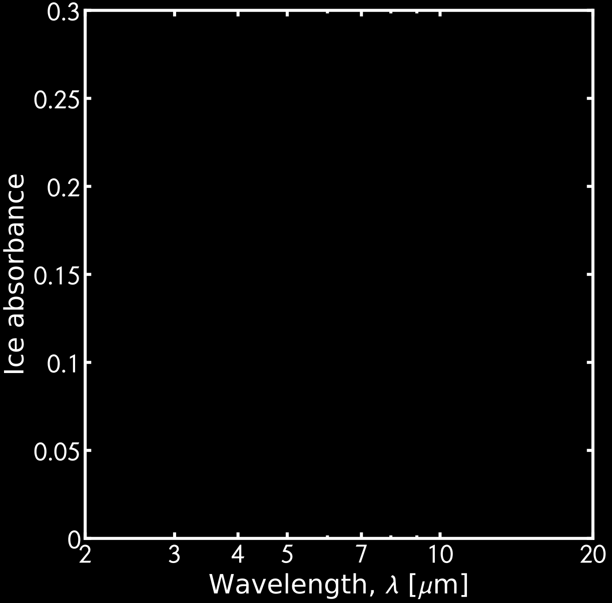

Ice properties

- Dense, UV-shielded regions ($A(V) \gtrsim 1$) → molecules freeze on grains.
- Most abundant species: H_2O, CO & CO_2.
- Characteristic spectral signatures: MIR absorption bands.

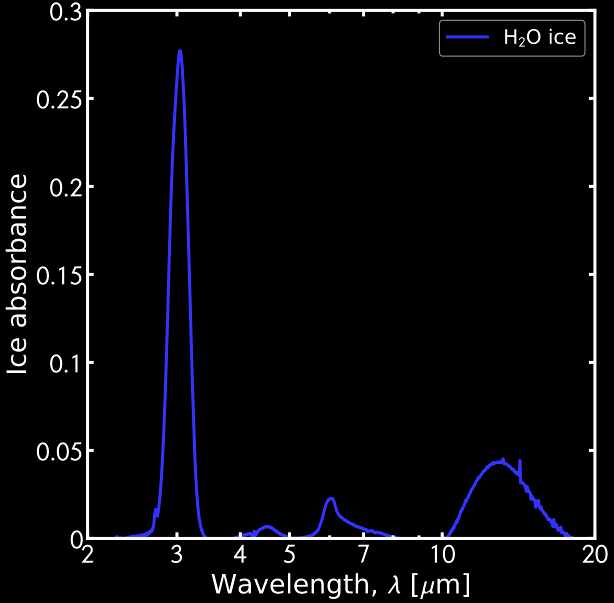

Ice properties

- Dense, UV-shielded regions ($A(V) \gtrsim 1$) → molecules freeze on grains.
- Most abundant species: H_2O, CO & CO_2.
- Characteristic spectral signatures: MIR absorption bands.

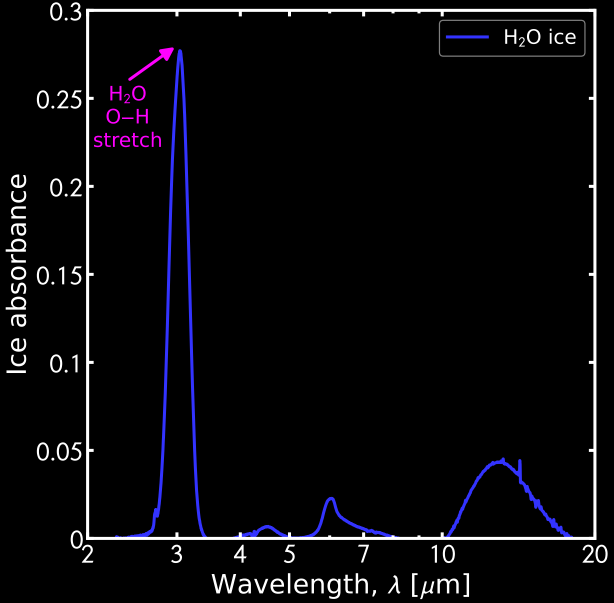

Ice properties

- Dense, UV-shielded regions ($A(V) \gtrsim 1$) → molecules freeze on grains.
- Most abundant species: H_2O, CO & CO_2.
- Characteristic spectral signatures: MIR absorption bands.

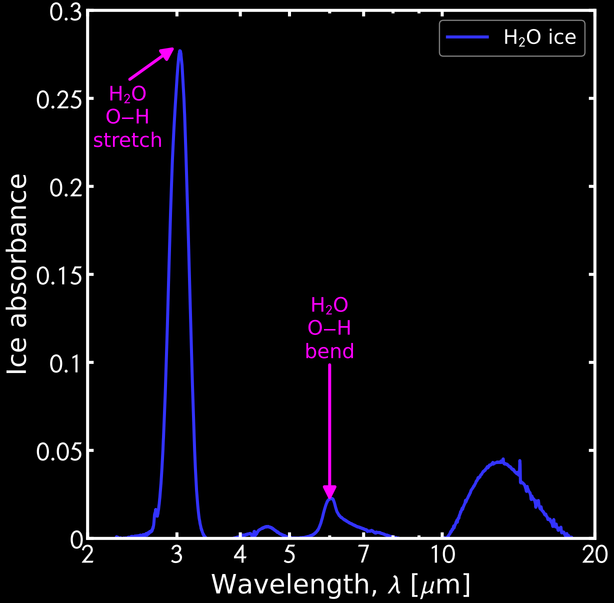

Ice properties

- Dense, UV-shielded regions ($A(V) \gtrsim 1$) $\rightarrow$ molecules freeze on grains.
- Most abundant species: H_2O, CO & CO_2.
- Characteristic spectral signatures: MIR absorption bands.

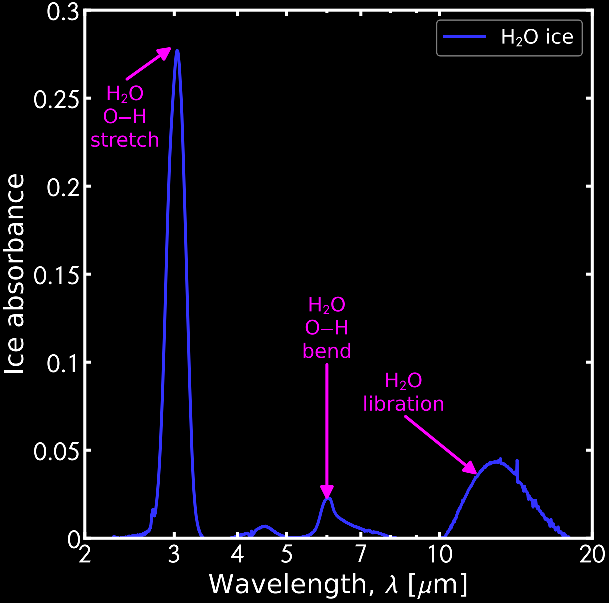

Ice properties

- Dense, UV-shielded regions ($A(V) \gtrsim 1$) $\rightarrow$ molecules freeze on grains.
- Most abundant species: H_2O, CO & CO_2.
- Characteristic spectral signatures: MIR absorption bands.

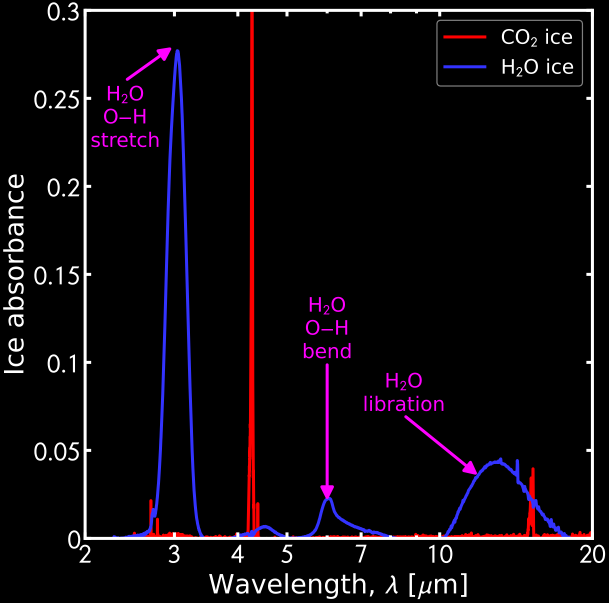

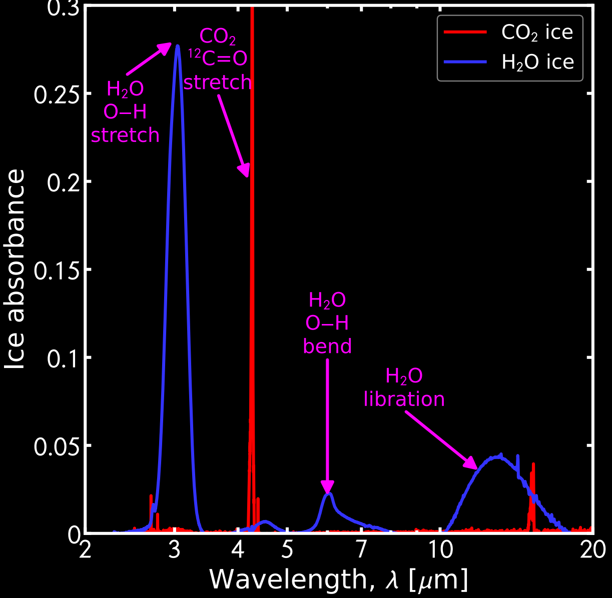

Ice properties

- Dense, UV-shielded regions ($A(V) \gtrsim 1$) $\rightarrow$ molecules freeze on grains.
- Most abundant species: H_2O, CO & CO_2.
- Characteristic spectral signatures: MIR absorption bands.

Ice properties

- Dense, UV-shielded regions ($A(V) \gtrsim 1$) $\rightarrow$ molecules freeze on grains.
- Most abundant species: H_2O, CO & CO_2.
- Characteristic spectral signatures: MIR absorption bands.

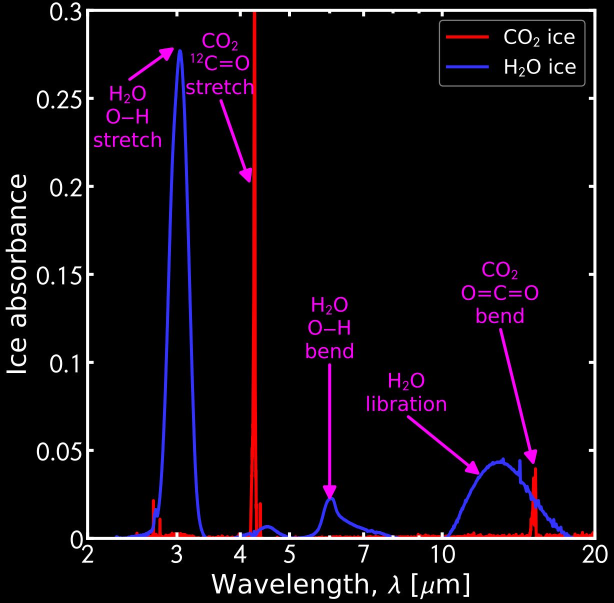

Ice properties

- Dense, UV-shielded regions ($A(V) \gtrsim 1$) → molecules freeze on grains.
- Most abundant species: H_2O, CO & CO_2.
- Characteristic spectral signatures: MIR absorption bands.

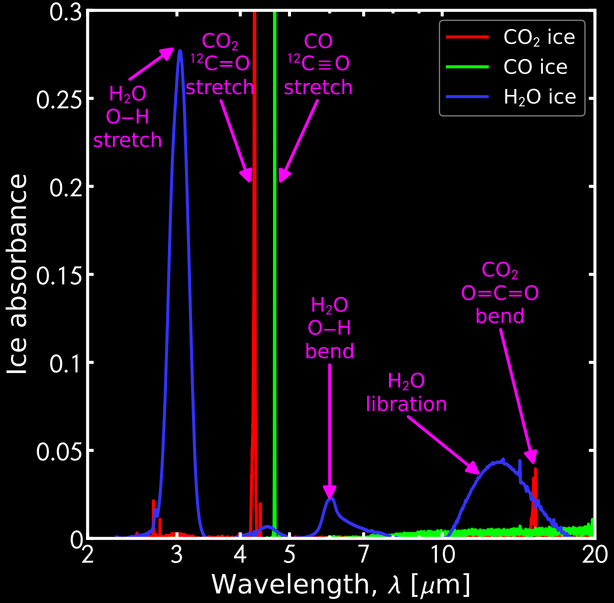

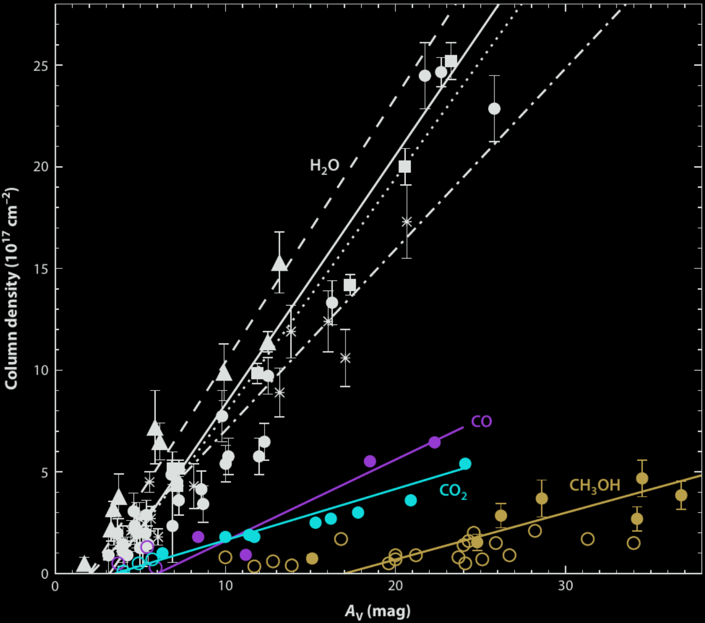

(Boogert et al., 2015)

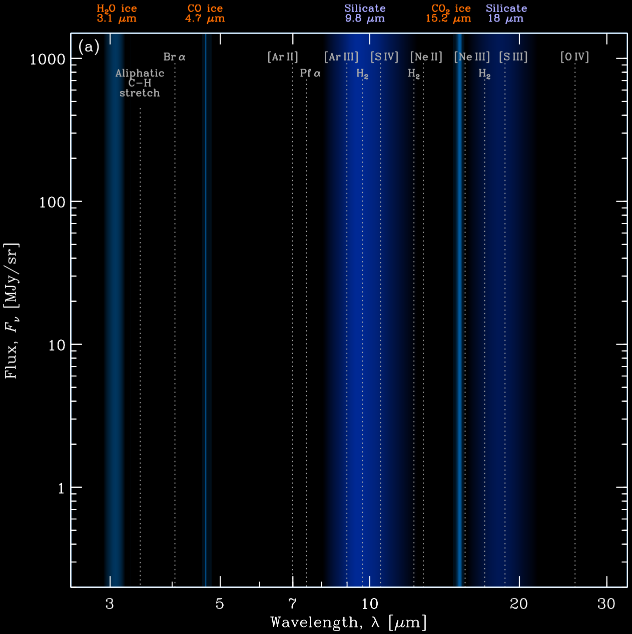

(Galliano et al., 2018)

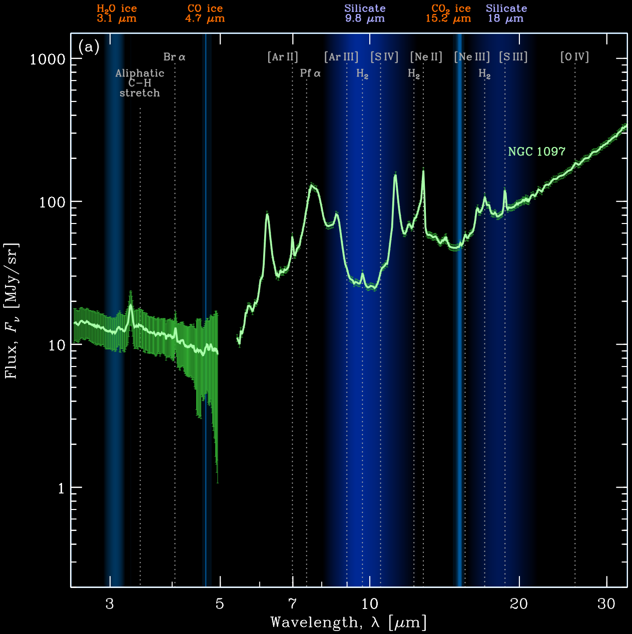

(Galliano et al., 2018)

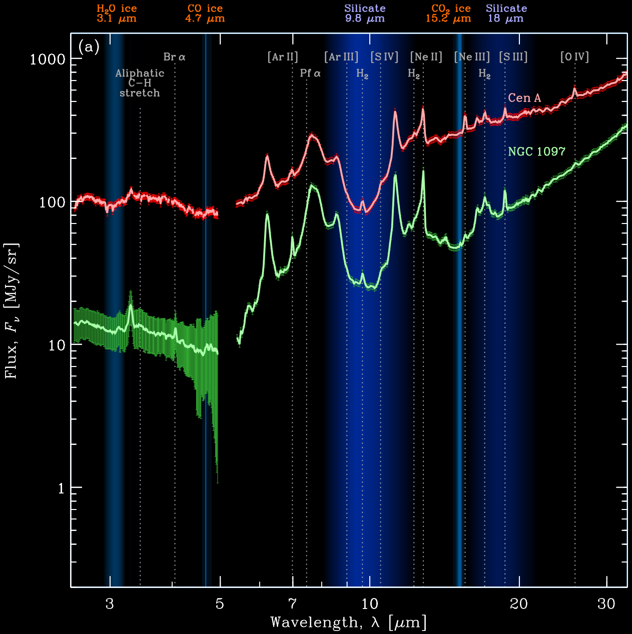

(Galliano et al., 2018)

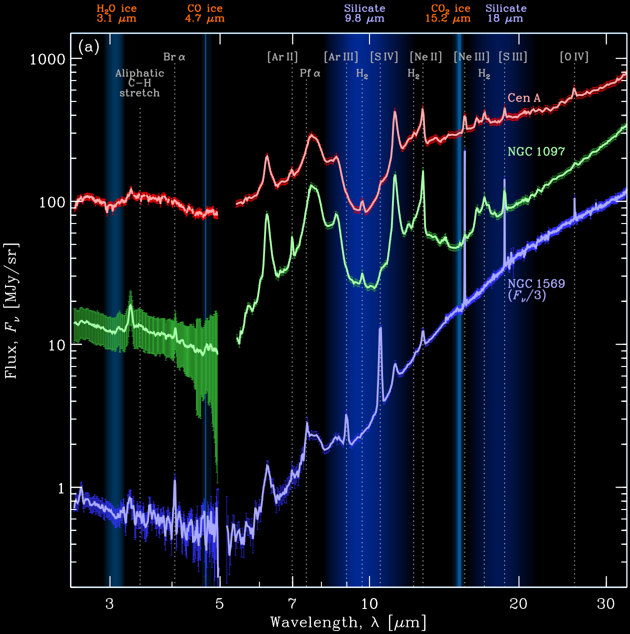

(Galliano et al., 2018)

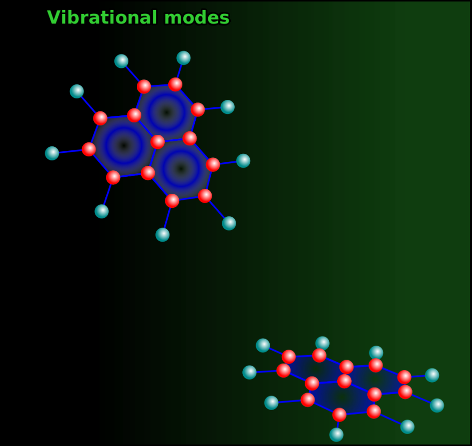
Vibrational modes

Vibrational modes

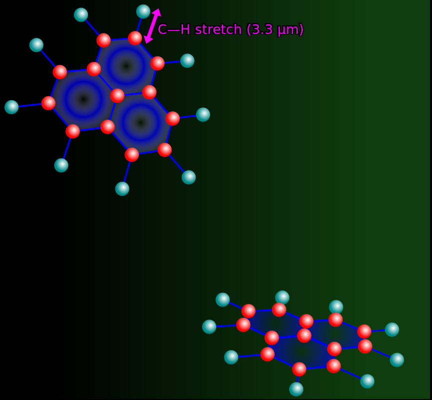

Vibrational modes

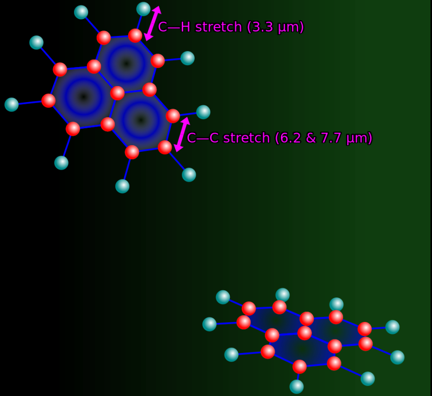

Vibrational modes

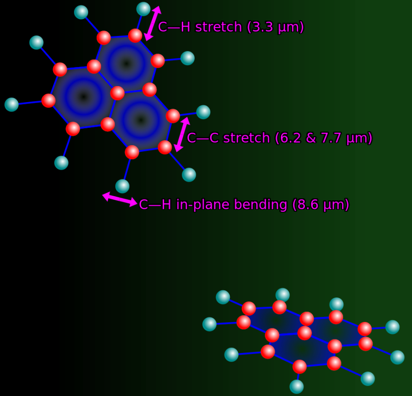

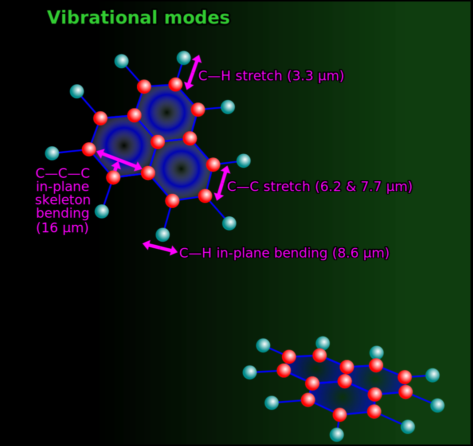
Vibrational modes
C—H stretch (3.3 µm)
C—C—C in-plane skeleton bending (16 µm)
C—C stretch (6.2 & 7.7 µm)
C—H in-plane bending (8.6 µm)

Vibrational modes

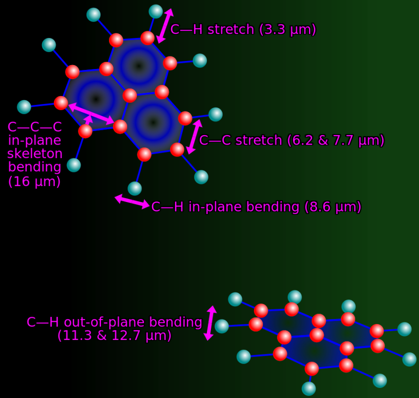

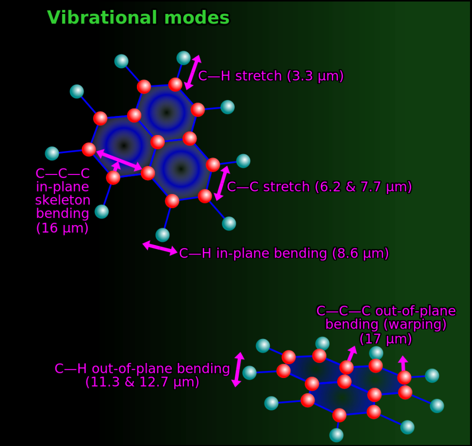
Vibrational modes
C—H stretch (3.3 µm)
C—C—C in-plane skeleton bending (16 µm)
C—C stretch (6.2 & 7.7 µm)
C—H in-plane bending (8.6 µm)
C—C—C out-of-plane bending (warping) (17 µm)
C—H out-of-plane bending (11.3 & 12.7 µm)

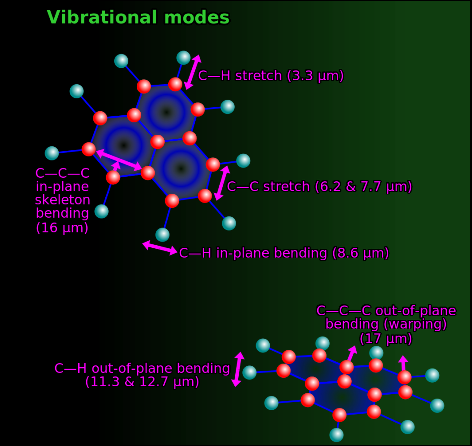

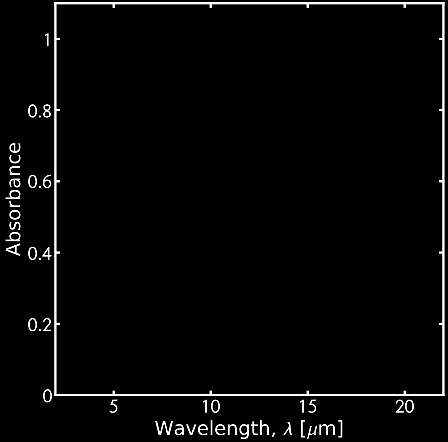

Laboratory data (Allamandola et al., 1999)

Molecules | Polycyclic Aromatic Hydrocarbons (PAHs)

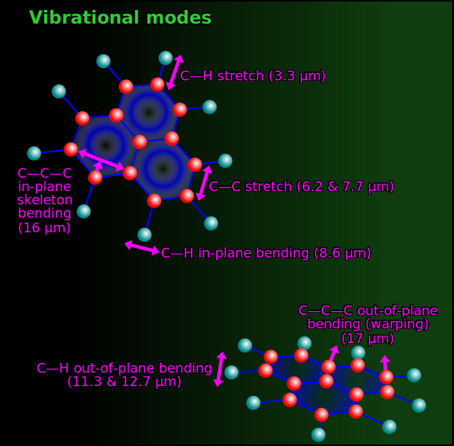

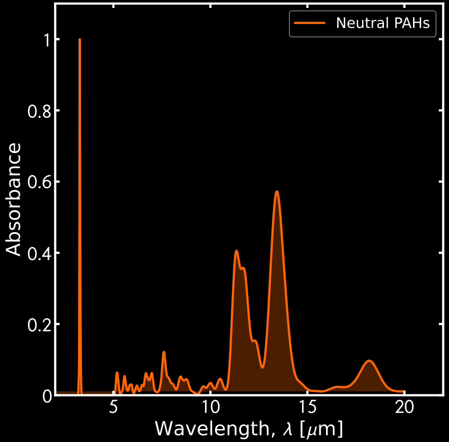

Laboratory data (Allamandola et al., 1999)

Molecules | Polycyclic Aromatic Hydrocarbons (PAHs)

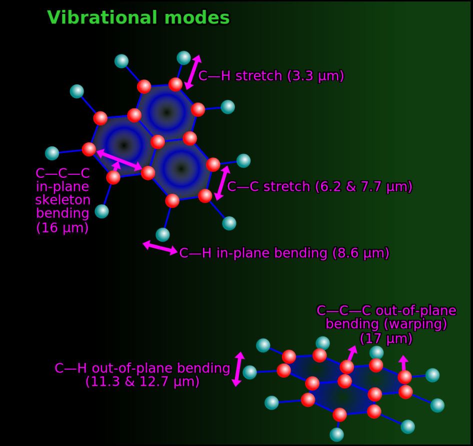

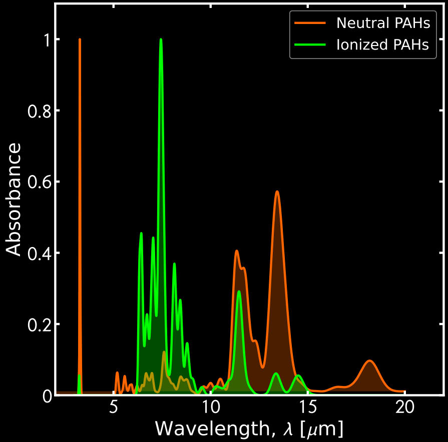

Laboratory data (Allamandola et al., 1999)

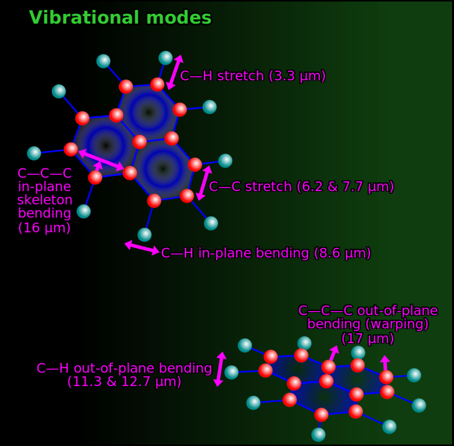

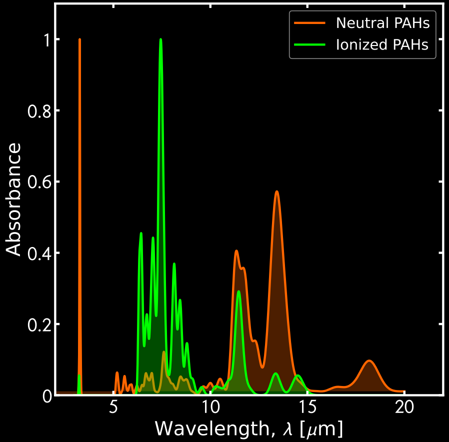

Laboratory data (Allamandola et al., 1999)

Astrophysical significance of PAHs

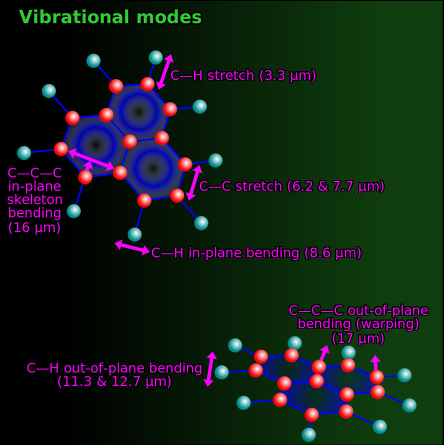

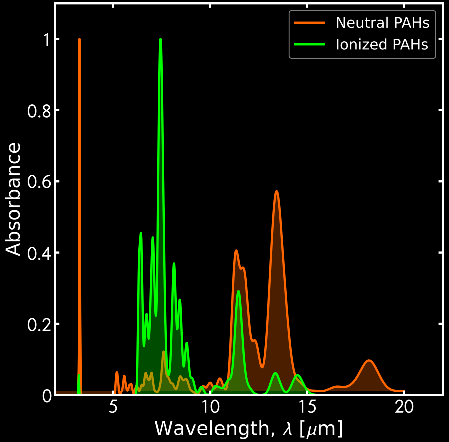

Laboratory data (Allamandola et al., 1999)

Astrophysical significance of PAHs

- Carry the bright mid-IR emission bands.

Molecules | Polycyclic Aromatic Hydrocarbons (PAHs)

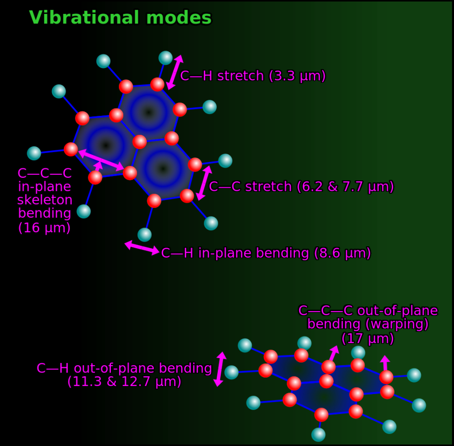

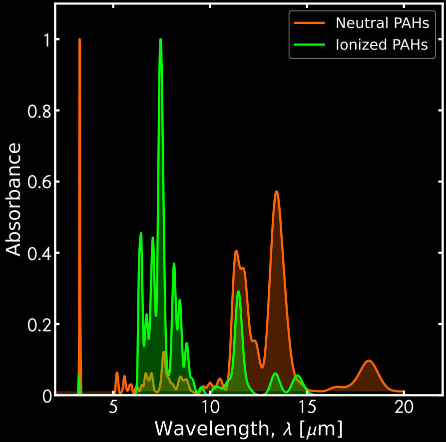

Laboratory data (Allamandola et al., 1999)

Astrophysical significance of PAHs

- Carry the bright mid-IR emission bands.
- Responsible for the photoelectric heating of the neutral gas.

Molecules | Polycyclic Aromatic Hydrocarbons (PAHs)

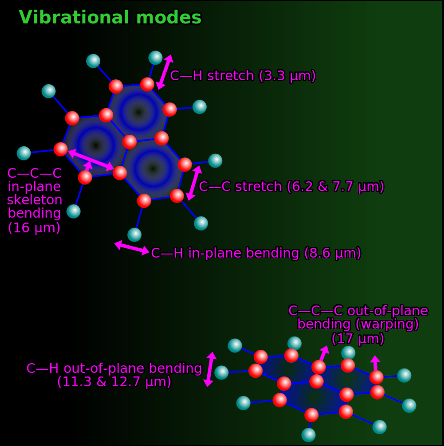

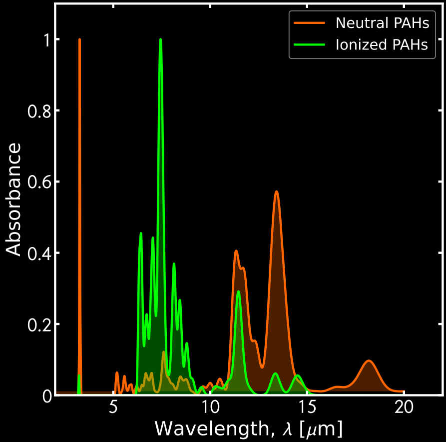

Laboratory data (Allamandola et al., 1999)

Astrophysical significance of PAHs

- Carry the bright mid-IR emission bands.
- Responsible for the photoelectric heating of the neutral gas.
- Milky Way: $\simeq 40\,\%$ of $L_{\rm IR}$ & $15\,\%$ of $L_{\rm bol}$.

The recent explosion of the detection of large molecules in the ISM

The recent explosion of the detection of large molecules in the ISM

- Guélin & Cernicharo (2022) count 256 species detected, using radiotelescopes.

The recent explosion of the detection of large molecules in the ISM

- Guélin & Cernicharo (2022) count 256 species detected, using radiotelescopes.

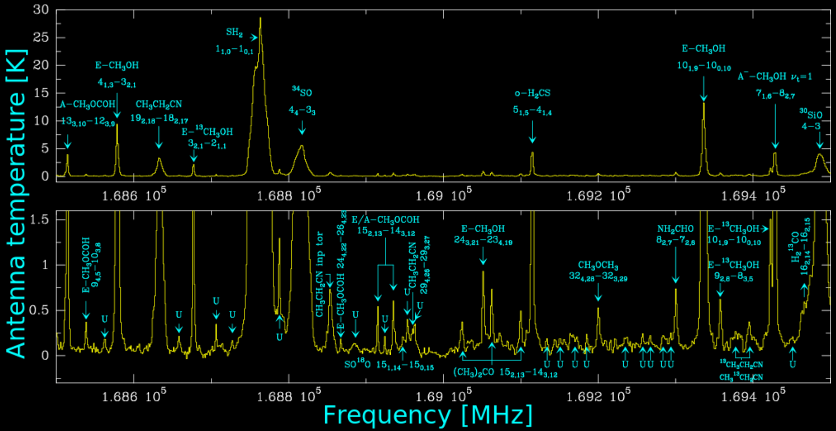

Credit: $\lambda \simeq 2$ mm spectrum of the Orion-KL star-forming cloud with the IRAM-30m radiotelescope (Tercero et al., 2010).

The recent explosion of the detection of large molecules in the ISM

- Guélin & Cernicharo (2022) count 256 species detected, using radiotelescopes.
- Relevant for understanding pre-biotic chemistry → no amino acids found to date.

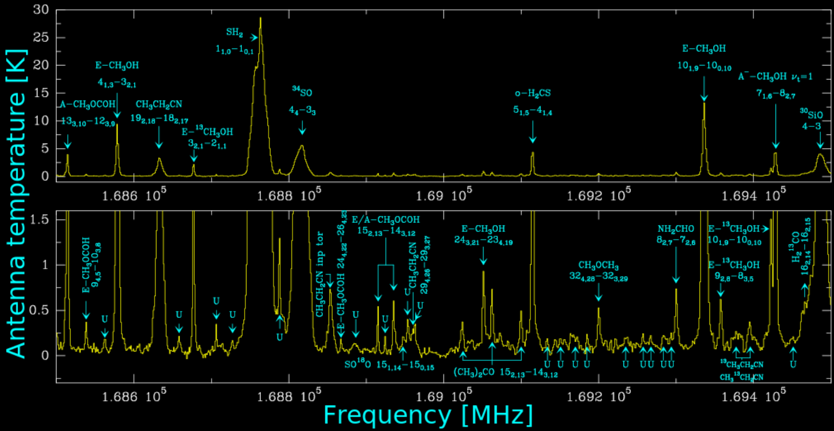

Credit: $\lambda \simeq 2$ mm spectrum of the Orion-KL star-forming cloud with the IRAM-30m radiotelescope (Tercero et al., 2010).

The recent explosion of the detection of large molecules in the ISM

- Guélin & Cernicharo (2022) count 256 species detected, using radiotelescopes.
- Relevant for understanding pre-biotic chemistry → no amino acids found to date.
- Detection of NH_2-CH_2-CN, a precursor of glycine (Belloche et al., 2008).

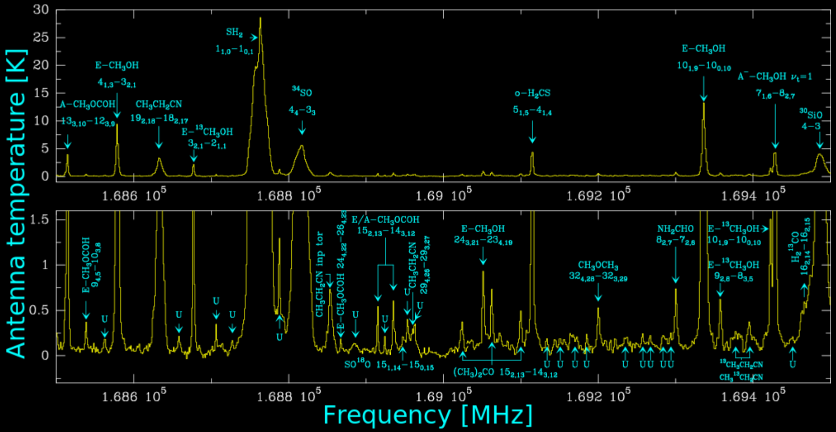

Credit: $\lambda \simeq 2$ mm spectrum of the Orion-KL star-forming cloud with the IRAM-30m radiotelescope (Tercero et al., 2010).

Molecules | Diffuse Interstellar Bands (DIBs)

A century-old enigma

A century-old enigma

- Ubiquitous visible-to-near-IR absorption features (Heger, 1922).

A century-old enigma

- Ubiquitous visible-to-near-IR absorption features (Heger, 1922).

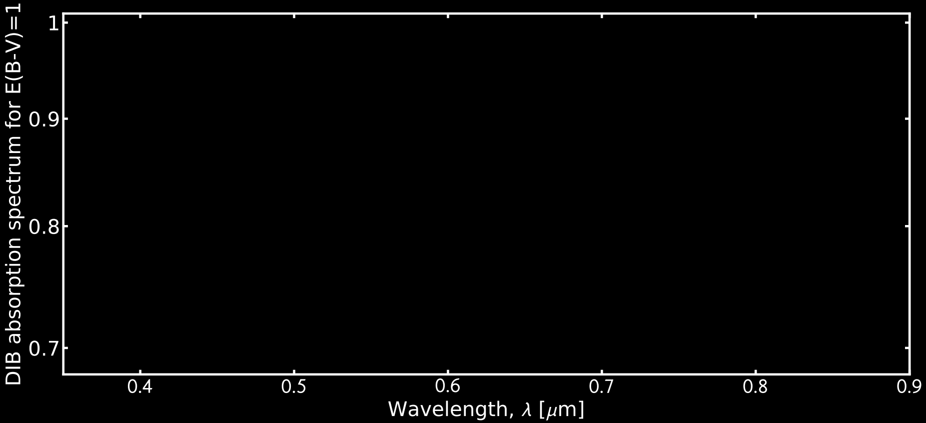

Data from Jenniskens & Désert (1994).

A century-old enigma

- Ubiquitous visible-to-near-IR absorption features (Heger, 1922).

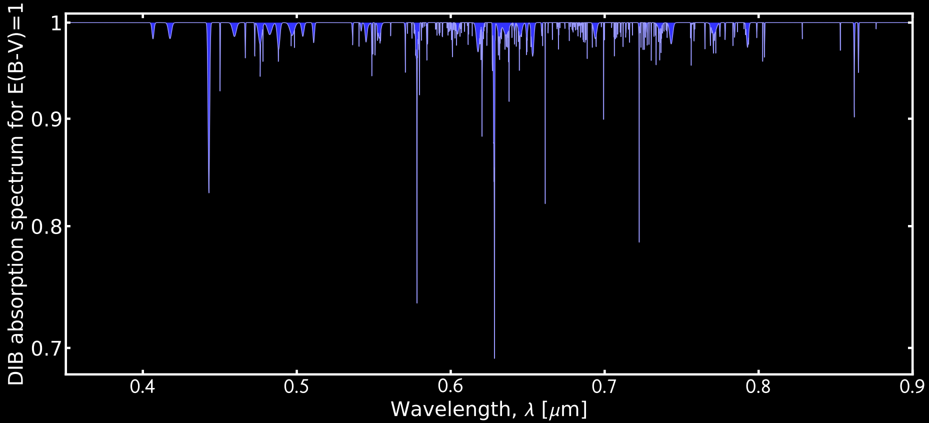

Data from Jenniskens & Désert (1994).

A century-old enigma

- Ubiquitous visible-to-near-IR absorption features (Heger, 1922).
- Interstellar origin (Merrill, 1934).

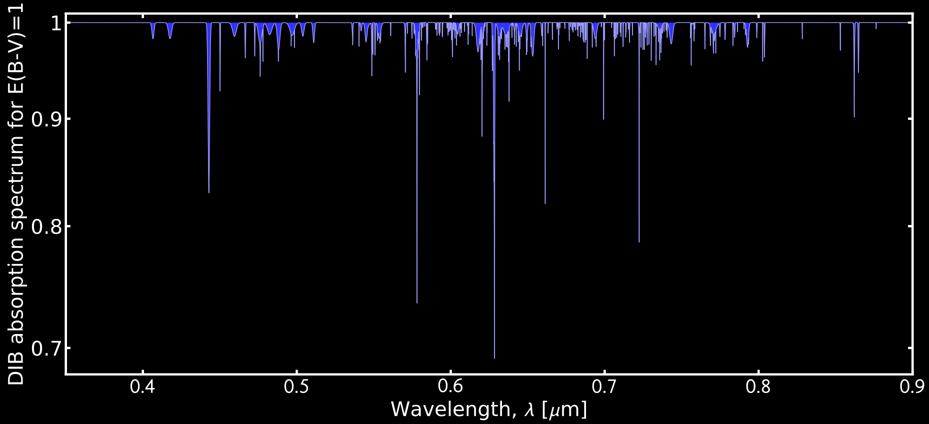

Data from Jenniskens & Désert (1994).

A century-old enigma

- Ubiquitous visible-to-near-IR absorption features (Heger, 1922).
- Interstellar origin (Merrill, 1934).
- More than 500 bands have been detected (Fan et al., 2019).

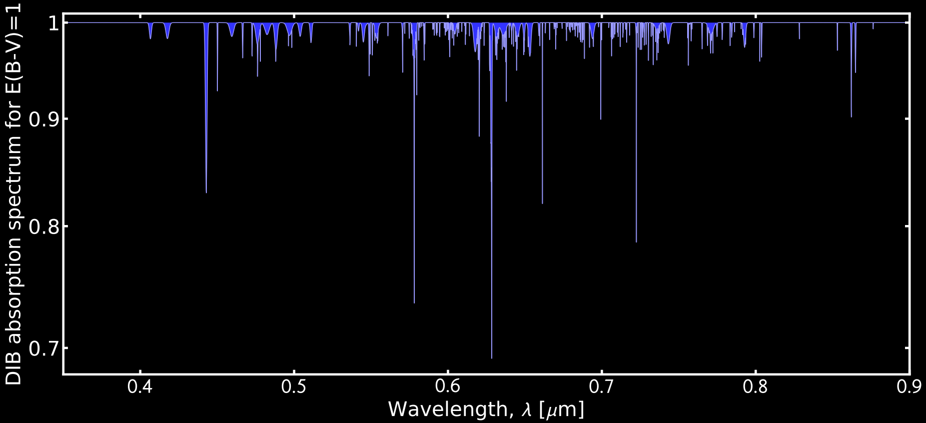

Data from Jenniskens & Désert (1994).

A century-old enigma

- Ubiquitous visible-to-near-IR absorption features (Heger, 1922).
- Interstellar origin (Merrill, 1934).
- More than 500 bands have been detected (Fan et al., 2019).
- Origin still unknown.

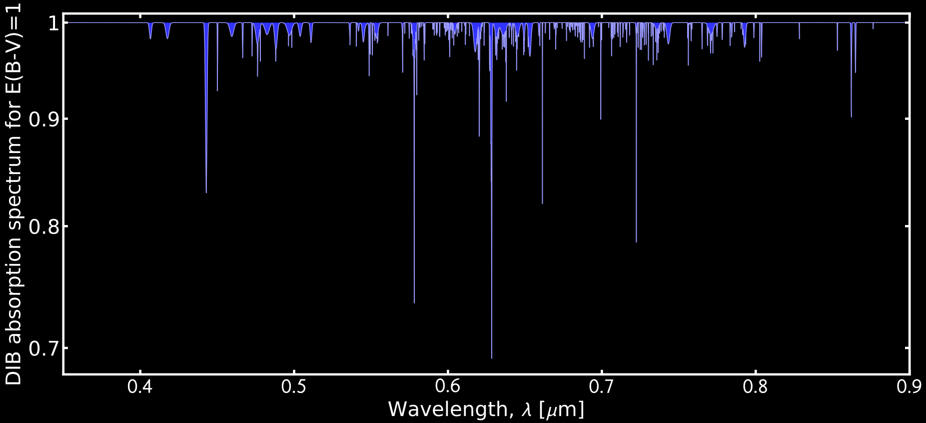

Data from Jenniskens & Désert (1994).

Characteristics of the carriers

Characteristics of the carriers

- Line width $\gtrsim 1$ Å $\Rightarrow$ no free-flying atoms.

Characteristics of the carriers

- Line width $\gtrsim 1$ Å $\Rightarrow$ no free-flying atoms.
- Must come from molecules with $\simeq 100$ atoms (MacIsaac et al., 2022).

Characteristics of the carriers

- Line width $\gtrsim 1$ Å $\Rightarrow$ no free-flying atoms.
- Must come from molecules with $\simeq 100$ atoms (MacIsaac et al., 2022).
- Cationic buckminsterfullerene (C_{60}^{+}) $\Rightarrow$ 2, maybe 4 near-IR DIBs (Campbell et al. 2015; Walker et al. 2015).

Characteristics of the carriers

- Line width $\gtrsim 1$ Å $\Rightarrow$ no free-flying atoms.
- Must come from molecules with $\simeq 100$ atoms (MacIsaac et al., 2022).
- Cationic buckminsterfullerene (C_{60}^{+}) $\Rightarrow$ 2, maybe 4 near-IR DIBs (Campbell et al. 2015; Walker et al. 2015).

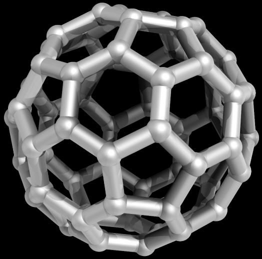

Buckminsterfullerene (C_{60})

Molecules | The Only DIB Identification to Date: Fullerene

Characteristics of the carriers

- Line width $\gtrsim 1$ Å $\Rightarrow$ no free-flying atoms.
- Must come from molecules with $\simeq 100$ atoms (MacIsaac et al., 2022).
- Cationic buckminsterfullerene (C_{60}^+) $\Rightarrow$ 2, maybe 4 near-IR DIBs (Campbell et al. 2015; Walker et al. 2015).
- Buckminsterfullerene also detected in emission in the mid-IR (Cami et al., 2010).

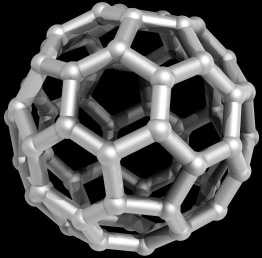

Buckminsterfullerene (C_{60})

The Only DIB Identification to Date: Fullerene

Characteristics of the carriers

- Line width $\gtrsim 1$ Å $\Rightarrow$ no free-flying atoms.
- Must come from molecules with $\simeq 100$ atoms (MacIsaac et al., 2022).
- Cationic buckminsterfullerene (C_{60}^+) $\Rightarrow$ 2, maybe 4 near-IR DIBs (Campbell et al. 2015; Walker et al. 2015).
- Buckminsterfullerene also detected in emission in the mid-IR (Cami et al., 2010).

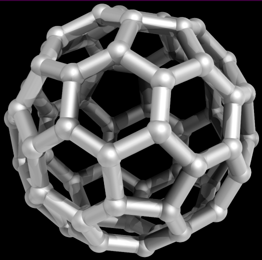

Buckminsterfullerene (C_{60})

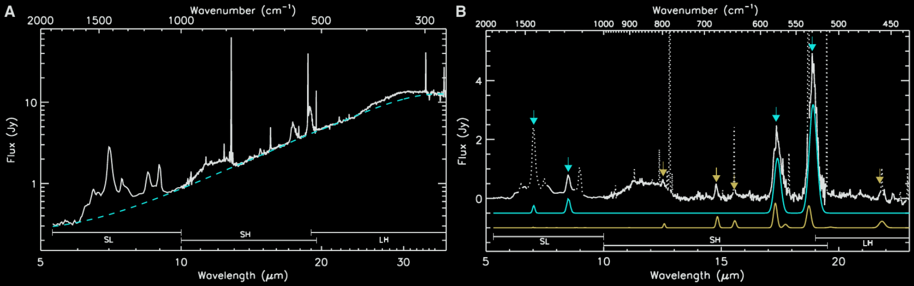

(Cami et al. 2010; using the *Spitzer* space telescope)

Outline of the Lecture

Dust | From Atoms & Molecules to Solids

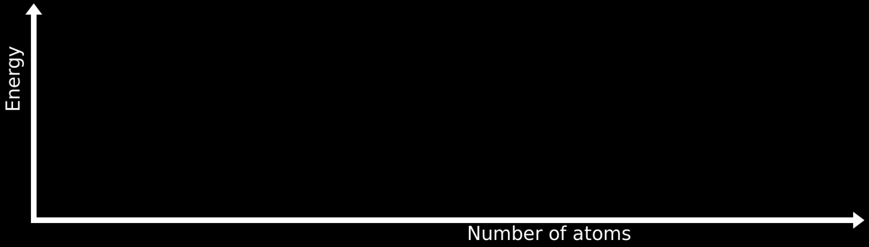

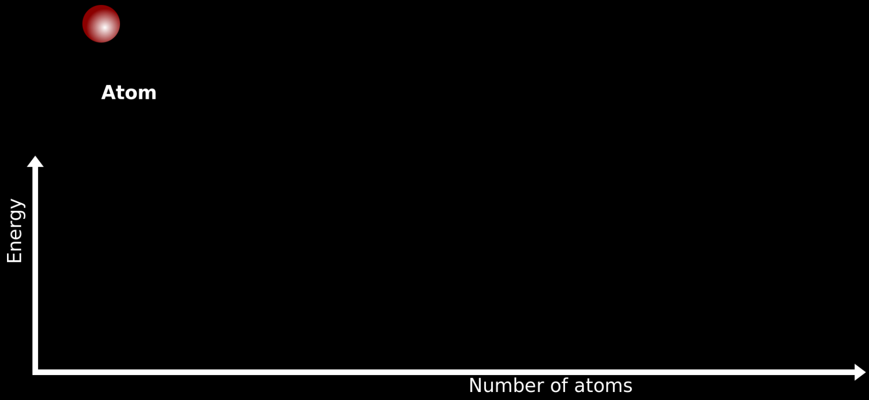
Atom
Energy
Number of atoms

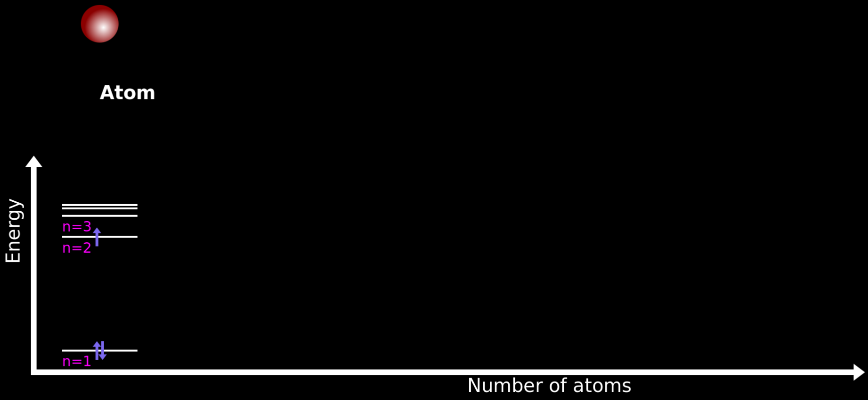
Atom
Energy
n=3
n=2
n=1
Number of atoms

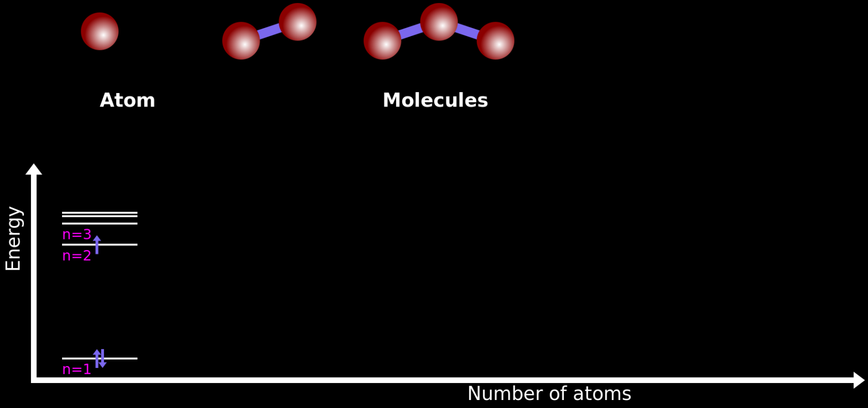

Atom
Molecules
Energy
n=3
n=2
n=1
Number of atoms

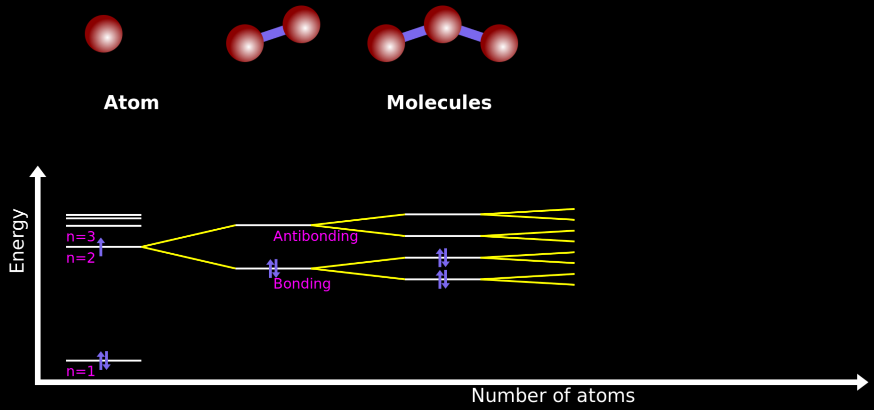
Atom
Molecules
Energy
n=3
n=2
n=1
Antibonding
Bonding
Number of atoms

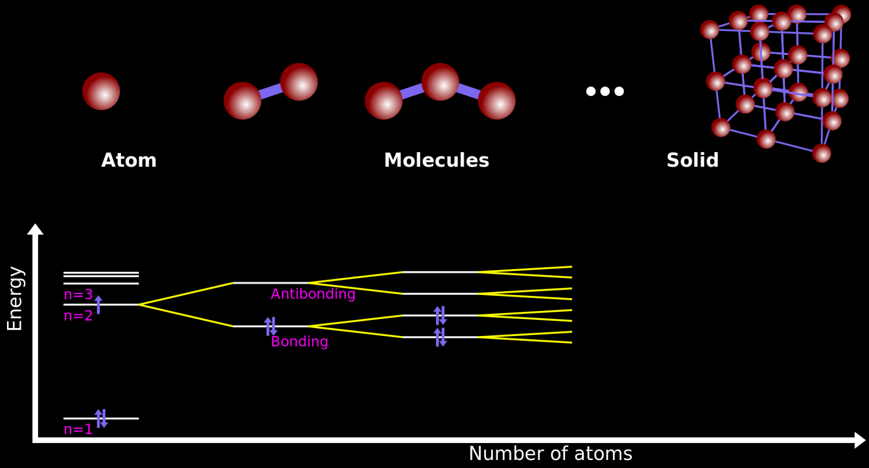
Atom
Molecules
Solid
Energy
n=3
n=2
n=1
Antibonding
Bonding
Number of atoms

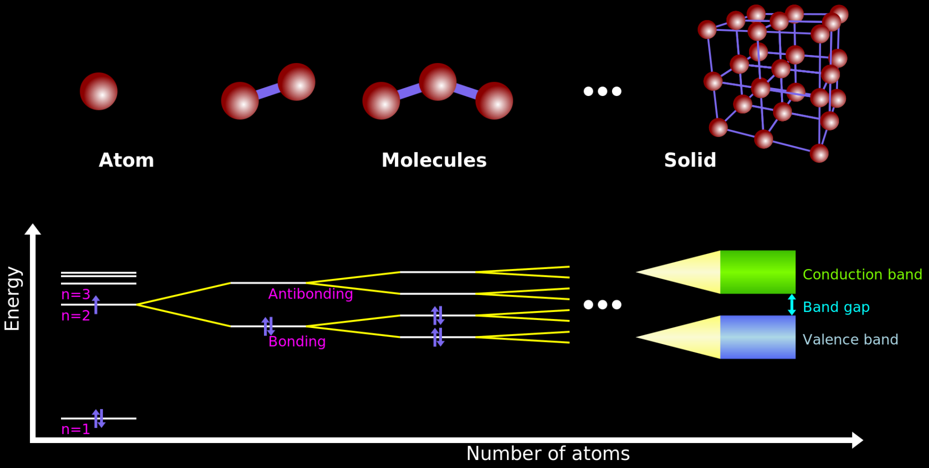
Atom
Molecules
Solid
Energy
n=3
n=2
n=1
Antibonding
Bonding
Conduction band
Band gap
Valence band
Number of atoms

The Fermi-Dirac distribution

The Fermi-Dirac distribution

Energy distribution of electrons:

$$f(E) \equiv \frac{1}{\exp\left(\frac{E - E_\mathrm{F}}{kT}\right) + 1}.$$

The Fermi-Dirac distribution

Energy distribution of electrons:

$$f(E) \equiv \frac{1}{\exp\left(\frac{E-E_\mathrm{F}}{kT}\right)+1}.$$

Fermi level, E_F: maximum energy at $T = 0$ K.

The Fermi-Dirac distribution

Energy distribution of electrons:

$$f(E) \equiv \frac{1}{\exp\left(\frac{E-E_F}{kT}\right)+1}.$$

Fermi level, E_F: maximum energy at $T=0$ K.

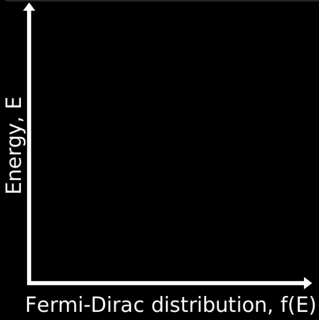

The Fermi-Dirac distribution

Energy distribution of electrons:

$$f(E) \equiv \frac{1}{\exp\left(\frac{E-E_\mathrm{F}}{kT}\right)+1}.$$

Fermi level, E_F: maximum energy at $T = 0$ K.

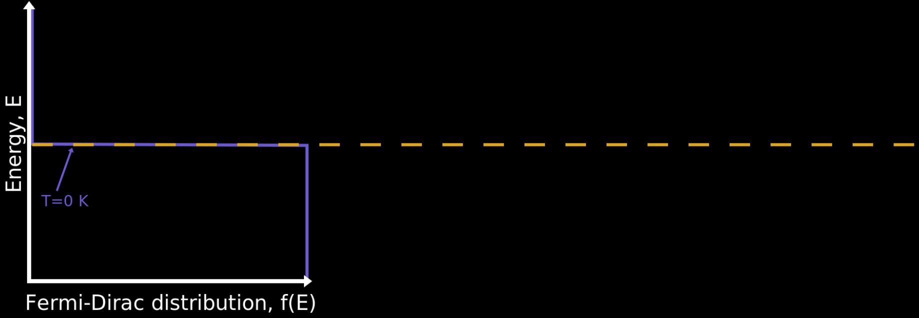

The Fermi-Dirac distribution

Energy distribution of electrons:

$$f(E) \equiv \frac{1}{\exp\left(\frac{E-E_F}{kT}\right)+1}.$$

Fermi level, E_F: maximum energy at $T = 0$ K.

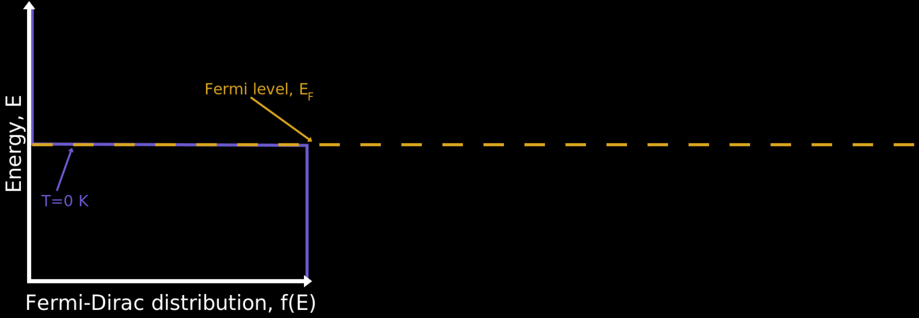

The Fermi-Dirac distribution

Energy distribution of electrons:

$$f(E) \equiv \frac{1}{\exp\left(\frac{E-E_\mathrm{F}}{kT}\right)+1}.$$

Fermi level, E_F: maximum energy at $T=0$ K.

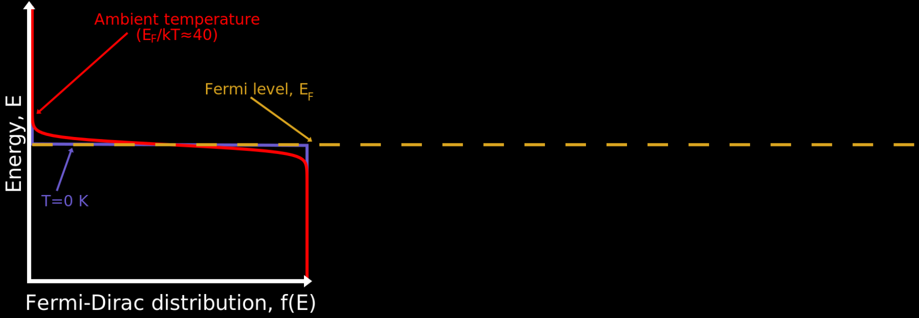

The Fermi-Dirac distribution

Energy distribution of electrons:

$$f(E) \equiv \frac{1}{\exp\left(\frac{E-E_F}{kT}\right)+1}.$$

Fermi level, E_F: maximum energy at $T = 0$ K.

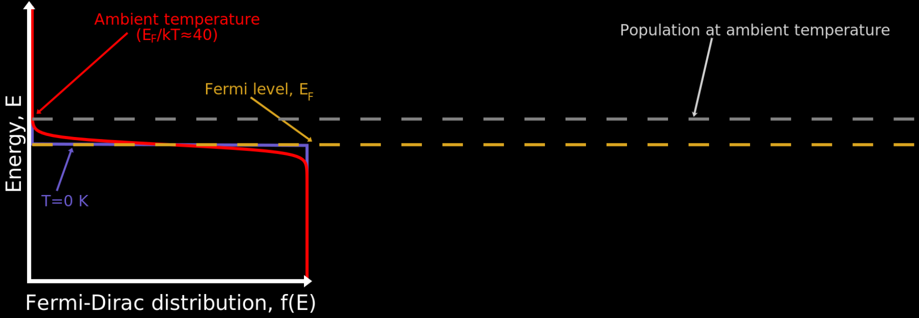

The Fermi-Dirac distribution

Energy distribution of electrons:

$$f(E) \equiv \frac{1}{\exp\left(\frac{E-E_F}{kT}\right)+1}.$$

Fermi level, E_F: maximum energy at $T = 0$ K.

Two and a half types of solids

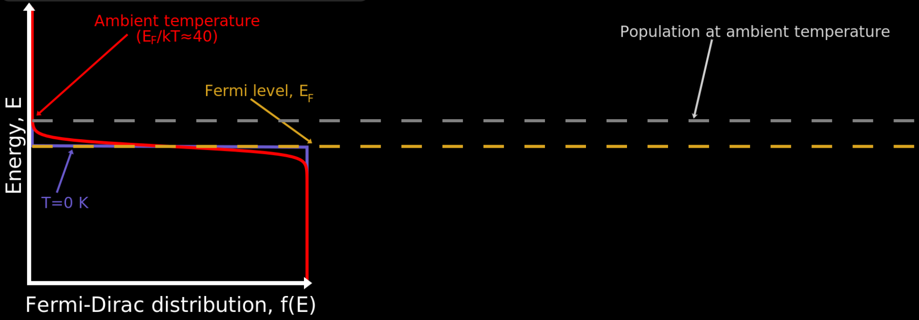

The Fermi-Dirac distribution

Energy distribution of electrons:

$$f(E) \equiv \frac{1}{\exp\left(\frac{E-E_F}{kT}\right)+1}.$$

Fermi level, E_F: maximum energy at $T = 0$ K.

Two and a half types of solids

Insulator (or dielectric): solid where the valence electrons are tied to their nucleus.

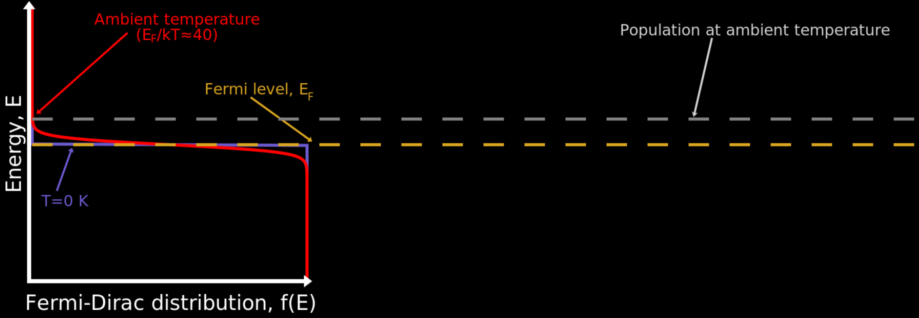

The Fermi-Dirac distribution

Energy distribution of electrons:

$$f(E) \equiv \frac{1}{\exp\left(\frac{E-E_F}{kT}\right)+1}.$$

Fermi level, E_F: maximum energy at $T = 0$ K.

Two and a half types of solids

Insulator (or dielectric): solid where the valence electrons are tied to their nucleus.

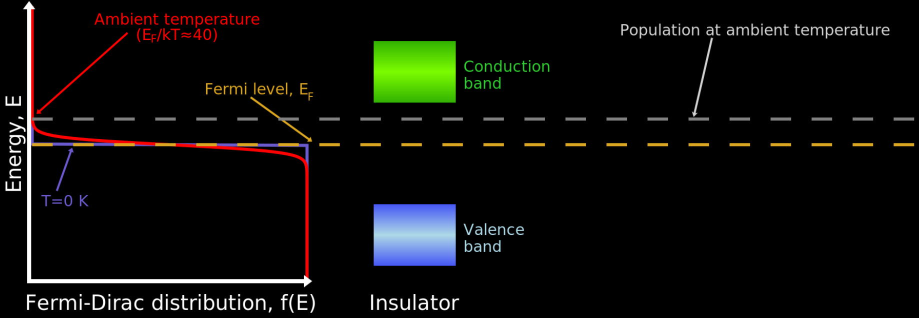

The Fermi-Dirac distribution

Energy distribution of electrons:

$$f(E) \equiv \frac{1}{\exp\left(\frac{E-E_F}{kT}\right)+1}.$$

Fermi level, E_F: maximum energy at $T = 0$ K.

Two and a half types of solids

Insulator (or dielectric): solid where the valence electrons are tied to their nucleus.

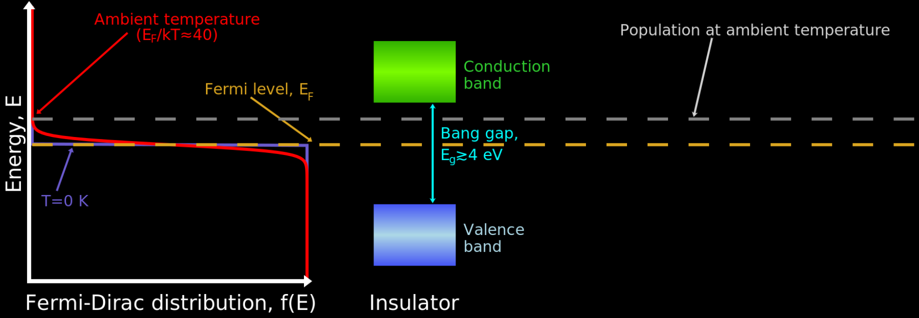

The Fermi-Dirac distribution

Energy distribution of electrons:

$$f(E) \equiv \frac{1}{\exp\left(\frac{E-E_F}{kT}\right)+1}.$$

Fermi level, E_F: maximum energy at $T = 0$ K.

Two and a half types of solids

Insulator (or dielectric): solid where the valence electrons are tied to their nucleus.

Conductor: solid where the valence electrons are free to roam the lattice.

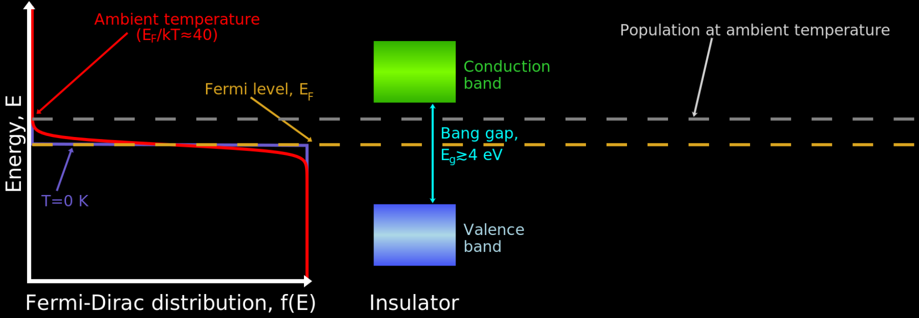

Dust | Insulators, Semiconductors & Conductors

The Fermi-Dirac distribution

Energy distribution of electrons:

$$f(E) \equiv \frac{1}{\exp\left(\frac{E - E_F}{kT}\right) + 1}.$$

Fermi level, E_F: maximum energy at $T = 0$ K.

Two and a half types of solids

Insulator (or dielectric): solid where the valence electrons are tied to their nucleus.

Conductor: solid where the valence electrons are free to roam the lattice.

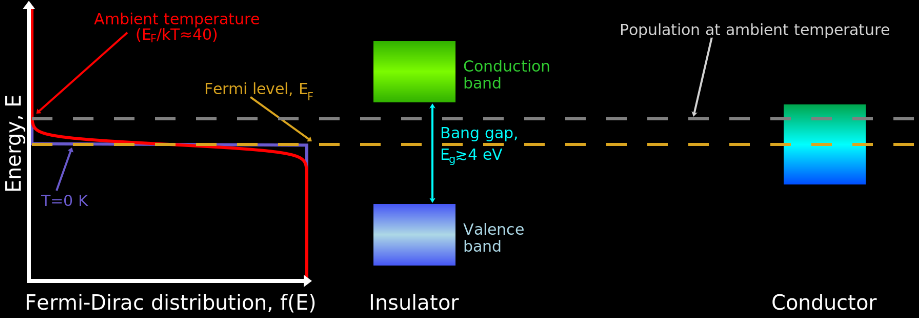

The Fermi-Dirac distribution

Energy distribution of electrons:

$$f(E) \equiv \frac{1}{\exp\left(\frac{E-E_F}{kT}\right)+1}.$$

Fermi level, E_F: maximum energy at $T = 0$ K.

Two and a half types of solids

Insulator (or dielectric): solid where the valence electrons are tied to their nucleus.

Conductor: solid where the valence electrons are free to roam the lattice.

Semiconductor: insulator at $T = 0$ K & conductor at ambient temperature.

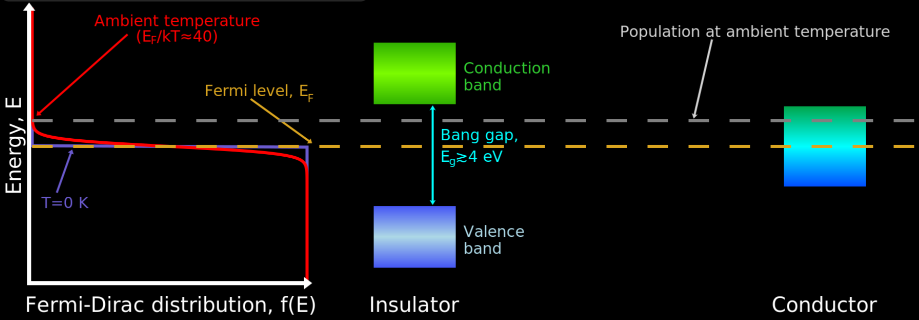

The Fermi-Dirac distribution

Energy distribution of electrons:

$$f(E) \equiv \frac{1}{\exp\left(\frac{E - E_F}{kT}\right) + 1}.$$

Fermi level, E_F: maximum energy at $T = 0$ K.

Two and a half types of solids

Insulator (or dielectric): solid where the valence electrons are tied to their nucleus.

Conductor: solid where the valence electrons are free to roam the lattice.

Semiconductor: insulator at $T = 0$ K & conductor at ambient temperature.

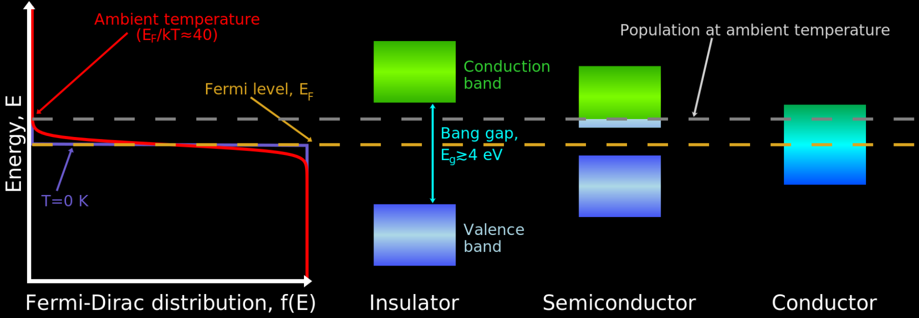

The Fermi-Dirac distribution

Energy distribution of electrons:

$$f(E) \equiv \frac{1}{\exp\left(\frac{E-E_F}{kT}\right)+1}.$$

Fermi level, E_F: maximum energy at $T = 0$ K.

Two and a half types of solids

Insulator (or dielectric): solid where the valence electrons are tied to their nucleus.

Conductor: solid where the valence electrons are free to roam the lattice.

Semiconductor: insulator at $T = 0$ K & conductor at ambient temperature.

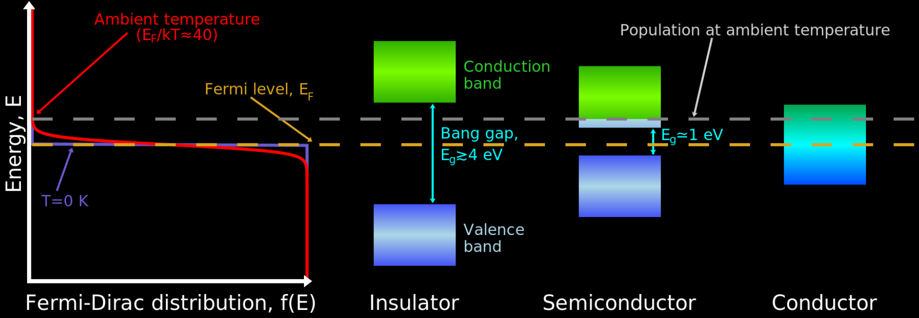

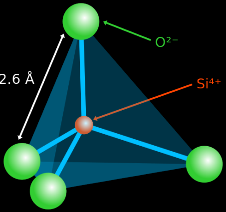

(a) Silica tetrahedron

Dust | Structure of the Main Interstellar Grain Candidates

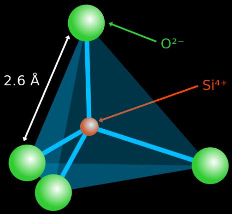

(a) Silica tetrahedron

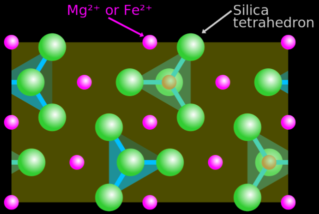

(b) Olivine crystal

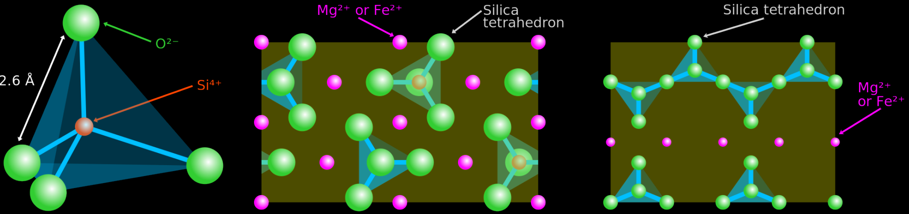

(a) Silica tetrahedron (b) Olivine crystal (c) Pyroxene crystal

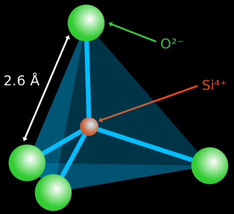

(a) Silica tetrahedron

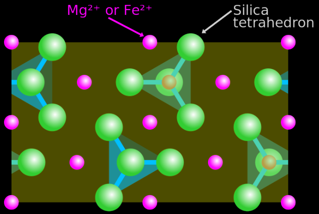

(b) Olivine crystal

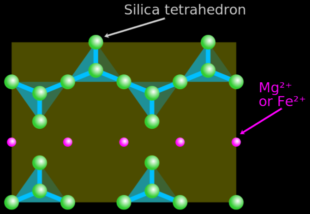

(c) Pyroxene crystal

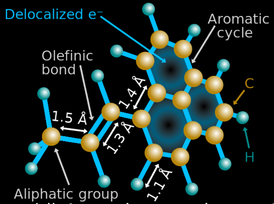

(d) Amorphous carbon, a-C(:H)

Dust | Structure of the Main Interstellar Grain Candidates

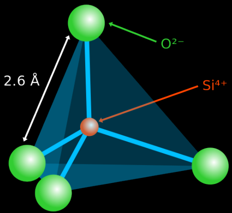

(a) Silica tetrahedron

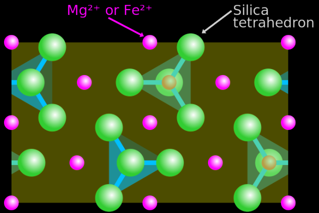

(b) Olivine crystal

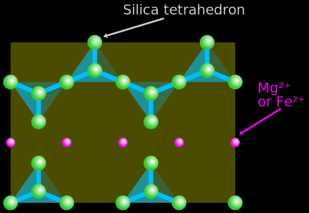

(c) Pyroxene crystal

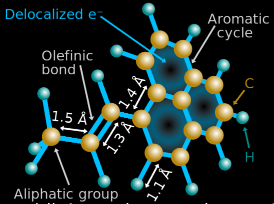

(d) Amorphous carbon, a-C(:H)

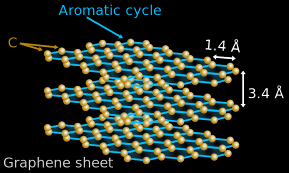

(e) Graphite

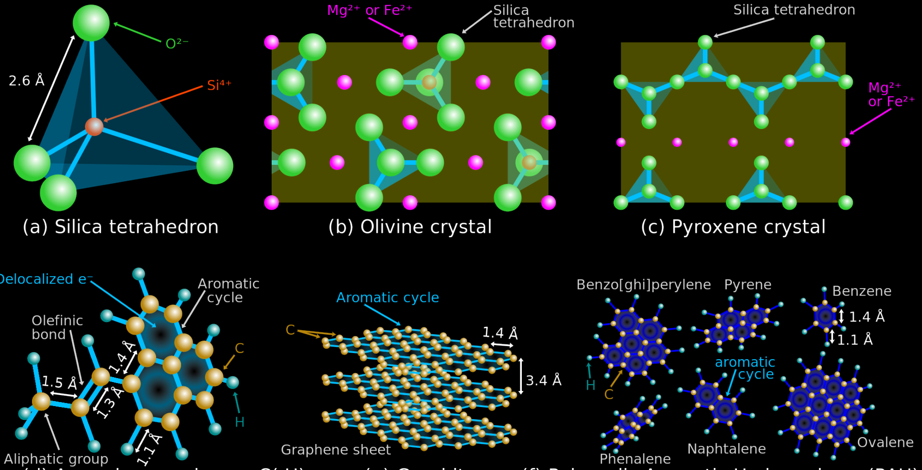

(a) Silica tetrahedron (b) Olivine crystal (c) Pyroxene crystal

(d) Amorphous carbon, a-C(:H) (e) Graphite (f) Polycyclic Aromatic Hydrocarbons (PAH)

Dust | Macroscopic Appearance of Interstellar Grain Materials

Forsterite

Dust | Macroscopic Appearance of Interstellar Grain Materials

Forsterite

Enstatite

Forsterite

Enstatite

Graphite

Forsterite

Enstatite

Graphite

Soot $\simeq$ a-C(:H)

Forsterite

Enstatite

PAHs

Graphite

Soot $\simeq$ a-C(:H)


Background Stars
Dusty Cloud


Non-extincted optical photon
Background Stars
Dusty Cloud

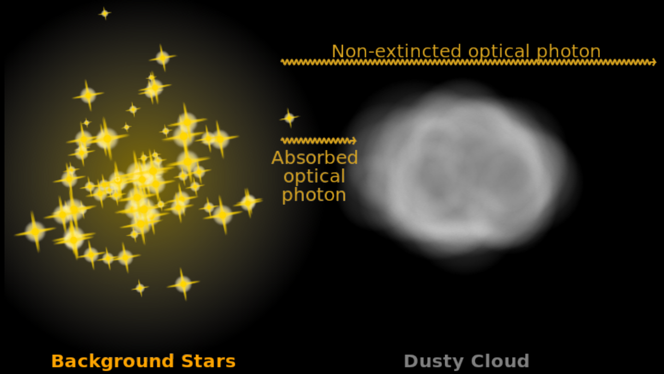
Non-extincted optical photon
Absorbed optical photon
Background Stars
Dusty Cloud

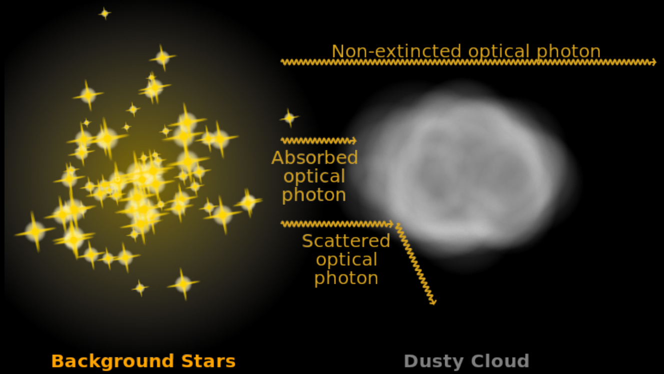
Non-extincted optical photon
Absorbed optical photon
Scattered optical photon
Background Stars
Dusty Cloud

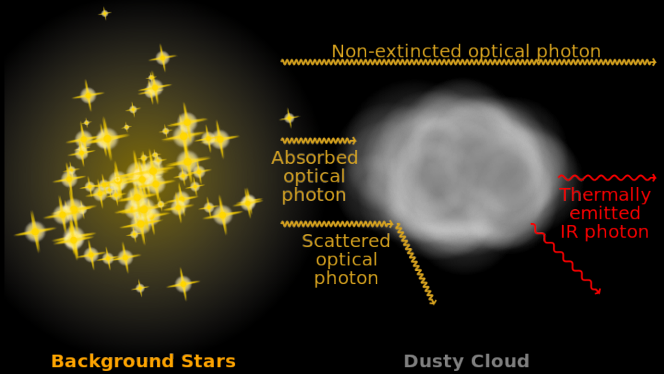
Non-extincted optical photon
Absorbed optical photon
Scattered optical photon
Thermally emitted IR photon
Background Stars
Dusty Cloud

Dust | Scattering, Absorption & Emission

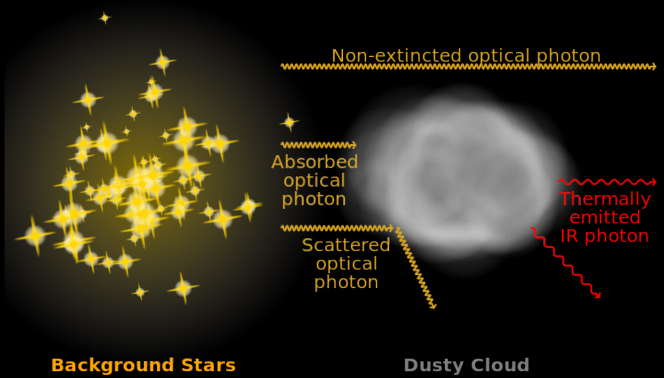

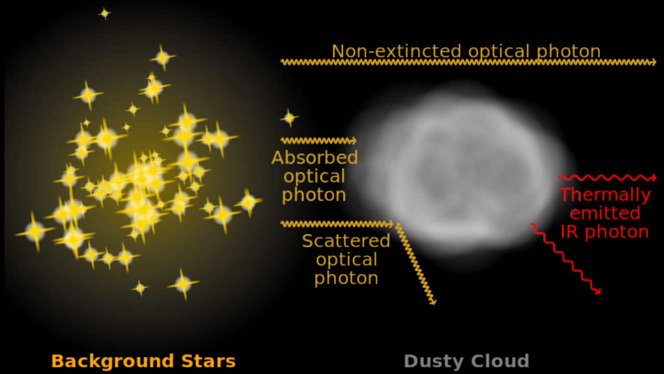
Non-extincted optical photon
Absorbed optical photon
Scattered optical photon
Thermally emitted IR photon
Background Stars
Dusty Cloud


Extinction
Optical
Emission
Infrared

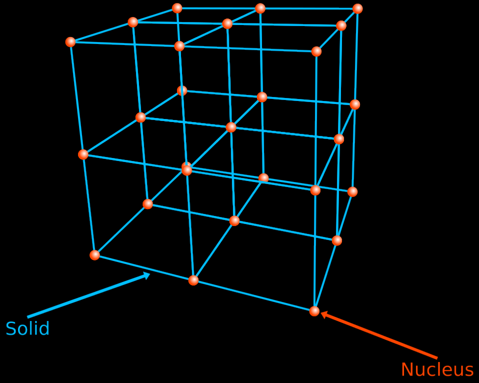
Solid
Nucleus

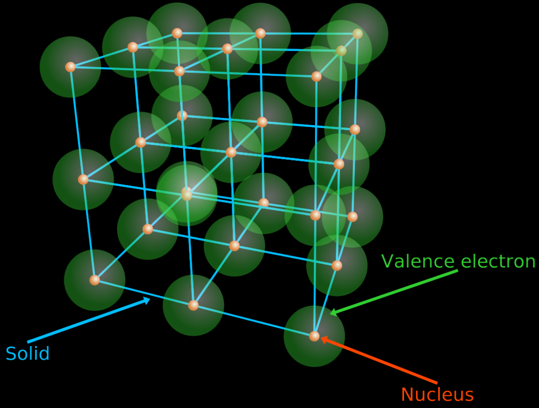
Valence electron
Solid
Nucleus

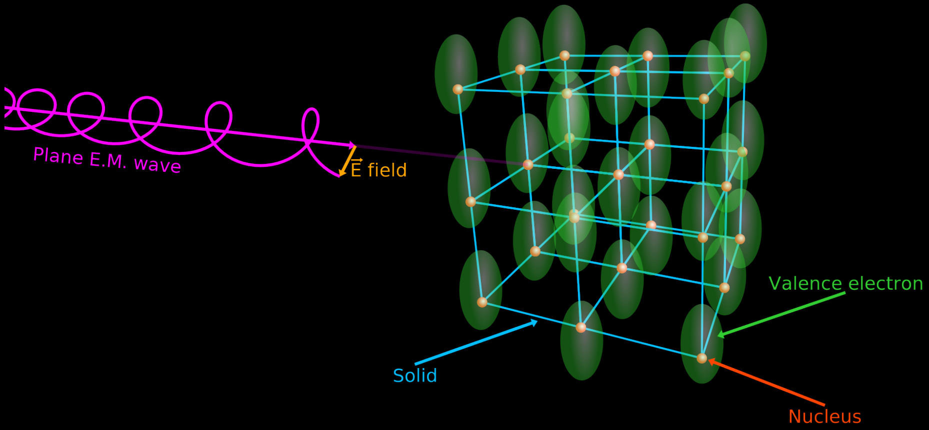
Plane E.M. wave
$\vec{E}$ field
Valence electron
Solid
Nucleus

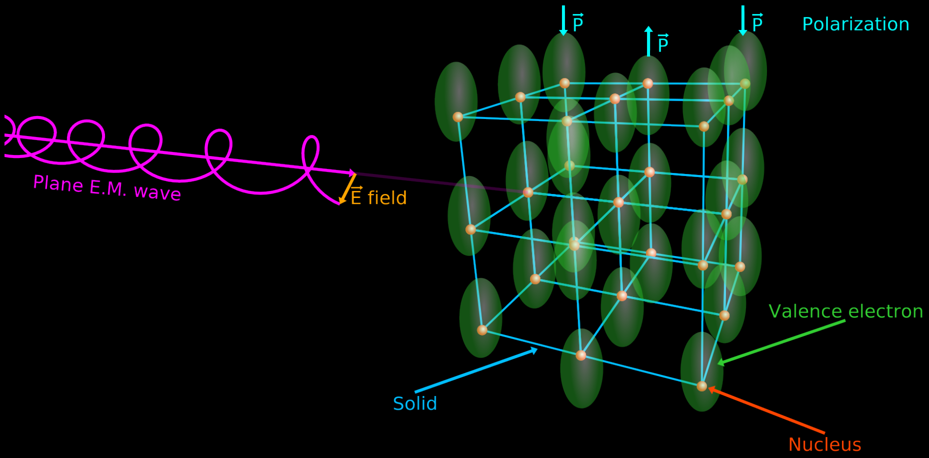

$\vec{P}$
$\vec{P}$
$\vec{P}$
Polarization
Plane E.M. wave
$\vec{E}$ field
Valence electron
Solid
Nucleus

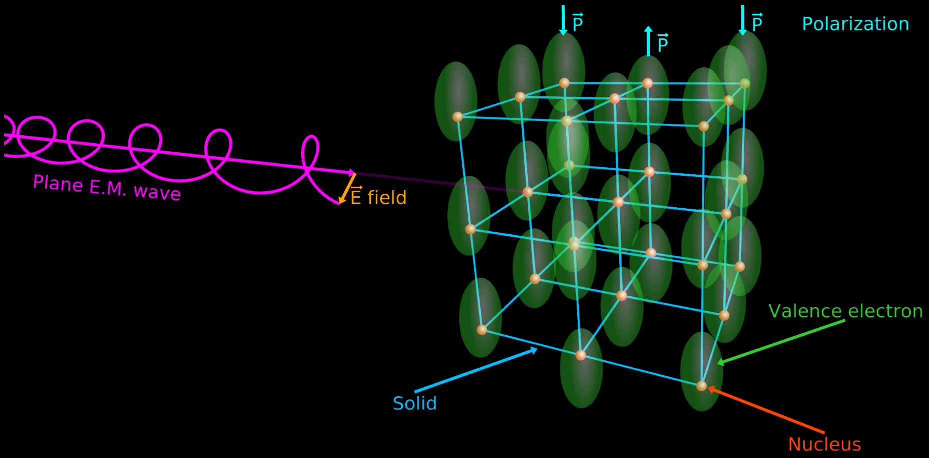

Absorption & scattering:

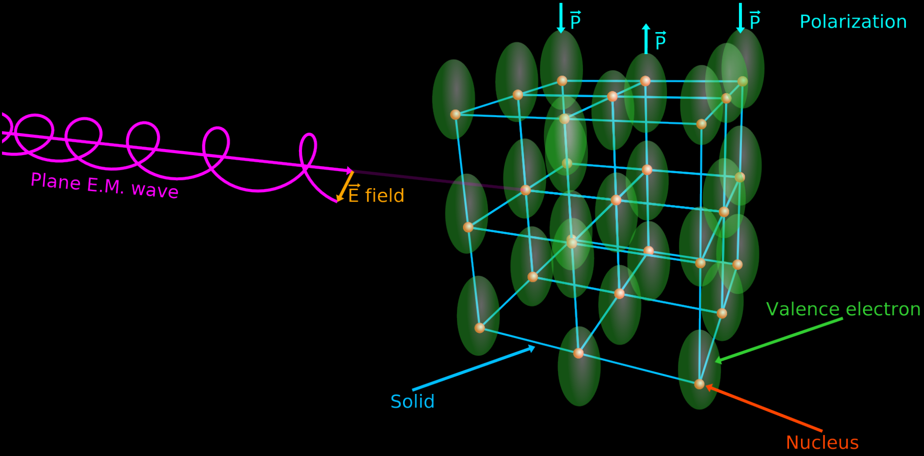

Absorption & scattering: $\underbrace{\vec{D}}_{\text{electric displacement field}} = \epsilon_0 \vec{E}$

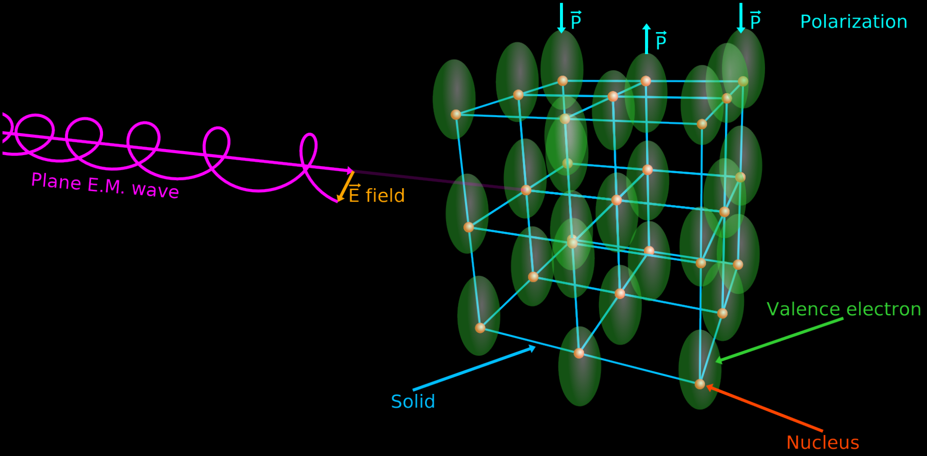

Absorption & scattering: $\underbrace{\vec{D}}_{\text{electric displacement field}} = \epsilon_0 \vec{E} + \underbrace{\vec{P}}_{\text{induced dipoles}}$

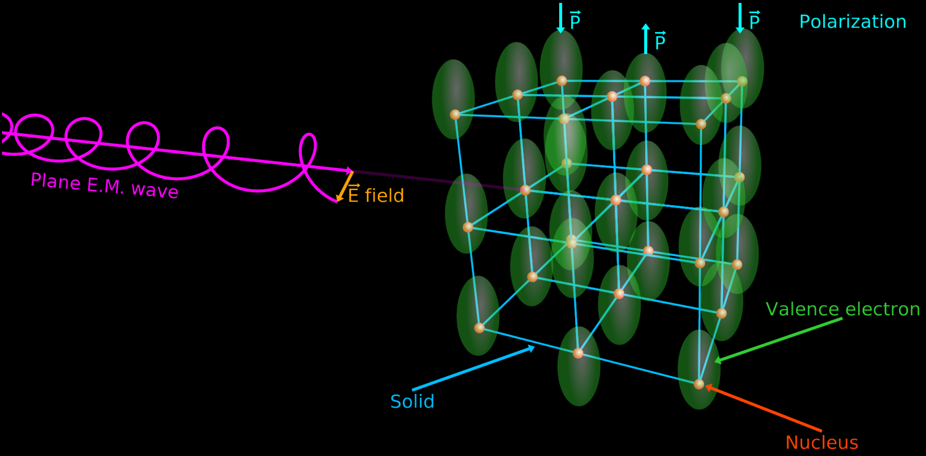

Absorption & scattering:

$$\underbrace{\vec{D}}_{\text{electric displacement field}} = \epsilon_0 \vec{E} + \underbrace{\vec{P}}_{\text{induced dipoles}} = \epsilon_0 \times \underbrace{\epsilon_r}_{\text{relative permittivity}} \times \vec{E}$$

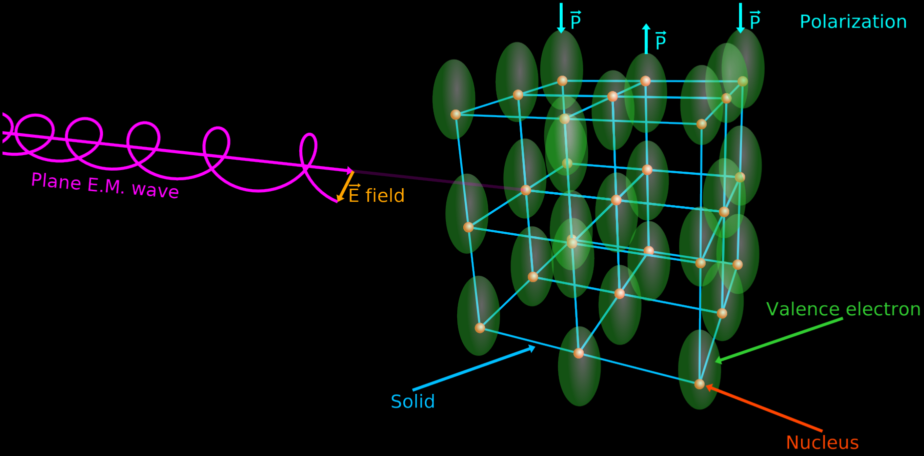

Absorption & scattering: $\underbrace{\vec{D}}_{\text{electric displacement field}} = \epsilon_0 \vec{E} + \underbrace{\vec{P}}_{\text{induced dipoles}} = \epsilon_0 \times \underbrace{\epsilon_r}_{\text{relative permittivity}} \times \vec{E}$

Emission:

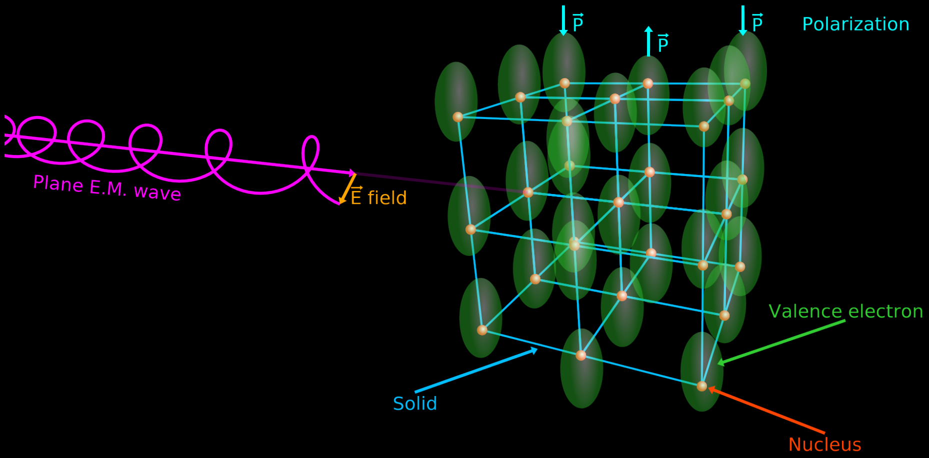

Absorption & scattering: $\underbrace{\vec{D}}_{\text{electric displacement field}} = \epsilon_0 \vec{E} + \underbrace{\vec{P}}_{\text{induced dipoles}} = \epsilon_0 \times \underbrace{\epsilon_r}_{\text{relative permittivity}} \times \vec{E}$

Emission: dissipation $\Rightarrow$ collision with the lattice

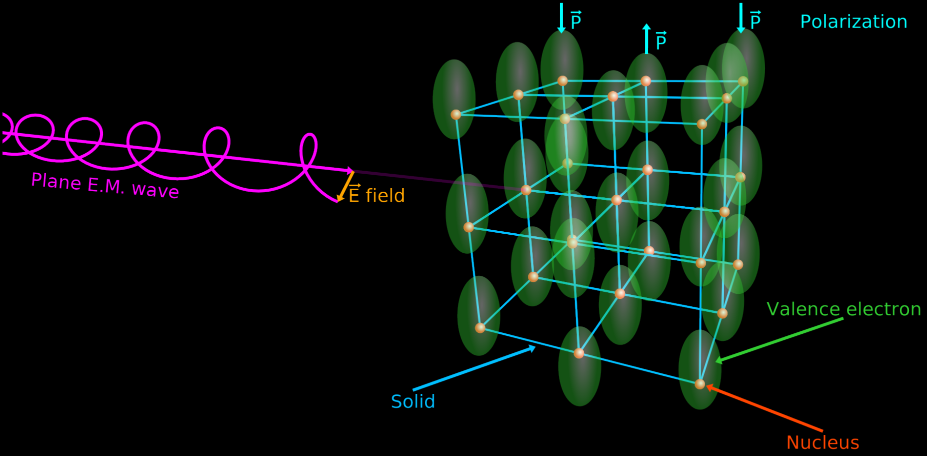

Absorption & scattering: $\underbrace{\vec{D}}_{\text{electric displacement field}} = \epsilon_0 \vec{E} + \underbrace{\vec{P}}_{\text{induced dipoles}} = \epsilon_0 \times \underbrace{\epsilon_r}_{\text{relative permittivity}} \times \vec{E}$

Emission: dissipation ⇒ collision with the lattice ⇒ thermal radiation.

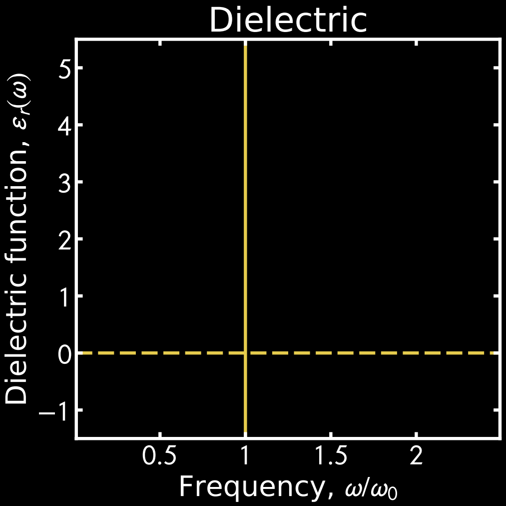

Dielectric
Dielectric function, $\varepsilon_r(\omega)$
5
4
3
2
1
0
−1
0.5
1
1.5
2
Frequency, ω/ω_0

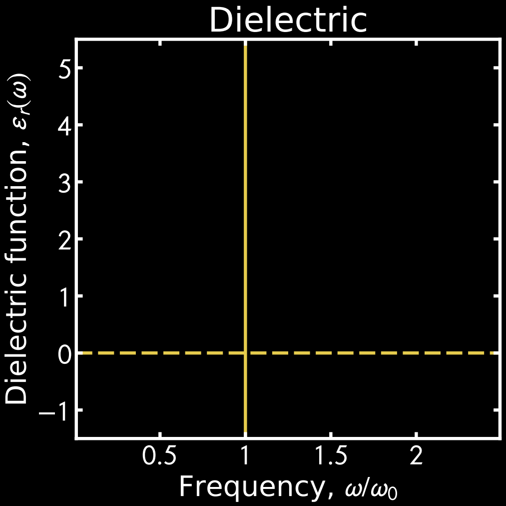

Absorption: attenuation $\Rightarrow$ function of $\text{Im}(\epsilon_r)$.

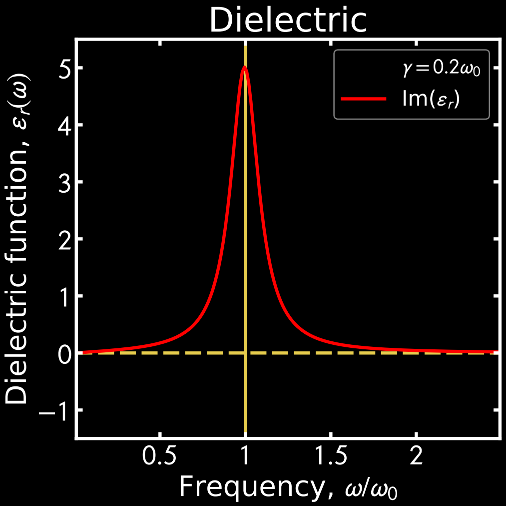

Absorption: attenuation ⇒ function of Im(ϵ_r).

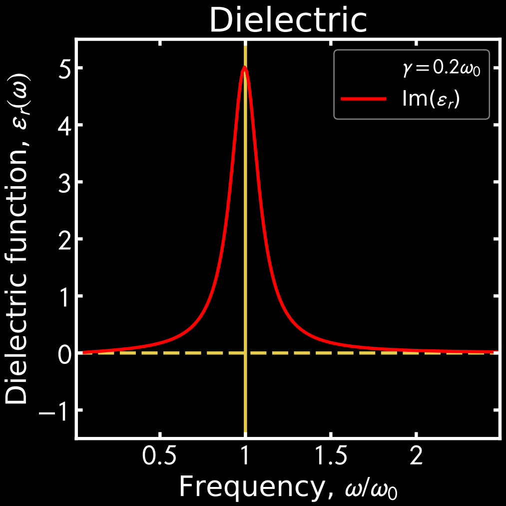

Absorption: attenuation $\Rightarrow$ function of $\mathrm{Im}(\epsilon_r)$.

Kramers-Kronig relations: causality relations $\Rightarrow$ $\mathrm{Re}(\epsilon_r) = f[\mathrm{Im}(\epsilon_r)]$.

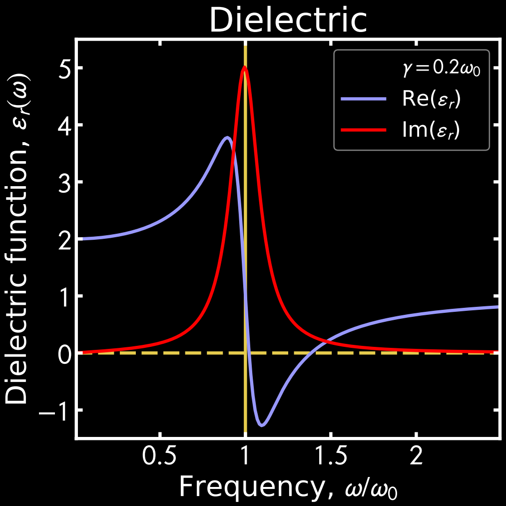

Absorption: attenuation $\Rightarrow$ function of Im(ϵ_r).

Kramers-Kronig relations: causality relations $\Rightarrow$ $\mathrm{Re}(\epsilon_r) = f[\mathrm{Im}(\epsilon_r)]$.

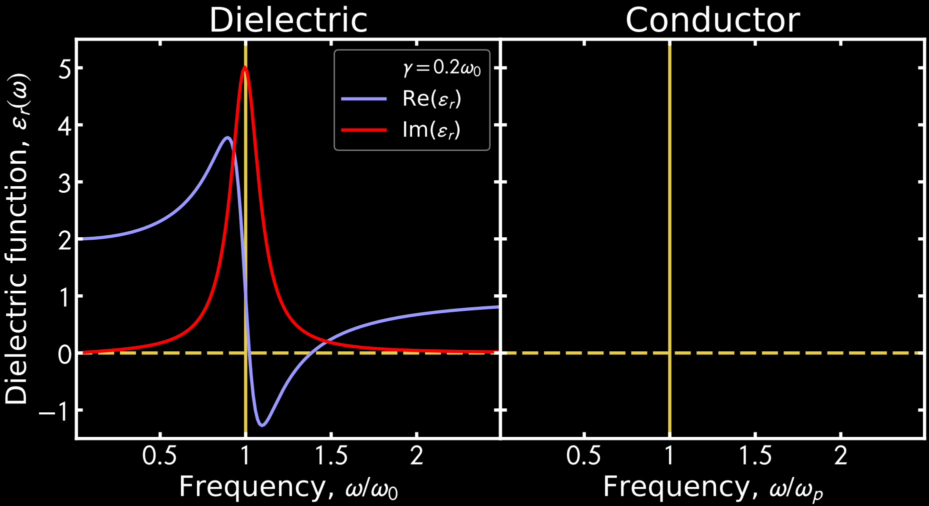

Absorption: attenuation $\Rightarrow$ function of Im(ϵ_r).

Kramers-Kronig relations: causality relations $\Rightarrow \mathrm{Re}(\epsilon_r) = f[\mathrm{Im}(\epsilon_r)]$.

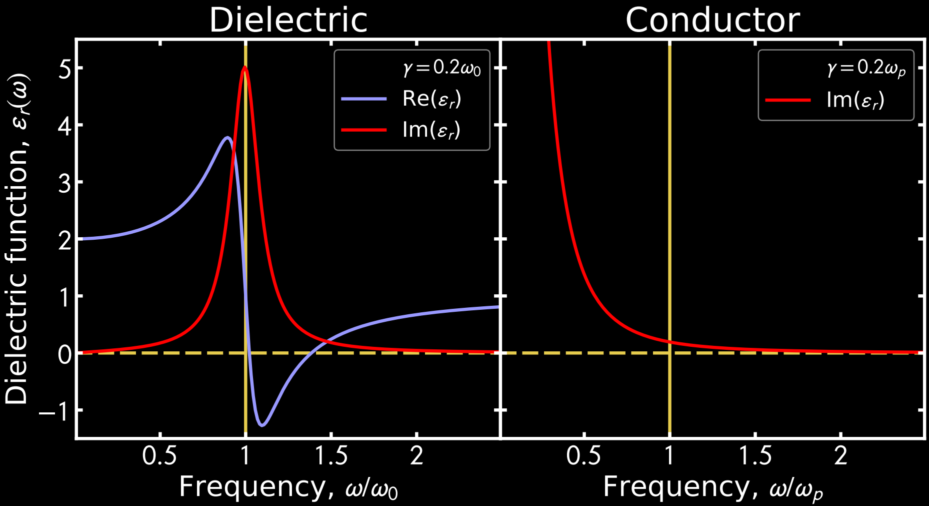

Absorption: attenuation $\Rightarrow$ function of $\mathrm{Im}(\epsilon_r)$.

Kramers-Kronig relations: causality relations $\Rightarrow \mathrm{Re}(\epsilon_r) = f[\mathrm{Im}(\epsilon_r)]$.

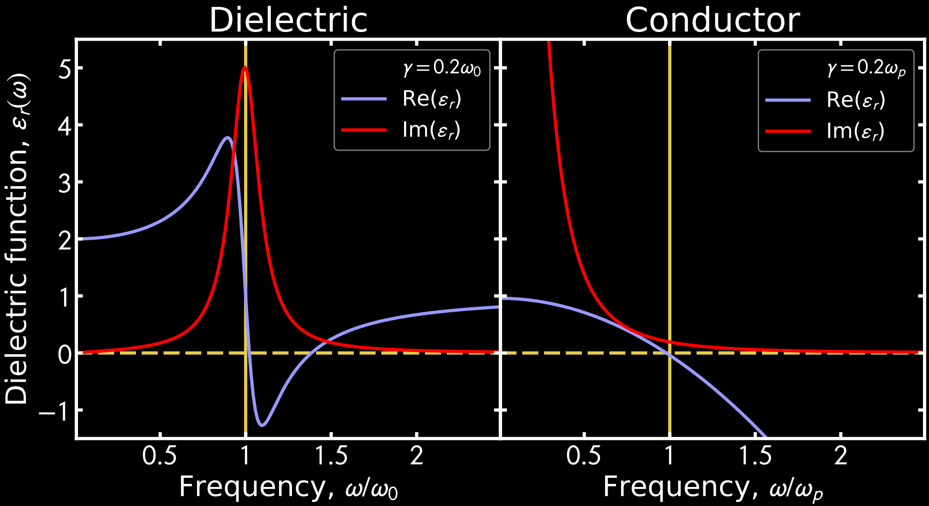

Absorption: attenuation ⇒ function of Im(ϵ_r).

Kramers-Kronig relations: causality relations ⇒ $\mathrm{Re}(\epsilon_r) = f[\mathrm{Im}(\epsilon_r)]$.

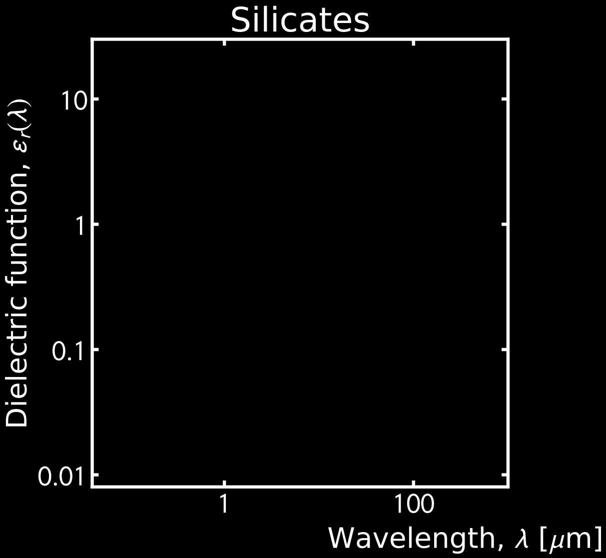
Silicates
10
1
0.1
0.01
Dielectric function, $\varepsilon_r(\lambda)$
1
100
Wavelength, λ [μm]

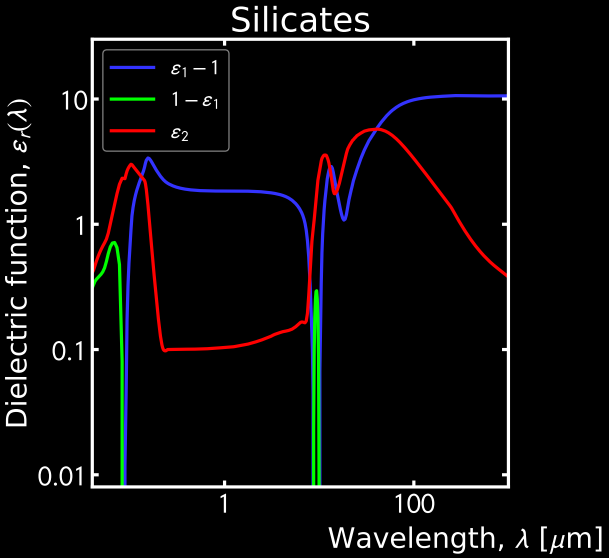

(Optical properties from Draine 2003

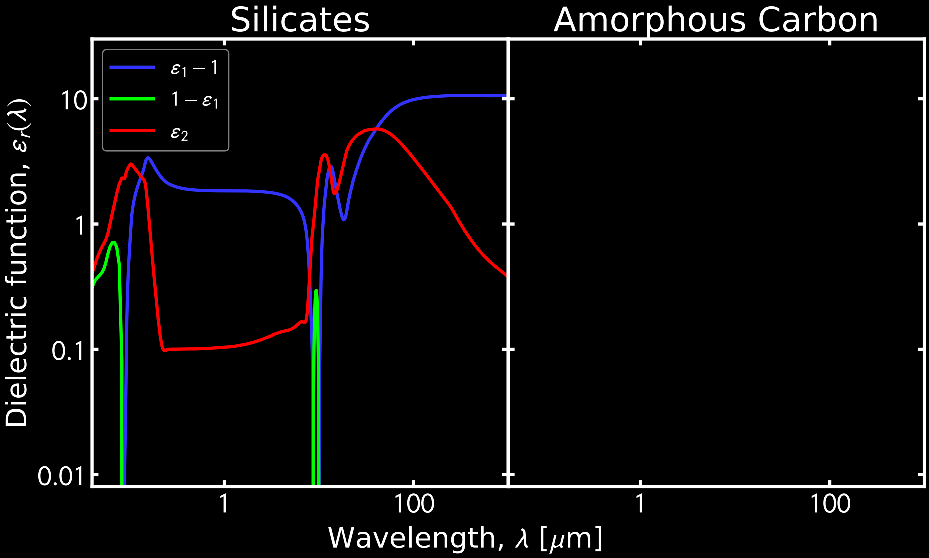

(Optical properties from Draine 2003

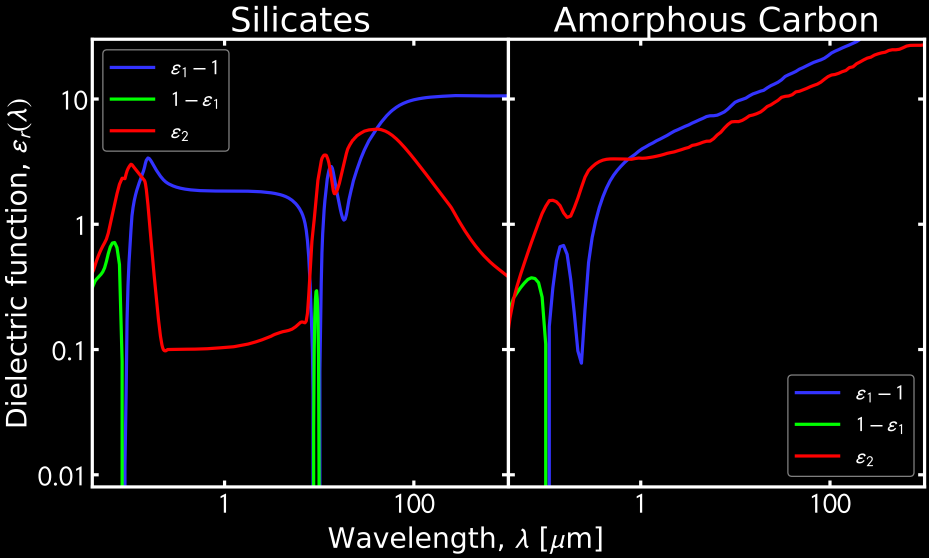

(Optical properties from Draine 2003 & Zubko et al. 1996)

Mie theory

Mie theory

Principle: solves absorption & scattering of a plane E.M. wave by a spherical homogeneous grain

Mie theory

Principle: solves absorption & scattering of a plane E.M. wave by a spherical homogeneous grain
$\rightarrow$ Maxwell equations + spherical harmonics expansion.

Mie theory

Principle: solves absorption & scattering of a plane E.M. wave by a spherical homogeneous grain $\rightarrow$ Maxwell equations + spherical harmonics expansion.

Results: depend only on $x \equiv 2\pi a/\lambda$ (a: grain radius):

Mie theory

Principle: solves absorption & scattering of a plane E.M. wave by a spherical homogeneous grain $\rightarrow$ Maxwell equations + spherical harmonics expansion.

Results: depend only on $x \equiv 2\pi a/\lambda$ (a: grain radius):

$$\underbrace{C_{\text{abs}}(\lambda, a)}_{\text{absorption cross-section}} \equiv$$

Mie theory

Principle: solves absorption & scattering of a plane E.M. wave by a spherical homogeneous grain → Maxwell equations + spherical harmonics expansion.

Results: depend only on $x \equiv 2\pi a/\lambda$ (a: grain radius):

$$\underbrace{C_{\rm abs}(\lambda, a)}_{\text{absorption cross-section}} \equiv \underbrace{\pi a^2}_{\text{cross-section}} \times$$

Mie theory

Principle: solves absorption & scattering of a plane E.M. wave by a spherical homogeneous grain $\rightarrow$ Maxwell equations + spherical harmonics expansion.

Results: depend only on $x \equiv 2\pi a/\lambda$ (a: grain radius):

$$\underbrace{C_{\rm abs}(\lambda, a)}_{\text{absorption cross-section}} \equiv \underbrace{\pi a^2}_{\text{cross-section}} \times \underbrace{Q_{\rm abs}(x)}_{\text{absorption efficiency}}$$

Mie theory

Principle: solves absorption & scattering of a plane E.M. wave by a spherical homogeneous grain $\rightarrow$ Maxwell equations + spherical harmonics expansion.

Results: depend only on $x \equiv 2\pi a/\lambda$ (a: grain radius):

$$\underbrace{C_{\rm abs}(\lambda, a)}_{\text{absorption cross-section}} \equiv \underbrace{\pi a^2}_{\text{cross-section}} \times \underbrace{Q_{\rm abs}(x)}_{\text{absorption efficiency}}$$

$$\underbrace{C_{\rm sca}(\lambda, a)}_{\text{scattering cross-section}} \equiv \underbrace{\pi a^2}_{\text{cross-section}} \times \underbrace{Q_{\rm sca}(x)}_{\text{scattering efficiency}}$$

Mie theory

Principle: solves absorption & scattering of a plane E.M. wave by a spherical homogeneous grain
→ Maxwell equations + spherical harmonics expansion.

Results: depend only on $x \equiv 2\pi a/\lambda$ (a: grain radius):

$$\underbrace{C_{\rm abs}(\lambda, a)}_{\text{absorption cross-section}} \equiv \underbrace{\pi a^2}_{\text{cross-section}} \times \underbrace{Q_{\rm abs}(x)}_{\text{absorption efficiency}}$$

$$\underbrace{C_{\rm sca}(\lambda, a)}_{\text{scattering cross-section}} \equiv \underbrace{\pi a^2}_{\text{cross-section}} \times \underbrace{Q_{\rm sca}(x)}_{\text{scattering efficiency}}$$

$$\underbrace{g(\lambda, a)}_{\text{asymmetry parameter}} \equiv$$

Mie theory

Principle: solves absorption & scattering of a plane E.M. wave by a spherical homogeneous grain $\rightarrow$ Maxwell equations + spherical harmonics expansion.

Results: depend only on $x \equiv 2\pi a/\lambda$ (a: grain radius):

$$\underbrace{C_{\rm abs}(\lambda, a)}_{\text{absorption cross-section}} \equiv \underbrace{\pi a^2}_{\text{cross-section}} \times \underbrace{Q_{\rm abs}(x)}_{\text{absorption efficiency}}$$

$$\underbrace{C_{\rm sca}(\lambda, a)}_{\text{scattering cross-section}} \equiv \underbrace{\pi a^2}_{\text{cross-section}} \times \underbrace{Q_{\rm sca}(x)}_{\text{scattering efficiency}}$$

$$\underbrace{g(\lambda, a)}_{\text{asymmetry parameter}} \equiv \langle \underbrace{\cos\theta}_{\text{scattering angle}} \rangle(x)$$

Mie theory

Principle: solves absorption & scattering of a plane E.M. wave by a spherical homogeneous grain
$\rightarrow$ Maxwell equations + spherical harmonics expansion.

Results: depend only on $x \equiv 2\pi a/\lambda$ (a: grain radius):

$$\underbrace{C_{\rm abs}(\lambda,a)}_{\text{absorption cross-section}} \equiv \underbrace{\pi a^2}_{\text{cross-section}} \times \underbrace{Q_{\rm abs}(x)}_{\text{absorption efficiency}}$$

$$\underbrace{C_{\rm sca}(\lambda,a)}_{\text{scattering cross-section}} \equiv \underbrace{\pi a^2}_{\text{cross-section}} \times \underbrace{Q_{\rm sca}(x)}_{\text{scattering efficiency}}$$

$$\underbrace{g(\lambda,a)}_{\text{asymmetry parameter}} \equiv \langle \underbrace{\cos\theta}_{\text{scattering angle}} \rangle(x)$$

Limit behaviors of the optical properties

Mie theory

Principle: solves absorption & scattering of a plane E.M. wave by a spherical homogeneous grain $\rightarrow$ Maxwell equations + spherical harmonics expansion.

Results: depend only on $x \equiv 2\pi a/\lambda$ (a: grain radius):

$$\underbrace{C_{\rm abs}(\lambda, a)}_{\text{absorption cross-section}} \equiv \underbrace{\pi a^2}_{\text{cross-section}} \times \underbrace{Q_{\rm abs}(x)}_{\text{absorption efficiency}}$$

$$\underbrace{C_{\rm sca}(\lambda, a)}_{\text{scattering cross-section}} \equiv \underbrace{\pi a^2}_{\text{cross-section}} \times \underbrace{Q_{\rm sca}(x)}_{\text{scattering efficiency}}$$

$$\underbrace{g(\lambda, a)}_{\text{asymmetry parameter}} \equiv \langle \underbrace{\cos\theta}_{\text{scattering angle}} \rangle(x)$$

Limit behaviors of the optical properties

Geometrical optics $(x \gg 1)$

Mie theory

Principle: solves absorption & scattering of a plane E.M. wave by a spherical homogeneous grain $\rightarrow$ Maxwell equations + spherical harmonics expansion.

Results: depend only on $x \equiv 2\pi a/\lambda$ (a: grain radius):

$$\underbrace{C_{\rm abs}(\lambda,a)}_{\text{absorption cross-section}} \equiv \underbrace{\pi a^2}_{\text{cross-section}} \times \underbrace{Q_{\rm abs}(x)}_{\text{absorption efficiency}}$$

$$\underbrace{C_{\rm sca}(\lambda,a)}_{\text{scattering cross-section}} \equiv \underbrace{\pi a^2}_{\text{cross-section}} \times \underbrace{Q_{\rm sca}(x)}_{\text{scattering efficiency}}$$

$$\underbrace{g(\lambda,a)}_{\text{asymmetry parameter}} \equiv \langle \underbrace{\cos\theta}_{\text{scattering angle}} \rangle(x)$$

Limit behaviors of the optical properties

Geometrical optics $(x \gg 1)$ grain $\simeq$ screen:

Mie theory

Principle: solves absorption & scattering of a plane E.M. wave by a spherical homogeneous grain $\rightarrow$ Maxwell equations + spherical harmonics expansion.

Results: depend only on $x \equiv 2\pi a/\lambda$ (a: grain radius):

$$\underbrace{C_{\rm abs}(\lambda, a)}_{\text{absorption cross-section}} \equiv \underbrace{\pi a^2}_{\text{cross-section}} \times \underbrace{Q_{\rm abs}(x)}_{\text{absorption efficiency}}$$

$$\underbrace{C_{\rm sca}(\lambda, a)}_{\text{scattering cross-section}} \equiv \underbrace{\pi a^2}_{\text{cross-section}} \times \underbrace{Q_{\rm sca}(x)}_{\text{scattering efficiency}}$$

$$\underbrace{g(\lambda, a)}_{\text{asymmetry parameter}} \equiv \langle \underbrace{\cos\theta}_{\text{scattering angle}} \rangle(x)$$

Limit behaviors of the optical properties

Geometrical optics $(x \gg 1)$ grain $\simeq$ screen:

$$Q_{\rm abs} \simeq 1$$

Mie theory

Principle: solves absorption & scattering of a plane E.M. wave by a spherical homogeneous grain $\rightarrow$ Maxwell equations + spherical harmonics expansion.

Results: depend only on $x \equiv 2\pi a/\lambda$ (a: grain radius):

$$\underbrace{C_{\text{abs}}(\lambda, a)}_{\text{absorption cross-section}} \equiv \underbrace{\pi a^2}_{\text{cross-section}} \times \underbrace{Q_{\text{abs}}(x)}_{\text{absorption efficiency}}$$

$$\underbrace{C_{\text{sca}}(\lambda, a)}_{\text{scattering cross-section}} \equiv \underbrace{\pi a^2}_{\text{cross-section}} \times \underbrace{Q_{\text{sca}}(x)}_{\text{scattering efficiency}}$$

$$\underbrace{g(\lambda, a)}_{\text{asymmetry parameter}} \equiv \langle \underbrace{\cos\theta}_{\text{scattering angle}} \rangle(x)$$

Limit behaviors of the optical properties

Geometrical optics $(x \gg 1)$ grain $\simeq$ screen:

$$Q_{\text{abs}} \simeq 1 \quad Q_{\text{sca}} \simeq 1$$

Mie theory

Principle: solves absorption & scattering of a plane E.M. wave by a spherical homogeneous grain
→ Maxwell equations + spherical harmonics expansion.

Results: depend only on $x \equiv 2\pi a/\lambda$ (a: grain radius):

$$\underbrace{C_{\rm abs}(\lambda,a)}_{\text{absorption cross-section}} \equiv \underbrace{\pi a^2}_{\text{cross-section}} \times \underbrace{Q_{\rm abs}(x)}_{\text{absorption efficiency}}$$

$$\underbrace{C_{\rm sca}(\lambda,a)}_{\text{scattering cross-section}} \equiv \underbrace{\pi a^2}_{\text{cross-section}} \times \underbrace{Q_{\rm sca}(x)}_{\text{scattering efficiency}}$$

$$\underbrace{g(\lambda,a)}_{\text{asymmetry parameter}} \equiv \langle \underbrace{\cos\theta}_{\text{scattering angle}} \rangle(x)$$

Limit behaviors of the optical properties

Geometrical optics $(x \gg 1)$ grain $\simeq$ screen:

$$Q_{\rm abs} \simeq 1 \quad Q_{\rm sca} \simeq 1 \quad \langle\cos\theta\rangle \simeq 1.$$

Mie theory

Principle: solves absorption & scattering of a plane E.M. wave by a spherical homogeneous grain $\rightarrow$ Maxwell equations + spherical harmonics expansion.

Results: depend only on $x \equiv 2\pi a/\lambda$ (a: grain radius):

$$\underbrace{C_{\rm abs}(\lambda,a)}_{\text{absorption cross-section}} \equiv \underbrace{\pi a^2}_{\text{cross-section}} \times \underbrace{Q_{\rm abs}(x)}_{\text{absorption efficiency}}$$

$$\underbrace{C_{\rm sca}(\lambda,a)}_{\text{scattering cross-section}} \equiv \underbrace{\pi a^2}_{\text{cross-section}} \times \underbrace{Q_{\rm sca}(x)}_{\text{scattering efficiency}}$$

$$\underbrace{g(\lambda,a)}_{\text{asymmetry parameter}} \equiv \langle \underbrace{\cos\theta}_{\text{scattering angle}} \rangle(x)$$

Limit behaviors of the optical properties

Geometrical optics $(x \gg 1)$ grain $\simeq$ screen:

$$Q_{\rm abs} \simeq 1 \quad Q_{\rm sca} \simeq 1 \quad \langle\cos\theta\rangle \simeq 1.$$

Rayleigh regime $(x \ll 1)$

Mie theory

Principle: solves absorption & scattering of a plane E.M. wave by a spherical homogeneous grain $\rightarrow$ Maxwell equations + spherical harmonics expansion.

Results: depend only on $x \equiv 2\pi a/\lambda$ (a: grain radius):

$$\underbrace{C_{\rm abs}(\lambda, a)}_{\text{absorption cross-section}} \equiv \underbrace{\pi a^2}_{\text{cross-section}} \times \underbrace{Q_{\rm abs}(x)}_{\text{absorption efficiency}}$$

$$\underbrace{C_{\rm sca}(\lambda, a)}_{\text{scattering cross-section}} \equiv \underbrace{\pi a^2}_{\text{cross-section}} \times \underbrace{Q_{\rm sca}(x)}_{\text{scattering efficiency}}$$

$$\underbrace{g(\lambda, a)}_{\text{asymmetry parameter}} \equiv \langle \underbrace{\cos\theta}_{\text{scattering angle}} \rangle(x)$$

Limit behaviors of the optical properties

Geometrical optics $(x \gg 1)$ grain $\simeq$ screen:

$$Q_{\rm abs} \simeq 1 \quad Q_{\rm sca} \simeq 1 \quad \langle\cos\theta\rangle \simeq 1.$$

Rayleigh regime $(x \ll 1)$ grain $\simeq$ dipole:

Mie theory

Principle: solves absorption & scattering of a plane E.M. wave by a spherical homogeneous grain
→ Maxwell equations + spherical harmonics expansion.

Results: depend only on $x \equiv 2\pi a/\lambda$ (a: grain radius):

$$\underbrace{C_{\rm abs}(\lambda, a)}_{\text{absorption cross-section}} \equiv \underbrace{\pi a^2}_{\text{cross-section}} \times \underbrace{Q_{\rm abs}(x)}_{\text{absorption efficiency}}$$

$$\underbrace{C_{\rm sca}(\lambda, a)}_{\text{scattering cross-section}} \equiv \underbrace{\pi a^2}_{\text{cross-section}} \times \underbrace{Q_{\rm sca}(x)}_{\text{scattering efficiency}}$$

$$\underbrace{g(\lambda, a)}_{\text{asymmetry parameter}} \equiv \langle \underbrace{\cos\theta}_{\text{scattering angle}} \rangle(x)$$

Limit behaviors of the optical properties

Geometrical optics $(x \gg 1)$ grain $\simeq$ screen:

$$Q_{\rm abs} \simeq 1 \quad Q_{\rm sca} \simeq 1 \quad \langle\cos\theta\rangle \simeq 1.$$

Rayleigh regime $(x \ll 1)$ grain $\simeq$ dipole:

$$Q_{\rm abs} \propto \lambda^{-2}$$

Mie theory

Principle: solves absorption & scattering of a plane E.M. wave by a spherical homogeneous grain $\rightarrow$ Maxwell equations + spherical harmonics expansion.

Results: depend only on $x \equiv 2\pi a/\lambda$ (a: grain radius):

$$\underbrace{C_{\rm abs}(\lambda, a)}_{\text{absorption cross-section}} \equiv \underbrace{\pi a^2}_{\text{cross-section}} \times \underbrace{Q_{\rm abs}(x)}_{\text{absorption efficiency}}$$

$$\underbrace{C_{\rm sca}(\lambda, a)}_{\text{scattering cross-section}} \equiv \underbrace{\pi a^2}_{\text{cross-section}} \times \underbrace{Q_{\rm sca}(x)}_{\text{scattering efficiency}}$$

$$\underbrace{g(\lambda, a)}_{\text{asymmetry parameter}} \equiv \langle \underbrace{\cos\theta}_{\text{scattering angle}} \rangle(x)$$

Limit behaviors of the optical properties

Geometrical optics ($x \gg 1$) grain $\simeq$ screen:

$$Q_{\rm abs} \simeq 1 \quad Q_{\rm sca} \simeq 1 \quad \langle\cos\theta\rangle \simeq 1.$$

Rayleigh regime ($x \ll 1$) grain $\simeq$ dipole:

$$Q_{\rm abs} \propto \lambda^{-2} \quad Q_{\rm sca} \propto \lambda^{-4}$$

Mie theory

Principle: solves absorption & scattering of a plane E.M. wave by a spherical homogeneous grain
$\rightarrow$ Maxwell equations + spherical harmonics expansion.

Results: depend only on $x \equiv 2\pi a/\lambda$ (a: grain radius):

$$\underbrace{C_{\rm abs}(\lambda, a)}_{\text{absorption cross-section}} \equiv \underbrace{\pi a^2}_{\text{cross-section}} \times \underbrace{Q_{\rm abs}(x)}_{\text{absorption efficiency}}$$

$$\underbrace{C_{\rm sca}(\lambda, a)}_{\text{scattering cross-section}} \equiv \underbrace{\pi a^2}_{\text{cross-section}} \times \underbrace{Q_{\rm sca}(x)}_{\text{scattering efficiency}}$$

$$\underbrace{g(\lambda, a)}_{\text{asymmetry parameter}} \equiv \langle \underbrace{\cos\theta}_{\text{scattering angle}} \rangle(x)$$

Limit behaviors of the optical properties

Geometrical optics $(x \gg 1)$ grain $\simeq$ screen:

$$Q_{\rm abs} \simeq 1 \quad Q_{\rm sca} \simeq 1 \quad \langle\cos\theta\rangle \simeq 1.$$

Rayleigh regime $(x \ll 1)$ grain $\simeq$ dipole:

$$Q_{\rm abs} \propto \lambda^{-2} \quad Q_{\rm sca} \propto \lambda^{-4} \quad \langle\cos\theta\rangle \simeq 0.$$


Geometrical optics
Grain
Incident photons
Scattered photons

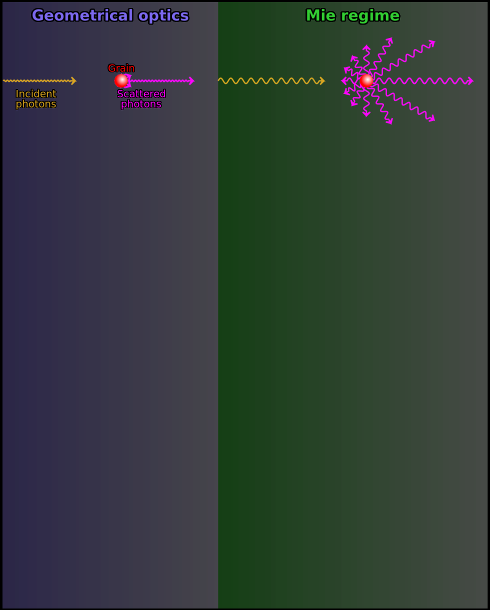
Geometrical optics
Mie regime
Grain
Incident photons
Scattered photons

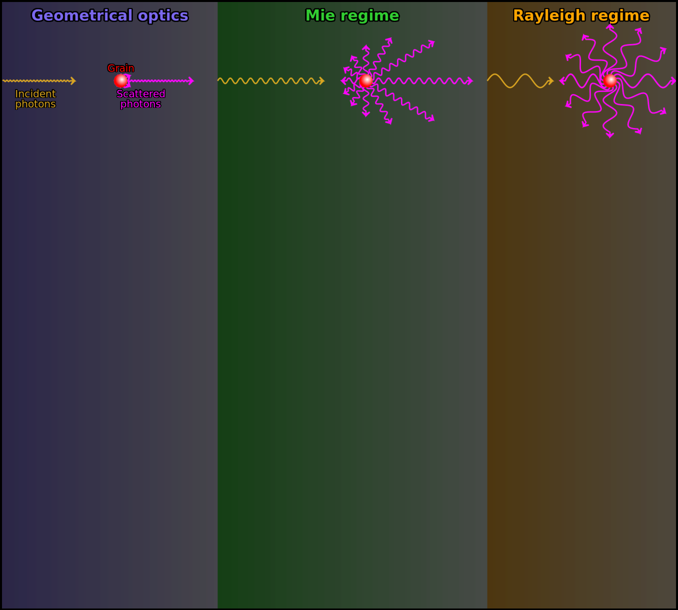
Geometrical optics
Mie regime
Rayleigh regime
Grain
Incident photons
Scattered photons

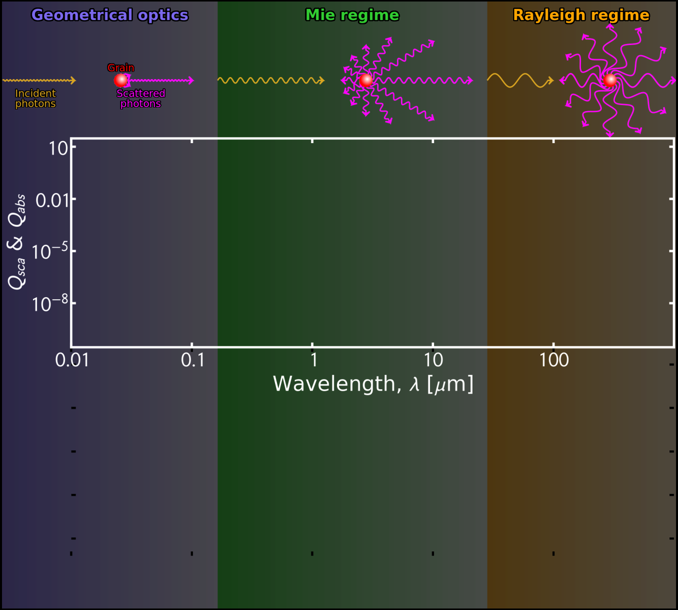
Geometrical optics
Mie regime
Rayleigh regime
Grain
Incident photons
Scattered photons
Q_{sca} & Q_{abs}
10
0.01
10^{-5}
10^{-8}
0.01
0.1
1
10
100
Wavelength, λ [μm]

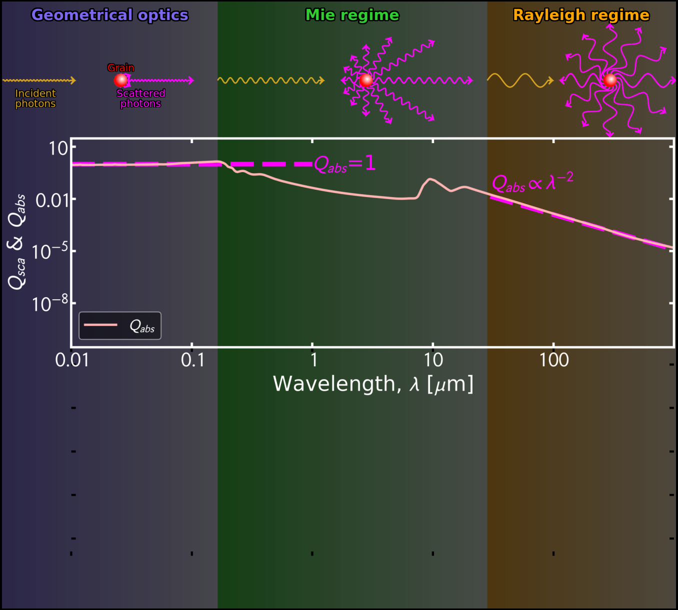
Geometrical optics
Mie regime
Rayleigh regime
Grain
Incident photons
Scattered photons
Q_{abs}=1
$Q_{abs} \propto \lambda^{-2}$
10
0.01
10^{-5}
10^{-8}
Q_{sca} & Q_{abs}
Q_{abs}
0.01
0.1
1
10
100
Wavelength, λ [μm]

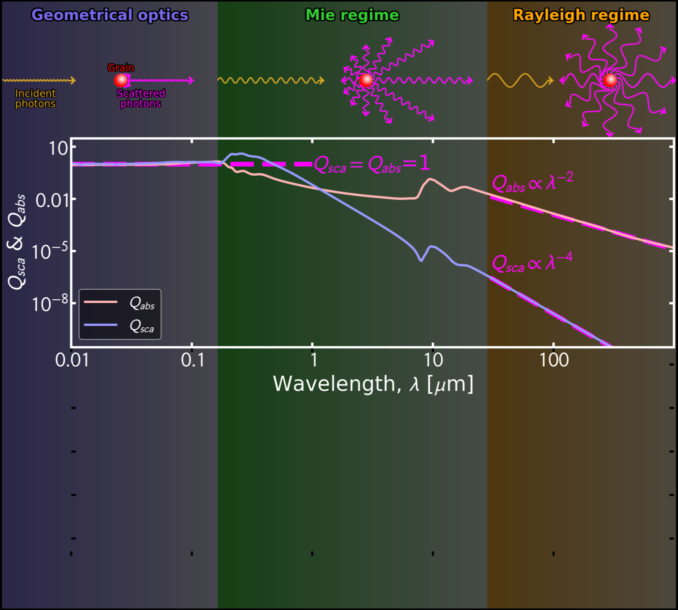
Geometrical optics
Mie regime
Rayleigh regime
Grain
Incident photons
Scattered photons
$Q_{sca} = Q_{abs} = 1$
$Q_{abs} \propto \lambda^{-2}$
$Q_{sca} \propto \lambda^{-4}$
Q_{sca} & Q_{abs}
10
0.01
10^{-5}
10^{-8}
Q_{abs}
Q_{sca}
0.01
0.1
1
10
100
Wavelength, λ [μm]

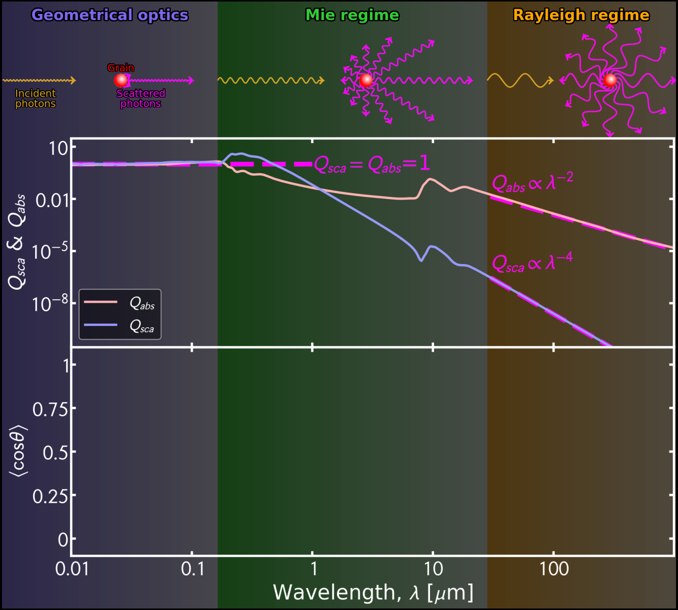
Geometrical optics
Mie regime
Rayleigh regime
Grain
Incident photons
Scattered photons
$Q_{sca} = Q_{abs} = 1$
$Q_{abs} \propto \lambda^{-2}$
$Q_{sca} \propto \lambda^{-4}$
Q_{abs}
Q_{sca}
Q_{sca} & Q_{abs}
10
0.01
10^{-5}
10^{-8}
$\langle \cos\theta \rangle$
1
0.75
0.5
0.25
0
0.01
0.1
1
10
100
Wavelength, λ [μm]

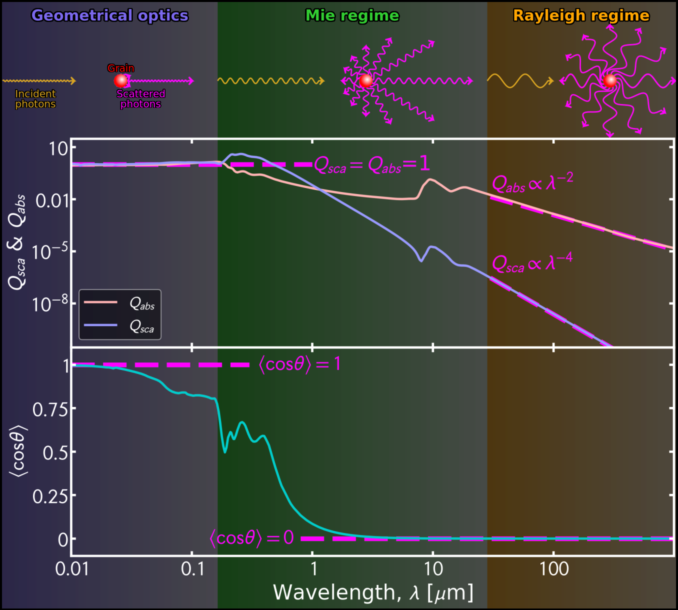

Geometrical optics
Mie regime
Rayleigh regime
Grain
Incident photons
Scattered photons
$Q_{sca} = Q_{abs} = 1$
$Q_{abs} \propto \lambda^{-2}$
$Q_{sca} \propto \lambda^{-4}$
Q_{abs}
Q_{sca}
Q_{sca} & Q_{abs}
10
0.01
10^{-5}
10^{-8}
$\langle\cos\theta\rangle = 1$
$\langle\cos\theta\rangle = 0$
$\langle\cos\theta\rangle$
1
0.75
0.5
0.25
0
0.01
0.1
1
10
100
Wavelength, λ [μm]

Dust | Cross-Sections of Grains with Arbitrary Shape & Composition

Different methods for different cases

Different methods for different cases

Composite grains: Effective Medium Theory (EMT; Bohren & Huffman 1983).

Different methods for different cases

Composite grains: Effective Medium Theory (EMT; Bohren & Huffman 1983).

Aggregates & arbitrary shapes: Discrete Dipole Approximation (DDA; Draine & Flatau 1994).

Different methods for different cases

Composite grains: Effective Medium Theory (EMT; Bohren & Huffman 1983).

Aggregates & arbitrary shapes: Discrete Dipole Approximation (DDA; Draine & Flatau 1994).

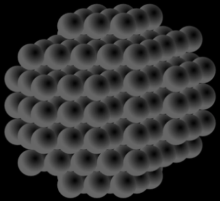

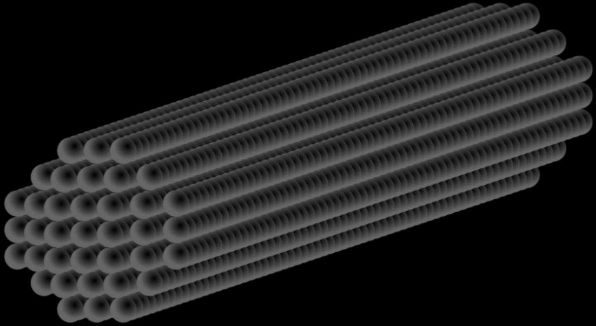

Dust | Polarization by Elongated Dust Grains

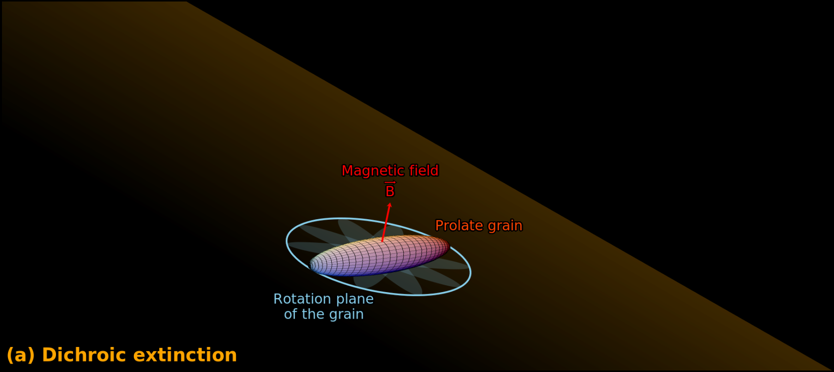

(a) Dichroic extinction

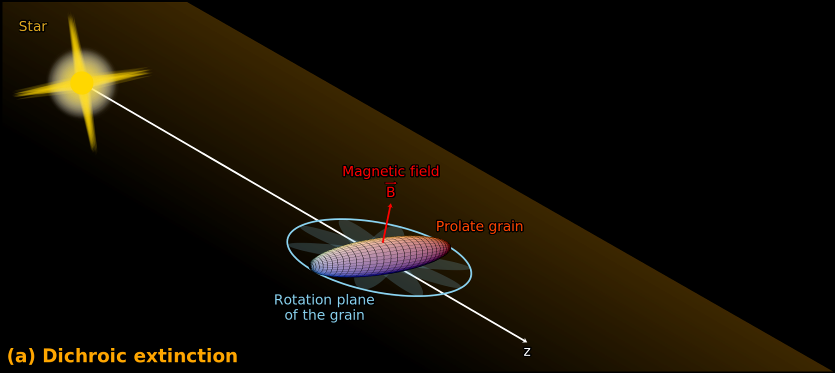
Star
Magnetic field
B
Prolate grain
Rotation plane
of the grain
z
(a) Dichroic extinction

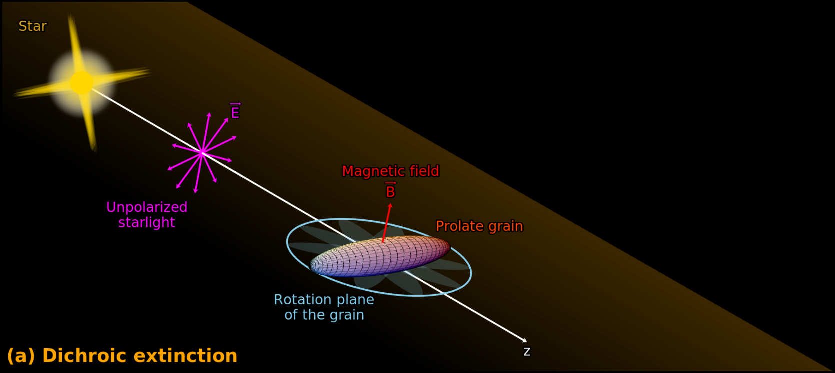
Star
E
Unpolarized
starlight
Magnetic field
B
Prolate grain
Rotation plane
of the grain
z
(a) Dichroic extinction

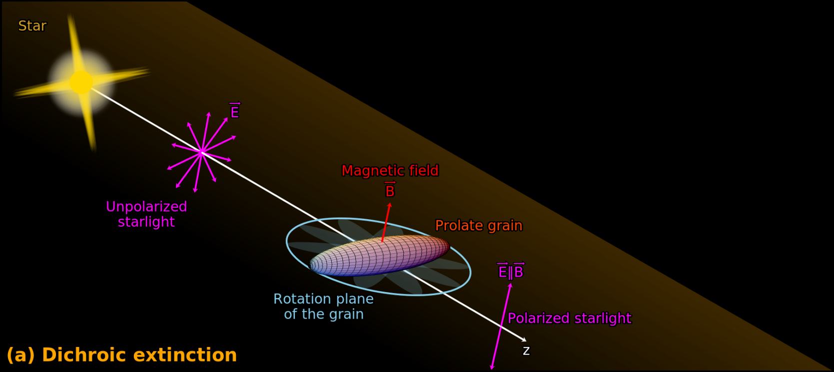

(a) Dichroic extinction

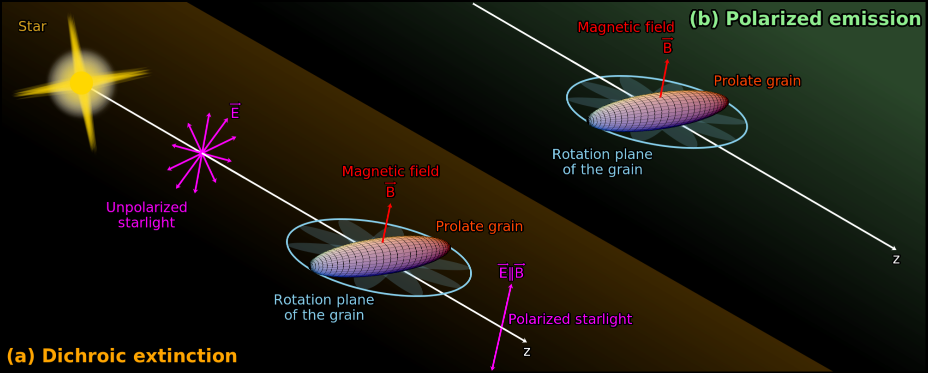
Star
$\vec{E}$
Unpolarized starlight
Magnetic field
$\vec{B}$
Prolate grain
Rotation plane of the grain
$\vec{E} \parallel \vec{B}$
Polarized starlight
z
(a) Dichroic extinction
(b) Polarized emission
Magnetic field
$\vec{B}$
Prolate grain
Rotation plane of the grain
z

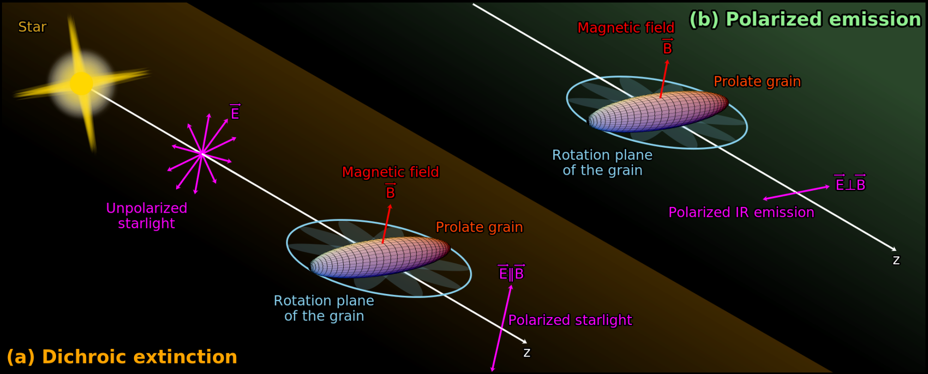
Star
$\vec{E}$
Unpolarized starlight
Magnetic field
$\vec{B}$
Prolate grain
Rotation plane of the grain
$\vec{E} \parallel \vec{B}$
Polarized starlight
z
(a) Dichroic extinction
(b) Polarized emission
Magnetic field
$\vec{B}$
Prolate grain
Rotation plane of the grain
$\vec{E} \perp \vec{B}$
Polarized IR emission
z

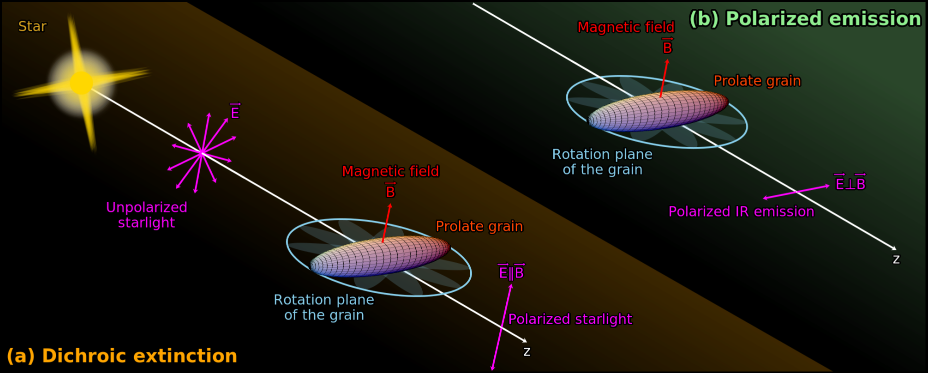

Dust-induced polarization is widely used to study $\vec{B}$.

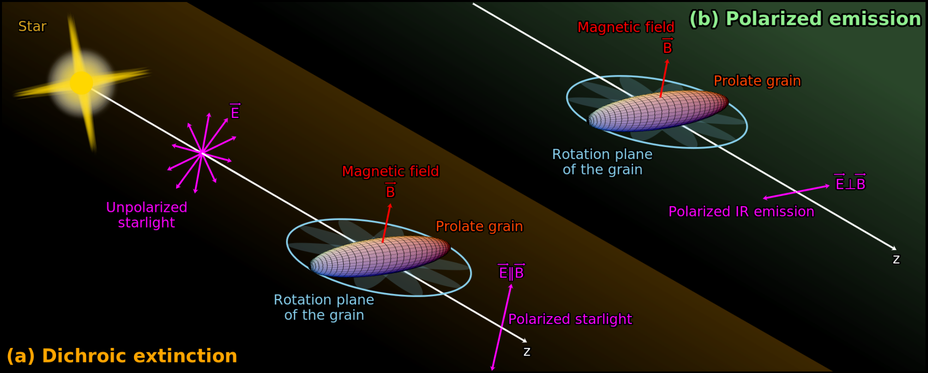

Dust-induced polarization is widely used to study $\overrightarrow{B}$.

(Planck Collaboration et al., 2020)

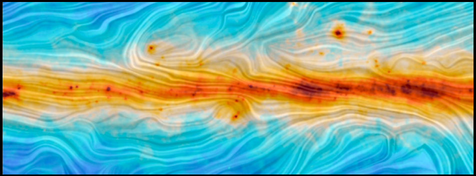

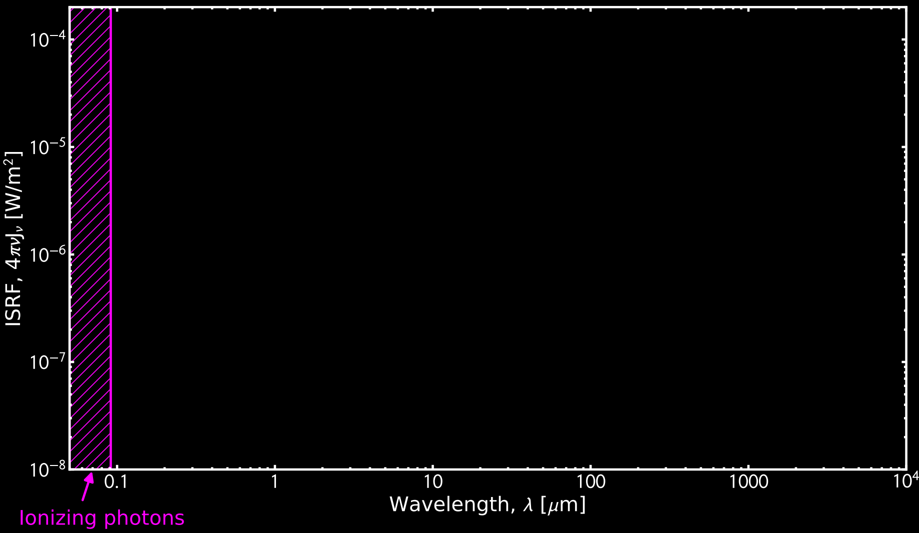

10^{-4}
10^{-5}
10^{-6}
10^{-7}
10^{-8}
ISRF, $4\pi\nu J_\nu$ [W/m^2]
0.1
1
10
100
1000
10^4
Wavelength, λ [μm]
Ionizing photons

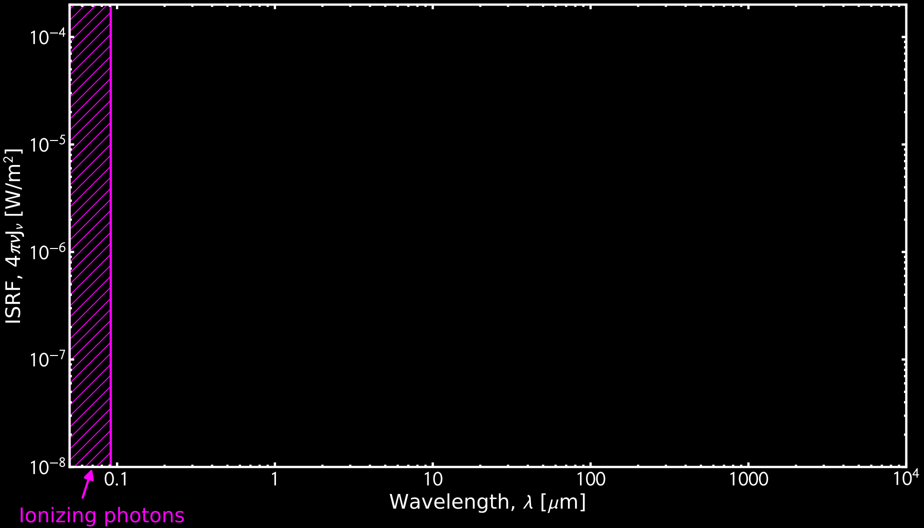

Starlight intensity, U: $\int_{0.0912\,\mu m}^{8\,\mu m} 4\pi J_\lambda(\lambda)\,\mathrm{d}\lambda = U \times 2.2 \times 10^{-5}\ \mathrm{W/m^2}$ (Mathis et al., 1983).

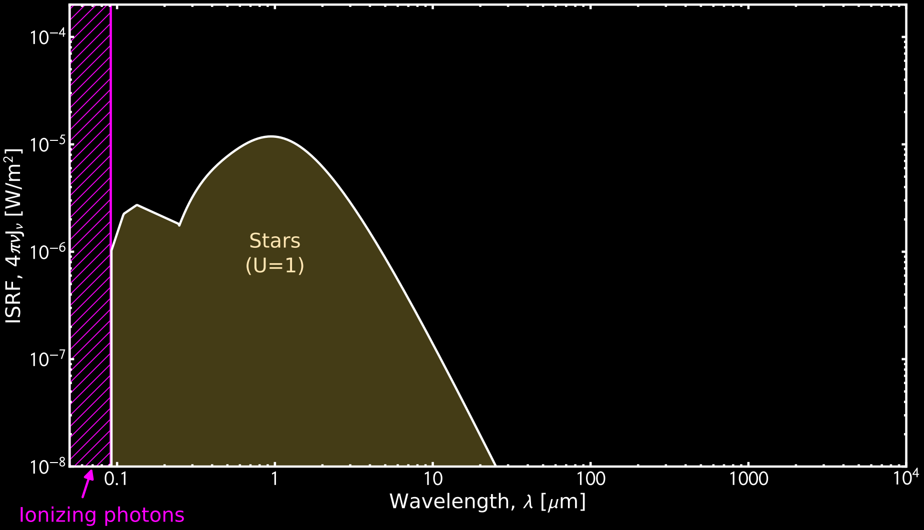

Starlight intensity, U**:** $\int_{0.0912\,\mu m}^{8\,\mu m} 4\pi J_\lambda(\lambda)\,\mathrm{d}\lambda = U \times 2.2 \times 10^{-5}\ \mathrm{W/m^2}$ (Mathis et al., 1983).

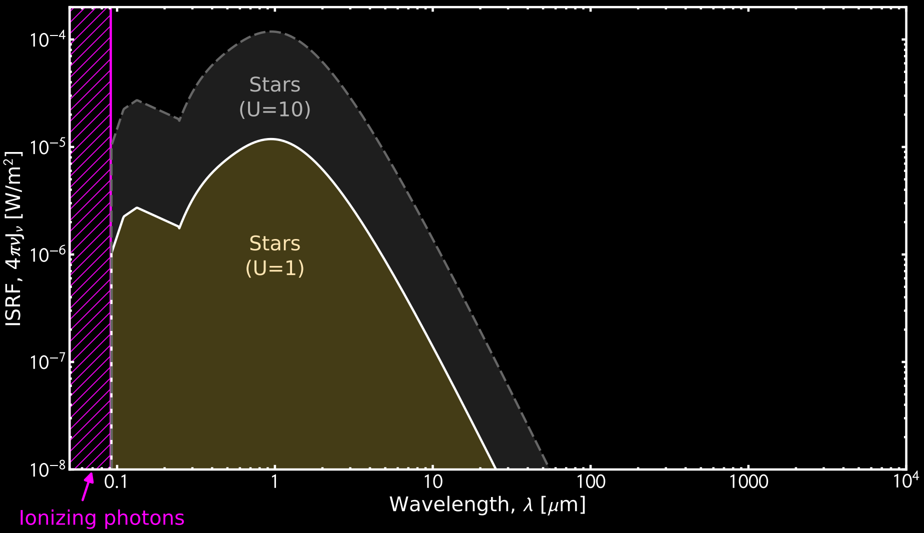

Starlight intensity, U: $\int_{0.0912\,\mu m}^{8\,\mu m} 4\pi J_\lambda(\lambda)\,\mathrm{d}\lambda = U \times 2.2 \times 10^{-5}\ \mathrm{W/m^2}$ (Mathis et al., 1983).

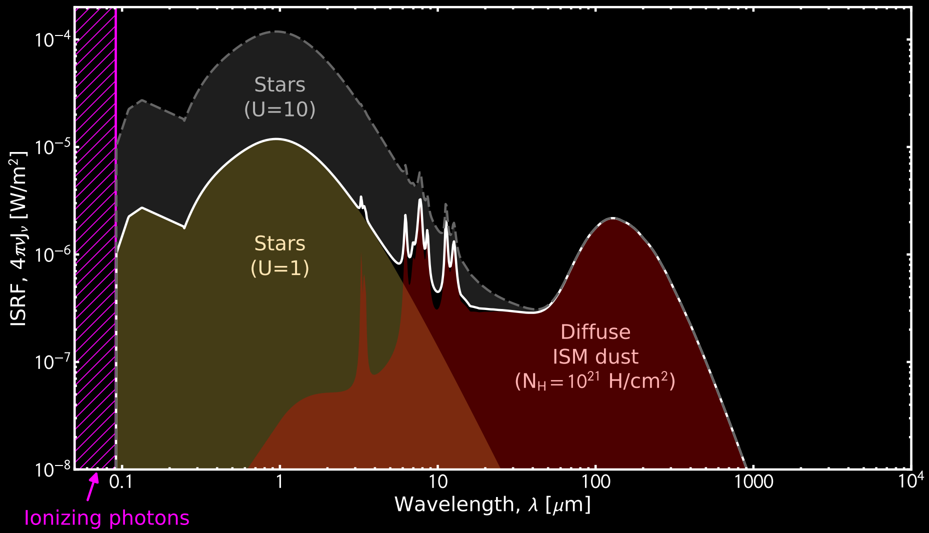

Starlight intensity, U: $\int_{0.0912\,\mu m}^{8\,\mu m} 4\pi J_\lambda(\lambda)\,\mathrm{d}\lambda = U \times 2.2 \times 10^{-5}\ \mathrm{W/m^2}$ (Mathis et al., 1983).

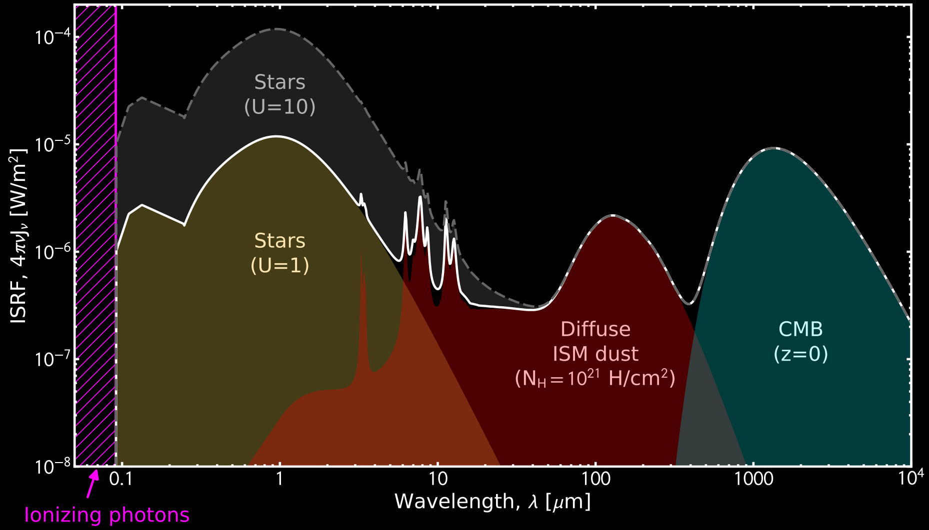

Starlight intensity, U: $\int_{0.0912\,\mu m}^{8\,\mu m} 4\pi J_\lambda(\lambda)\,d\lambda = U \times 2.2 \times 10^{-5}$ W/m^2 (Mathis et al., 1983).

Dust | The Interstellar Radiation Field

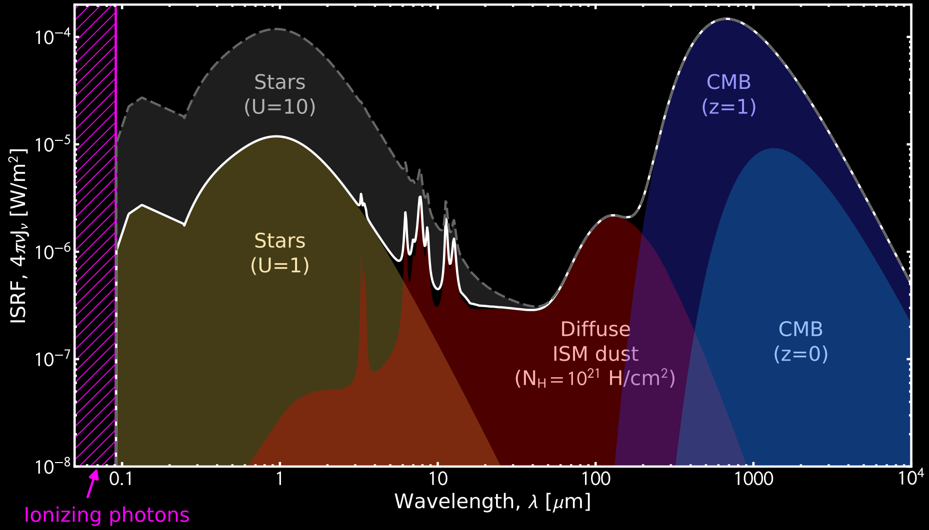

Starlight intensity, ***U*****:** $\int_{0.0912\,\mu m}^{8\,\mu m} 4\pi J_\lambda(\lambda)\,d\lambda = U \times 2.2 \times 10^{-5}\ \mathrm{W/m^2}$ (Mathis et al., 1983).

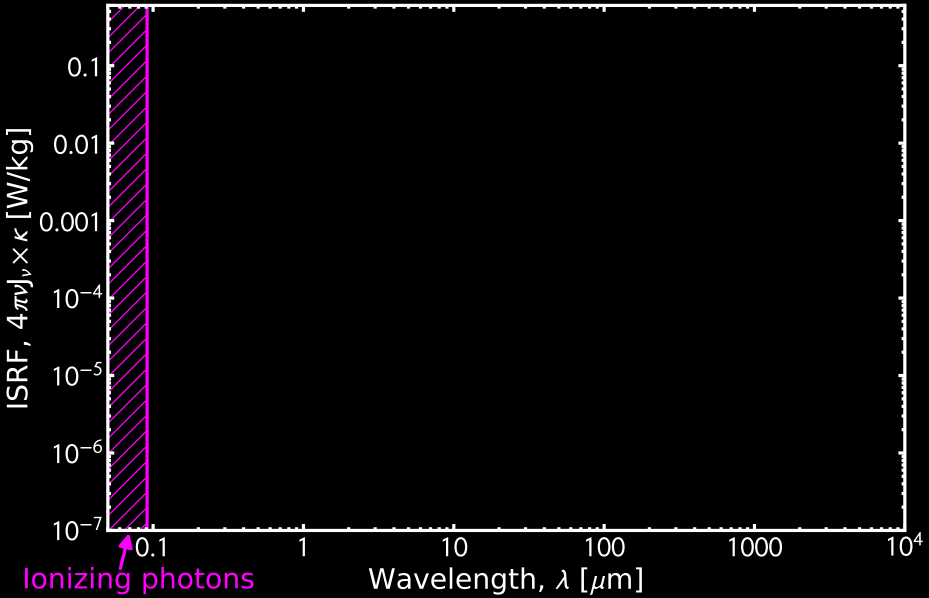

ISRF, $4\pi\nu J_\nu \times \kappa$ [W/kg]
0.1
0.01
0.001
10^{-4}
10^{-5}
10^{-6}
10^{-7}
0.1
1
10
100
1000
10^4
Wavelength, λ [μm]
Ionizing photons

$\int^{8\,\mu m}$

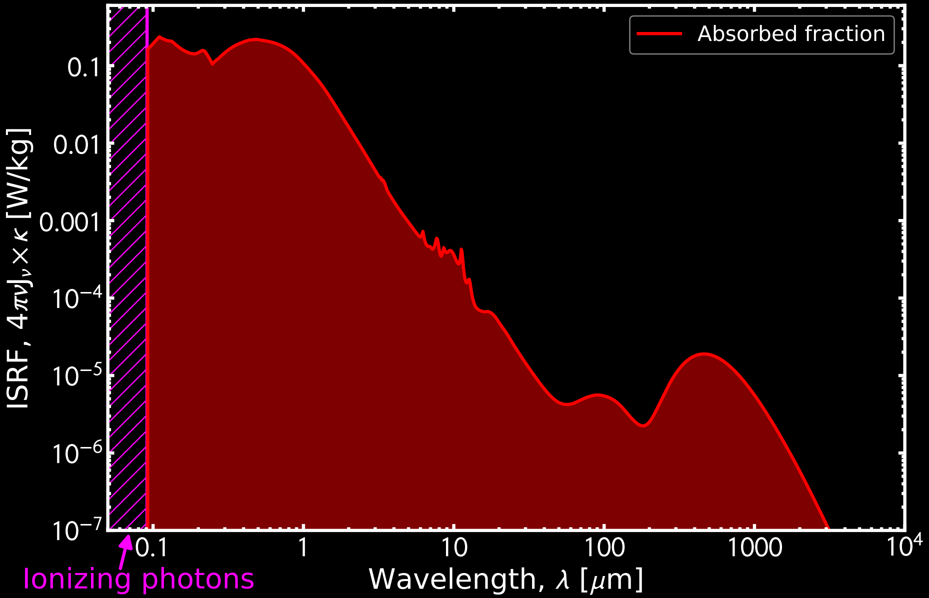
Absorbed fraction
ISRF, $4\pi\nu J_\nu \times \kappa$ [W/kg]
0.1
0.01
0.001
10^{-4}
10^{-5}
10^{-6}
10^{-7}
0.1
1
10
100
1000
10^4
Wavelength, λ [μm]
Ionizing photons

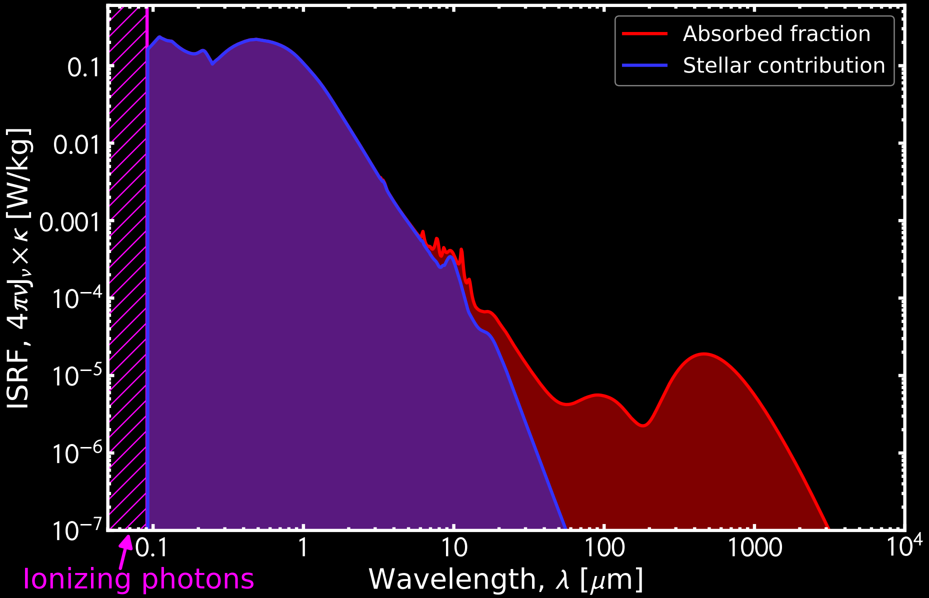
Absorbed fraction
Stellar contribution
0.1
0.01
0.001
10^{-4}
10^{-5}
10^{-6}
10^{-7}
ISRF, $4\pi\nu J_\nu \times \kappa$ [W/kg]
0.1
1
10
100
1000
10^4
Wavelength, λ [μm]
Ionizing photons

$\int^{8\,\mu m}$

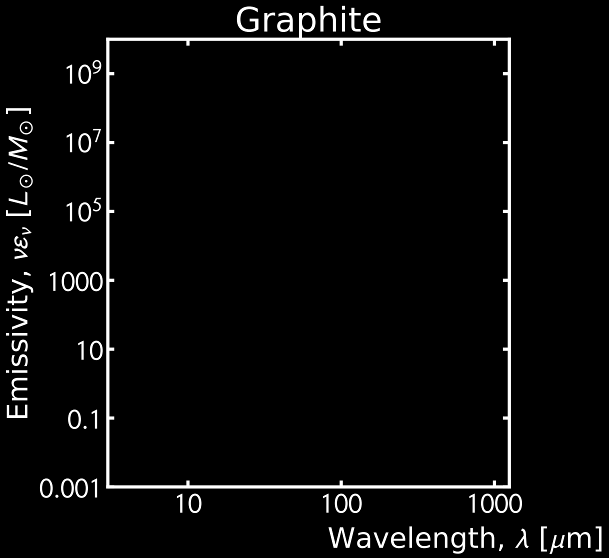
Graphite
10^9
10^7
10^5
1000
10
0.1
0.001
10
100
1000
Emissivity, $\nu\varepsilon_\nu$ $[L_\odot/M_\odot]$
Wavelength, λ [μm]

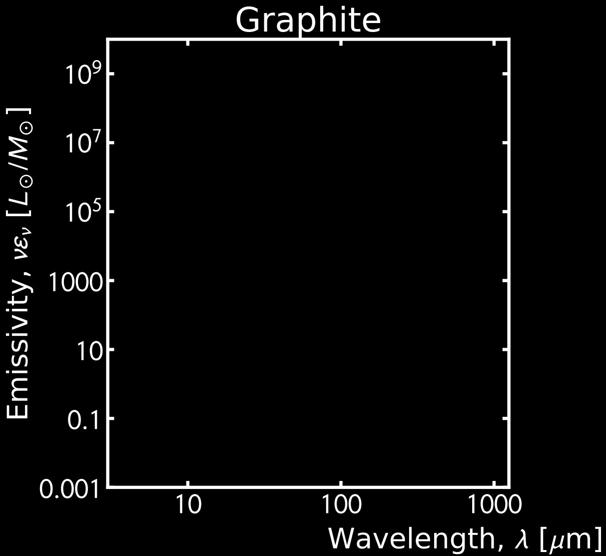

Large grains: $\epsilon_\nu \propto \frac{Q_{abs}(\lambda, a)}{a} \times B_\nu(\lambda, T)$.

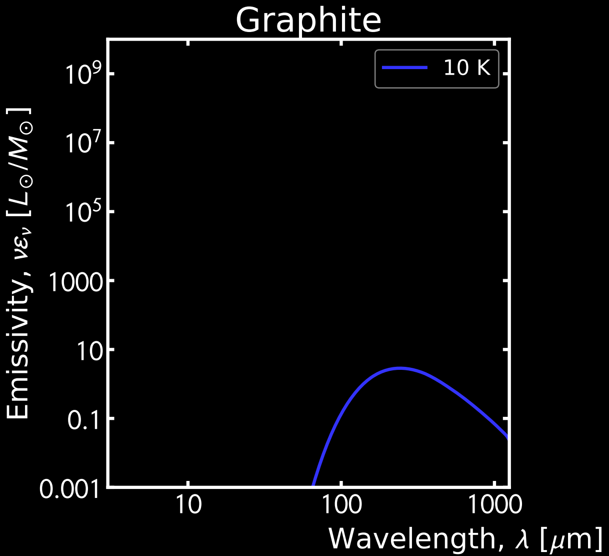

Large grains: $\epsilon_\nu \propto \frac{Q_{abs}(\lambda, a)}{a} \times B_\nu(\lambda, T)$. (Optical properties from Draine 2003)

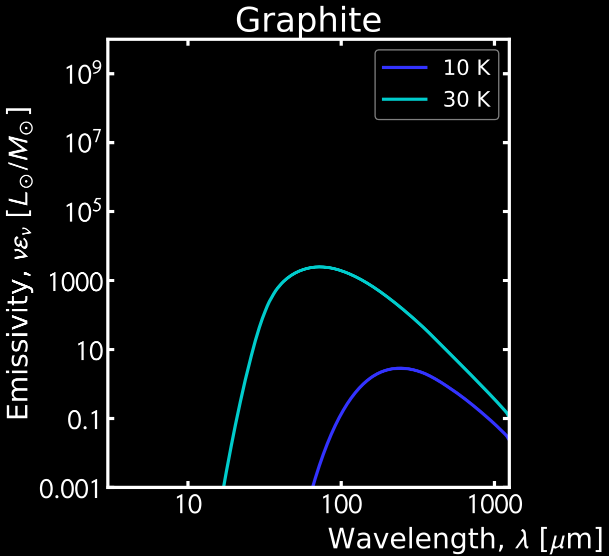

Large grains: $\epsilon_\nu \propto \frac{Q_{abs}(\lambda, a)}{a} \times B_\nu(\lambda, T)$. (Optical properties from Draine 2003)

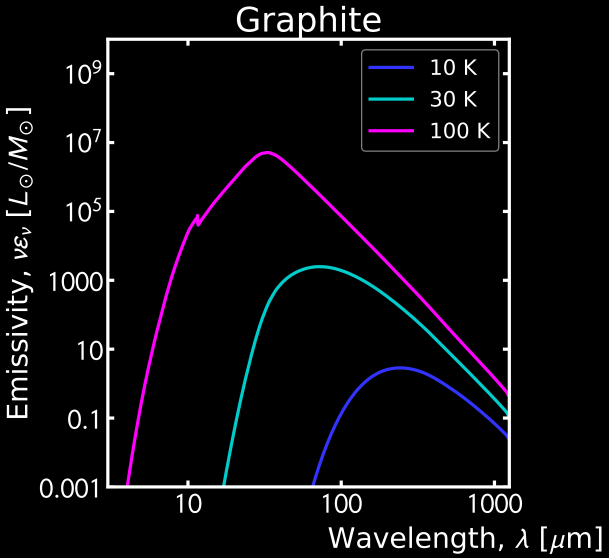

Large grains: $\epsilon_\nu \propto \frac{Q_{abs}(\lambda, a)}{a} \times B_\nu(\lambda, T)$.

(Optical properties from Draine 2003)

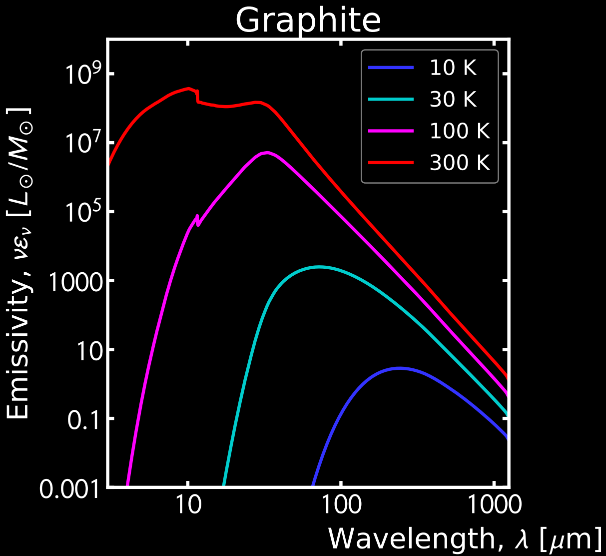

Large grains: $\epsilon_\nu \propto \frac{Q_{abs}(\lambda, a)}{a} \times B_\nu(\lambda, T)$.

(Optical properties from Draine 2003)

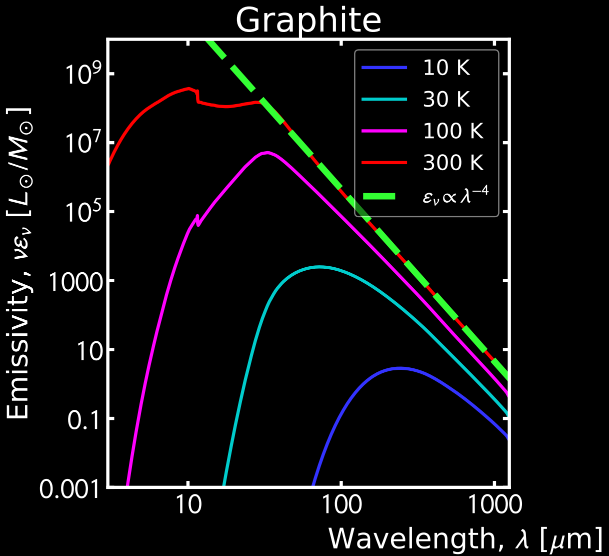

Large grains: $\epsilon_\nu \propto \frac{Q_{abs}(\lambda, a)}{a} \times B_\nu(\lambda, T)$. (Optical properties from Draine 2003)

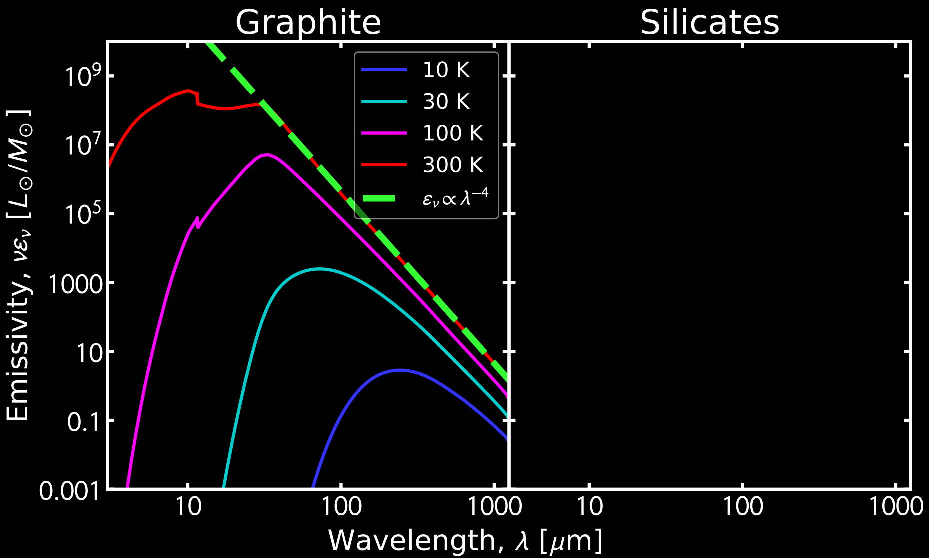

Large grains: $\epsilon_\nu \propto \frac{Q_{abs}(\lambda, a)}{a} \times B_\nu(\lambda, T)$.

(Optical properties from Draine 2003)

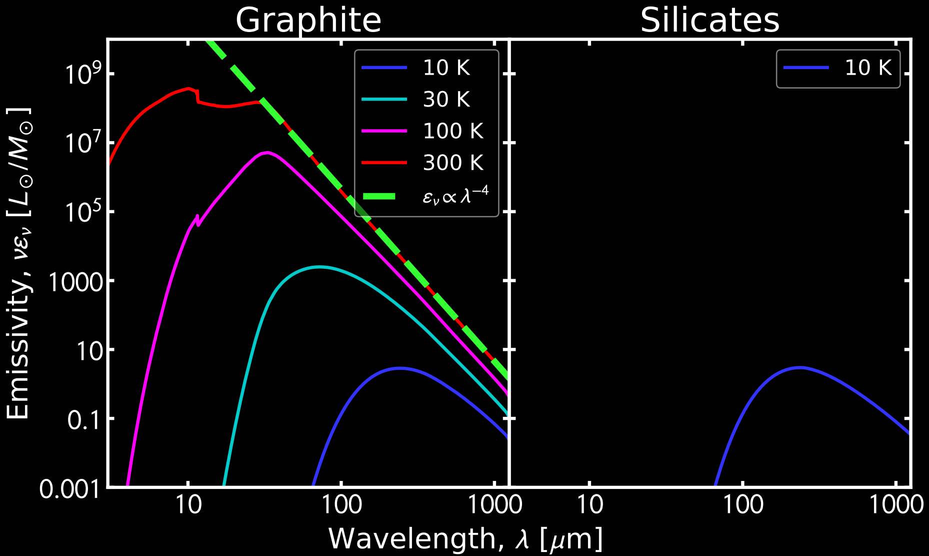

Large grains: $\epsilon_\nu \propto \frac{Q_{abs}(\lambda, a)}{a} \times B_\nu(\lambda, T)$.

(Optical properties from Draine 2003)

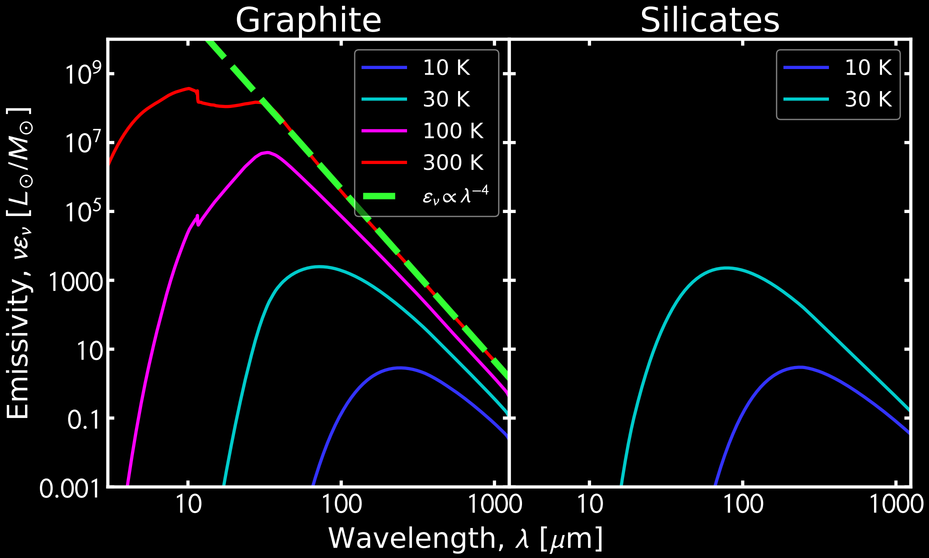

Large grains: $\epsilon_\nu \propto \frac{Q_{abs}(\lambda, a)}{a} \times B_\nu(\lambda, T)$.

(Optical properties from Draine 2003)

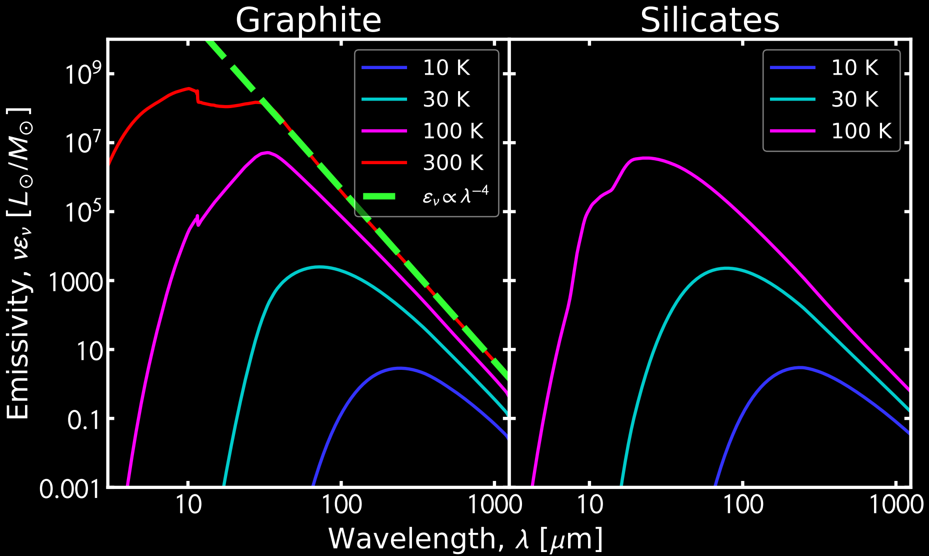

Large grains: $\epsilon_\nu \propto \frac{Q_{abs}(\lambda, a)}{a} \times B_\nu(\lambda, T)$.

(Optical properties from Draine 2003)

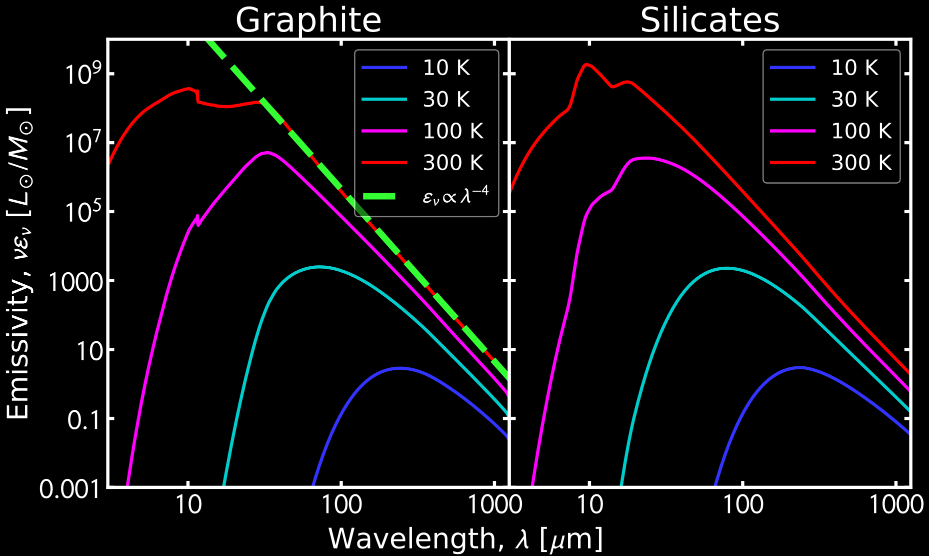

Large grains: $\epsilon_\nu \propto \frac{Q_{abs}(\lambda, a)}{a} \times B_\nu(\lambda, T)$.

(Optical properties from Draine 2003)

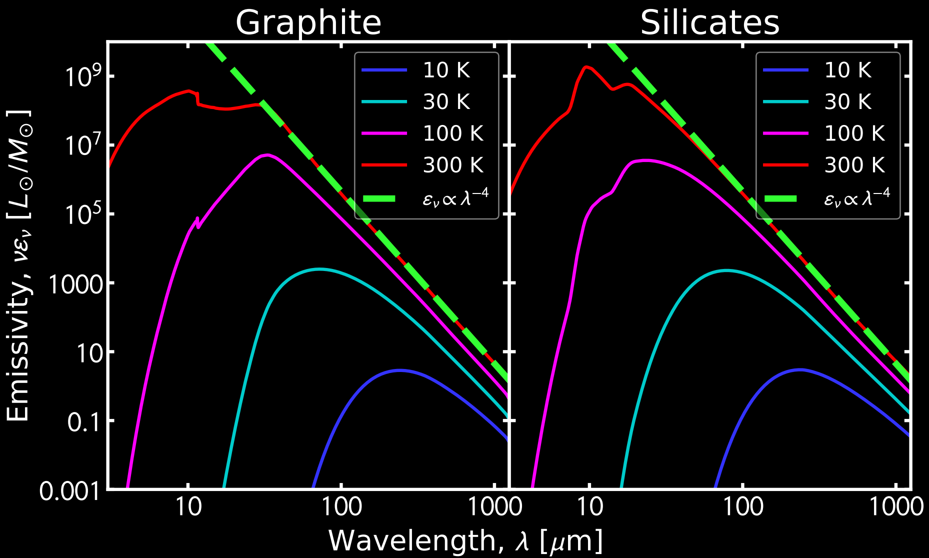

Large grains: $\epsilon_\nu \propto \frac{Q_{abs}(\lambda, a)}{a} \times B_\nu(\lambda, T)$.

(Optical properties from Draine 2003)

$F_\nu(\lambda) \propto$

$$F_\nu(\lambda) \propto \qquad\qquad \times B_\nu(\lambda, T)$$

$$F_\nu(\lambda) \propto \qquad \times (\lambda_0/\lambda)^\beta \times B_\nu(\lambda, T)$$

$$F_\nu(\lambda) \propto M_{\rm dust} \times (\lambda_0/\lambda)^\beta \times B_\nu(\lambda, T)$$

$$F_\nu(\lambda) \propto M_{\rm dust} \times (\lambda_0/\lambda)^\beta \times B_\nu(\lambda, T)$$

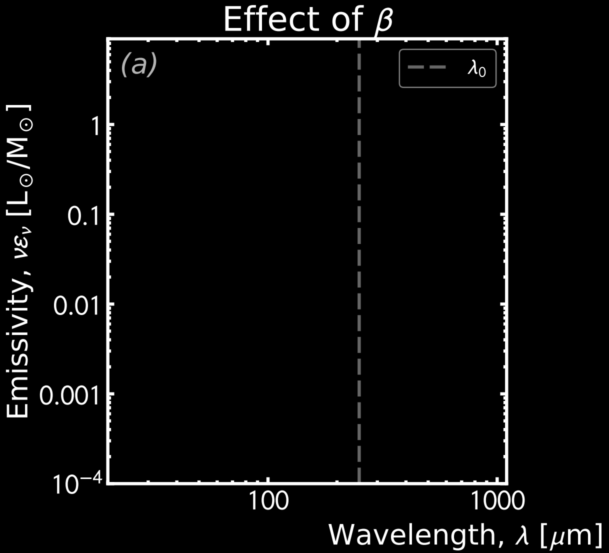

$$F_\nu(\lambda) \propto M_{\text{dust}} \times (\lambda_0/\lambda)^\beta \times B_\nu(\lambda, T)$$

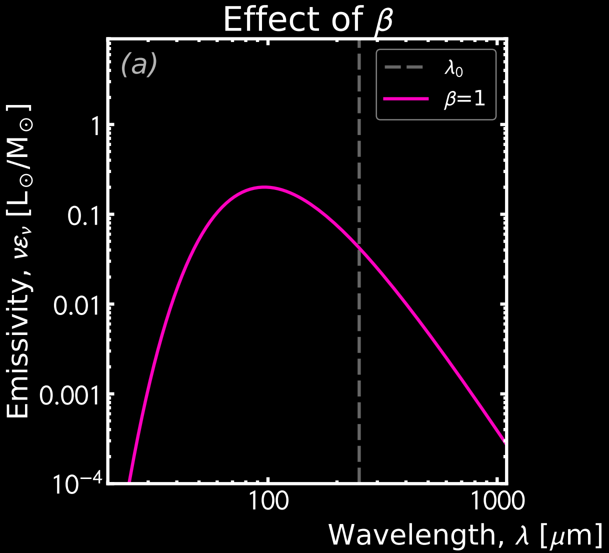

$$F_\nu(\lambda) \propto M_{\rm dust} \times (\lambda_0/\lambda)^\beta \times B_\nu(\lambda, T)$$

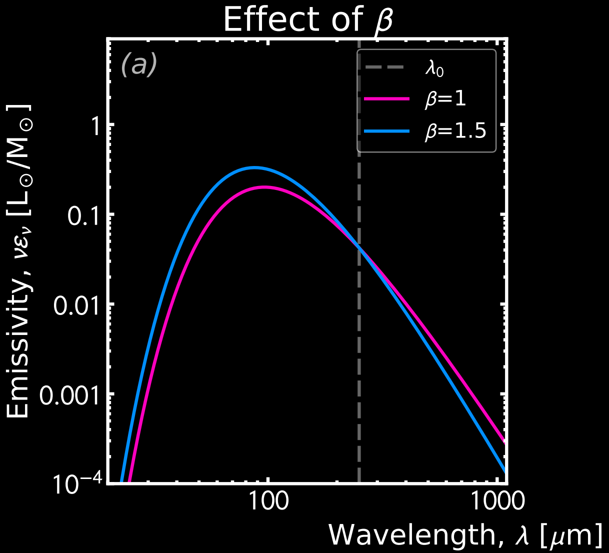

$$F_\nu(\lambda) \propto M_{\rm dust} \times (\lambda_0/\lambda)^\beta \times B_\nu(\lambda, T)$$

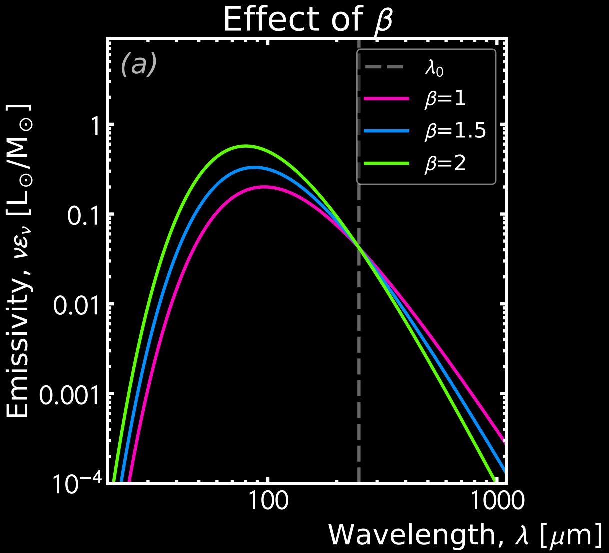

$$F_\nu(\lambda) \propto M_{\rm dust} \times (\lambda_0/\lambda)^\beta \times B_\nu(\lambda, T)$$

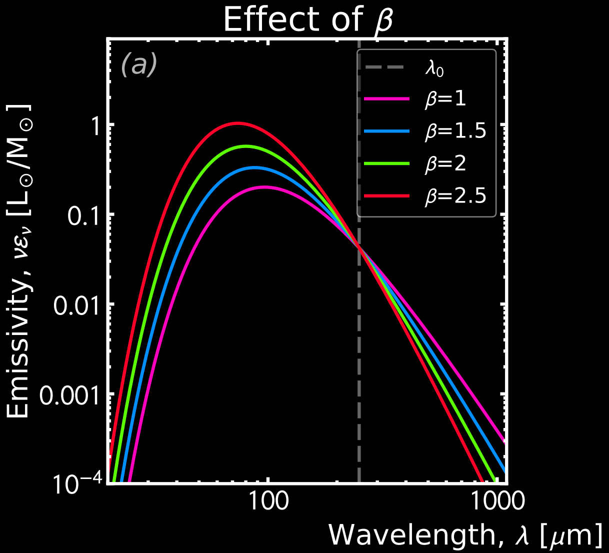

$$F_\nu(\lambda) \propto M_{\rm dust} \times (\lambda_0/\lambda)^\beta \times B_\nu(\lambda, T)$$

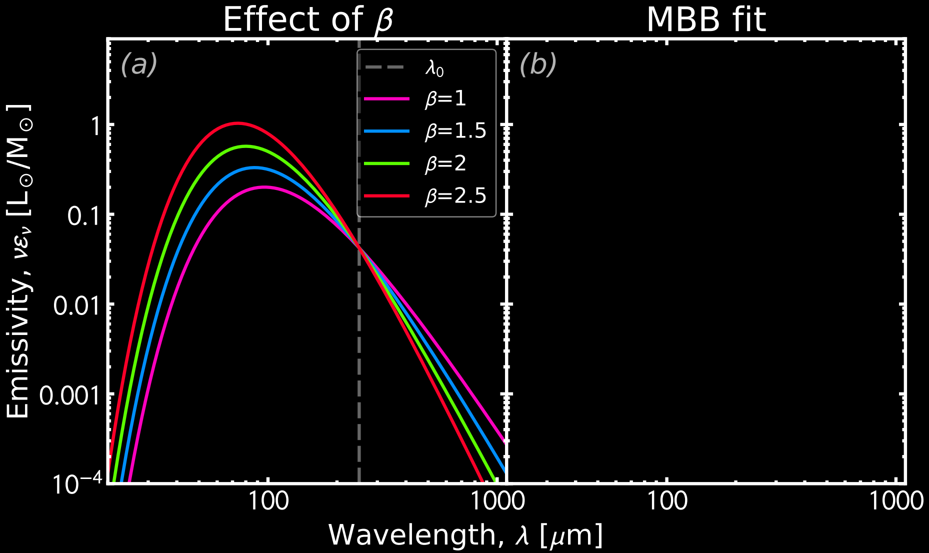

$$F_\nu(\lambda) \propto M_{\rm dust} \times (\lambda_0/\lambda)^\beta \times B_\nu(\lambda, T)$$

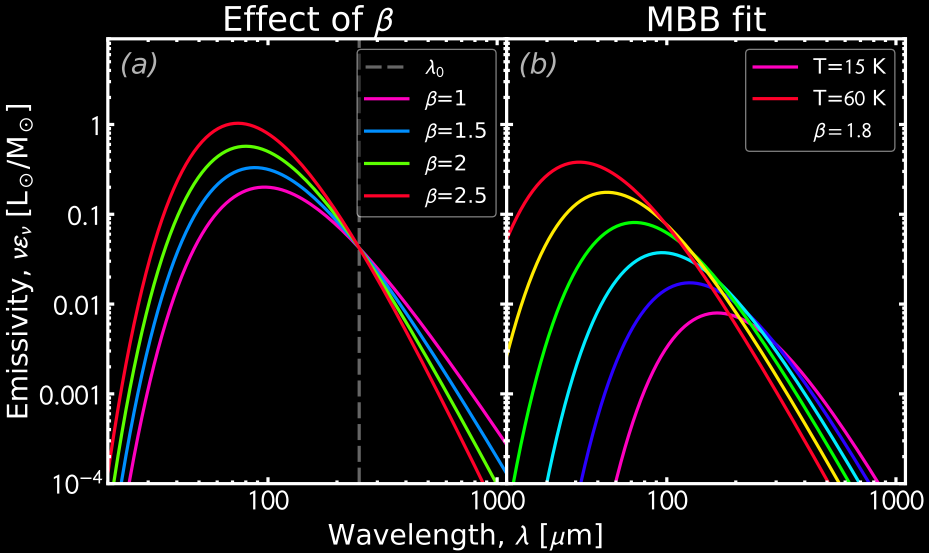

$$F_\nu(\lambda) \propto M_{\rm dust} \times (\lambda_0/\lambda)^\beta \times B_\nu(\lambda, T)$$

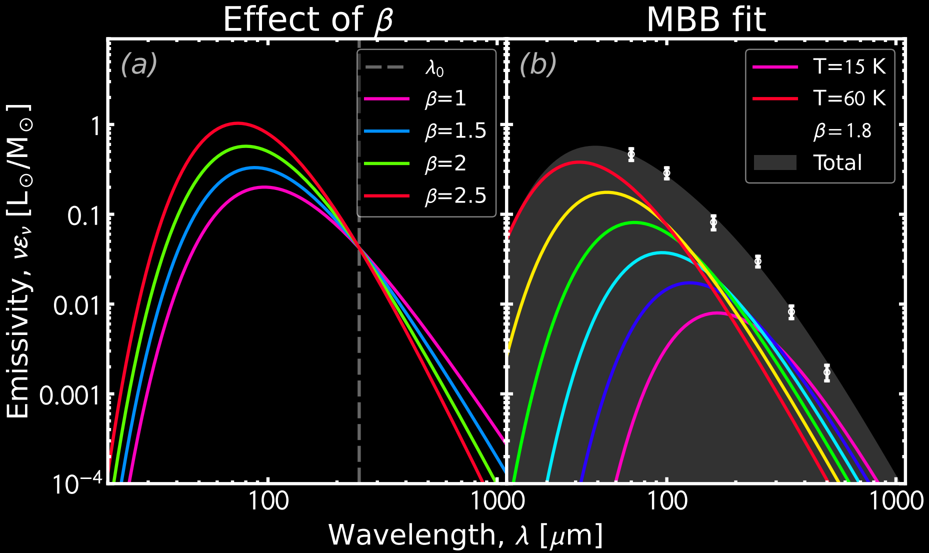

$$F_\nu(\lambda) \propto M_{\rm dust} \times (\lambda_0/\lambda)^\beta \times B_\nu(\lambda, T)$$

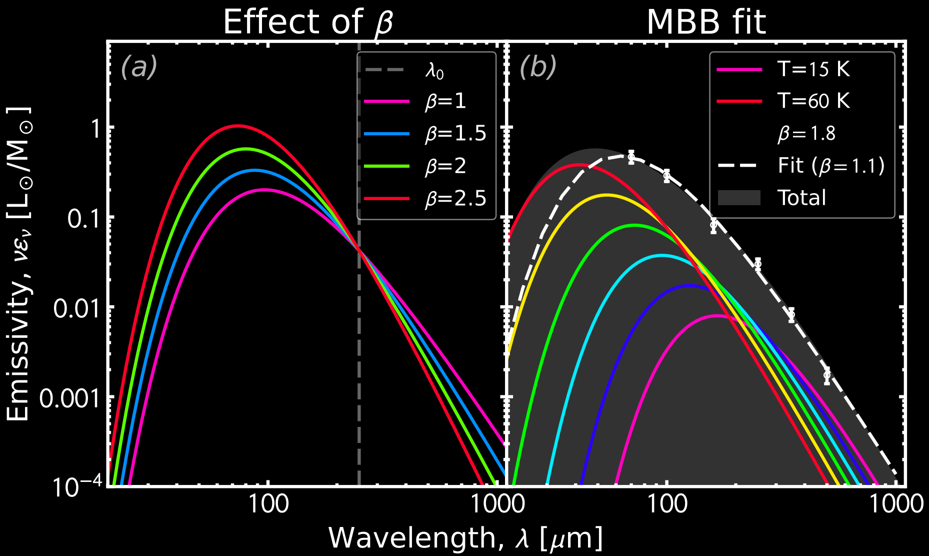

Distribution of harmonic oscillators in a solid lattice

Distribution of harmonic oscillators in a solid lattice

Debye temperature: $\lambda_\mathrm{D} = 2d_\mathrm{at}$ is the shortest phonon wavelength possible $\Rightarrow$ $T_\mathrm{D} \equiv hc/\lambda_\mathrm{D} k$.

Distribution of harmonic oscillators in a solid lattice

Debye temperature: $\lambda_D = 2d_{at}$ is the shortest phonon wavelength possible $\Rightarrow T_D \equiv hc/\lambda_D k$.

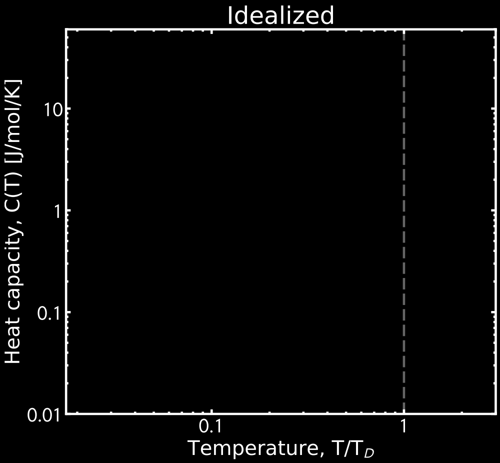

Distribution of harmonic oscillators in a solid lattice

Debye temperature: $\lambda_{\rm D} = 2d_{\rm at}$ is the shortest phonon wavelength possible $\Rightarrow$ $T_{\rm D} \equiv hc/\lambda_{\rm D}k$.

Dulong-Petit regime: high temperature ($T \gg T_{\rm D}$) limit: $C(T) \simeq 3Nk \rightarrow$ classical expression.

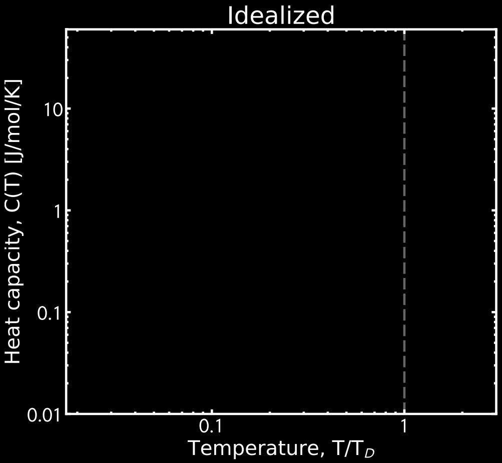

Distribution of harmonic oscillators in a solid lattice

Debye temperature: $\lambda_\mathrm{D} = 2d_\mathrm{at}$ is the shortest phonon wavelength possible $\Rightarrow T_\mathrm{D} \equiv hc/\lambda_\mathrm{D} k$.

Dulong-Petit regime: high temperature ($T \gg T_\mathrm{D}$) limit: $C(T) \simeq 3Nk \rightarrow$ classical expression.

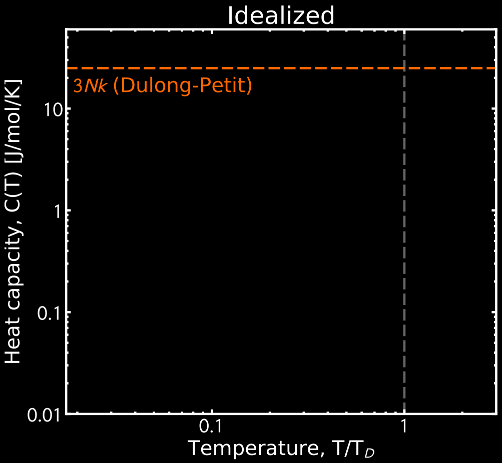

Distribution of harmonic oscillators in a solid lattice

Debye temperature: $\lambda_\mathrm{D} = 2d_\mathrm{at}$ is the shortest phonon wavelength possible $\Rightarrow T_\mathrm{D} \equiv hc/\lambda_\mathrm{D}k$.

Dulong-Petit regime: high temperature ($T \gg T_\mathrm{D}$) limit: $C(T) \simeq 3Nk \rightarrow$ classical expression.

Debye regime: low temperature ($T \ll T_\mathrm{D}$) limit: $C(T) \propto T^3 \rightarrow$ accounts for mode quantification.

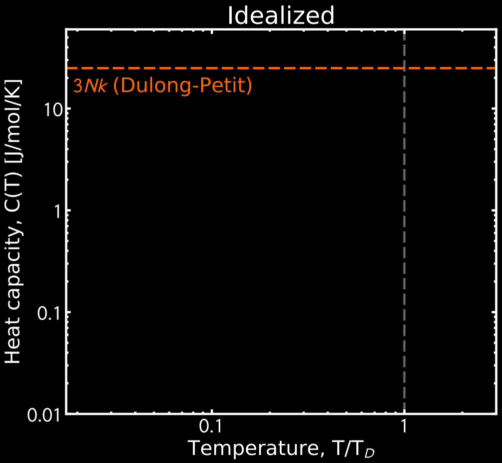

Distribution of harmonic oscillators in a solid lattice

Debye temperature: $\lambda_D = 2d_{at}$ is the shortest phonon wavelength possible $\Rightarrow T_D \equiv hc/\lambda_D k$.

Dulong-Petit regime: high temperature ($T \gg T_D$) limit: $C(T) \simeq 3Nk \rightarrow$ classical expression.

Debye regime: low temperature ($T \ll T_D$) limit: $C(T) \propto T^3 \rightarrow$ accounts for mode quantification.

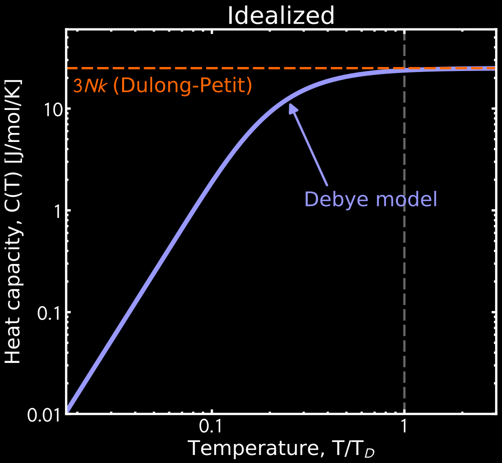

Distribution of harmonic oscillators in a solid lattice

Debye temperature: $\lambda_D = 2d_{at}$ is the shortest phonon wavelength possible $\Rightarrow T_D \equiv hc/\lambda_D k$.

Dulong-Petit regime: high temperature ($T \gg T_D$) limit: $C(T) \simeq 3Nk \rightarrow$ classical expression.

Debye regime: low temperature ($T \ll T_D$) limit: $C(T) \propto T^3 \rightarrow$ accounts for mode quantification.

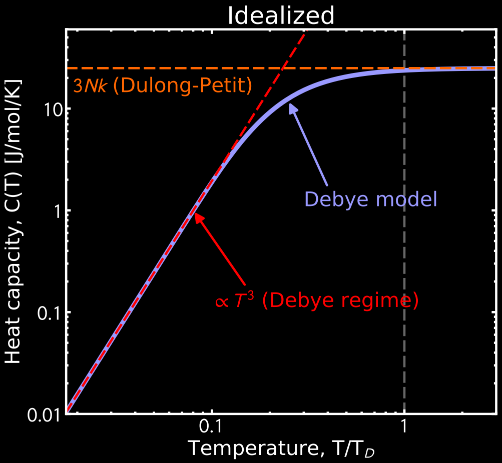

Distribution of harmonic oscillators in a solid lattice

Debye temperature: $\lambda_D = 2d_{at}$ is the shortest phonon wavelength possible $\Rightarrow T_D \equiv hc/\lambda_D k$.

Dulong-Petit regime: high temperature ($T \gg T_D$) limit: $C(T) \simeq 3Nk \rightarrow$ classical expression.

Debye regime: low temperature ($T \ll T_D$) limit: $C(T) \propto T^3 \rightarrow$ accounts for mode quantification.

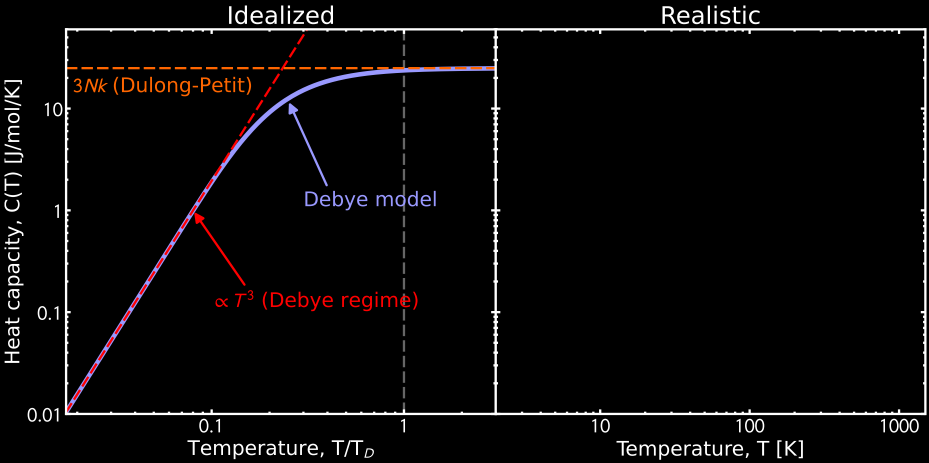

Distribution of harmonic oscillators in a solid lattice

Debye temperature: $\lambda_D = 2d_{at}$ is the shortest phonon wavelength possible $\Rightarrow T_D \equiv hc/\lambda_D k$.

Dulong-Petit regime: high temperature ($T \gg T_D$) limit: $C(T) \simeq 3Nk \rightarrow$ classical expression.

Debye regime: low temperature ($T \ll T_D$) limit: $C(T) \propto T^3 \rightarrow$ accounts for mode quantification.

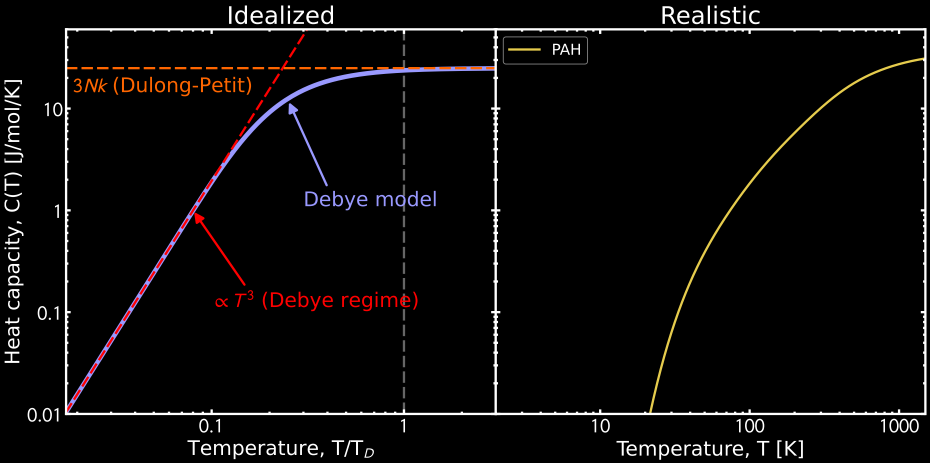

Distribution of harmonic oscillators in a solid lattice

Debye temperature: $\lambda_D = 2d_{at}$ is the shortest phonon wavelength possible $\Rightarrow$ $T_D \equiv hc/\lambda_D k$.

Dulong-Petit regime: high temperature ($T \gg T_D$) limit: $C(T) \simeq 3Nk \rightarrow$ classical expression.

Debye regime: low temperature ($T \ll T_D$) limit: $C(T) \propto T^3 \rightarrow$ accounts for mode quantification.

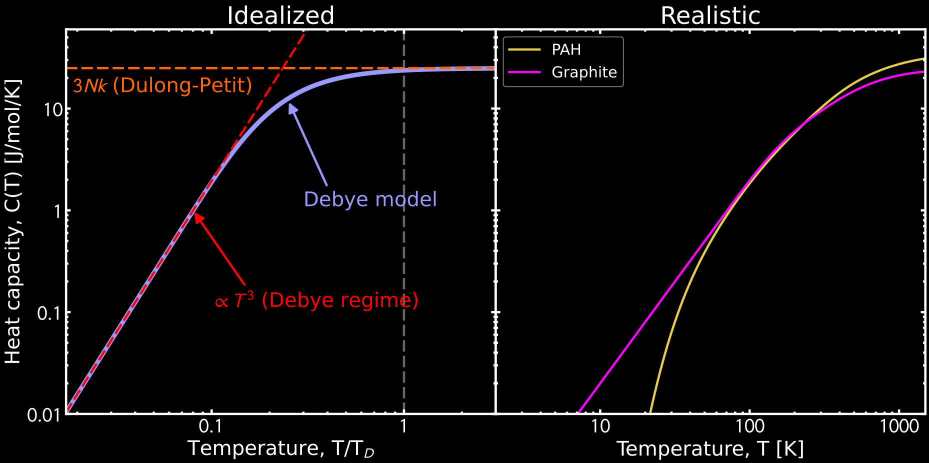

Distribution of harmonic oscillators in a solid lattice

Debye temperature: $\lambda_D = 2d_{at}$ is the shortest phonon wavelength possible $\Rightarrow$ $T_D \equiv hc/\lambda_D k$.

Dulong-Petit regime: high temperature ($T \gg T_D$) limit: $C(T) \simeq 3Nk$ $\rightarrow$ classical expression.

Debye regime: low temperature ($T \ll T_D$) limit: $C(T) \propto T^3$ $\rightarrow$ accounts for mode quantification.

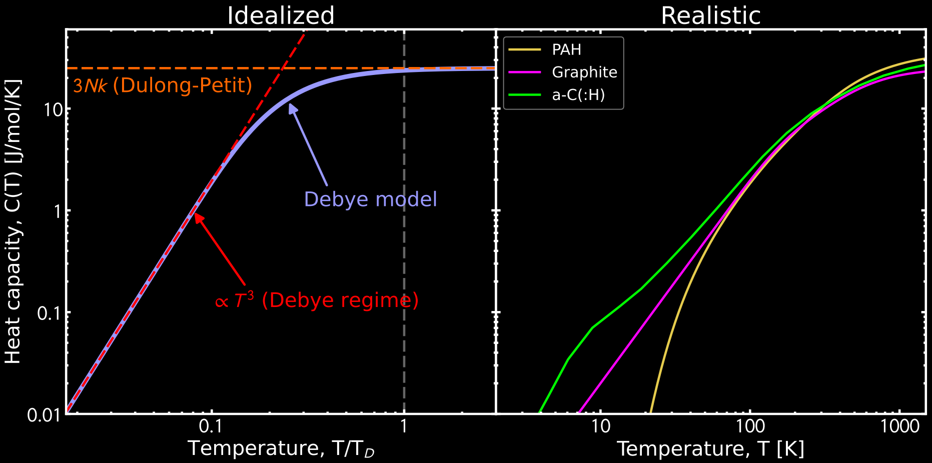

Distribution of harmonic oscillators in a solid lattice

Debye temperature: $\lambda_D = 2d_{at}$ is the shortest phonon wavelength possible $\Rightarrow T_D \equiv hc/\lambda_D k$.

Dulong-Petit regime: high temperature $(T \gg T_D)$ limit: $C(T) \simeq 3Nk \rightarrow$ classical expression.

Debye regime: low temperature $(T \ll T_D)$ limit: $C(T) \propto T^3 \rightarrow$ accounts for mode quantification.

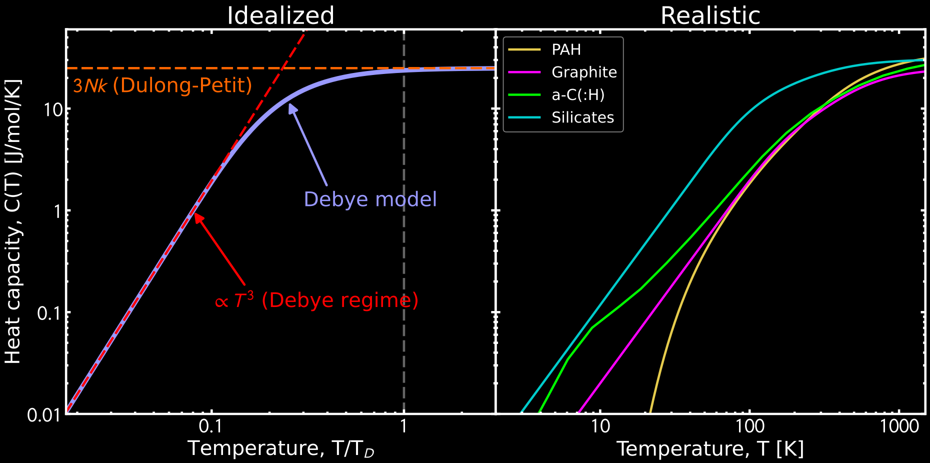

Dust | Stochastic Heating: Temperature Fluctuations

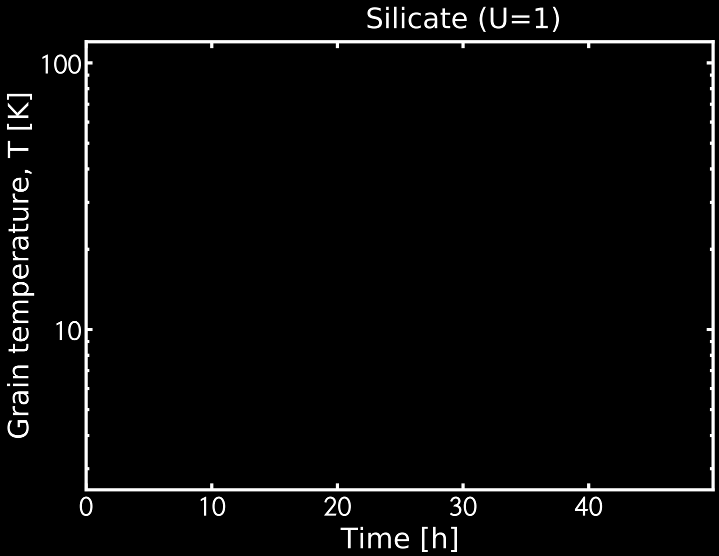
Silicate (U=1)
100
10
Grain temperature, T [K]
0
10
20
30
40
Time [h]

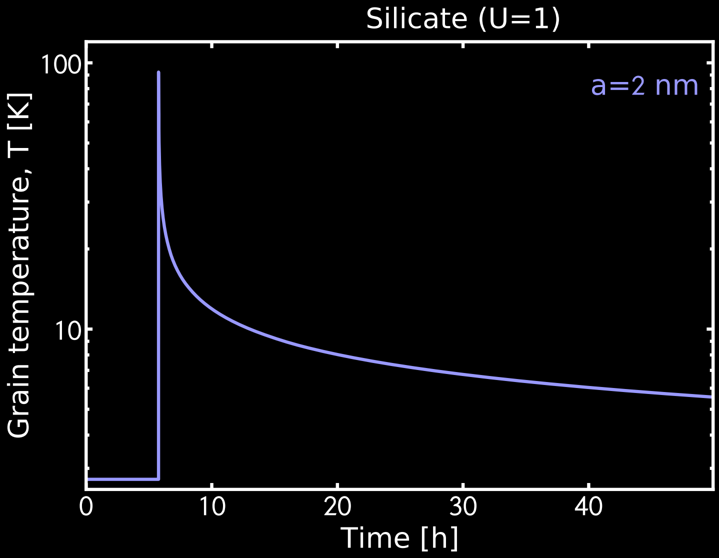
Silicate (U=1)
a=2 nm
Grain temperature, T [K]
100
10
0
10
20
30
40
Time [h]

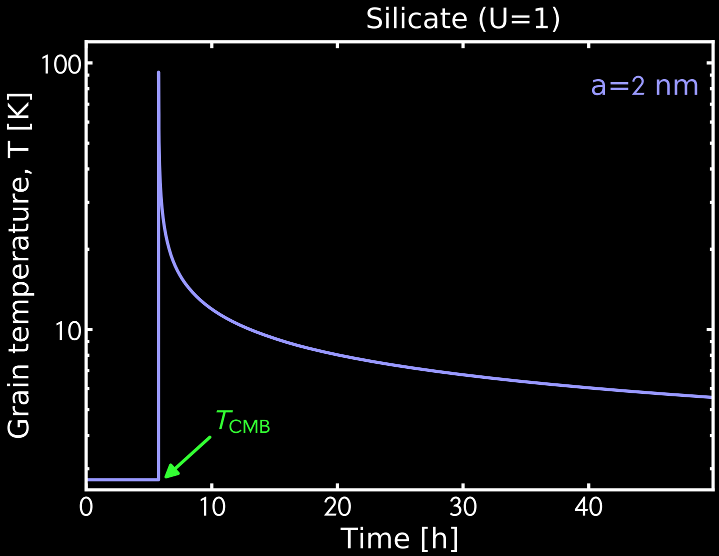
Silicate (U=1)
a=2 nm
$T_{\rm CMB}$
Grain temperature, T [K]
100
10
Time [h]
0
10
20
30
40

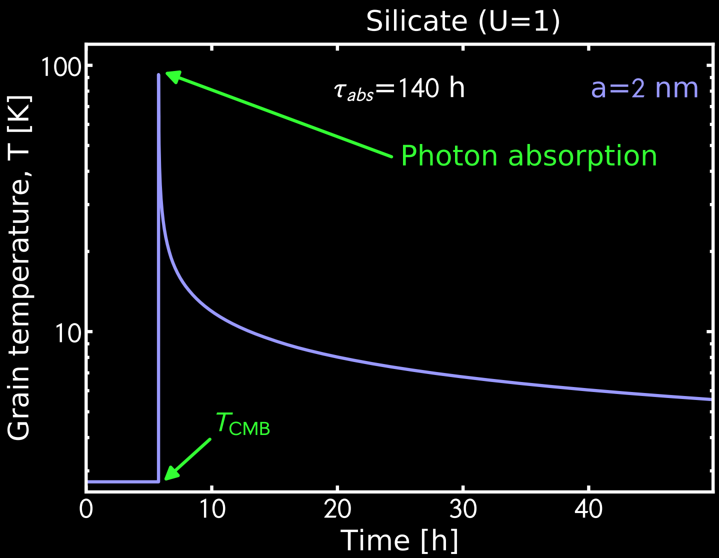
Silicate (U=1)
τ_{abs}=140 h
a=2 nm
Photon absorption
$T_{\rm CMB}$
100
10
Grain temperature, T [K]
0
10
20
30
40
Time [h]

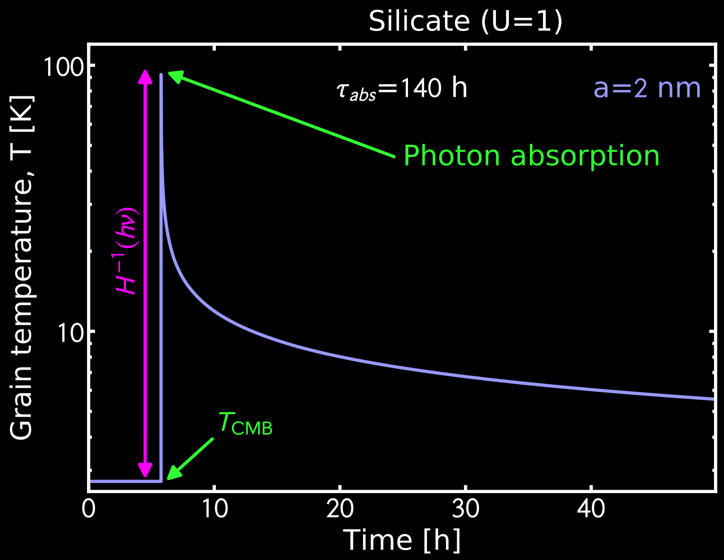

Silicate (U=1)
τ_{abs}=140 h
a=2 nm
Photon absorption
$H^{-1}(h\nu)$
$T_{\rm CMB}$
Grain temperature, T [K]
100
10
0
10
20
30
40
Time [h]

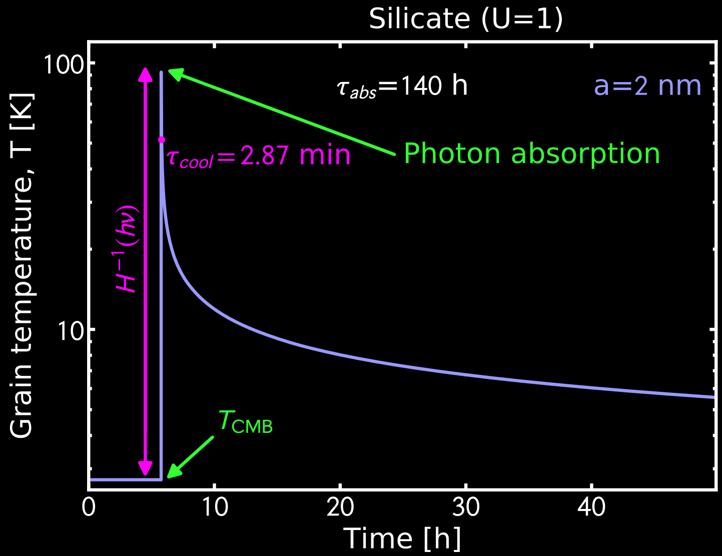
Silicate (U=1)
τ_{abs}=140 h
a=2 nm
τ_{cool}=2.87 min
Photon absorption
$H^{-1}(h\nu)$
$T_{\rm CMB}$
Grain temperature, T [K]
100
10
0
10
20
30
40
Time [h]

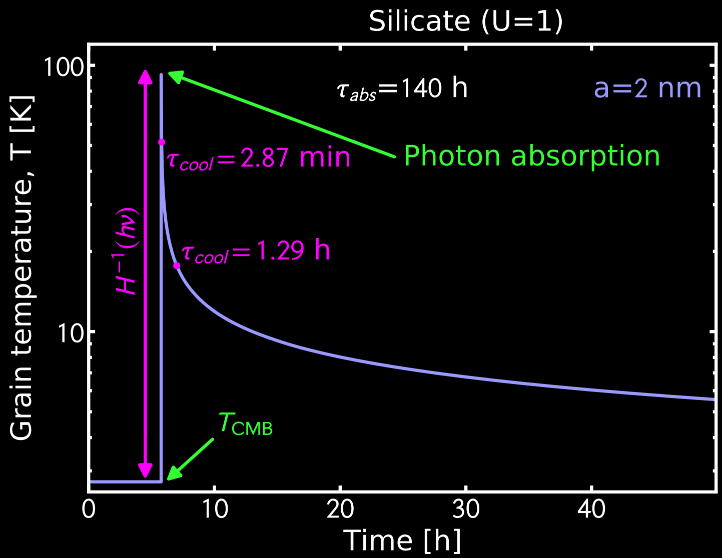
Silicate (U=1)
τ_{abs}=140 h
a=2 nm
Photon absorption
τ_{cool} = 2.87 min
τ_{cool} = 1.29 h
$H^{-1}(h\nu)$
T_{CMB}
100
10
0
10
20
30
40
Time [h]
Grain temperature, T [K]

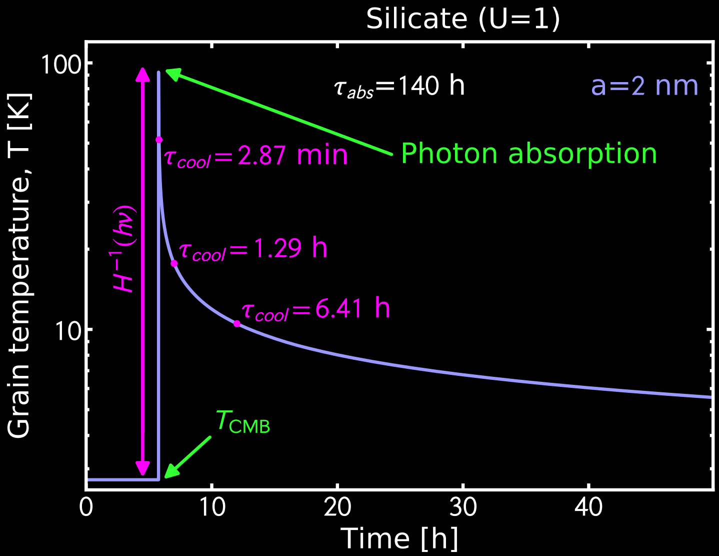
Silicate (U=1)
τ_{abs}=140 h
a=2 nm
Photon absorption
τ_{cool}=2.87 min
τ_{cool}=1.29 h
τ_{cool}=6.41 h
$H^{-1}(h\nu)$
T_{CMB}
Grain temperature, T [K]
100
10
0
10
20
30
40
Time [h]

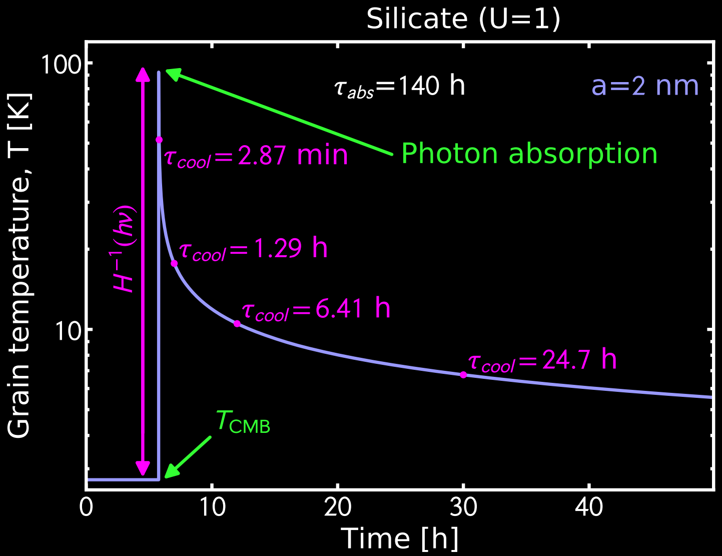

Silicate (U=1)
τ_{abs}=140 h
a=2 nm
Photon absorption
τ_{cool} = 2.87 min
τ_{cool} = 1.29 h
τ_{cool} = 6.41 h
τ_{cool} = 24.7 h
$H^{-1}(h\nu)$
T_{CMB}
100
10
Grain temperature, T [K]
0
10
20
30
40
Time [h]

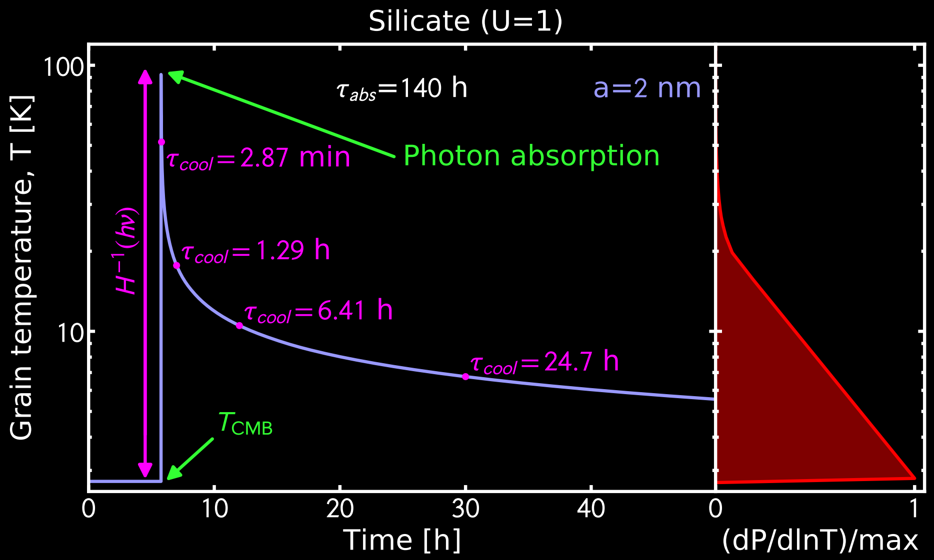
Silicate (U=1)
Grain temperature, T [K]
100
10
τ_{abs}=140 h
a=2 nm
Photon absorption
τ_{cool}=2.87 min
τ_{cool}=1.29 h
τ_{cool}=6.41 h
τ_{cool}=24.7 h
$H^{-1}(h\nu)$
T_{CMB}
0
10
20
30
40
0
1
Time [h]
(dP/dlnT)/max

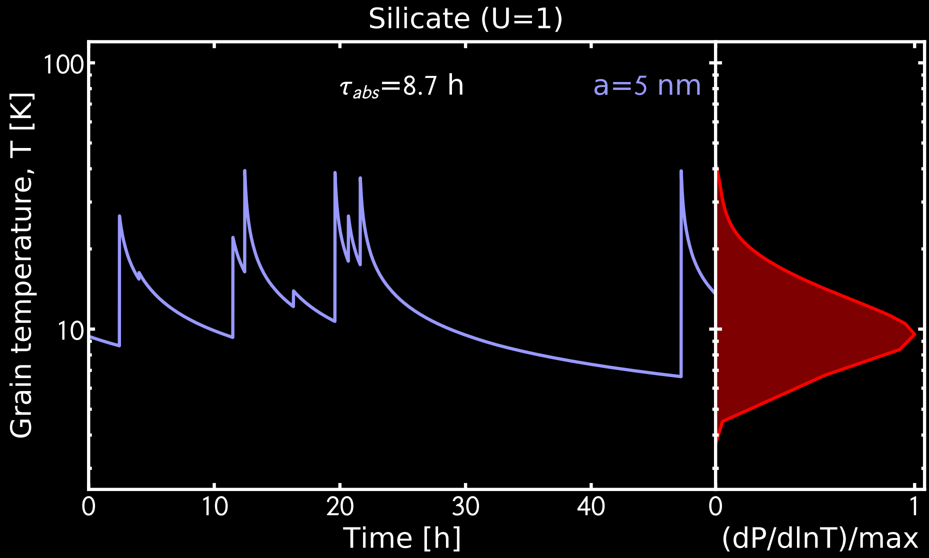
Silicate (U=1)
τ_{abs}=8.7 h
a=5 nm
Grain temperature, T [K]
100
10
0
10
20
30
40
0
1
Time [h]
(dP/dlnT)/max

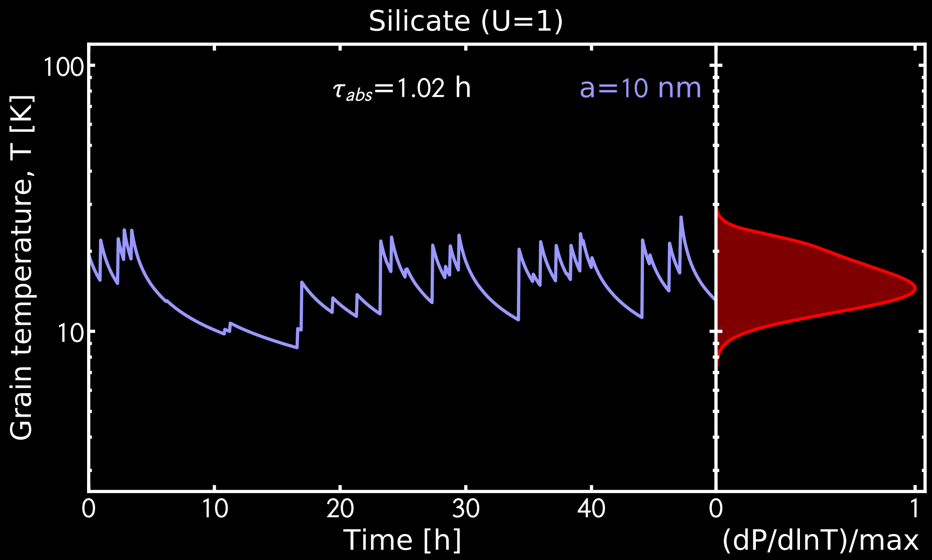

Silicate (U=1)
τ_{abs}=1.02 h
a=10 nm
Grain temperature, T [K]
100
10
0
10
20
30
40
Time [h]
0
1
(dP/dlnT)/max

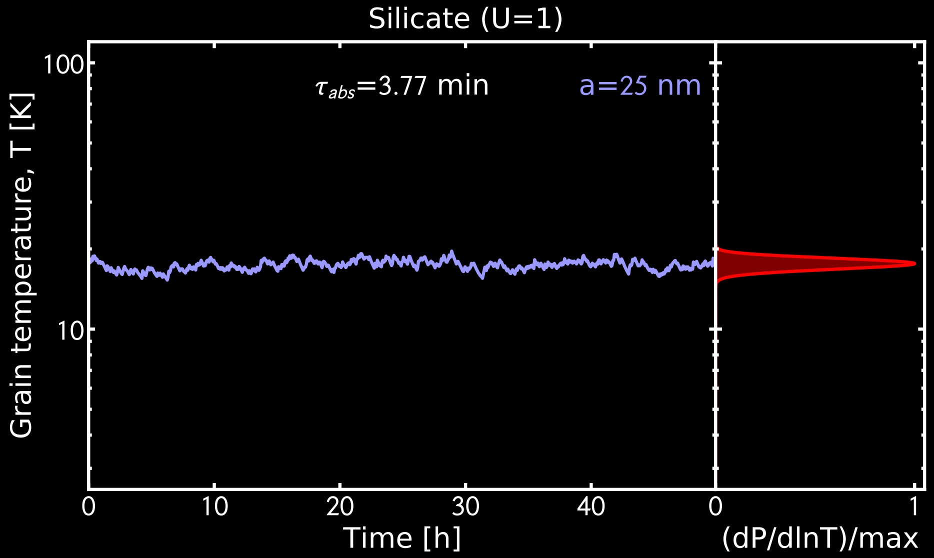
Silicate (U=1)
τ_{abs}=3.77 min
a=25 nm
100
10
Grain temperature, T [K]
0
10
20
30
40
Time [h]
0
1
(dP/dlnT)/max

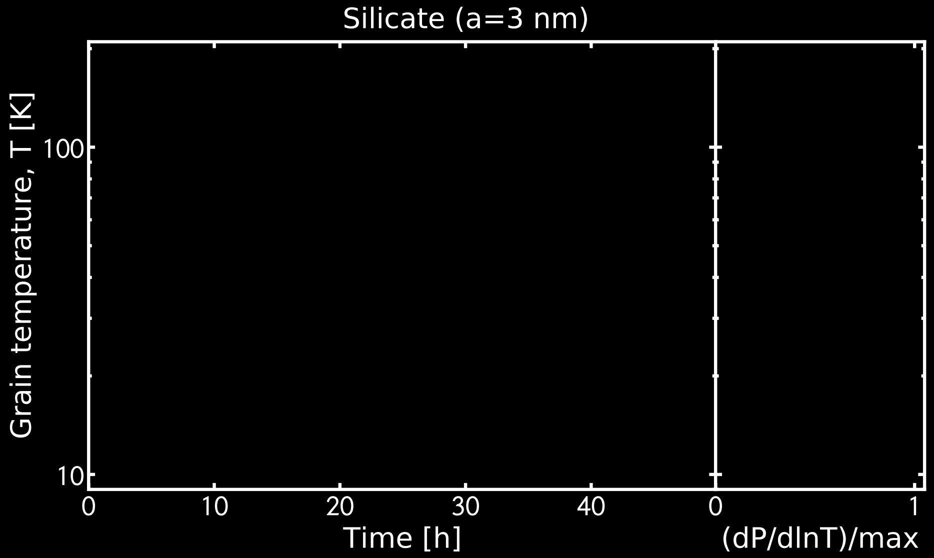
Silicate (a=3 nm)
Grain temperature, T [K]
100
10
0
10
20
30
40
Time [h]
0
1
(dP/dlnT)/max

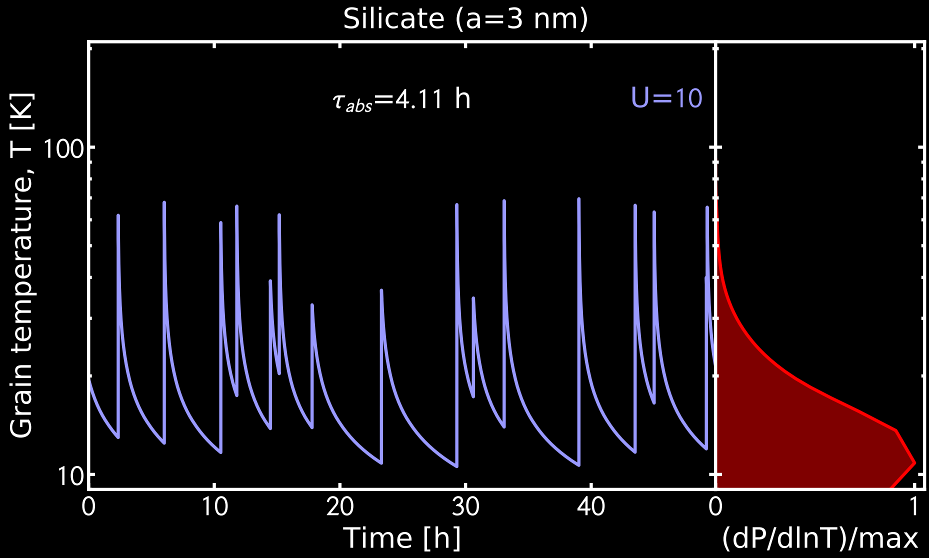
Silicate (a=3 nm)
τabs=4.11 h
U=10
Grain temperature, T [K]
100
10
0
10
20
30
40
Time [h]
0
1
(dP/dlnT)/max

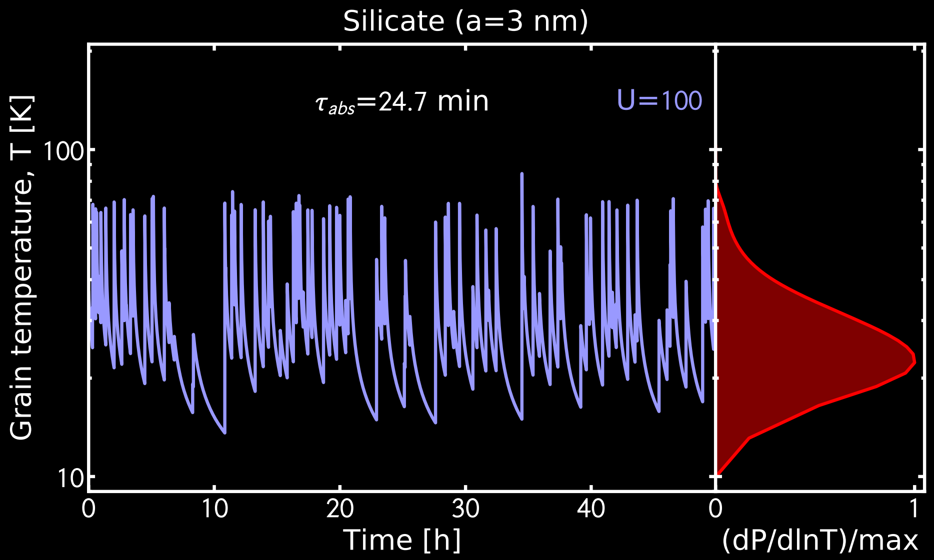

Silicate (a=3 nm)
τ_{abs}=24.7 min
U=100
Grain temperature, T [K]
100
10
0
10
20
30
40
0
1
Time [h]
(dP/dlnT)/max

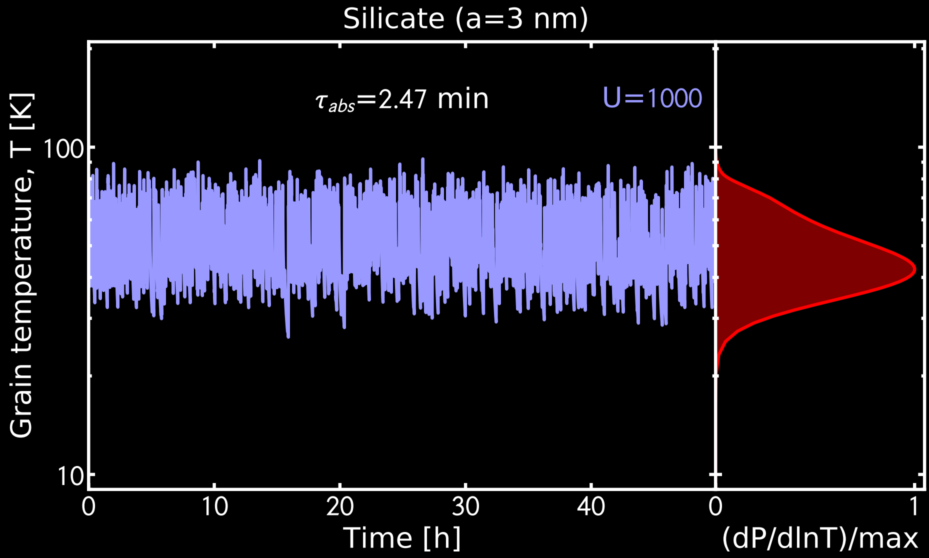
Silicate (a=3 nm)
τ_{abs}=2.47 min
U=1000
Grain temperature, T [K]
100
10
0
10
20
30
40
Time [h]
0
1
(dP/dlnT)/max

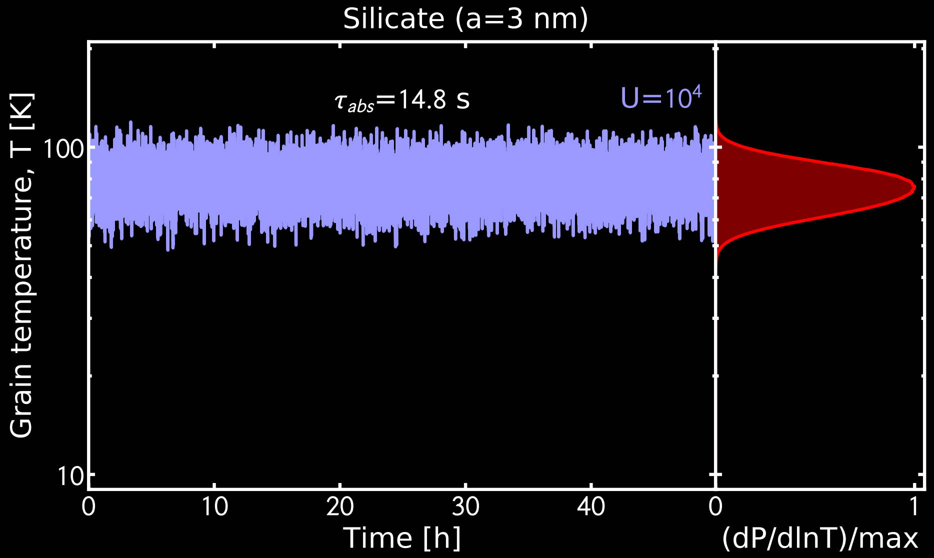
Silicate (a=3 nm)
τ_{abs}=14.8 s
U=10^4
Grain temperature, T [K]
100
10
0
10
20
30
40
Time [h]
0
1
(dP/dlnT)/max

Dust | Stochastic Heating: Emission Spectra of Silicates

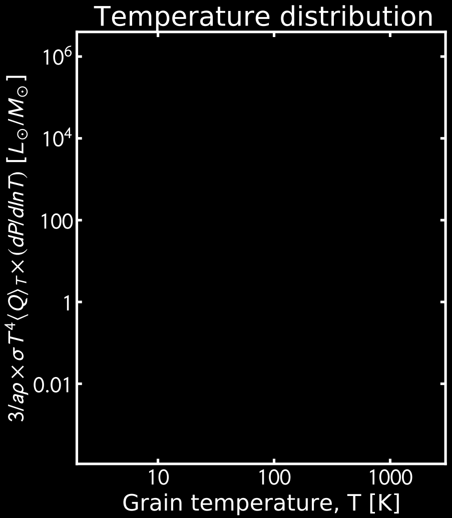
Temperature distribution
$3/a\rho \times \sigma T^4 \langle Q \rangle_T \times (dP/d\ln T)$ [$L_\odot/M_\odot$]
10^6
10^4
100
1
0.01
10
100
1000
Grain temperature, T [K]

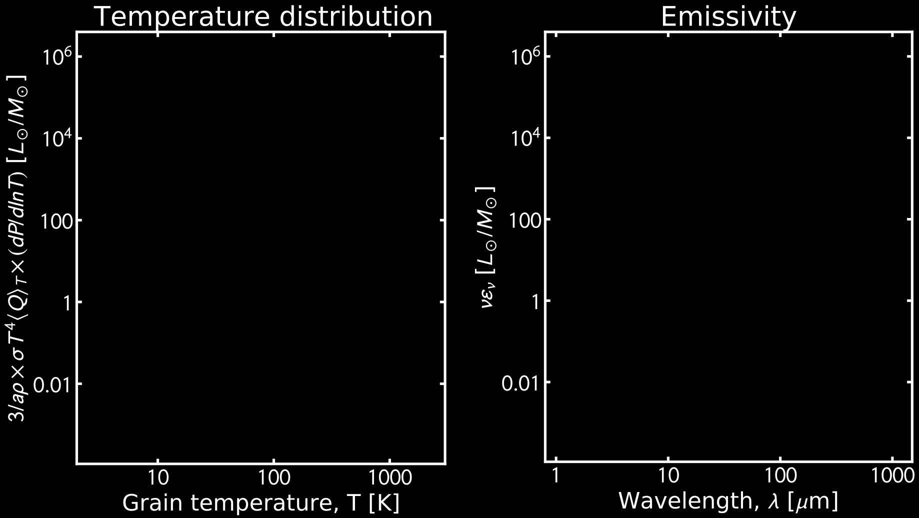
Temperature distribution
10^6
10^4
100
1
0.01
10
100
1000
Grain temperature, T [K]
$3/a\rho \times \sigma T^4 \langle Q \rangle_T \times (dP/d\ln T)$ [$L_\odot/M_\odot$]
Emissivity
10^6
10^4
100
1
0.01
1
10
100
1000
Wavelength, λ [μm]
$\nu\varepsilon_\nu$ [$L_\odot/M_\odot$]

Dust | Stochastic Heating: Emission Spectra of Silicates

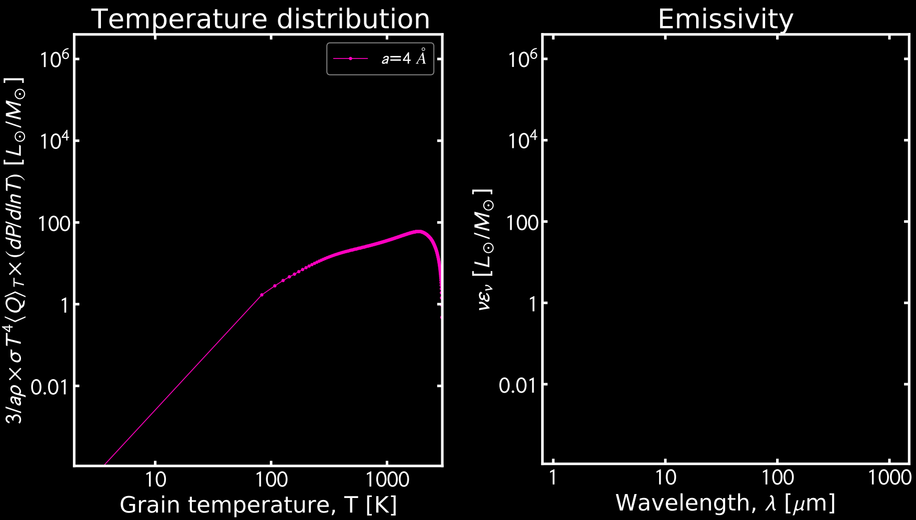

(solution using the numerical method of Guhathakurta & Draine 1989)

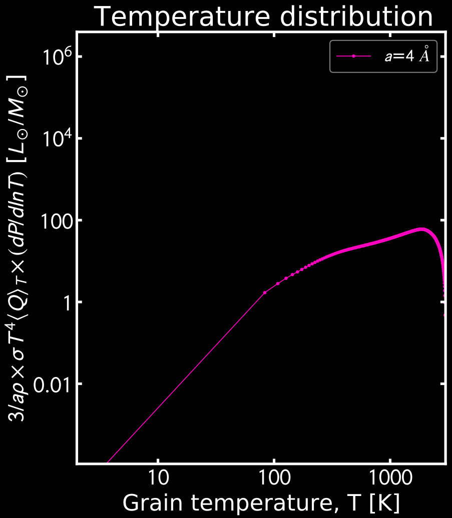

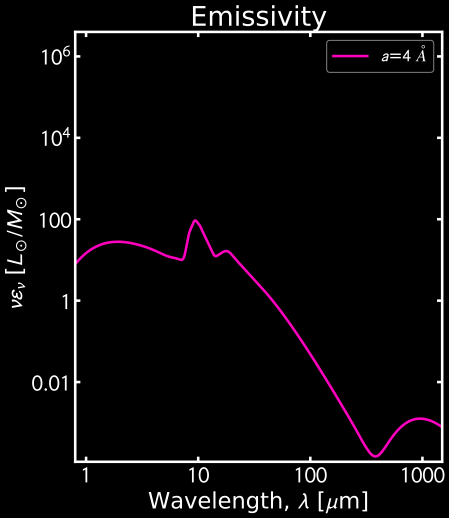

(solution using the numerical method of Guhathakurta & Draine 1989)

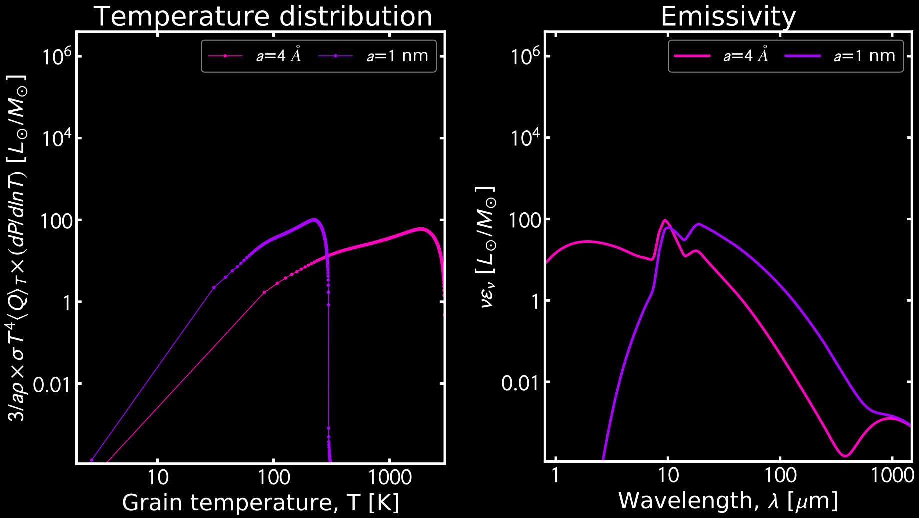

(solution using the numerical method of Guhathakurta & Draine 1989)

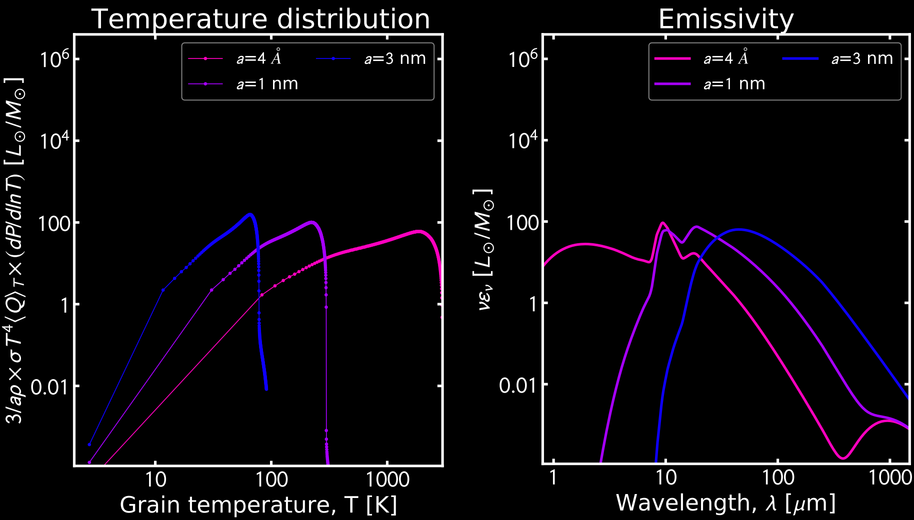

(solution using the numerical method of Guhathakurta & Draine 1989)

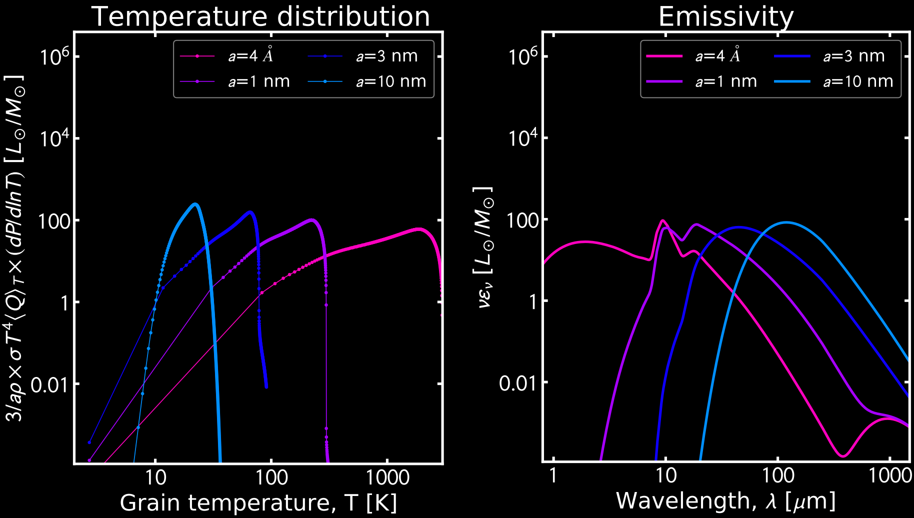

(solution using the numerical method of Guhathakurta & Draine 1989)

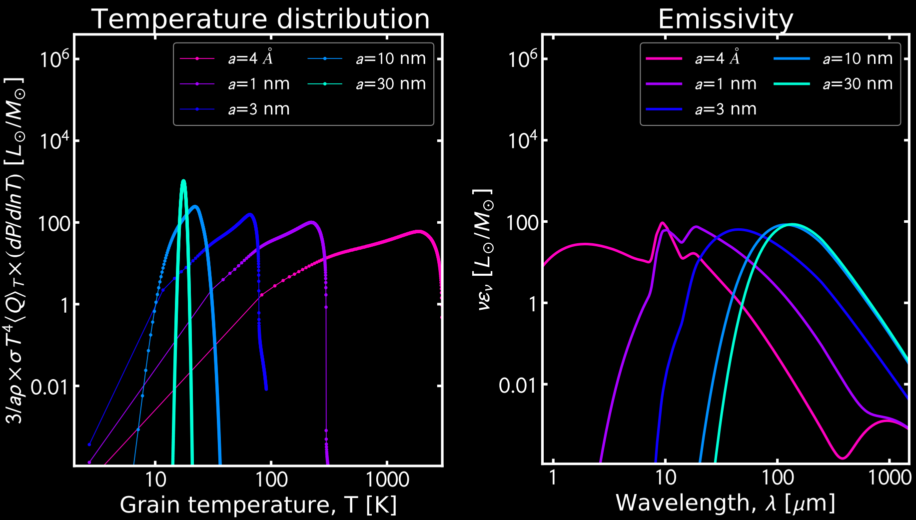

(solution using the numerical method of Guhathakurta & Draine 1989)

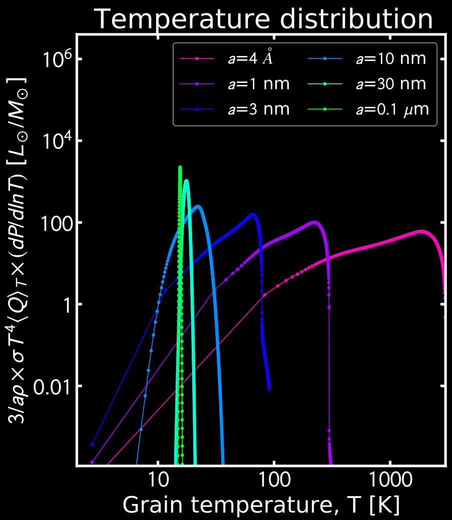

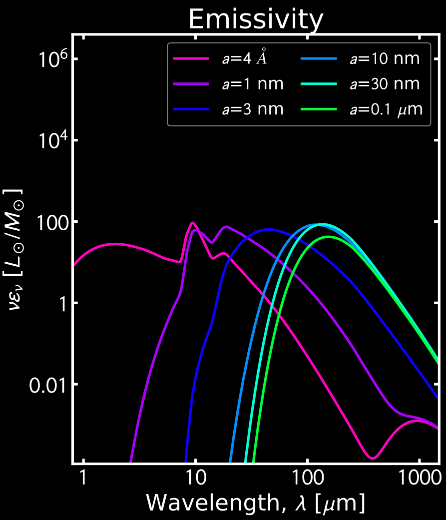

(solution using the numerical method of Guhathakurta & Draine 1989)

Dust | Stochastic Heating: Emission Spectra of Silicates

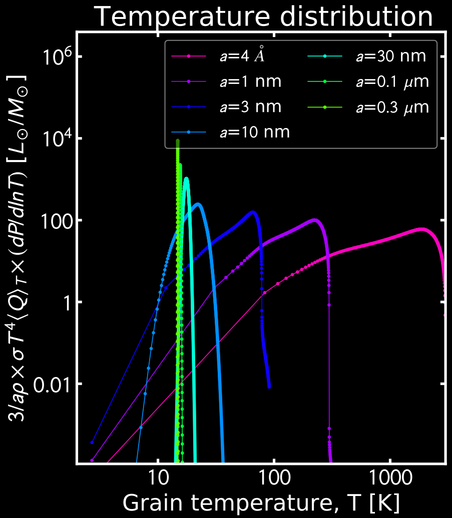

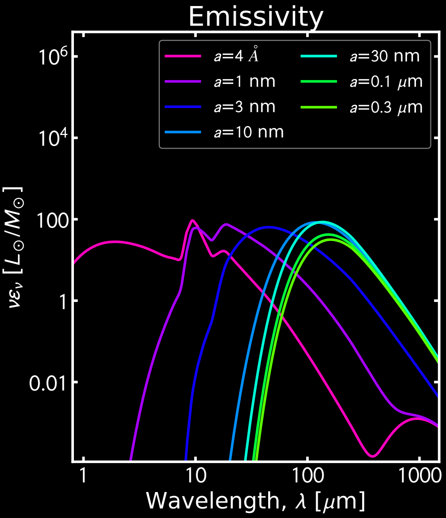

(solution using the numerical method of Guhathakurta & Draine 1989)

Dust | Stochastic Heating: Emission Spectra of Silicates

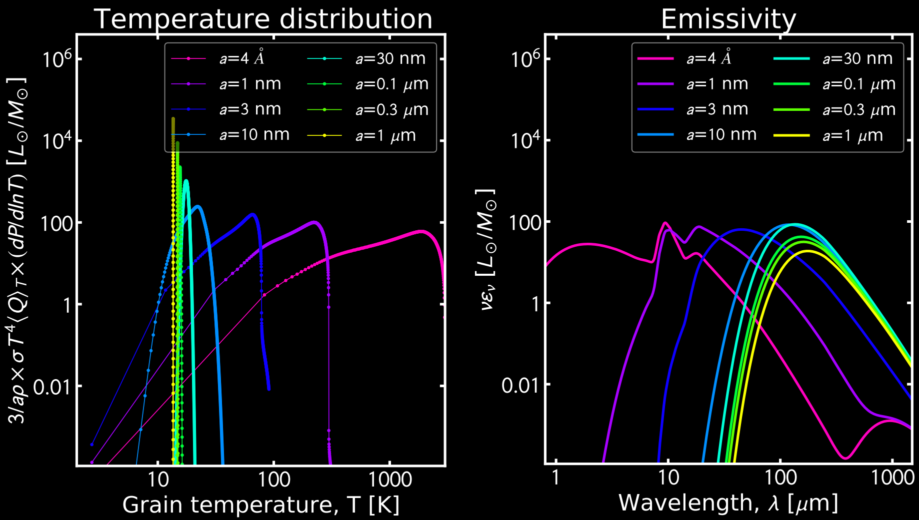

(solution using the numerical method of Guhathakurta & Draine 1989)

Dust | Stochastic Heating: Emission Spectra of Silicates

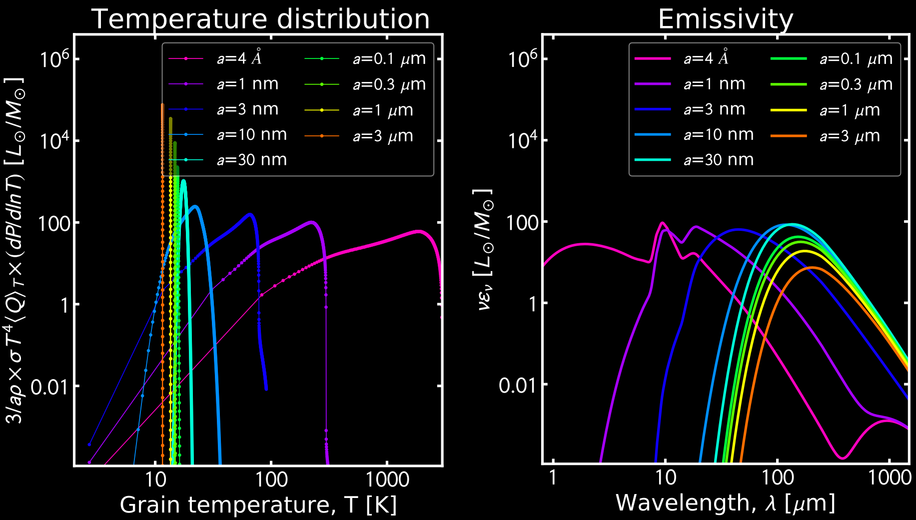

(solution using the numerical method of Guhathakurta & Draine 1989)

Dust | Stochastic Heating: Emission Spectra of Silicates

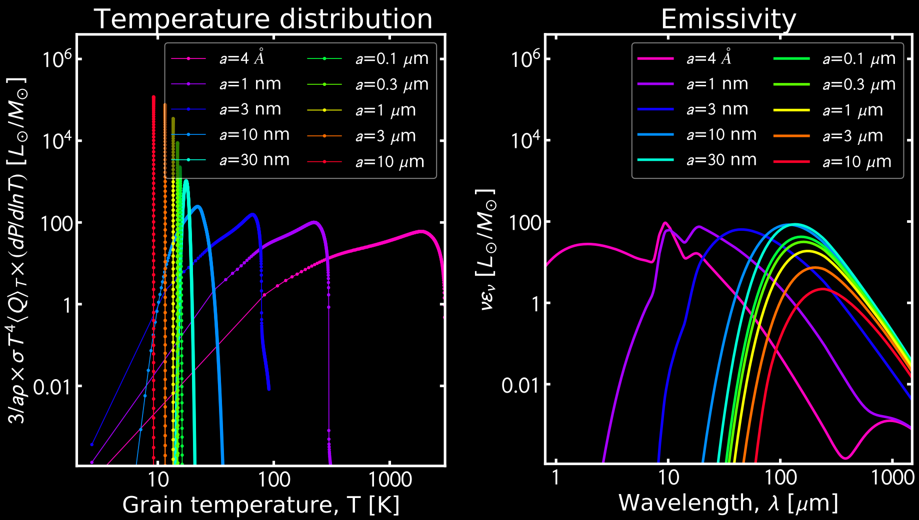

(solution using the numerical method of Guhathakurta & Draine 1989)

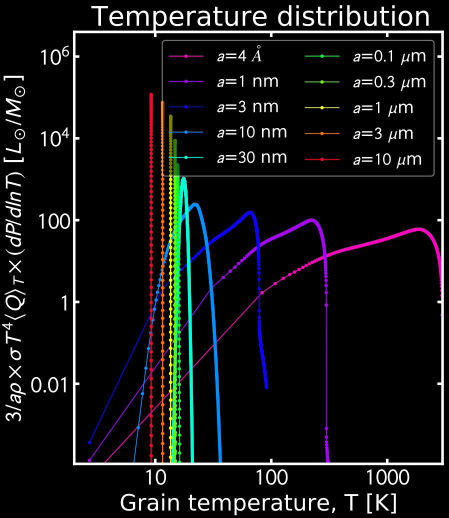

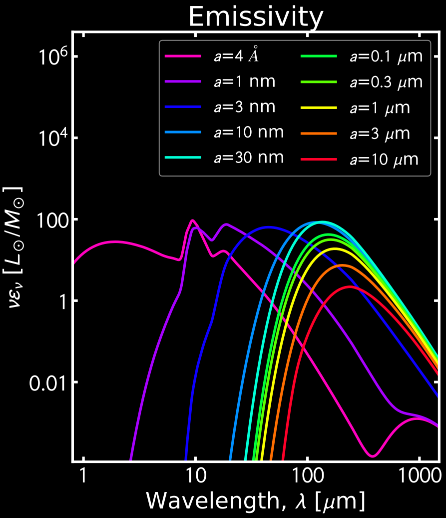

(solution using the numerical method of Guhathakurta & Draine 1989)

In the ISM ⇒ range of sizes.

Physical ingredients

Physical ingredients

- Set of optical properties & heat capacities: *e.g.* astrosilicates, PAHs, a-C(:H), *etc.*

Physical ingredients

- Set of optical properties & heat capacities: *e.g.* astrosilicates, PAHs, a-C(:H), *etc.*
- Size distribution of each species $\rightarrow$ power-law, log-normal, *etc.*

Physical ingredients

- Set of optical properties & heat capacities: *e.g.* astrosilicates, PAHs, a-C(:H), *etc.*
- Size distribution of each species $\rightarrow$ power-law, log-normal, *etc.*
- Abundances relative to the gas.

Dust | What is a Dust Model? How is it Build & Used?

Physical ingredients

- Set of optical properties & heat capacities: *e.g.* astrosilicates, PAHs, a-C(:H), *etc.*
- Size distribution of each species → power-law, log-normal, *etc.*
- Abundances relative to the gas.

Empirical constraints

Exclusively from the Galactic diffuse ISM → well-studied, optically-thin & uniformly illuminated (*e.g.* Mathis et al., 1977; Désert et al., 1990; Draine & Li, 2001, 2007; Zubko et al., 2004; Compiègne et al., 2011; Jones et al., 2013; Guillet et al., 2017; Jones et al., 2017; Siebenmorgen, 2023; Hensley & Draine, 2023; Ysard et al., 2024).

Dust | What is a Dust Model? How is it Build & Used?

Physical ingredients

- Set of optical properties & heat capacities: *e.g.* astrosilicates, PAHs, a-C(:H), *etc.*
- Size distribution of each species → power-law, log-normal, *etc.*
- Abundances relative to the gas.

Empirical constraints

Exclusively from the Galactic diffuse ISM → well-studied, optically-thin & uniformly illuminated (*e.g.* Mathis et al., 1977; Désert et al., 1990; Draine & Li, 2001, 2007; Zubko et al., 2004; Compiègne et al., 2011; Jones et al., 2013; Guillet et al., 2017; Jones et al., 2017; Siebenmorgen, 2023; Hensley & Draine, 2023; Ysard et al., 2024).

- UV-MIR extinction;

Dust | What is a Dust Model? How is it Build & Used?

Physical ingredients

- Set of optical properties & heat capacities: *e.g.* astrosilicates, PAHs, a-C(:H), *etc.*
- Size distribution of each species → power-law, log-normal, *etc.*
- Abundances relative to the gas.

Empirical constraints

Exclusively from the Galactic diffuse ISM → well-studied, optically-thin & uniformly illuminated (*e.g.* Mathis et al., 1977; Désert et al., 1990; Draine & Li, 2001, 2007; Zubko et al., 2004; Compiègne et al., 2011; Jones et al., 2013; Guillet et al., 2017; Jones et al., 2017; Siebenmorgen, 2023; Hensley & Draine, 2023; Ysard et al., 2024).

- UV-MIR extinction;
- IR emission;

Physical ingredients

- Set of optical properties & heat capacities: *e.g.* astrosilicates, PAHs, a-C(:H), *etc.*
- Size distribution of each species → power-law, log-normal, *etc.*
- Abundances relative to the gas.

Empirical constraints

Exclusively from the Galactic diffuse ISM → well-studied, optically-thin & uniformly illuminated (*e.g.* Mathis et al., 1977; Désert et al., 1990; Draine & Li, 2001, 2007; Zubko et al., 2004; Compiègne et al., 2011; Jones et al., 2013; Guillet et al., 2017; Jones et al., 2017; Siebenmorgen, 2023; Hensley & Draine, 2023; Ysard et al., 2024).

- UV-MIR extinction;
- IR emission;
- Depletions;

Physical ingredients

- Set of optical properties & heat capacities: *e.g.* astrosilicates, PAHs, a-C(:H), *etc.*
- Size distribution of each species → power-law, log-normal, *etc.*
- Abundances relative to the gas.

Empirical constraints

Exclusively from the Galactic diffuse ISM → well-studied, optically-thin & uniformly illuminated (*e.g.* Mathis et al., 1977; Désert et al., 1990; Draine & Li, 2001, 2007; Zubko et al., 2004; Compiègne et al., 2011; Jones et al., 2013; Guillet et al., 2017; Jones et al., 2017; Siebenmorgen, 2023; Hensley & Draine, 2023; Ysard et al., 2024).

- UV-MIR extinction;
- IR emission;
- Depletions;
- Visible & IR polarization;

Dust | What is a Dust Model? How is it Build & Used?

Physical ingredients

- Set of optical properties & heat capacities: *e.g.* astrosilicates, PAHs, a-C(:H), *etc.*
- Size distribution of each species → power-law, log-normal, *etc.*
- Abundances relative to the gas.

Empirical constraints

Exclusively from the Galactic diffuse ISM → well-studied, optically-thin & uniformly illuminated (*e.g.* Mathis et al., 1977; Désert et al., 1990; Draine & Li, 2001, 2007; Zubko et al., 2004; Compiègne et al., 2011; Jones et al., 2013; Guillet et al., 2017; Jones et al., 2017; Siebenmorgen, 2023; Hensley & Draine, 2023; Ysard et al., 2024).

- UV-MIR extinction;
- IR emission;
- Depletions;
- Visible & IR polarization;
- Laboratory data;

Dust | What is a Dust Model? How is it Build & Used?

Physical ingredients

- Set of optical properties & heat capacities: *e.g.* astrosilicates, PAHs, a-C(:H), *etc.*
- Size distribution of each species → power-law, log-normal, *etc.*
- Abundances relative to the gas.

Empirical constraints

Exclusively from the Galactic diffuse ISM → well-studied, optically-thin & uniformly illuminated (*e.g.* Mathis et al., 1977; Désert et al., 1990; Draine & Li, 2001, 2007; Zubko et al., 2004; Compiègne et al., 2011; Jones et al., 2013; Guillet et al., 2017; Jones et al., 2017; Siebenmorgen, 2023; Hensley & Draine, 2023; Ysard et al., 2024).

- UV-MIR extinction;
- IR emission;
- Depletions;
- Visible & IR polarization;
- Laboratory data;
- Broad knowledge from IDPs.

Dust | What is a Dust Model? How is it Build & Used?

Physical ingredients

- Set of optical properties & heat capacities: *e.g.* astrosilicates, PAHs, a-C(:H), *etc.*
- Size distribution of each species → power-law, log-normal, *etc.*
- Abundances relative to the gas.

Empirical constraints

Exclusively from the Galactic diffuse ISM → well-studied, optically-thin & uniformly illuminated (*e.g.* Mathis et al., 1977; Désert et al., 1990; Draine & Li, 2001, 2007; Zubko et al., 2004; Compiègne et al., 2011; Jones et al., 2013; Guillet et al., 2017; Jones et al., 2017; Siebenmorgen, 2023; Hensley & Draine, 2023; Ysard et al., 2024).

- UV-MIR extinction;
- IR emission;
- Depletions;
- Visible & IR polarization;
- Laboratory data;
- Broad knowledge from IDPs.

Usefulness for studying galaxies @ all z:

⇒ provides a framework to model observations & infer:

Dust | What is a Dust Model? How is it Build & Used?

Physical ingredients

- Set of optical properties & heat capacities: *e.g.* astrosilicates, PAHs, a-C(:H), *etc.*
- Size distribution of each species → power-law, log-normal, *etc.*
- Abundances relative to the gas.

Empirical constraints

Exclusively from the Galactic diffuse ISM → well-studied, optically-thin & uniformly illuminated (*e.g.* Mathis et al., 1977; Désert et al., 1990; Draine & Li, 2001, 2007; Zubko et al., 2004; Compiègne et al., 2011; Jones et al., 2013; Guillet et al., 2017; Jones et al., 2017; Siebenmorgen, 2023; Hensley & Draine, 2023; Ysard et al., 2024).

- UV-MIR extinction;
- IR emission;
- Depletions;
- Visible & IR polarization;
- Laboratory data;
- Broad knowledge from IDPs.

Usefulness for studying galaxies @ all z:

⇒ provides a framework to model observations & infer:

- Total dust mass;

Physical ingredients

- Set of optical properties & heat capacities: *e.g.* astrosilicates, PAHs, a-C(:H), *etc.*
- Size distribution of each species → power-law, log-normal, *etc.*
- Abundances relative to the gas.

Empirical constraints

Exclusively from the Galactic diffuse ISM → well-studied, optically-thin & uniformly illuminated (*e.g.* Mathis et al., 1977; Désert et al., 1990; Draine & Li, 2001, 2007; Zubko et al., 2004; Compiègne et al., 2011; Jones et al., 2013; Guillet et al., 2017; Jones et al., 2017; Siebenmorgen, 2023; Hensley & Draine, 2023; Ysard et al., 2024).

- UV-MIR extinction;
- IR emission;
- Depletions;
- Visible & IR polarization;
- Laboratory data;
- Broad knowledge from IDPs.

Usefulness for studying galaxies @ all z:

⇒ provides a framework to model observations & infer:

- Total dust mass;
- Heating *i.e.* varying U (starlight intensity);

Dust | What is a Dust Model? How is it Build & Used?

Physical ingredients

- Set of optical properties & heat capacities: *e.g.* astrosilicates, PAHs, a-C(:H), *etc.*
- Size distribution of each species → power-law, log-normal, *etc.*
- Abundances relative to the gas.

Empirical constraints

Exclusively from the Galactic diffuse ISM → well-studied, optically-thin & uniformly illuminated (*e.g.* Mathis et al., 1977; Désert et al., 1990; Draine & Li, 2001, 2007; Zubko et al., 2004; Compiègne et al., 2011; Jones et al., 2013; Guillet et al., 2017; Jones et al., 2017; Siebenmorgen, 2023; Hensley & Draine, 2023; Ysard et al., 2024).

- UV-MIR extinction;
- IR emission;
- Depletions;
- Visible & IR polarization;
- Laboratory data;
- Broad knowledge from IDPs.

Usefulness for studying galaxies @ all z:

⇒ provides a framework to model observations & infer:

- Total dust mass;
- Heating *i.e.* varying U (starlight intensity);
- Total thermally-emitted power;

Dust | What is a Dust Model? How is it Build & Used?

Physical ingredients

- Set of optical properties & heat capacities: *e.g.* astrosilicates, PAHs, a-C(:H), *etc.*
- Size distribution of each species → power-law, log-normal, *etc.*
- Abundances relative to the gas.

Empirical constraints

Exclusively from the Galactic diffuse ISM → well-studied, optically-thin & uniformly illuminated (*e.g.* Mathis et al., 1977; Désert et al., 1990; Draine & Li, 2001, 2007; Zubko et al., 2004; Compiègne et al., 2011; Jones et al., 2013; Guillet et al., 2017; Jones et al., 2017; Siebenmorgen, 2023; Hensley & Draine, 2023; Ysard et al., 2024).

- UV-MIR extinction;
- IR emission;
- Depletions;
- Visible & IR polarization;
- Laboratory data;
- Broad knowledge from IDPs.

Usefulness for studying galaxies @ all z:

⇒ provides a framework to model observations & infer:

- Total dust mass;
- Heating *i.e.* varying U (starlight intensity);
- Total thermally-emitted power;
- In a limited extent, the fraction of small grains.

Dust | What is a Dust Model? How is it Build & Used?

Physical ingredients

- Set of optical properties & heat capacities: *e.g.* astrosilicates, PAHs, a-C(:H), *etc.*
- Size distribution of each species → power-law, log-normal, *etc.*
- Abundances relative to the gas.

Empirical constraints

Exclusively from the Galactic diffuse ISM → well-studied, optically-thin & uniformly illuminated (*e.g.* Mathis et al., 1977; Désert et al., 1990; Draine & Li, 2001, 2007; Zubko et al., 2004; Compiègne et al., 2011; Jones et al., 2013; Guillet et al., 2017; Jones et al., 2017; Siebenmorgen, 2023; Hensley & Draine, 2023; Ysard et al., 2024).

- UV-MIR extinction;
- IR emission;
- Depletions;
- Visible & IR polarization;
- Laboratory data;
- Broad knowledge from IDPs.

Usefulness for studying galaxies @ all z:

⇒ provides a framework to model observations & infer:

- Total dust mass;
- Heating *i.e.* varying U (starlight intensity);
- Total thermally-emitted power;
- In a limited extent, the fraction of small grains.

⇒ Bias due to the assumption of Galactic properties.

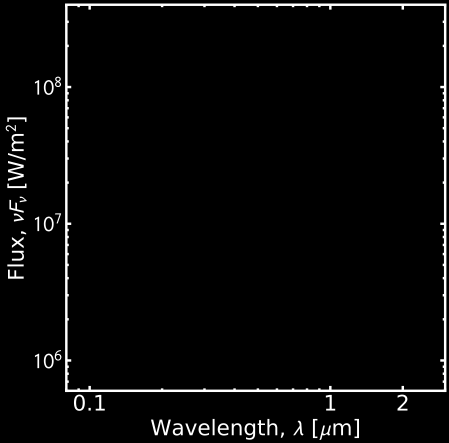

10^8
10^7
10^6
Flux, νF_ν [W/m^2]
0.1
1
2
Wavelength, λ [μm]

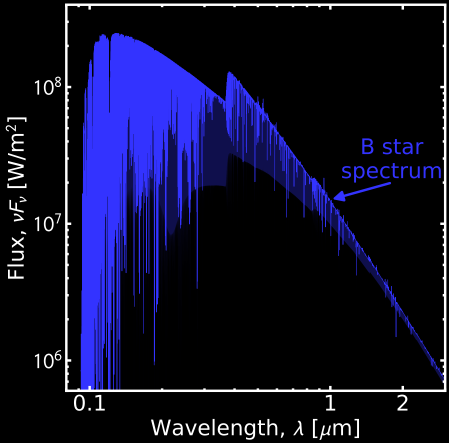
B star spectrum
Flux, νF_ν [W/m^2]
10^8
10^7
10^6
0.1
1
2
Wavelength, λ [μm]

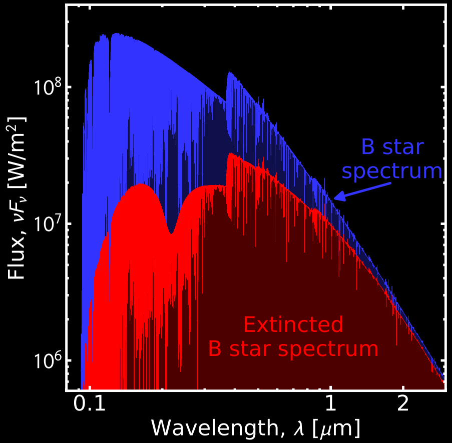
B star
spectrum
Extincted
B star spectrum
Flux, νF_ν [W/m^2]
10^8
10^7
10^6
0.1
1
2
Wavelength, λ [μm]

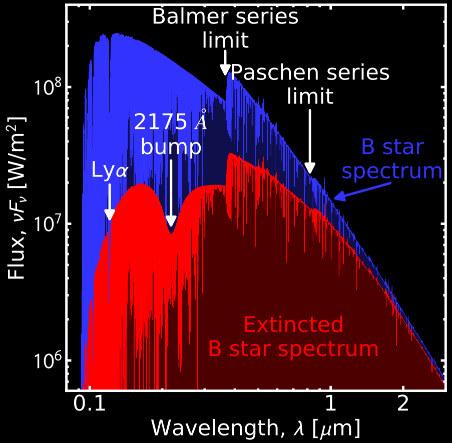
Balmer series
limit
Paschen series
limit
2175 Å
bump
Lyα
B star
spectrum
Extincted
B star spectrum
10^8
10^7
10^6
Flux, νF_ν [W/m^2]
0.1
1
2
Wavelength, λ [μm]

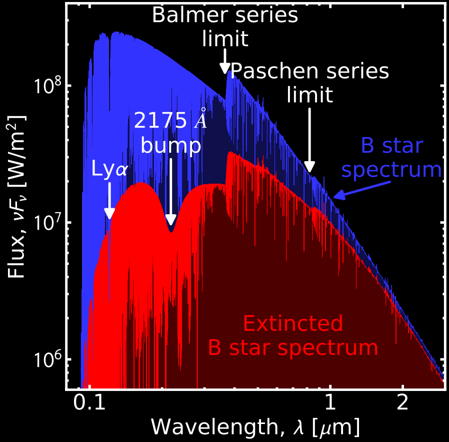

Selective extinction in magnitude

$$F_\nu^{\text{obs}}(\lambda) = F_\nu^{\text{int}}(\lambda) \times \exp[-\tau(\lambda)]$$

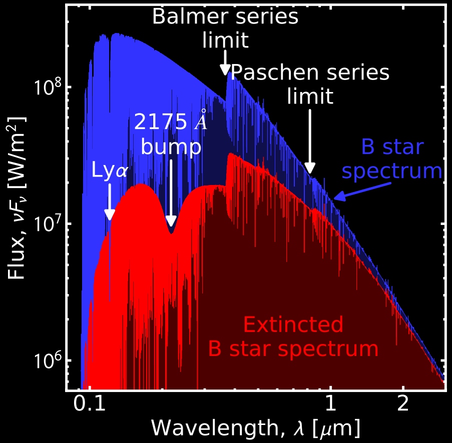

Selective extinction in magnitude

$$F_\nu^{\text{obs}}(\lambda) = F_\nu^{\text{int}}(\lambda) \times \exp[-\tau(\lambda)]$$

Amplitude: $A(\lambda) = 1.086 \times \tau(\lambda)$

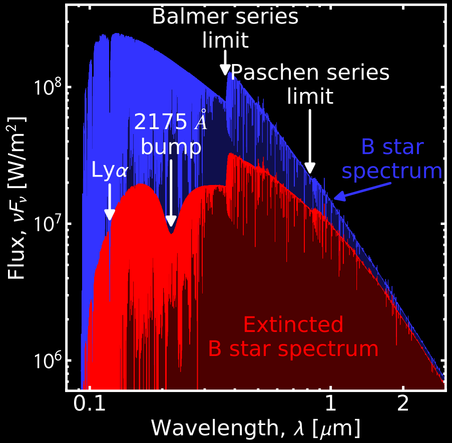

Selective extinction in magnitude

$$F_\nu^{\text{obs}}(\lambda) = F_\nu^{\text{int}}(\lambda) \times \exp[-\tau(\lambda)]$$

Amplitude: $A(\lambda) = 1.086 \times \tau(\lambda) \propto \mathrm{N(H)}$

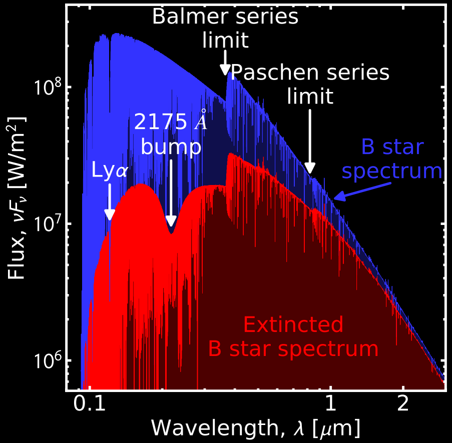

Selective extinction in magnitude

$$F_\nu^{\text{obs}}(\lambda) = F_\nu^{\text{int}}(\lambda) \times \exp[-\tau(\lambda)]$$

Amplitude: $A(\lambda) = 1.086 \times \tau(\lambda) \propto \text{N(H)}$

Slope: $R(V) \equiv \dfrac{A(V)}{A(B) - A(V)}$

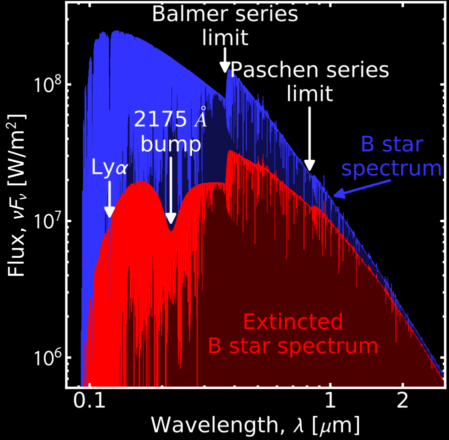

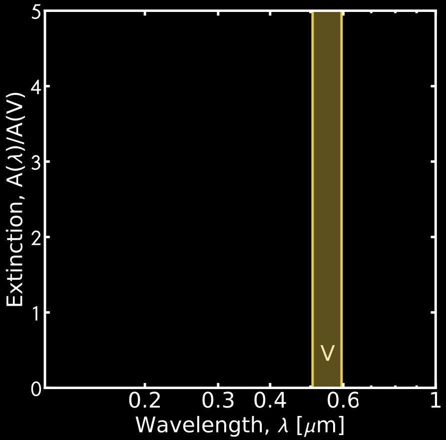

Selective extinction in magnitude

$$F_\nu^{\rm obs}(\lambda) = F_\nu^{\rm int}(\lambda) \times \exp[-\tau(\lambda)]$$

Amplitude: $A(\lambda) = 1.086 \times \tau(\lambda) \propto \mathrm{N(H)}$

Slope: $R(V) \equiv \dfrac{A(V)}{A(B) - A(V)}$

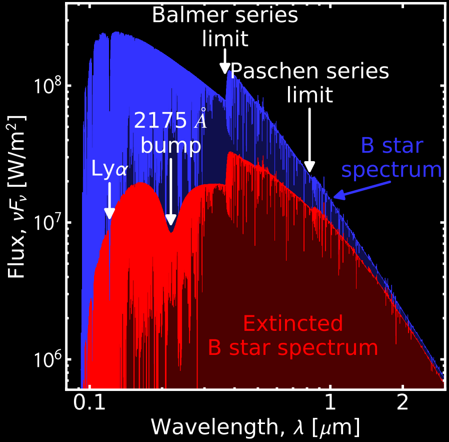

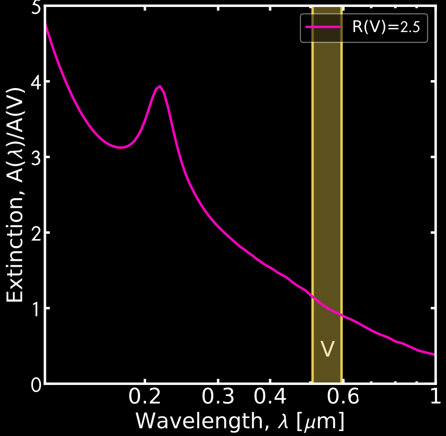

Selective extinction in magnitude

$$F_\nu^{\text{obs}}(\lambda) = F_\nu^{\text{int}}(\lambda) \times \exp[-\tau(\lambda)]$$

Amplitude: $A(\lambda) = 1.086 \times \tau(\lambda) \propto \text{N(H)}$

Slope: $R(V) \equiv \dfrac{A(V)}{A(B) - A(V)}$

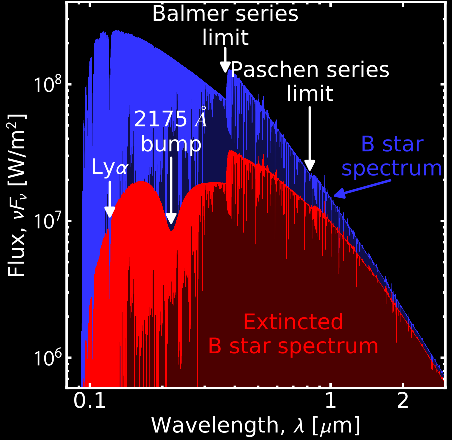

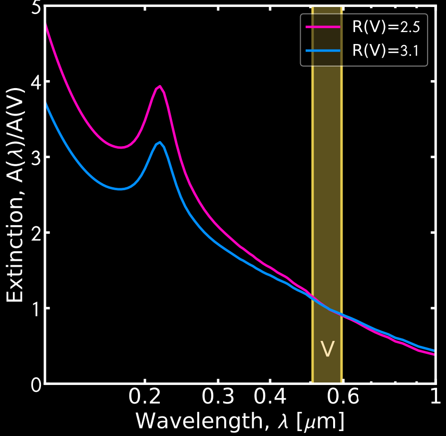

Selective extinction in magnitude

$$F_\nu^{\text{obs}}(\lambda) = F_\nu^{\text{int}}(\lambda) \times \exp[-\tau(\lambda)]$$

Amplitude: $A(\lambda) = 1.086 \times \tau(\lambda) \propto \text{N(H)}$

Slope: $R(V) \equiv \dfrac{A(V)}{A(B) - A(V)}$

Dust | Galactic Dust Observables: the Extinction Curve

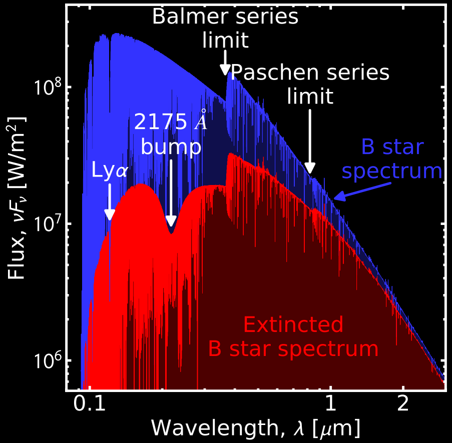

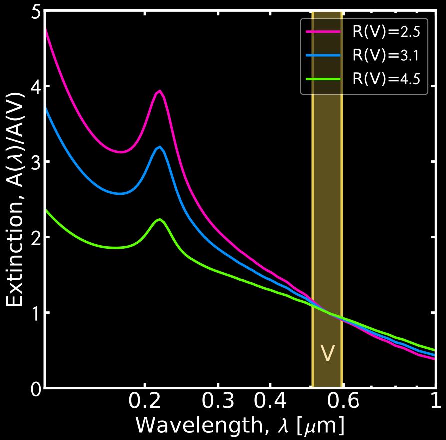

Selective extinction in magnitude

$$F_\nu^{\text{obs}}(\lambda) = F_\nu^{\text{int}}(\lambda) \times \exp[-\tau(\lambda)]$$

Amplitude: $A(\lambda) = 1.086 \times \tau(\lambda) \propto \text{N(H)}$

Slope: $R(V) \equiv \dfrac{A(V)}{A(B) - A(V)}$

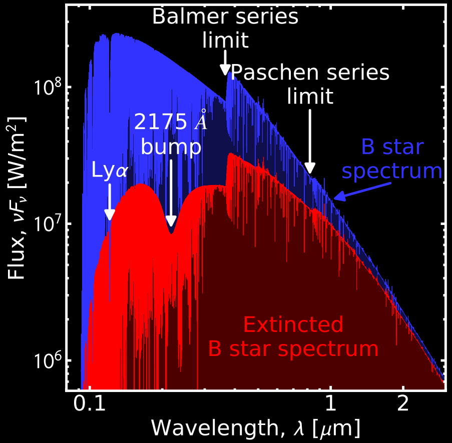

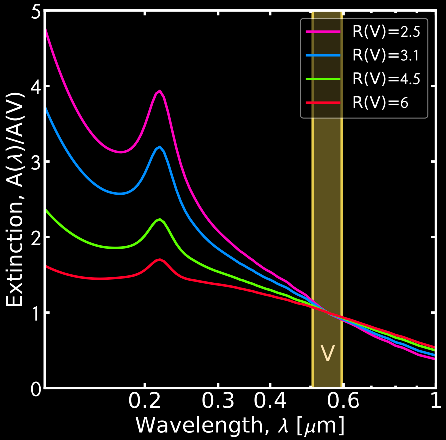

Selective extinction in magnitude

$$F_\nu^{\text{obs}}(\lambda) = F_\nu^{\text{int}}(\lambda) \times \exp[-\tau(\lambda)]$$

Amplitude: $A(\lambda) = 1.086 \times \tau(\lambda) \propto \text{N(H)}$

Slope: $R(V) \equiv \dfrac{A(V)}{A(B) - A(V)}$

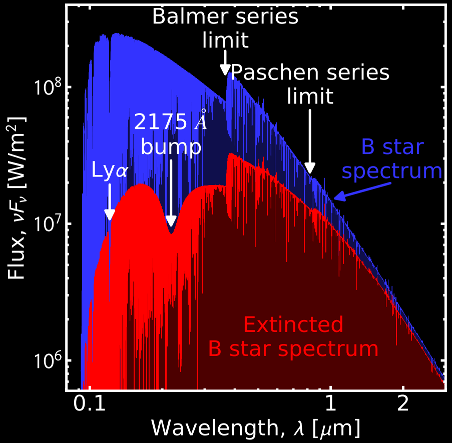

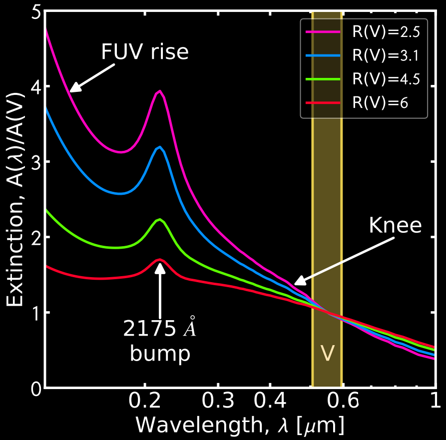

Selective extinction in magnitude

$$F_\nu^{\text{obs}}(\lambda) = F_\nu^{\text{int}}(\lambda) \times \exp[-\tau(\lambda)]$$

Amplitude: $A(\lambda) = 1.086 \times \tau(\lambda) \propto \mathrm{N(H)}$

Slope: $R(V) \equiv \dfrac{A(V)}{A(B) - A(V)}$

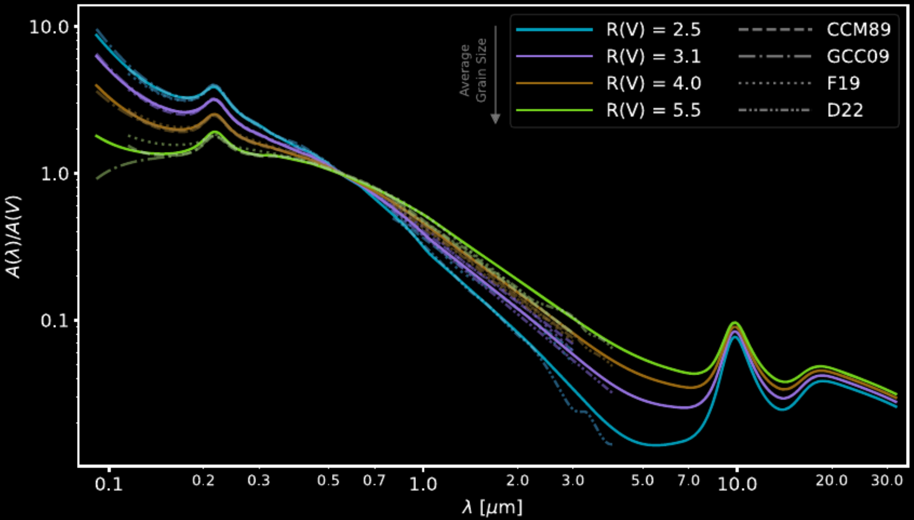

(Gordon et al., 2023)

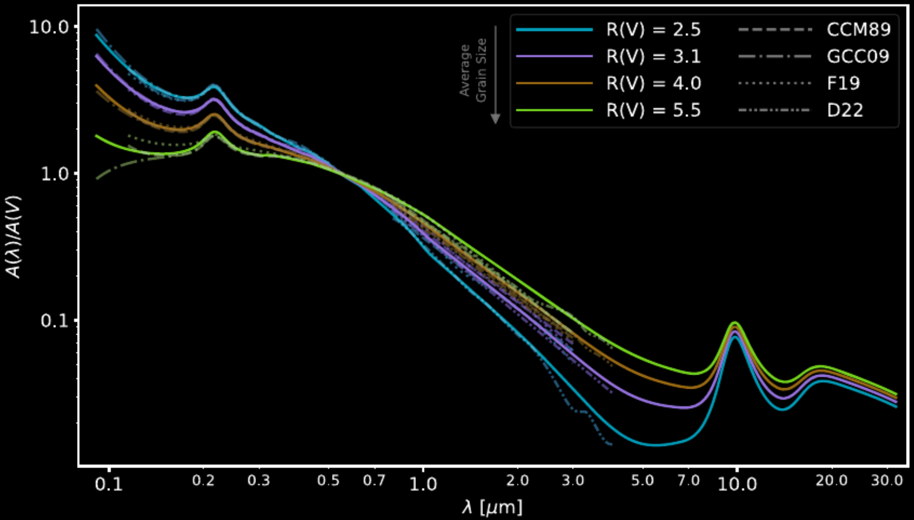

(Gordon et al., 2023)

⇒ size distribution, properties of carbonaceous & silicate grains, and optical properties.

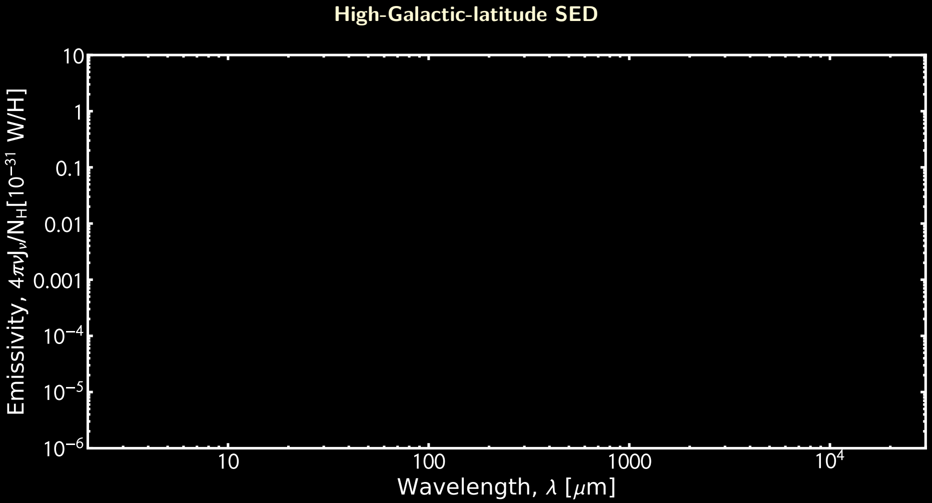

Data homogenized by Hensley & Draine (2021).

High-Galactic-latitude SED

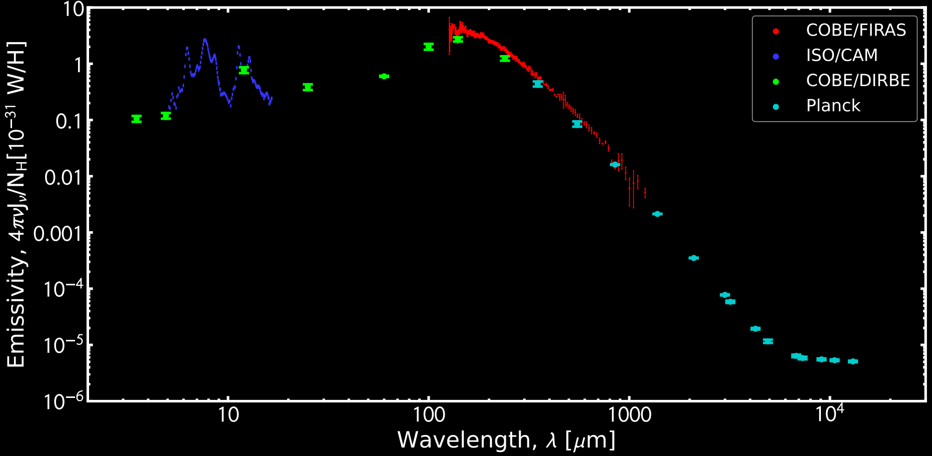

Data homogenized by Hensley & Draine (2021).

High-Galactic-latitude SED

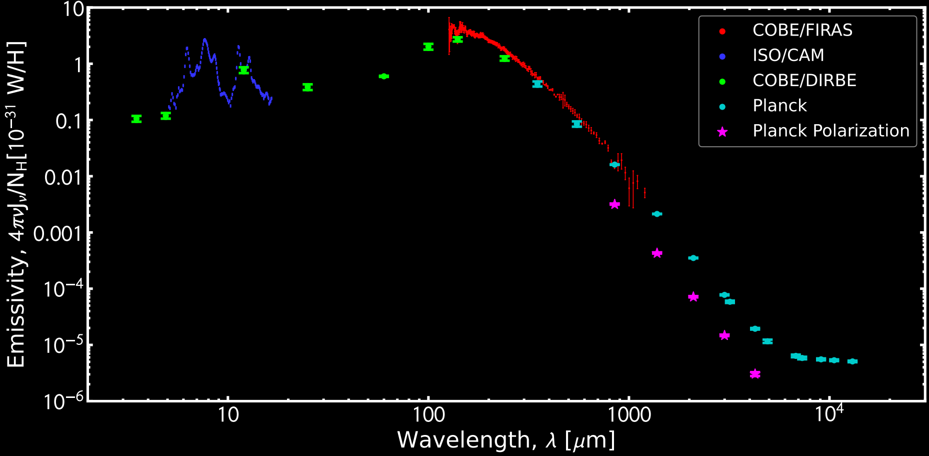

Data homogenized by Hensley & Draine (2021).

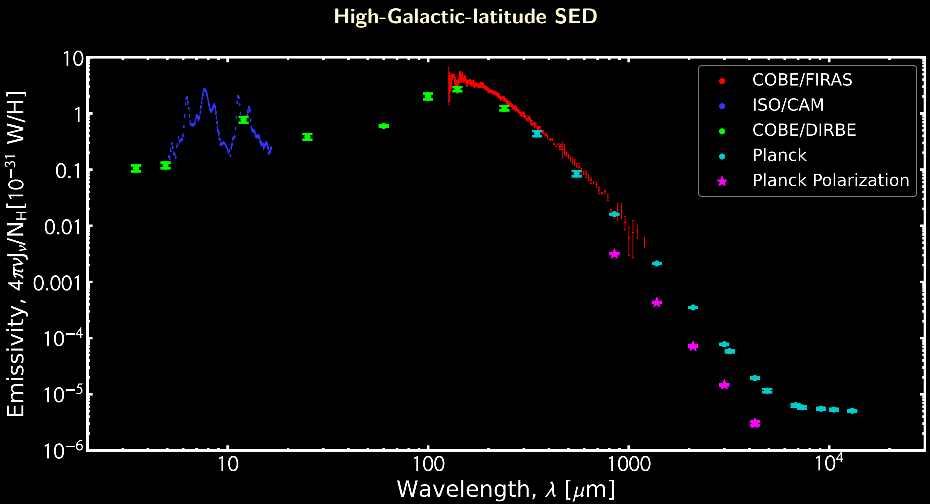

Data homogenized by Hensley & Draine (2021).

⇒ size distribution, optical properties & grain shapes.

$$\underbrace{\delta(E)}_{\text{depletion of E}} \equiv$$

$$\underbrace{\delta(E)}_{\text{depletion of E}} \equiv \underbrace{\log\left(\frac{N_\mathrm{E}}{N_\mathrm{H}}\right)_\mathrm{gas}}_{\text{abundance in the gas}} -$$

$$\underbrace{\delta(E)}_{\text{depletion of E}} \equiv \underbrace{\log\left(\frac{N_\text{E}}{N_\text{H}}\right)_\text{gas}}_{\text{abundance in the gas}} - \underbrace{\log\left(\frac{N_\text{E}}{N_\text{H}}\right)_\odot}_{\text{total abundance}}$$

Dust | The Elemental Depletions

$$\underbrace{\delta(E)}_{\text{depletion of E}} \equiv \underbrace{\log\left(\frac{N_\mathrm{E}}{N_\mathrm{H}}\right)_\mathrm{gas}}_{\text{abundance in the gas}} - \underbrace{\log\left(\frac{N_\mathrm{E}}{N_\mathrm{H}}\right)_\odot}_{\text{total abundance}} \simeq A_\mathrm{E} \times \underbrace{F_\star}_{\text{depletion strength}} + B_\mathrm{E}$$

(Jenkins, 2009)

$$\underbrace{\delta(E)}_{\text{depletion of E}} \equiv \underbrace{\log\left(\frac{N_E}{N_H}\right)_{\text{gas}}}_{\text{abundance in the gas}} - \underbrace{\log\left(\frac{N_E}{N_H}\right)_{\odot}}_{\text{total abundance}} \simeq A_E \times \underbrace{F_\star}_{\text{depletion strength}} + B_E$$

(Jenkins, 2009)

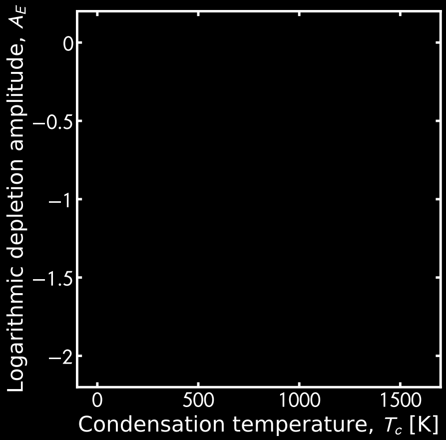

$$\underbrace{\delta(E)}_{\text{depletion of E}} \equiv \underbrace{\log\left(\frac{N_\text{E}}{N_\text{H}}\right)_\text{gas}}_{\text{abundance in the gas}} - \underbrace{\log\left(\frac{N_\text{E}}{N_\text{H}}\right)_\odot}_{\text{total abundance}} \simeq A_\text{E} \times \underbrace{F_\star}_{\text{depletion strength}} + B_\text{E} \quad \text{(Jenkins, 2009)}$$

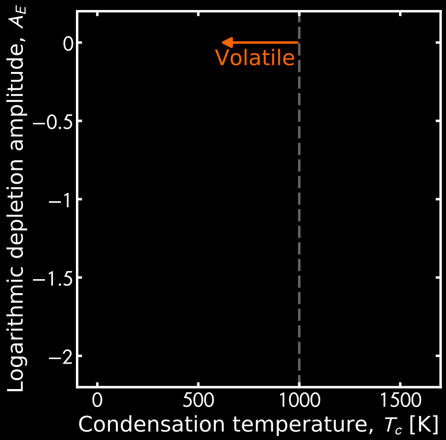

$$\underbrace{\delta(E)}_{\text{depletion of E}} \equiv \underbrace{\log\left(\frac{N_E}{N_H}\right)_{\text{gas}}}_{\text{abundance in the gas}} - \underbrace{\log\left(\frac{N_E}{N_H}\right)_{\odot}}_{\text{total abundance}} \simeq A_E \times \underbrace{F_\star}_{\text{depletion strength}} + B_E$$

(Jenkins, 2009)

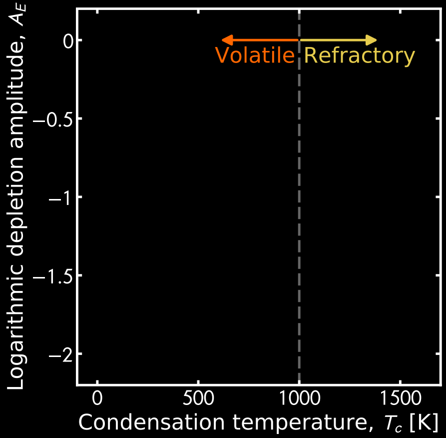

Dust | The Elemental Depletions

$$\underbrace{\delta(E)}_{\text{depletion of E}} \equiv \underbrace{\log\left(\frac{N_E}{N_H}\right)_{\text{gas}}}_{\text{abundance in the gas}} - \underbrace{\log\left(\frac{N_E}{N_H}\right)_{\odot}}_{\text{total abundance}} \simeq A_E \times \underbrace{F_\star}_{\text{depletion strength}} + B_E$$

(Jenkins, 2009)

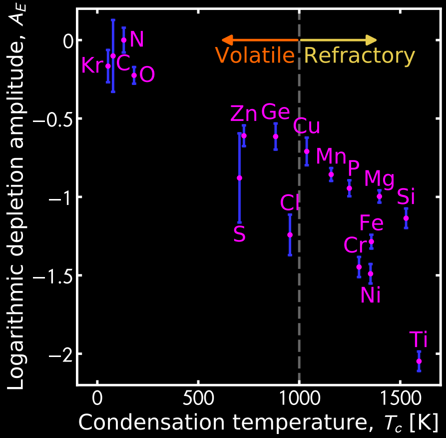

$$\underbrace{\delta(E)}_{\text{depletion of E}} \equiv \underbrace{\log\left(\frac{N_E}{N_H}\right)_{\text{gas}}}_{\text{abundance in the gas}} - \underbrace{\log\left(\frac{N_E}{N_H}\right)_{\odot}}_{\text{total abundance}} \simeq A_E \times \underbrace{F_\star}_{\text{depletion strength}} + B_E$$

(Jenkins, 2009)

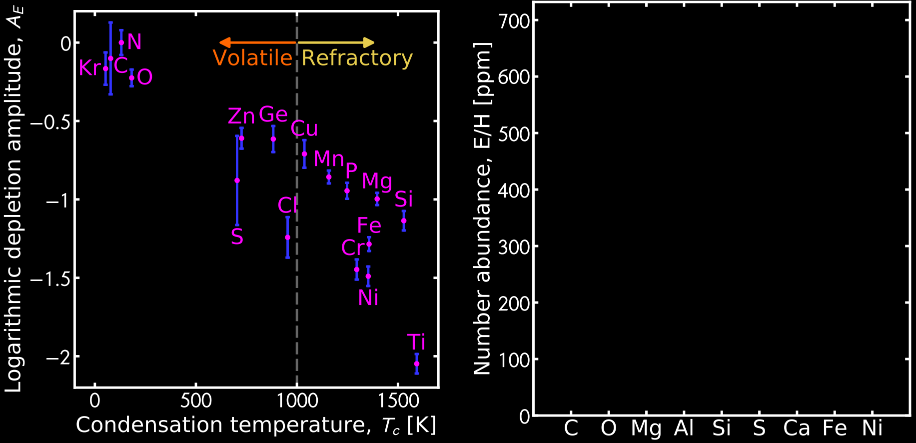

Dust | The Elemental Depletions

$$\underbrace{\delta(E)}_{\text{depletion of E}} \equiv \underbrace{\log\left(\frac{N_E}{N_H}\right)_{\text{gas}}}_{\text{abundance in the gas}} - \underbrace{\log\left(\frac{N_E}{N_H}\right)_{\odot}}_{\text{total abundance}} \simeq A_E \times \underbrace{F_\star}_{\text{depletion strength}} + B_E$$

(Jenkins, 2009)

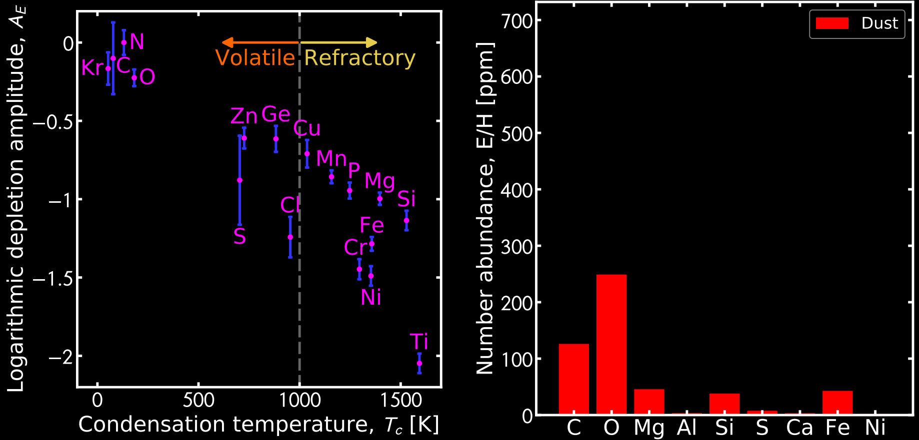

$$\underbrace{\delta(E)}_{\text{depletion of E}} \equiv \underbrace{\log\left(\frac{N_\mathrm{E}}{N_\mathrm{H}}\right)_\mathrm{gas}}_{\text{abundance in the gas}} - \underbrace{\log\left(\frac{N_\mathrm{E}}{N_\mathrm{H}}\right)_\odot}_{\text{total abundance}} \simeq A_\mathrm{E} \times \underbrace{F_\star}_{\text{depletion strength}} + B_\mathrm{E}$$

(Jenkins, 2009)

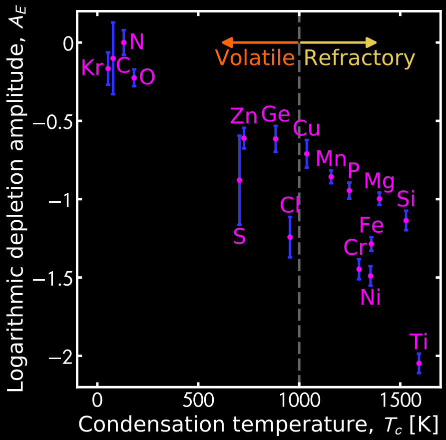

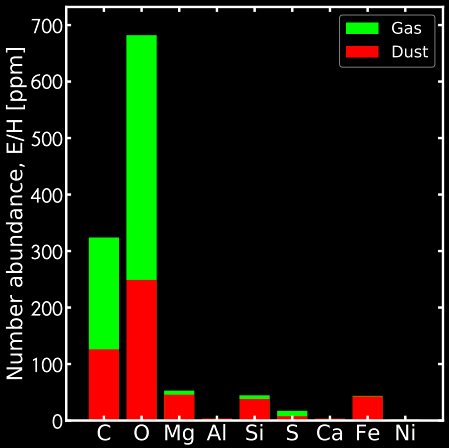

$$\underbrace{\delta(E)}_{\text{depletion of E}} \equiv \underbrace{\log\left(\frac{N_E}{N_H}\right)_{gas}}_{\text{abundance in the gas}} - \underbrace{\log\left(\frac{N_E}{N_H}\right)_{\odot}}_{\text{total abundance}} \simeq A_E \times \underbrace{F_\star}_{\text{depletion strength}} + B_E$$

(Jenkins, 2009)

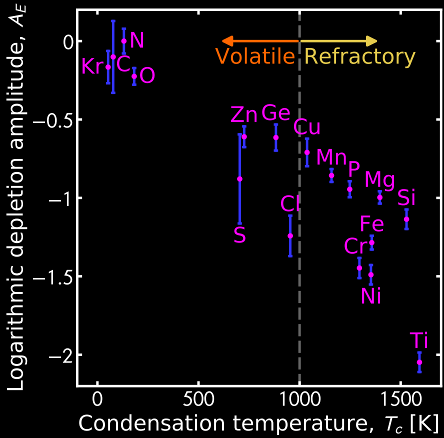

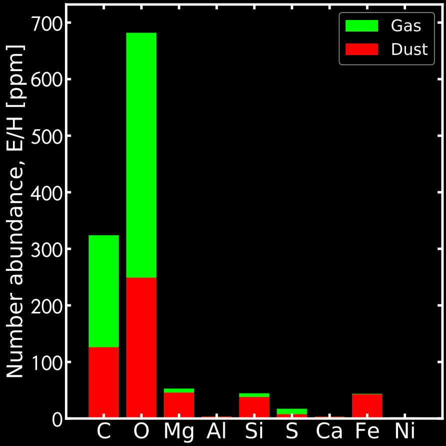

⇒ global dust stoichiometry.

Dust | Study of Interplanetary Dust Particles (IDP)

Pre-Solar grains locked-up in meteorites

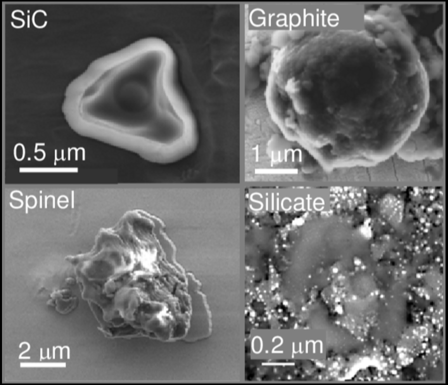

Pre-Solar grains locked-up in meteorites

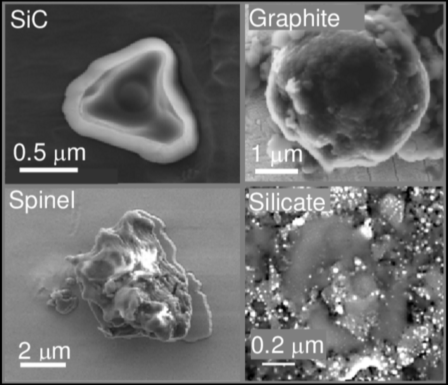

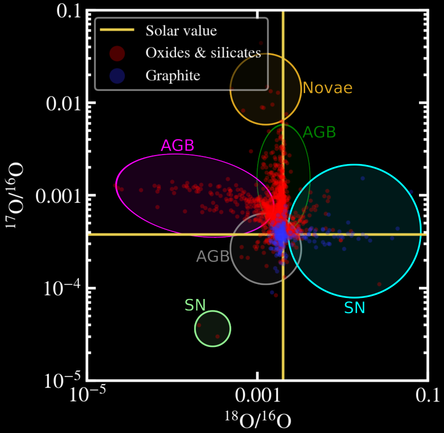

(Hoppe, 2010)

Pre-Solar grains locked-up in meteorites

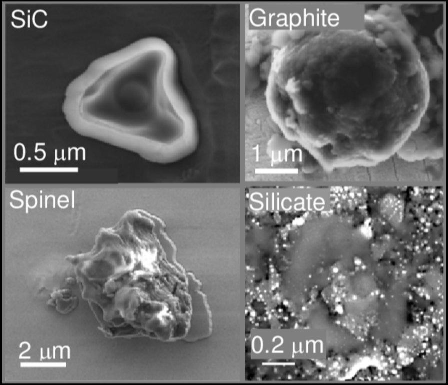

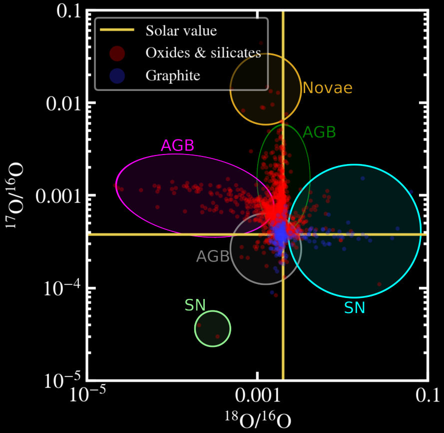

(Hoppe, 2010)

⇒ provides a sample of the types of solids in the ISM.

Dust | X-ray Absorption Edges

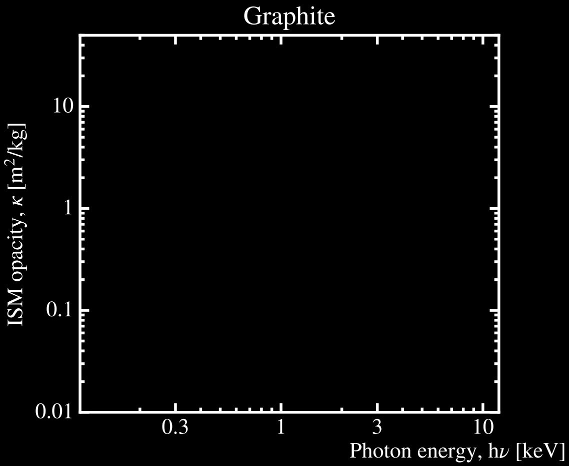

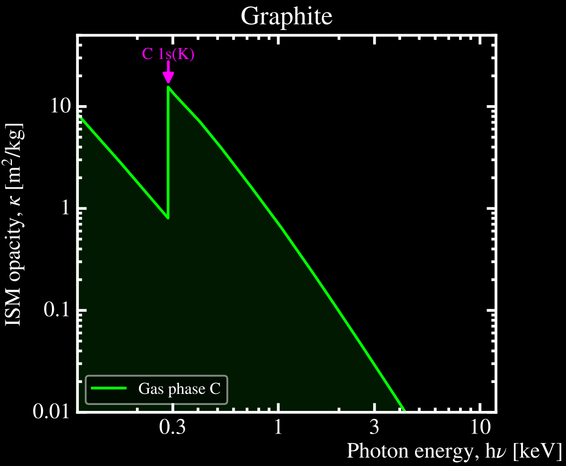
Graphite
C 1s(K)
Gas phase C
ISM opacity, κ [m^2/kg]
10
1
0.1
0.01
0.3
1
3
10
Photon energy, hν [keV]

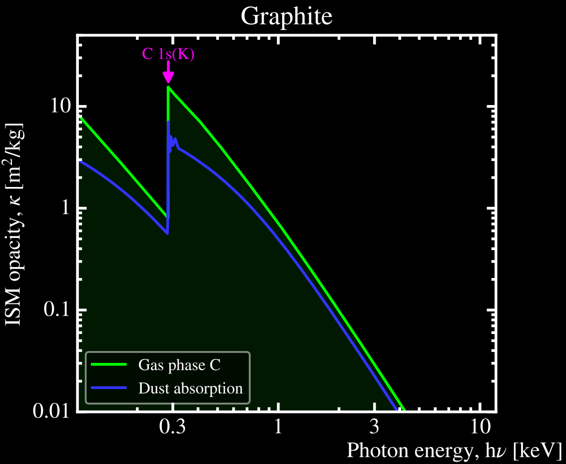
Graphite
C 1s(K)
ISM opacity, κ [m²/kg]
10
1
0.1
0.01
0.3
1
3
10
Photon energy, hν [keV]
Gas phase C
Dust absorption

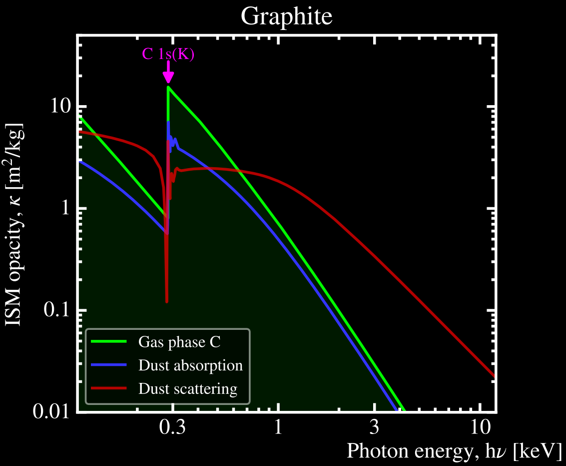
Graphite
C 1s(K)
ISM opacity, κ [m2/kg]
10
1
0.1
0.01
0.3
1
3
10
Photon energy, hν [keV]
Gas phase C
Dust absorption
Dust scattering

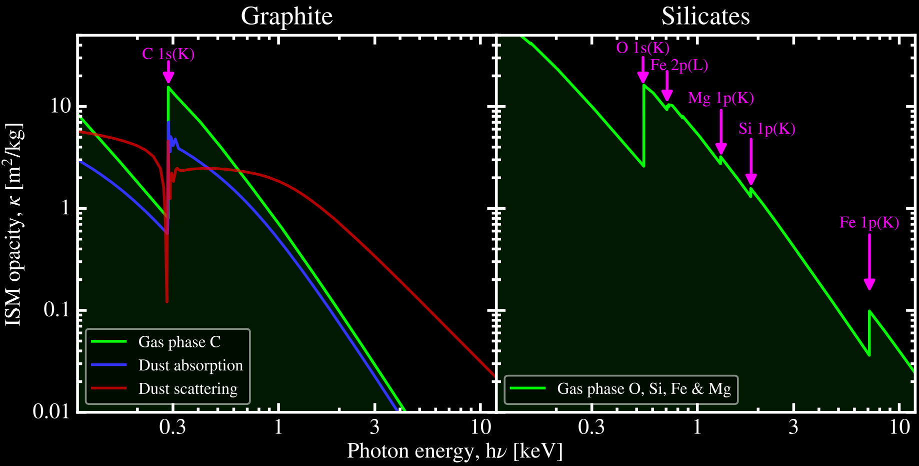
Graphite
Silicates
C 1s(K)
O 1s(K)
Fe 2p(L)
Mg 1p(K)
Si 1p(K)
Fe 1p(K)
ISM opacity, κ [m²/kg]
10
1
0.1
0.01
0.3
1
3
10
Photon energy, hν [keV]
Gas phase C
Dust absorption
Dust scattering
Gas phase O, Si, Fe & Mg

Dust | X-ray Absorption Edges

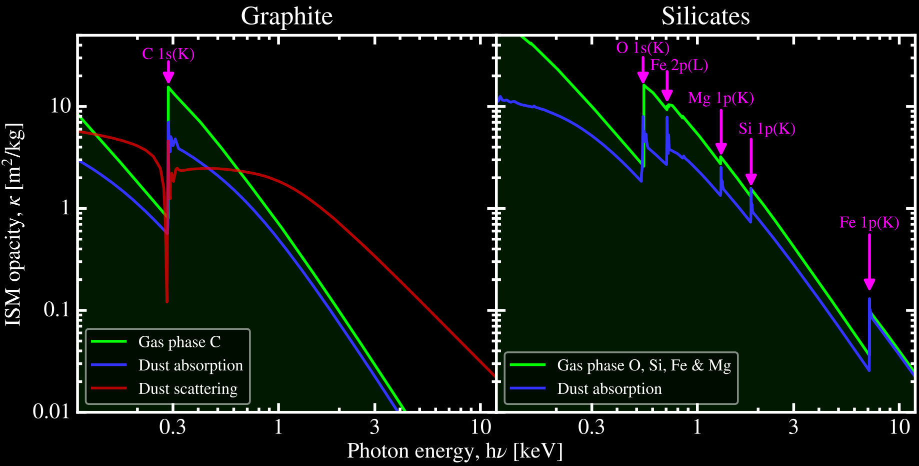

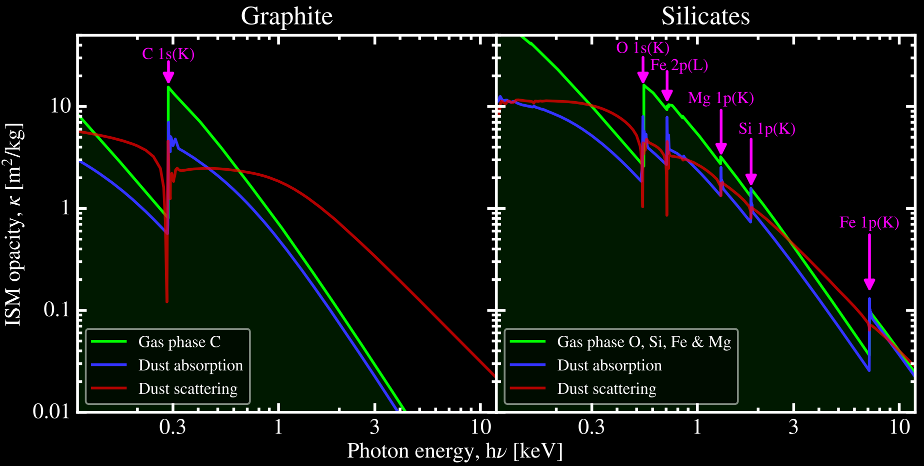
Graphite
Silicates
C 1s(K)
O 1s(K)
Fe 2p(L)
Mg 1p(K)
Si 1p(K)
Fe 1p(K)
Gas phase C
Dust absorption
Dust scattering
Gas phase O, Si, Fe & Mg
Dust absorption
Dust scattering
ISM opacity, κ [m2/kg]
10
1
0.1
0.01
0.3
1
3
10
Photon energy, hν [keV]

Dust | X-ray Absorption Edges

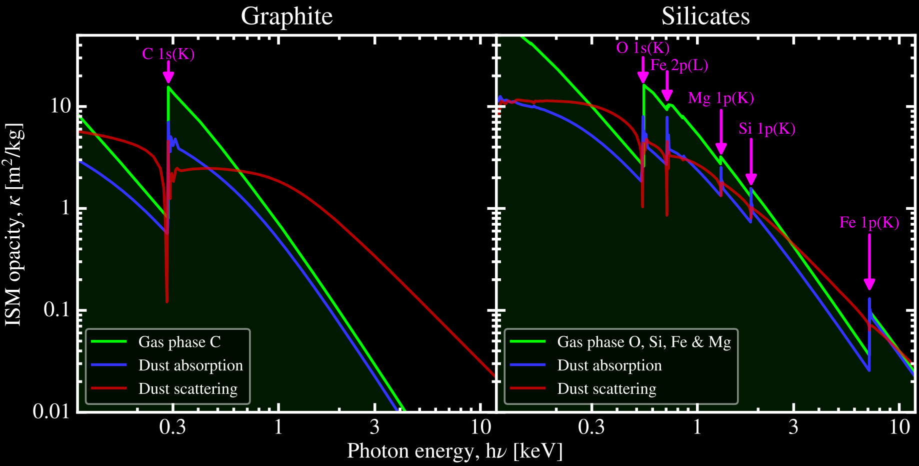

See *e.g.* Zeegers et al. (2017) & Rogantini et al. (2020).

Dust | X-ray Absorption Edges

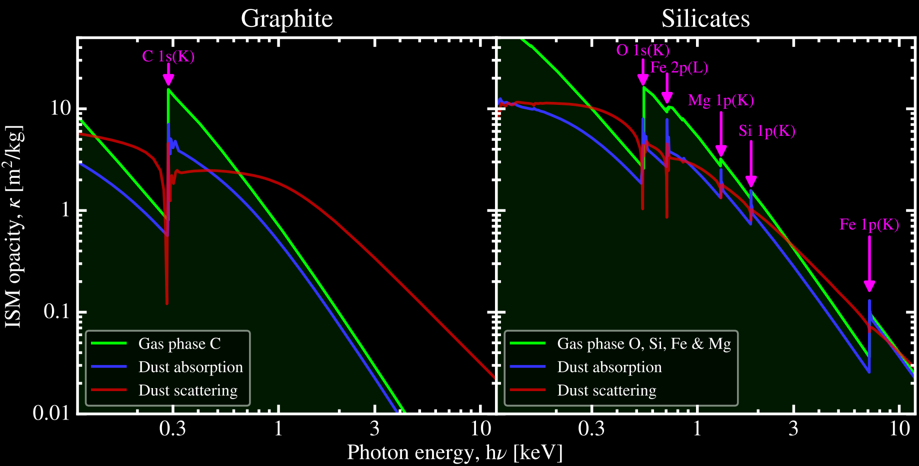

See *e.g.* Zeegers et al. (2017) & Rogantini et al. (2020).

⇒ constrain the grain structure.

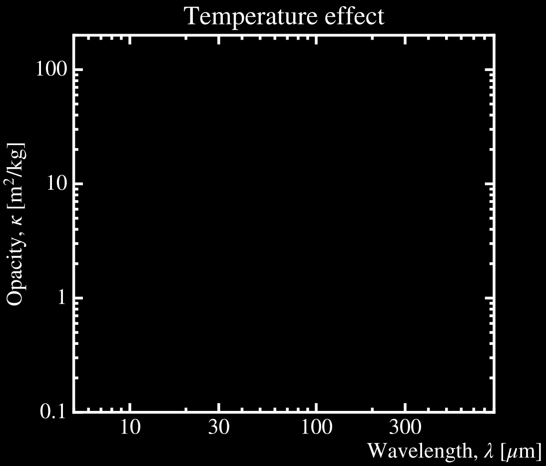

(Demyk et al., 2017a,b)

Dust | Laboratory Experiments on Dust Analogs

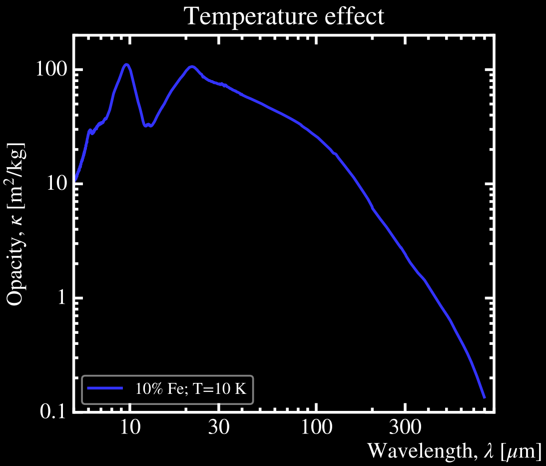

(Demyk et al., 2017a,b)

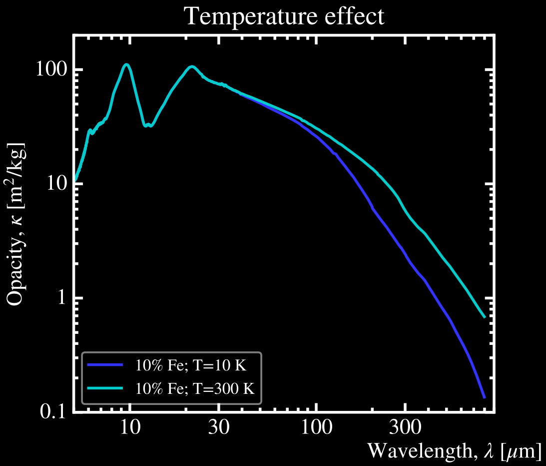

(Demyk et al., 2017a,b)

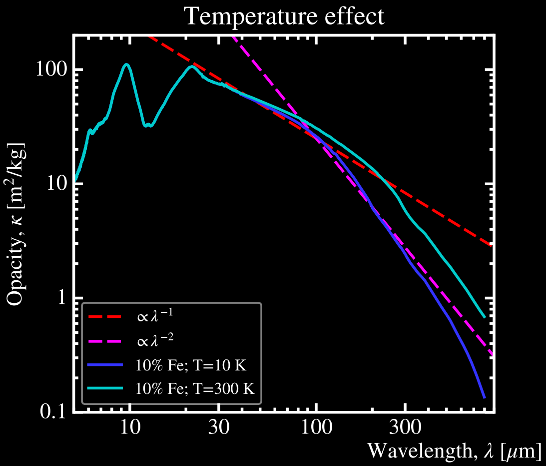

(Demyk et al., 2017a,b)

Dust | Laboratory Experiments on Dust Analogs

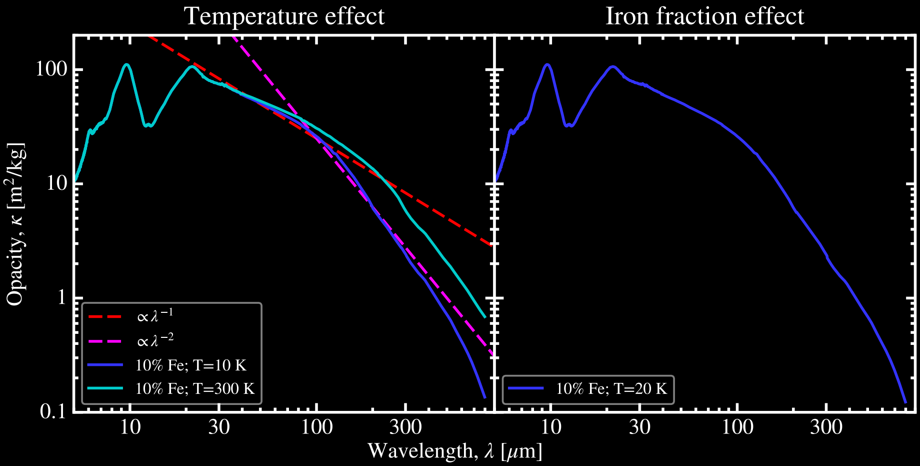

(Demyk et al., 2017a,b)

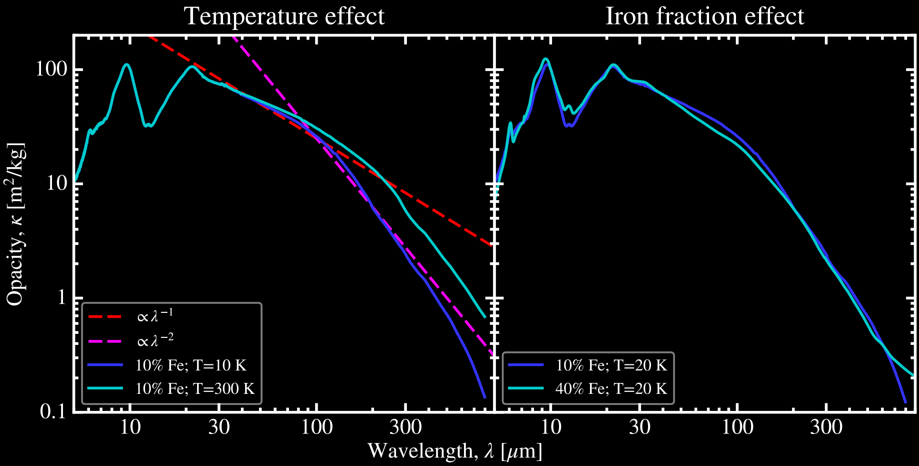

(Demyk et al., 2017a,b)

Dust | Laboratory Experiments on Dust Analogs

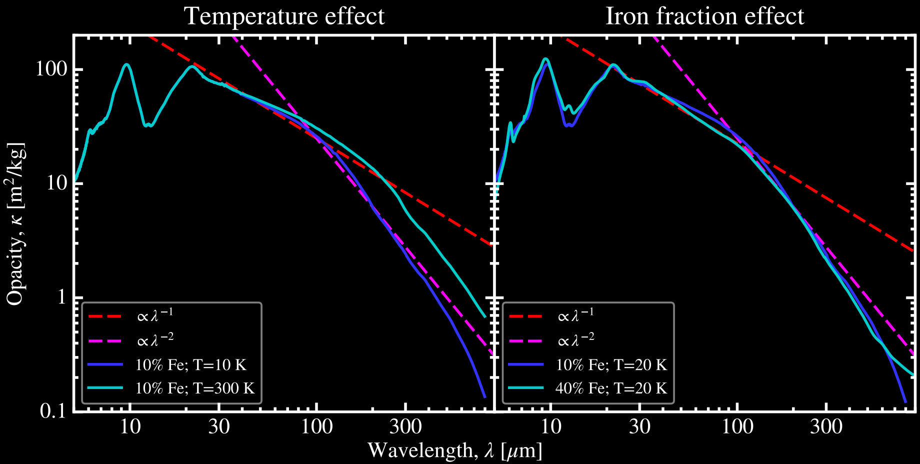

(Demyk et al., 2017a,b)

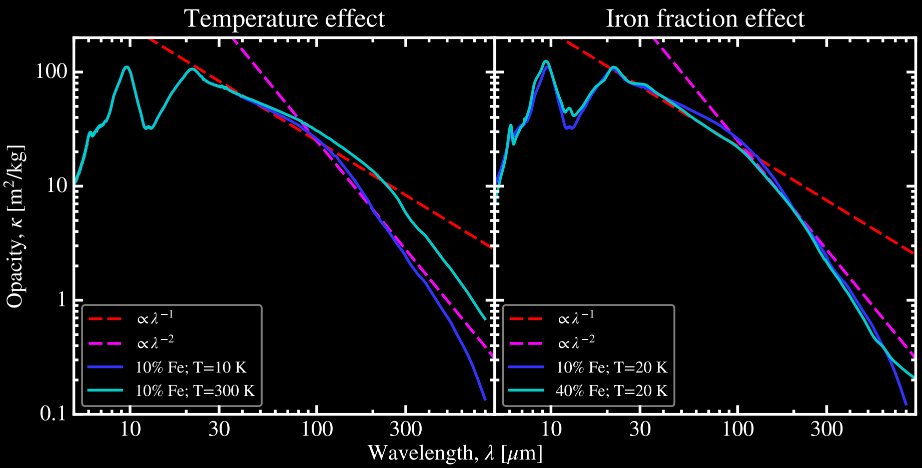

(Demyk et al., 2017a,b)

⇒ provide realistic optical properties.

Example: the THEMIS model (Jones et al., 2017)

Dust | A Model of the Diffuse Galactic ISM (1/2)

Example: the THEMIS model (Jones et al., 2017)

- heavily based on laboratory data.

Example: the THEMIS model (Jones et al., 2017)

- heavily based on laboratory data.
- a-C(:H) and coated amorphous silicates with Fe and FeS inclusions.

Example: the THEMIS model (Jones et al., 2017)

- heavily based on laboratory data.
- a-C(:H) and coated amorphous silicates with Fe and FeS inclusions.
- consistent with *Planck* data.

Example: the THEMIS model (Jones et al., 2017)

- heavily based on laboratory data.
- a-C(:H) and coated amorphous silicates with Fe and FeS inclusions.
- consistent with *Planck* data.

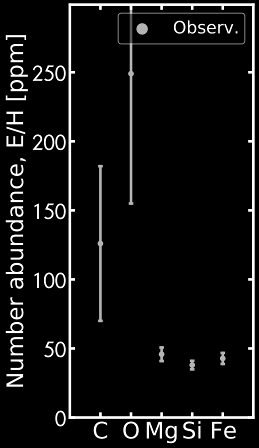

Example: the THEMIS model (Jones et al., 2017)

- heavily based on laboratory data.
- a-C(:H) and coated amorphous silicates with Fe and FeS inclusions.
- consistent with *Planck* data.

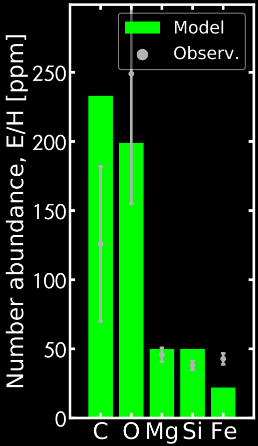

Example: the THEMIS model (Jones et al., 2017)

- heavily based on laboratory data.
- a-C(:H) and coated amorphous silicates with Fe and FeS inclusions.
- consistent with *Planck* data.

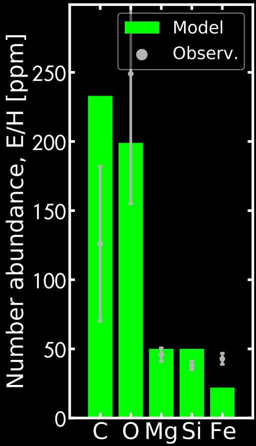

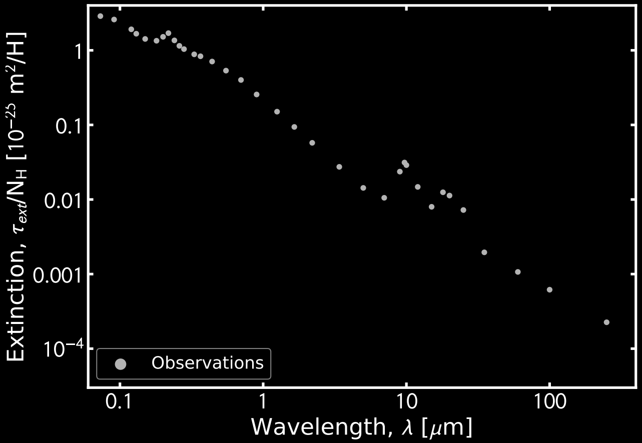

Example: the THEMIS model (Jones et al., 2017)

- heavily based on laboratory data.
- a-C(:H) and coated amorphous silicates with Fe and FeS inclusions.
- consistent with *Planck* data.

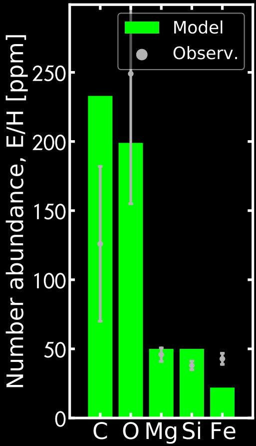

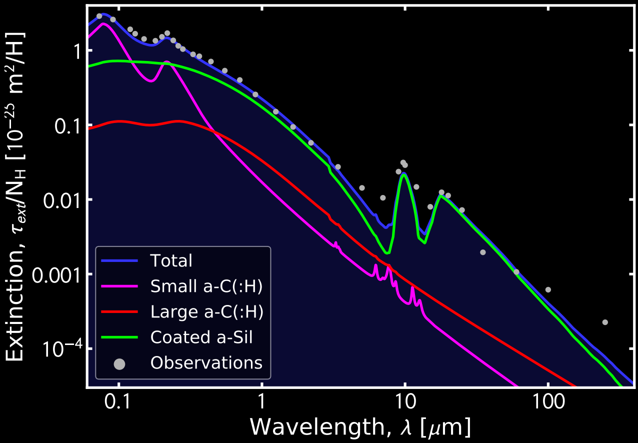

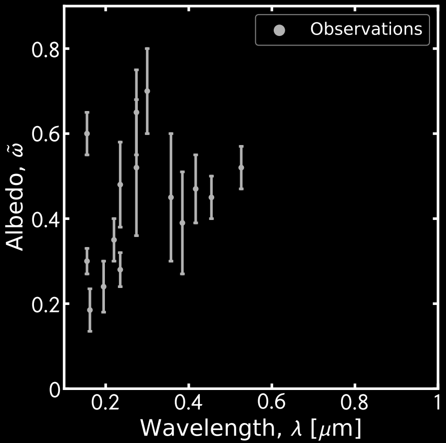
Observations
0
0.2
0.4
0.6
0.8
Albedo, $\tilde{\omega}$
0.2
0.4
0.6
0.8
1
Wavelength, λ [μm]

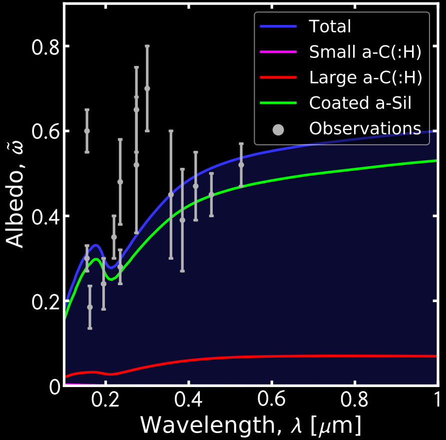

(THEMIS; Jones et al., 2017)

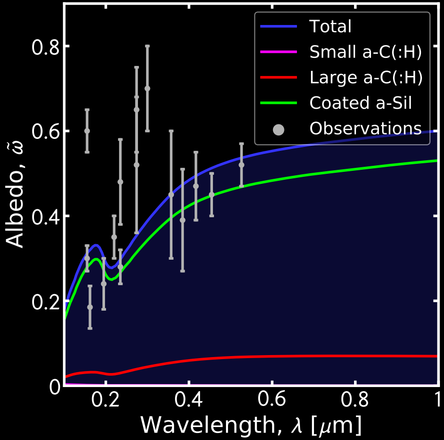

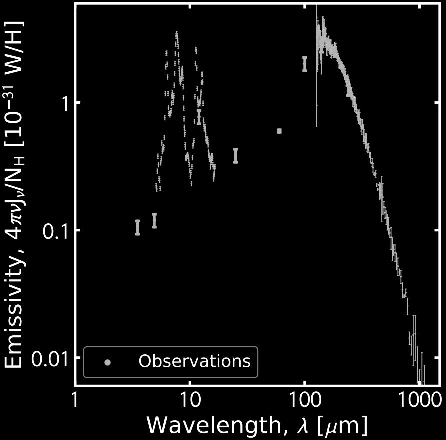

(THEMIS; Jones et al., 2017)

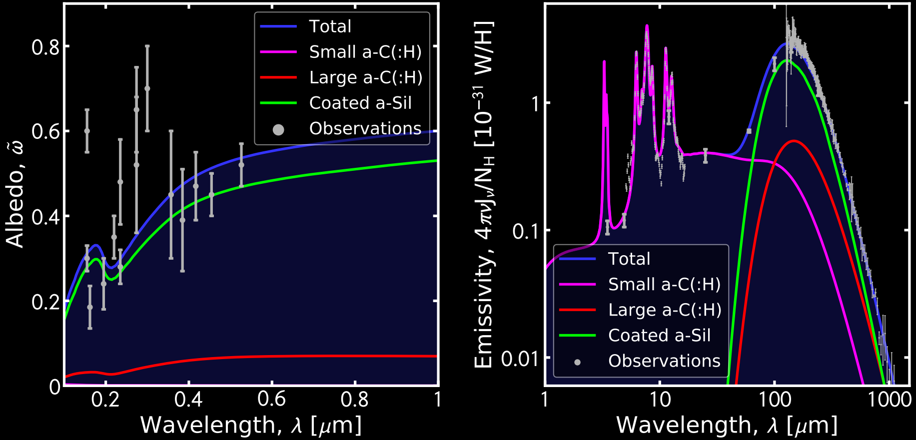

(THEMIS; Jones et al., 2017)

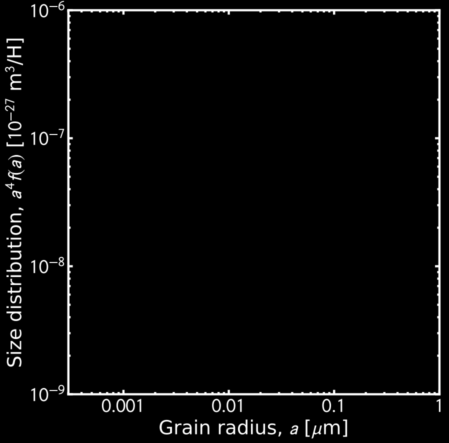

(Jones et al., 2017)

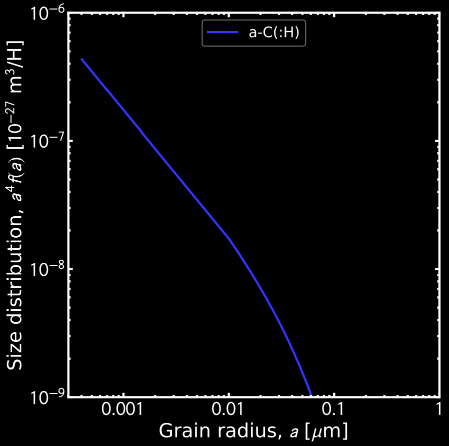

(Jones et al., 2017)

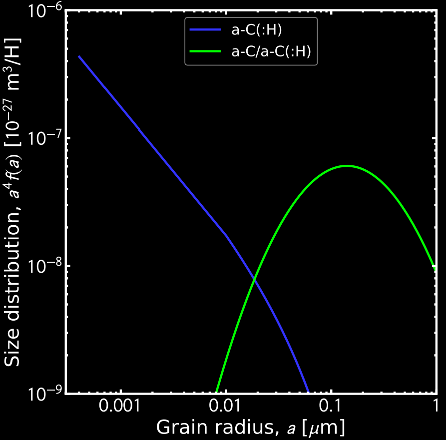

(Jones et al., 2017)

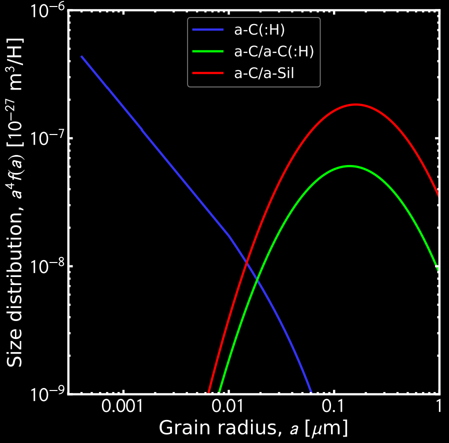

(Jones et al., 2017)

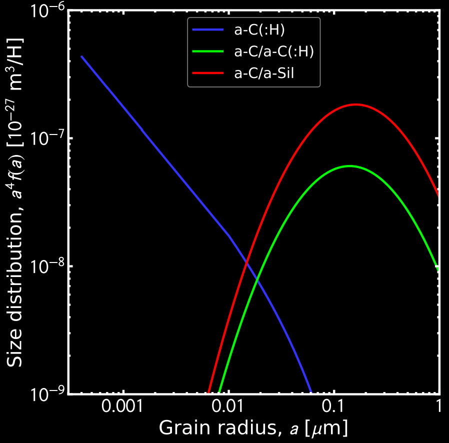

(Jones et al., 2017)

The MRN size distribution

The Mathis, Rumpl, & Nordsieck (1977, MRN) size distribution was the first attempt at accounting for the extinction curve with realistic grain optical properties: $f_{\text{MRN}}(a) \propto a^{-3.5}$.

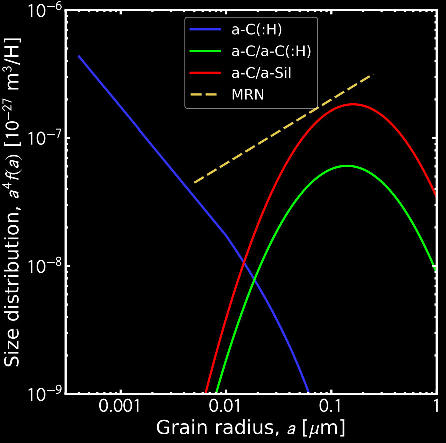

(Jones et al., 2017)

The MRN size distribution

The Mathis, Rumpl, & Nordsieck (1977, MRN) size distribution was the first attempt at accounting for the extinction curve with realistic grain optical properties: $f_{\text{MRN}}(a) \propto a^{-3.5}$.

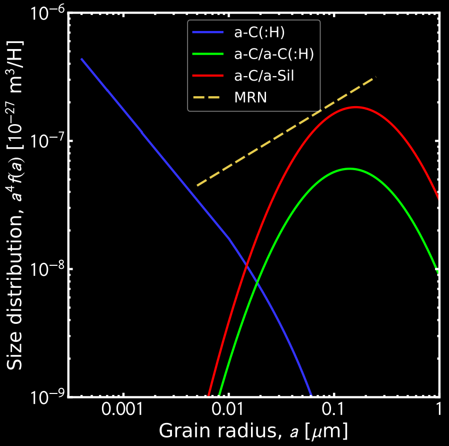

(Jones et al., 2017)

The MRN size distribution

The Mathis, Rumpl, & Nordsieck (1977, MRN) size distribution was the first attempt at accounting for the extinction curve with realistic grain optical properties: $f_{\mathrm{MRN}}(a) \propto a^{-3.5}$.

Average grain surface area & volume

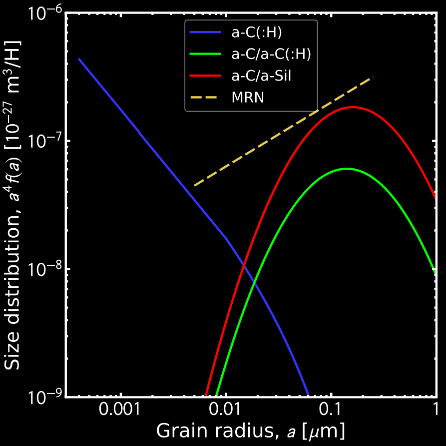

(Jones et al., 2017)

The MRN size distribution

The Mathis, Rumpl, & Nordsieck (1977, MRN) size distribution was the first attempt at accounting for the extinction curve with realistic grain optical properties: $f_{\text{MRN}}(a) \propto a^{-3.5}$.

Average grain surface area & volume

Surface, dominated by small grains:

$$\langle S_{\text{dust}} \rangle_a = \pi \int_{a_-}^{a_+} f_{\text{MRN}}(a) a^2 \, \mathrm{d}a \propto \frac{1}{\sqrt{a_-}} - \frac{1}{\sqrt{a_+}} \simeq \frac{1}{\sqrt{a_-}}.$$

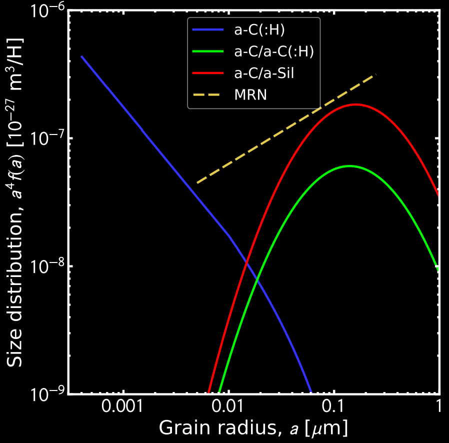

(Jones et al., 2017)

The MRN size distribution

The Mathis, Rumpl, & Nordsieck (1977, MRN) size distribution was the first attempt at accounting for the extinction curve with realistic grain optical properties: $f_{\rm MRN}(a) \propto a^{-3.5}$.

Average grain surface area & volume

Surface, dominated by small grains:

$$\langle S_{\rm dust}\rangle_a = \pi \int_{a_-}^{a_+} f_{\rm MRN}(a) a^2 \, {\rm d}a \propto \frac{1}{\sqrt{a_-}} - \frac{1}{\sqrt{a_+}} \simeq \frac{1}{\sqrt{a_-}}.$$

Volume, dominated by large grains:

$$\langle V_{\rm dust}\rangle_a = \frac{4\pi}{3} \int_{a_-}^{a_+} f_{\rm MRN}(a) a^3 \, {\rm d}a \propto \sqrt{a_+} - \sqrt{a_-} \simeq \sqrt{a_+}.$$

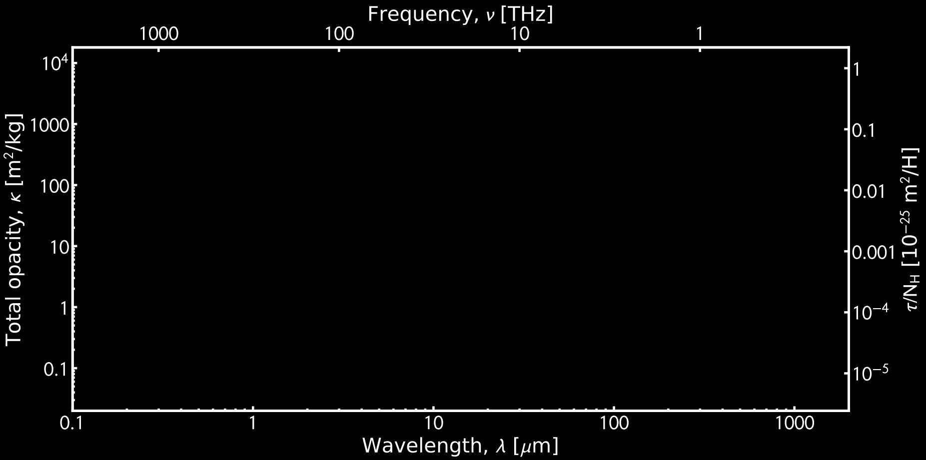
Frequency, ν [THz]
1000
100
10
1
Total opacity, κ [m^2/kg]
10^4
1000
100
10
1
0.1
τ/N_H [10^{-25} m^2/H]
1
0.1
0.01
0.001
10^{-4}
10^{-5}
0.1
1
10
100
1000
Wavelength, λ [μm]

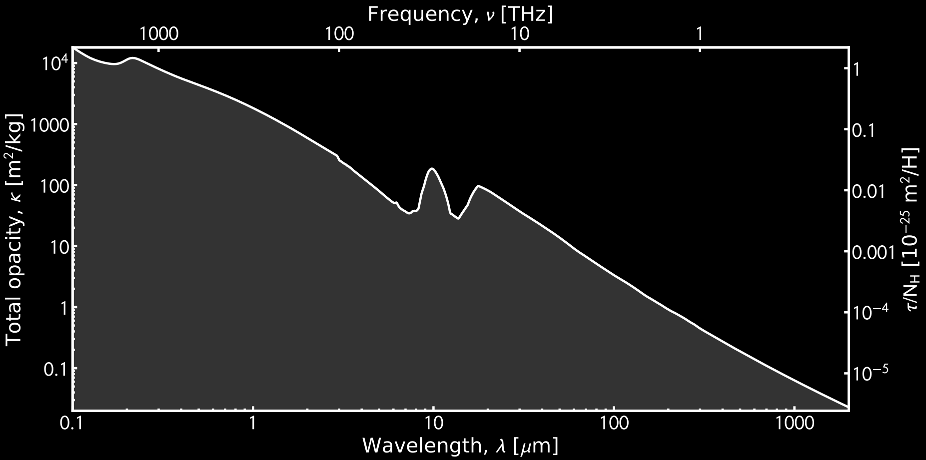
Frequency, ν [THz]
1000
100
10
1
Total opacity, κ [m²/kg]
10^4
1000
100
10
1
0.1
τ/N_H [10^−25 m²/H]
1
0.1
0.01
0.001
10^{-4}
10^{-5}
0.1
1
10
100
1000
Wavelength, λ [μm]

Dust | The Modeled Galactic Grain Opacity

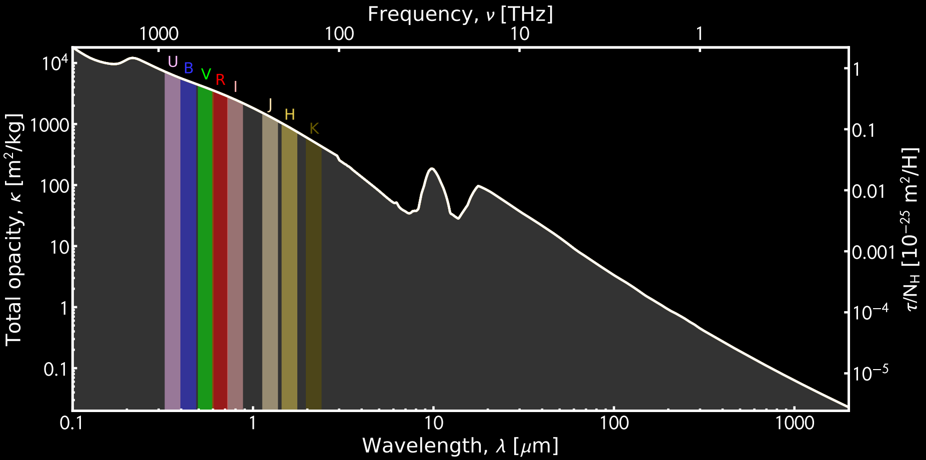

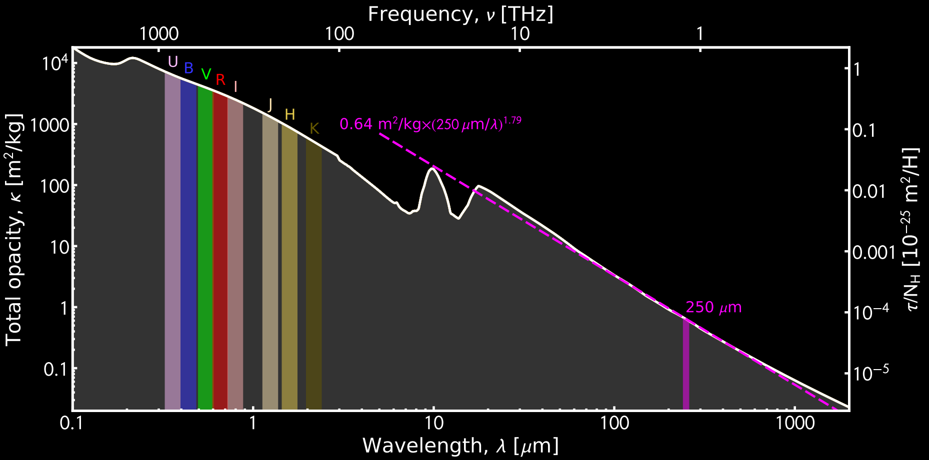

Frequency, ν [THz]
1000
100
10
1
Total opacity, κ [m²/kg]
τ/N_H [10⁻²⁵ m²/H]
U
B
V
R
I
J
H
K
0.64 m²/kg×(250 μm/λ)^1.79
250 μm
Wavelength, λ [μm]
0.1
1
10
100
1000

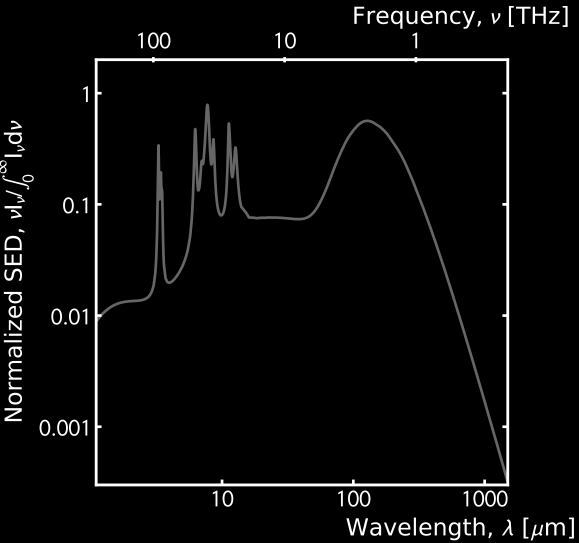
Frequency, ν [THz]
100
10
1
1
0.1
0.01
0.001
Normalized SED, $\nu I_\nu / \int_0^\infty I_\nu d\nu$
10
100
1000
Wavelength, λ [μm]

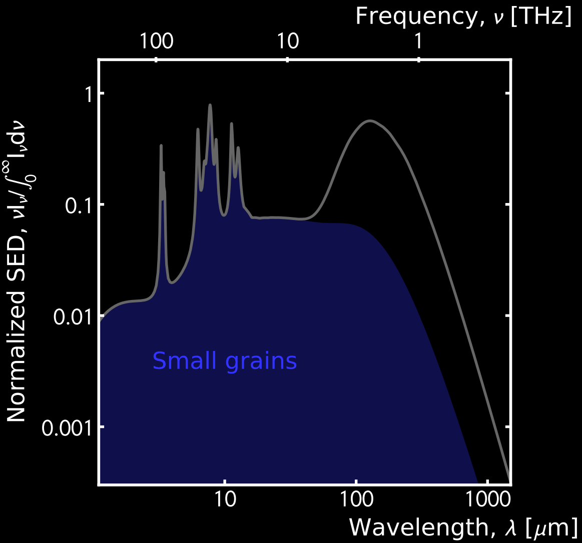
Frequency, ν [THz]
100
10
1
1
0.1
0.01
0.001
Normalized SED, $\nu I_\nu / \int_0^\infty I_\nu d\nu$
Small grains
10
100
1000
Wavelength, λ [μm]

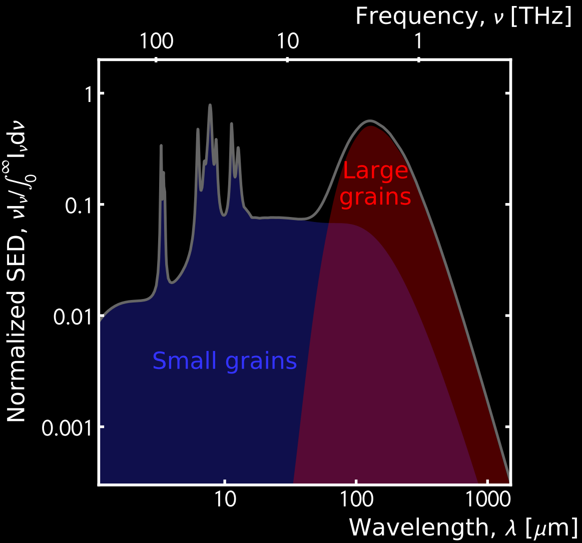
Frequency, ν [THz]
100
10
1
1
0.1
0.01
0.001
Normalized SED, $\nu I_\nu / \int_0^\infty I_\nu d\nu$
Large grains
Small grains
10
100
1000
Wavelength, λ [μm]

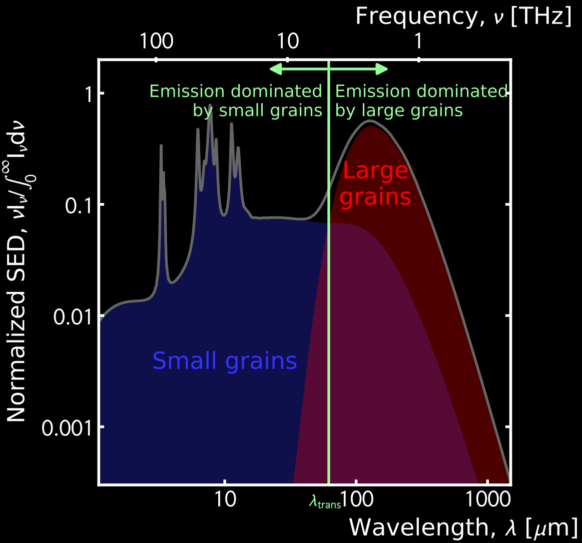
Frequency, ν [THz]
100
10
1
Emission dominated by small grains
Emission dominated by large grains
1
0.1
0.01
0.001
Normalized SED, $\nu I_\nu / \int_0^\infty I_\nu d\nu$
Large grains
Small grains
10
λ_{trans}
100
1000
Wavelength, λ [μm]

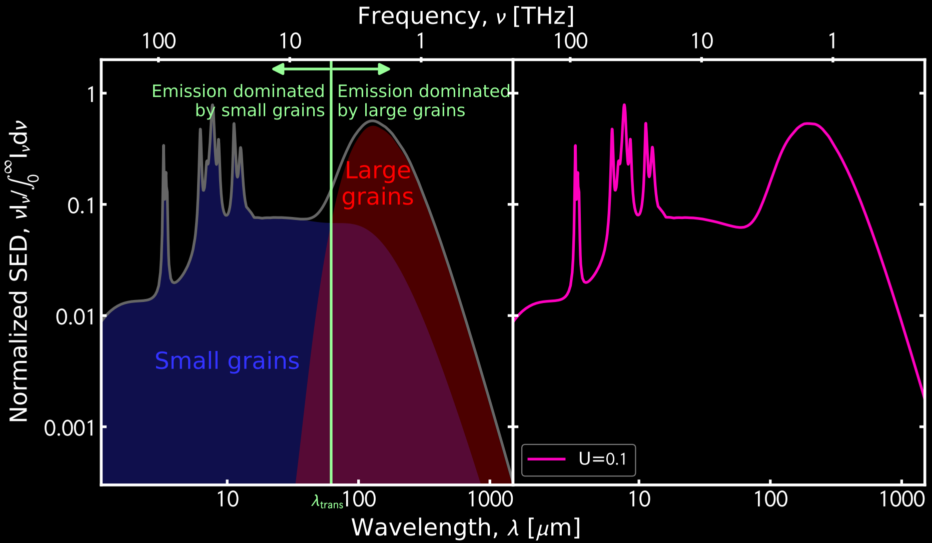
Frequency, ν [THz]
100
10
1
100
10
1
1
0.1
0.01
0.001
Normalized SED, $\nu I_\nu / \int_0^\infty I_\nu d\nu$
Emission dominated by small grains
Emission dominated by large grains
Large grains
Small grains
U=0.1
10
λ_{trans}
100
1000
10
100
1000
Wavelength, λ [μm]

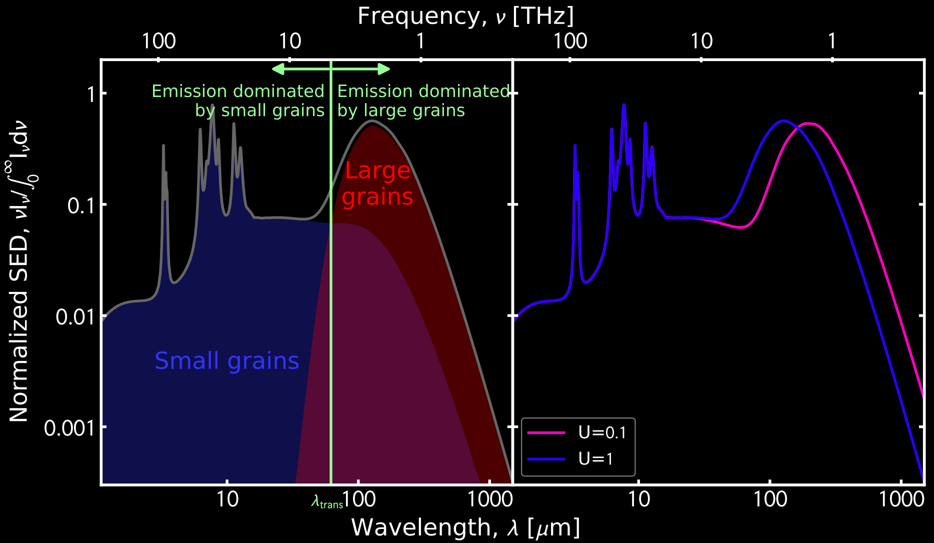
Frequency, ν [THz]
100
10
1
100
10
1
Emission dominated by small grains
Emission dominated by large grains
Large grains
Small grains
1
0.1
0.01
0.001
Normalized SED, $\nu I_\nu / \int_0^\infty I_\nu d\nu$
10
λ_{trans}
100
1000
10
100
1000
Wavelength, λ [μm]
U=0.1
U=1

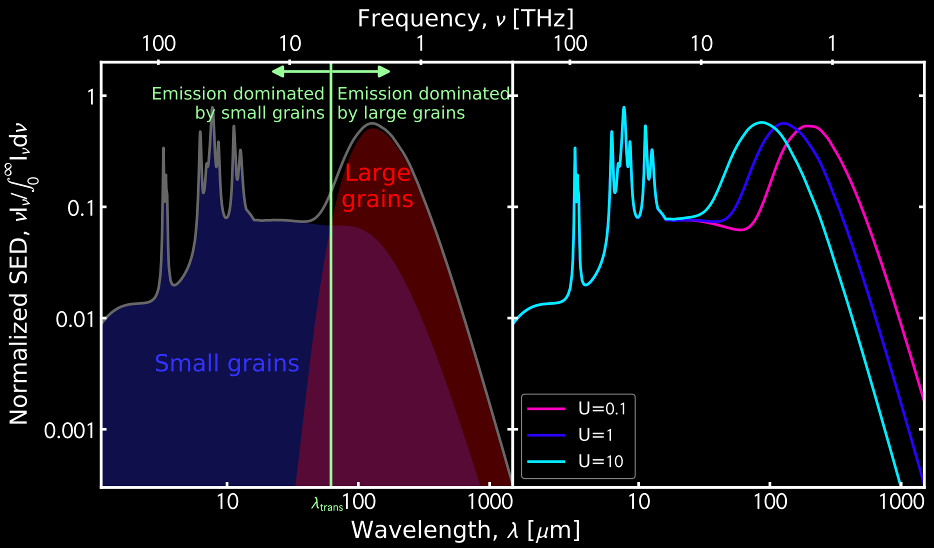

Frequency, ν [THz]
100
10
1
Emission dominated by small grains
Emission dominated by large grains
Large grains
Small grains
Normalized SED, $\nu I_\nu / \int_0^\infty I_\nu d\nu$
1
0.1
0.01
0.001
10
λ_{trans}
100
1000
Wavelength, λ [μm]
U=0.1
U=1
U=10

Dust | The Modeled Galactic Infrared Emission

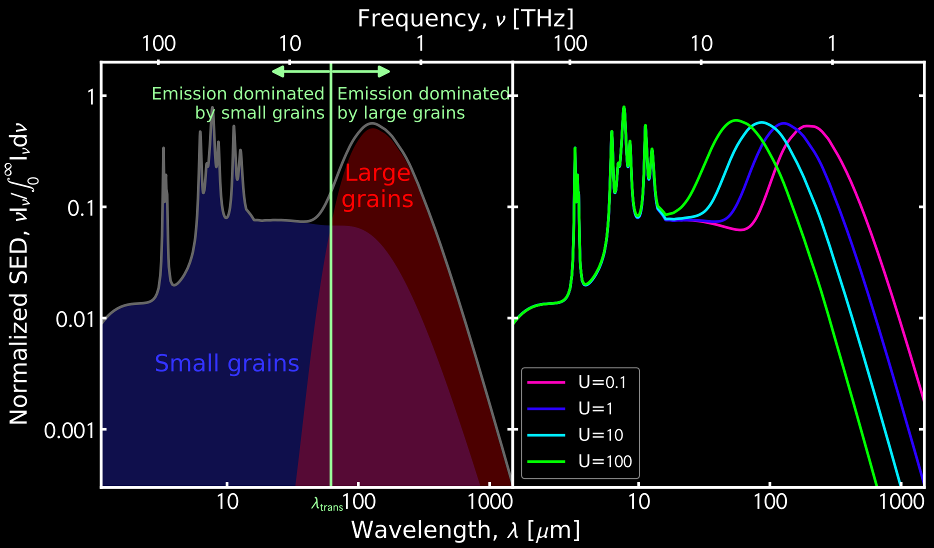

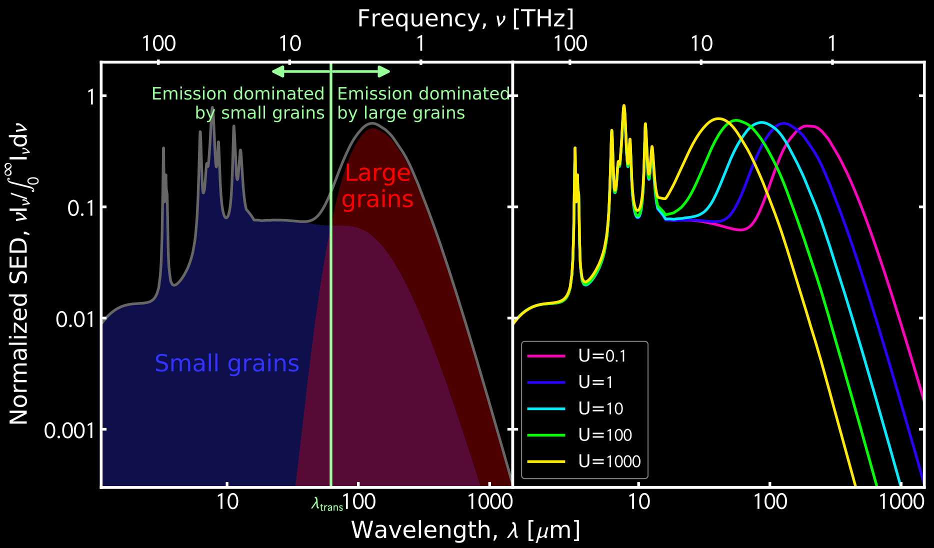

Frequency, ν [THz]
100
10
1
100
10
1
Emission dominated by small grains
Emission dominated by large grains
Large grains
Small grains
Normalized SED, $\nu I_\nu / \int_0^\infty I_\nu d\nu$
1
0.1
0.01
0.001
10
λ_{trans}
100
1000
10
100
1000
Wavelength, λ [μm]
U=0.1
U=1
U=10
U=100
U=1000

Dust | The Modeled Galactic Infrared Emission

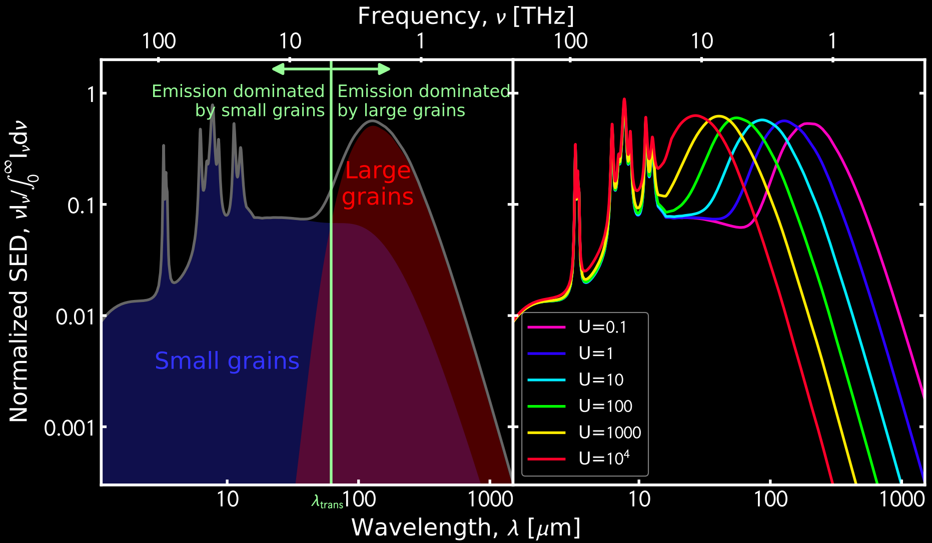

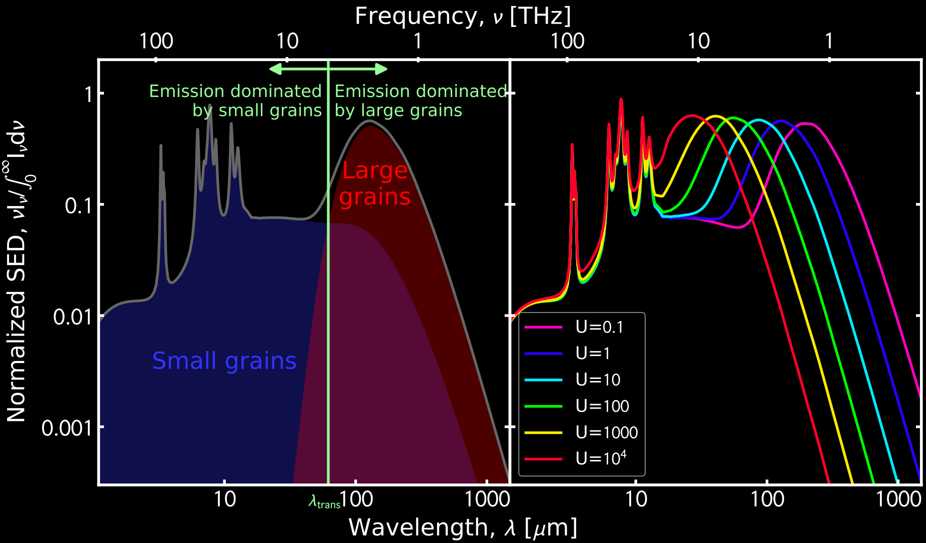

Galactic dust emissivity: $\epsilon_{dust} \simeq 221 \times U \, L_\odot / M_\odot$.

Outline of the Lecture

Neutral & ionized atoms

Neutral & ionized atoms

1. Atoms & molecules are excited by collisions & photons. They can be de-excited by collisions, photons or spontaneously. A line with a low spontaneous emission rate is called "*forbidden*".

Neutral & ionized atoms

1. Atoms & molecules are excited by collisions & photons. They can be de-excited by collisions, photons or spontaneously. A line with a low spontaneous emission rate is called "*forbidden*".
2. H^0 is opaque while H^+ is transparent to UV photons. The free-free emission is $F_\nu \propto \nu^{-0.12}$.

Neutral & ionized atoms

1. Atoms & molecules are excited by collisions & photons. They can be de-excited by collisions, photons or spontaneously. A line with a low spontaneous emission rate is called "*forbidden*".
2. H^0 is opaque while H^+ is transparent to UV photons. The free-free emission is $F_\nu \propto \nu^{-0.12}$.
3. Above $n_{\rm crit}$, the level populations are set by collisions $\Rightarrow$ the line emissivity is constant.

Neutral & ionized atoms

1. Atoms & molecules are excited by collisions & photons. They can be de-excited by collisions, photons or spontaneously. A line with a low spontaneous emission rate is called "*forbidden*".
2. H^0 is opaque while H^+ is transparent to UV photons. The free-free emission is $F_\nu \propto \nu^{-0.12}$.
3. Above $n_{\rm crit}$, the level populations are set by collisions $\Rightarrow$ the line emissivity is constant.

Molecules of astrophysical interest

Neutral & ionized atoms

1. Atoms & molecules are excited by collisions & photons. They can be de-excited by collisions, photons or spontaneously. A line with a low spontaneous emission rate is called "*forbidden*".
2. H^0 is opaque while H^+ is transparent to UV photons. The free-free emission is $F_\nu \propto \nu^{-0.12}$.
3. Above $n_{\rm crit}$, the level populations are set by collisions $\Rightarrow$ the line emissivity is constant.

Molecules of astrophysical interest

1. Molecules have electronic bands in the UV (Lyman-Werner), vibrational & rovibrational lines in the mid-IR, & rotational lines in the submm.

Conclusion | Take-Away Points

Neutral & ionized atoms

1. Atoms & molecules are excited by collisions & photons. They can be de-excited by collisions, photons or spontaneously. A line with a low spontaneous emission rate is called "*forbidden*".
2. H^0 is opaque while H^+ is transparent to UV photons. The free-free emission is $F_\nu \propto \nu^{-0.12}$.
3. Above n_{crit}, the level populations are set by collisions $\Rightarrow$ the line emissivity is constant.

Molecules of astrophysical interest

1. Molecules have electronic bands in the UV (Lyman-Werner), vibrational & rovibrational lines in the mid-IR, & rotational lines in the submm.
2. Strong molecular bonds are covalent (between 2 non-metals), ionic (between a metal & a non-metal) & metallic (between 2 metals). Van der Walls & H_2O are weaker bonds.

Conclusion | Take-Away Points

Neutral & ionized atoms

1. Atoms & molecules are excited by collisions & photons. They can be de-excited by collisions, photons or spontaneously. A line with a low spontaneous emission rate is called "*forbidden*".
2. H^0 is opaque while H^+ is transparent to UV photons. The free-free emission is $F_\nu \propto \nu^{-0.12}$.
3. Above $n_{\rm crit}$, the level populations are set by collisions $\Rightarrow$ the line emissivity is constant.

Molecules of astrophysical interest

1. Molecules have electronic bands in the UV (Lyman-Werner), vibrational & rovibrational lines in the mid-IR, & rotational lines in the submm.
2. Strong molecular bonds are covalent (between 2 non-metals), ionic (between a metal & a non-metal) & metallic (between 2 metals). Van der Walls & H_2O are weaker bonds.
3. H_2 is the most abundant molecule in the Universe. It does not have rotational lines. It exists in 2 forms: Ortho & Para.

Conclusion | Take-Away Points

Neutral & ionized atoms

1. Atoms & molecules are excited by collisions & photons. They can be de-excited by collisions, photons or spontaneously. A line with a low spontaneous emission rate is called "*forbidden*".
2. H^0 is opaque while H^+ is transparent to UV photons. The free-free emission is $F_\nu \propto \nu^{-0.12}$.
3. Above $n_{\rm crit}$, the level populations are set by collisions $\Rightarrow$ the line emissivity is constant.

Molecules of astrophysical interest

1. Molecules have electronic bands in the UV (Lyman-Werner), vibrational & rovibrational lines in the mid-IR, & rotational lines in the submm.
2. Strong molecular bonds are covalent (between 2 non-metals), ionic (between a metal & a non-metal) & metallic (between 2 metals). Van der Walls & H_2O are weaker bonds.
3. H_2 is the most abundant molecule in the Universe. It does not have rotational lines. It exists in 2 forms: Ortho & Para.

Interstellar dust

Conclusion | Take-Away Points

Neutral & ionized atoms

1. Atoms & molecules are excited by collisions & photons. They can be de-excited by collisions, photons or spontaneously. A line with a low spontaneous emission rate is called "*forbidden*".
2. H^0 is opaque while H^+ is transparent to UV photons. The free-free emission is $F_\nu \propto \nu^{-0.12}$.
3. Above $n_{\rm crit}$, the level populations are set by collisions $\Rightarrow$ the line emissivity is constant.

Molecules of astrophysical interest

1. Molecules have electronic bands in the UV (Lyman-Werner), vibrational & rovibrational lines in the mid-IR, & rotational lines in the submm.
2. Strong molecular bonds are covalent (between 2 non-metals), ionic (between a metal & a non-metal) & metallic (between 2 metals). Van der Walls & H_2O are weaker bonds.
3. H_2 is the most abundant molecule in the Universe. It does not have rotational lines. It exists in 2 forms: Ortho & Para.

Interstellar dust

1. Dust optical properties derive from the composition & solid-state structure of the grains.

Conclusion | Take-Away Points

Neutral & ionized atoms

1. Atoms & molecules are excited by collisions & photons. They can be de-excited by collisions, photons or spontaneously. A line with a low spontaneous emission rate is called "*forbidden*".
2. H^0 is opaque while H^+ is transparent to UV photons. The free-free emission is $F_\nu \propto \nu^{-0.12}$.
3. Above n_{crit}, the level populations are set by collisions $\Rightarrow$ the line emissivity is constant.

Molecules of astrophysical interest

1. Molecules have electronic bands in the UV (Lyman-Werner), vibrational & rovibrational lines in the mid-IR, & rotational lines in the submm.
2. Strong molecular bonds are covalent (between 2 non-metals), ionic (between a metal & a non-metal) & metallic (between 2 metals). Van der Walls & H_2O are weaker bonds.
3. H_2 is the most abundant molecule in the Universe. It does not have rotational lines. It exists in 2 forms: Ortho & Para.

Interstellar dust

1. Dust optical properties derive from the composition & solid-state structure of the grains.
2. Large grains ($a \gtrsim 0.02\ \mu$m) are at thermal equilibrium $\Rightarrow$ grey body. Small grains ($a \lesssim 0.02\ \mu$m) are stochastically heated $\Rightarrow$ broader & hotter emission spectrum.

Conclusion | Take-Away Points

Neutral & ionized atoms

1. Atoms & molecules are excited by collisions & photons. They can be de-excited by collisions, photons or spontaneously. A line with a low spontaneous emission rate is called "*forbidden*".
2. H^0 is opaque while H^+ is transparent to UV photons. The free-free emission is $F_\nu \propto \nu^{-0.12}$.
3. Above n_{crit}, the level populations are set by collisions $\Rightarrow$ the line emissivity is constant.

Molecules of astrophysical interest

1. Molecules have electronic bands in the UV (Lyman-Werner), vibrational & rovibrational lines in the mid-IR, & rotational lines in the submm.
2. Strong molecular bonds are covalent (between 2 non-metals), ionic (between a metal & a non-metal) & metallic (between 2 metals). Van der Walls & H_2O are weaker bonds.
3. H_2 is the most abundant molecule in the Universe. It does not have rotational lines. It exists in 2 forms: Ortho & Para.

Interstellar dust

1. Dust optical properties derive from the composition & solid-state structure of the grains.
2. Large grains ($a \gtrsim 0.02\ \mu$m) are at thermal equilibrium $\Rightarrow$ grey body. Small grains ($a \lesssim 0.02\ \mu$m) are stochastically heated $\Rightarrow$ broader & hotter emission spectrum.
3. Dust models are constrained by emission, extinction, depletion & polarization of the diffuse Galactic ISM. Surface area is dominated by small grains. Volume is dominated by large grains.

Allamandola, L. J., Hudgins, D. M., & Sandford, S. A. 1999, ApJ, 511, L115

Asplund, M., Grevesse, N., Sauval, A. J., & Scott, P. 2009, ARA&A, 47, 481

Belloche, A., Menten, K. M., Comito, C., et al. 2008, A&A, 482, 179

Bohren, C. F. & Huffman, D. R. 1983, Absorption and scattering of light by small particles (Wiley)

Boogert, A. C. A., Gerakines, P. A., & Whittet, D. C. B. 2015, ARA&A, 53, 541

Bransden, B. & Joachain, C. 1983, Physics of atoms and molecules (Longman)

Cami, J., Bernard-Salas, J., Peeters, E., & Malek, S. E. 2010, Science, 329, 1180

Campbell, E. K., Holz, M., Gerlich, D., & Maier, J. P. 2015, Nature, 523, 322

Compiègne, M., Verstraete, L., Jones, A., et al. 2011, A&A, 525, A103+

Demyk, K., Meny, C., Leroux, H., et al. 2017a, A&A, 606, A50

Demyk, K., Meny, C., Lu, X. H., et al. 2017b, A&A, 600, A123

Désert, F.-X., Boulanger, F., & Puget, J. L. 1990, A&A, 237, 215

Dopita, M. A. & Sutherland, R. S. 2003, Astrophysics of the diffuse universe (Springer)

Draine, B. T. 2003, ApJ, 598, 1017

Draine, B. T. 2011, Physics of the Interstellar and Intergalactic Medium (Princeton University Press)

Draine, B. T. & Flatau, P. J. 1994, J. Opt. Soc. Am. A, 11, 1491

Draine, B. T. & Li, A. 2001, ApJ, 551, 807

Draine, B. T. & Li, A. 2007, ApJ, 657, 810

Fan, H., Hobbs, L. M., Dahlstrom, J. A., et al. 2019, ApJ, 878, 151

Galliano, F. 2022, HDR, Université Paris-Saclay

Galliano, F., Galametz, M., & Jones, A. P. 2018, ARA&A, 56, 673

Gordon, K. D., Clayton, G. C., Decleir, M., et al. 2023, ApJ, 950, 86

Guélin, M. & Cernicharo, J. 2022, Frontiers in Astronomy and Space Sciences, 9, 787567

Guhathakurta, P. & Draine, B. T. 1989, ApJ, 345, 230

Guillet, V., Fanciullo, L., Verstraete, L., et al. 2017, ArXiv:1710.04598

Heger, M. L. 1922, Lick Observatory Bulletin, 10, 141

Hensley, B. S. & Draine, B. T. 2021, ApJ, 906, 73

Hensley, B. S. & Draine, B. T. 2023, ApJ, 948, 55

HI4PI Collaboration, Ben Bekhti, N., Flöer, L., et al. 2016, A&A, 594, A116

Hoppe, P. 2010, in Nuclei in the Cosmos, 21

Hummer, D. G. & Storey, P. J. 1987, MNRAS, 224, 801

Jenkins, E. B. 2009, ApJ, 700, 1299

Jenniskens, P. & Désert, F.-X. 1994, A&AS, 106

Jones, A. P., Fanciullo, L., Köhler, M., et al. 2013, A&A, 558, A62

Jones, A. P., Köhler, M., Ysard, N., Bocchio, M., & Verstraete, L. 2017, A&A, 602, A46

Jones, K. L., Koribalski, B. S., Elmouttie, M., & Haynes, R. F. 1999, MNRAS, 302, 649

Kalberla, P. M. W. & Kerp, J. 2009, ARA&A, 47, 27

Krügel, E. 2003, The physics of interstellar dust (IoP)

MacIsaac, H., Cami, J., Cox, N. L. J., et al. 2022, A&A, 662, A24

Mathis, J. S., Mezger, P. G., & Panagia, N. 1983, A&A, 128, 212

Mathis, J. S., Rumpl, W., & Nordsieck, K. H. 1977, ApJ, 217, 425

Merrill, P. W. 1934, PASP, 46, 206

Osterbrock, D. E. & Ferland, G. J. 2006, Astrophysics of gaseous nebulae and active galactic nuclei (University Science Books)

Planck Collaboration, Aghanim, N., Akrami, Y., et al. 2020, A&A, 641, A12

Rogantini, D., Costantini, E., Zeegers, S. T., et al. 2020, A&A, 641, A149

Rybicky, G. B. & Lightman, A. P. 1979, Radiative processes in astrophysics (Wiley)

Siebenmorgen, R. 2023, A&A, 670, A115

Smith, R. C., Points, S. D., Chu, Y. H., et al. 2005, in American Astronomical Society Meeting Abstracts, Vol. 207, American Astronomical Society Meeting Abstracts, 25.07

Tercero, B., Cernicharo, J., Pardo, J. R., & Goicoechea, J. R. 2010, A&A, 517, A96

Tielens, A. 2021, Molecular Astrophysics (Cambridge University Press)

Tielens, A. G. G. M. 2005, The Physics and Chemistry of the Interstellar Medium (Cambridge University Press)

Walker, G. A. H., Bohlender, D. A., Maier, J. P., & Campbell, E. K. 2015, ApJ, 812, L8

Walter, F., Brinks, E., de Blok, W. J. G., et al. 2008, AJ, 136, 2563

Wu, R., Galliano, F., & Onaka, T. 2018, in The Cosmic Wheel and the Legacy of the AKARI Archive: From Galaxies and Stars to Planets and Life, ed. T. Ootsubo, I. Yamamura, K. Murata, & T. Onaka, 133–136

Ysard, N., Jones, A. P., Guillet, V., et al. 2024, A&A, 684, A34

Zeegers, S. T., Costantini, E., de Vries, C. P., et al. 2017, A&A, 599, A117

Zubko, V., Dwek, E., & Arendt, R. G. 2004, ApJS, 152, 211

Zubko, V. G., Mennella, V., Colangeli, L., & Bussoletti, E. 1996, MNRAS, 282, 1321